DIFFUSION AND VISCOSITY COEFFICIENTS OF BINARY NON-ELECTROLYTE LIQUID MIXTURES

MOHAMMAD AFZAL AWAN

M.Sc. (CHEMISTRY)

M.Sc. (NUCLEAR ENGINEERING)

A Thesis submitted for the degree of

Doctor of Philosophy

of

the University of Glasgow

Department of Physical & Theoretical Chemistry,

The University,

Glasgow G12 8QQ

July, 1989

ProQuest LLC.
789 East Eisenhower Parkway
P.O. Box 1346
Ann Arbor, MI 48106 – 1346

Dedicated to my wife

Mrs. Bibi Gul Awan, B.A, L.L.B

for her patience, devotion and love.

CONTENTS

TABLES

FIGURES

ACKNOWLEDGEMENTS

The author wishes to express his sincere thanks to Dr. J. H. Dymond of Glasgow University and Dr. J. D. Isdale of the National Engineering Laboratory for their guidance and support for this research work.

The experimental work at high pressure was carried out at the National Engineering Laboratory, East Kilbride. The author is thankful to the Director, N.E.L., for permission to use the facilities of the laboratory and to the other members of staff who have helped in many ways.

The author is cordially thankful to the Ministry of Science and Technology, Government of Pakistan, for awarding the scholarship through the S & T scholarship Scheme.

DECLARATION

The work described in this thesis was carried out partly at the University of Glasgow and partly at the National Engineering Laboratory, East Kilbride during the period January, 1986 to November 1988. It is wholly original except where otherwise indicated in the text. Some of the results presented in chapters 2 and 5 have been published in the following papers.

(i) (p, ρ,T) of [0.5C_8H_{18} + 0.5(1-C_8H_{16})], [0.5$(CH_3)_2CHCH_2C(CH_3)_3$ +0.5 (1-C_8H_{16}) or 0.5C_8H_{18}], and [0.333C_8H_{18} + 0.333(1-C_8H_{16}) + 0.333$(CH_3)_2CHCH_2C(CH_3)_3$] in the range 298 to 373 K and 0.1 to 500 MPa, J.H. Dymond, R. Malhotra, M.A. Awan, J.D. Isdale and N.F. Glen, J. Chem. Thermodyn., 20 (1988), 1217.

(ii) Correlation of High Presure Diffusion and Viscosity Coefficients for n-Alkanes, J. H. Dymond and M. A. Awan, Int. J. Thermophys., 10 (1989), 941

Papers in the course of publication :

(i) Transport Properties of Nonelectrolyte Liquid Mixtures-VIII. Limiting Mutual Diffusion Coefficients of Fluorinated Benzenes in n- Hexane, M. A. Awan and J. H. Dymond, Int. J. Thermophys. (to be submitted).

(ii) Transport properties of Nonelectrolyte Liquid Mixtures-IX. Mutual Diffusion Coefficients for Toluene + n-Hexane and Toluene + Acetonitrile at Pressures up to 25 MPa, M. A. Awan and J. H. Dymond, Int. J. Thermophys. (to be submitted).

(iii) Transport Properties of nonelectrolyte Liquid Mixtures-X., Viscosity Coefficients for n-Hexane + Toluene System from 298 to 373 K at Presures up to 500 MPa, M. A. Awan and J. H. Dymond, N. F. Glen and J. D. Isdale, Int. J. Thermophys. (to be submitted).

(iv) Transport Properties of Nonelectrolyte Liquid Mixtures-XI., Viscosity Coefficients for the Toluene + Acetonitrile System from 298 to 373 K at Pressures up to 500 MPa or to the Freezing Pressure, M. A. Awan, J. H. Dymond, N. F. Glen and J. D. Isdale, Int. J. Thermophys. (to be submitted).

(v) (P, ρ, T) of [(1-x) C6H5CH3 + xC6H14] and [(1-x)C6H5CH3 + xCH3CN] in the range 298 to 373 K and 0.1 to 500 Mpa, M. A. Awan, J. H. Dymond, N. F. Glen and J. D. Isdale, J. Chem. Thermodyn. (to be submitted).

In addition the following papers have been presented at conferences:

(i) The State of the Kinetic Theory of Liquids Today.
J. H. Dymond, Eurotherm Seminar No.2, April 7-8, 1988, Stuttgart, Federal Republic of Germany.

(ii) Correlation of High Pressure Diffusion and Viscosity Coefficients for n-Alkanes.
J. H. Dymond and M. A. Awan. Paper presented at the 10th Symposium on Thermophysical Properties,June 20-23, 1988, Gaithersburg, Maryland, U.S.A.

SUMMARY

The Taylor Dispersion Technique has been applied to the measurement of mutual diffusion coefficients for liquid mixtures at elevated pressures. The systems studied were toluene plus n-hexane and toluene plus acetonitrile over the temperature range from 273 to 348 K and up to 25 MPa. The density and viscosity for the same mixtures have been measured from 298 to 373 K and up to 500 MPa. A self-centering falling body viscometer was used for the viscosity measurements, and densities were measured with a bellows volumometer. High pressure densities are also reported for the ternary mixture of n-octane, i-octane and oct-1-ene. Measurements were also made of the mutual diffusion coefficient of benzene and eight fluorinated benzenes at trace concentration in n-hexane from 213 to 333 K, at atmospheric pressure.

The results have been used to make a rigorous test of current theoretical and empirical relationships. The Tait equation fits the density data within 0.2%. The trace mutual diffusion coefficient data are satisfactorily accounted for on the basis of the rough hard-sphere model and the high pressure viscosity coefficient results are successfully correlated using a method based on consideration of hard-sphere theory. The Grunberg and Nissan equation satisfactorily reproduces the mixture viscosity data, with parameter G dependent on temperature, pressure and concentration.

An important development in the correlation of dense fluid transport properties on the basis of hard-sphere model is described, whereby diffusion and viscosity coefficients are considered simultaneously. This should lead to more reliable prediction methods for transport coefficients of dense fluids and fluid mixtures.

SYMBOLS AND ABBREVIATIONS

Except where specified otherwise the symbols used have the following meanings:

A	(i) Viscometer calibration constant
	(ii) Cross-sectional area of bellows
A_{12}	Translation-rotation coupling constant
B	Viscometer calibration constant
D_{12}	Mutual diffusion coefficient
De	Dean number
F	flow rate
F_{TR}	Transition flow rate
G	Grunberg and Nissan constant
G^*	Gibbs free energy
$g(\sigma)$	Radial distribution function at contact
K	Bulk modulus
$\bar{K}$	Secant bulk modulus
k	Boltzmann constant
L, l	Length
L_s	length of sinker
M	(i) Liquid mass in bellows
	(ii) Molecular weight
MD	Molecular dynamics
m	Mass per molecule
N	Avogadro constant
n	(i) Number of moles
	(ii) Constant in equation for the viscometer calibration

P	Pressure
Po	Atmospheric pressure
R	Universal Gas constant
Ro	Radius of diffusion tube
Rc	Radius of helix
Re	Reynolds number
r	Radius of capillary
r1	Radius of sinker
r2	Radius of viscometer tube
Sc	Schmidt number
T	Temperature
t	time
t*	Buoyancy corrected fall time
V	(i) Volume
	(ii) Velocity
Vo	Volume of close packing
V_M^E	Molar excess volume
x	mole fraction
α	Linear coefficient of expansion of steel
β	Linear coefficient of compressibility of steel
ρ, ρ_l	Density of liquid
ρ_o	Density at atmospheric pressure
ρ_s	Density of sinker
ξ	Packing fraction
η	Dynamic viscosity coefficient
η/ρ	Kinematic viscosity coefficient
σ	(i) Standard deviation of Gaussian peak
	(ii) Hard sphere diameter
λ	Coefficient of thermal conductivity

CHAPTER 1

INTRODUCTION

INTRODUCTION.

Transport properties of fluids and fluid mixtures play an important role in chemical engineering (for example, in plant design), in medicine (as in protein transportation in biological systems), in environmental engineering (air pollution, for example), in chemical processes (as in isotope separation) and in other disciplines. A study of transport properties is therefore extremely important both experimentally, to obtain precise measurements on systems of industrial importance and on key systems for testing theories, and theoretically, in order to provide information on the least well understood state of matter, the liquid. For accurate prediction of transport properties it is essential to develop theories of transport of dense fluids which have a molecular basis.

The theory of transport phenomena is well developed for dilute gases [1] made up of structureless spherical particles. Accurate prediction of diffusion, viscosity and thermal conductivity coefficients is possible, provided potential energy functions are accurately known. However, for dense fluids, problems arise because of many-body effects. These can be overcome, in principle, by the computer simulation technique of molecular dynamics [2-12]. The limitations of this method are the need for an accurate description of the pair intermolecular potential energy function for each substance, plus information concerning the non-additivity of the pair potential. An additional major disadvantage is the length of computing time involved in the calculations.

In view of these difficulties in calculating exactly the transport properties of dense fluids and their mixtures, it is necessary at present to use empirical methods or, preferably, semi-empirical methods which are based on theory. An outline of some of the currently used methods is given in Chapter 2. The most successful theoretical approach at this time is based on the hard-sphere model of a fluid [13] and this has been widely used for the successful correlation of experimental transport coefficient data for dense fluids and fluid mixtures [14-24]. However, values reported for the molecular parameter of a given substance often show significant variation. In order to resolve this difficulty and provide a sound foundation for further application of this approach, a careful analysis has been made of viscosity and diffusion data, simultaneously, since these properties exhibit a very strong density dependence, and a consistent set of parameters determined. The data used were for n-alkanes where extensive accurate measurements are available over wide temperature and pressure ranges. The results of this theoretical part of the project are included in Chapter 2.

For a rigorous test of any theory, it is necessary to have experimental measurements for selected systems over a wide range of experimental conditions.

Most of the experimental work on mixtures in the past has been concentrated in the case of mutual diffusion coefficients on measurements at trace concentrations over a limited temperature range, with little attention given to the pressure dependence. In this work, the Taylor dispersion technique is used to measure the mutual diffusion coefficients for benzene and eight fluorinated benzenes at trace con-

centration over the temperature range 213-333 K at atmospheric pressure. These systems show similar molecular interactions but have different size and mass ratios. The theory of the method is discussed in chapter 3, section 3.2 and the results are discussed in section 3.4.10. and 3.4.11.

High pressure mutual diffusion measurements were conducted for toluene + n-hexane mixtures over the temperature range 298 to 348 K at toluene mole fractions of 0, 0.25, 0.50, 0.75 and 1.0 up to 25 MPa. Measurents were also made for toluene + acetonitrile mixtures at temperatures from 273 to 248 K at a toluene mole fraction of 0, 0.2, 0.4, 0.6, 0.8 and 1.0 up to 24 MPa. The results for these non-ideal systems are presented in section 3.5.4. of Chapter 3. Prediction methods are available for the composition dependence of binary liquid mixtures [25-29] but in most cases knowledge of the thermodynamic factor is required.

In the case of viscosity coefficients at elevated pressures, previous measurements have been made almost exclusively on n-alkanes and their mixtures. Therefore, in this work an experimental study has been made of mixtures of toluene with n-hexane and with acetonitrile, where the molecular interactions will differ. Chapter 4 describes the methods used to measure the viscosity coefficient and density at atmospheric pressure. Results given in this chapter for toluene, acetonitrile and binary mixtures of toluene + n-hexane and toluene + acetonitrile at temperature from 298 to 348 K are used in the subsequent chapter to calculate the high pressure density and viscosity coefficient. High pressure densities were measured by using a bellows volumometer while high pressure viscosity coefficients were measured using the self-

centering falling body viscometer at the National Engineering Laboratory, East Kilbride, Glasgow. Both sets of apparatus are described in the later sections of Chapter 4.

The high pressure densities and coefficient of viscosity for binary mixtures of toluene + n-hexane and toluene + acetonitrile at temperatures from 298 to 373 K and at pressures up to 500 MPa are presented in Chapter 5. Density results are also presented for the equimolar mixture of n-octane, i-octane and oct-1-ene over the same temperature and pressure ranges, to supplement previous measurements on the equimolar binary mixtures [30].

The results presented in Chapter 5 are discussed in Chapter 6 in the light of current theories and correlation methods. Specifically, (a) the variation of molar excess volume with composition and pressure is described; (b) the densities are fitted to the modified Tait equation, and (c) the viscosity coefficients are correlated on the basis of the rough hard-sphere theory, and also fitted to a free volume form of equation and to the empirical Grunberg and Nissan equation.

Chapter 7 is devoted to various conclusions drawn from this research work, and includes a number of suggestions for future work.

CHAPTER 2

THEORIES OF TRANSPORT PROPERTIES FOR DENSE FLUIDS

2.1 INTRODUCTION.

The diffusion and high pressure viscosity coefficient data for liquids and liquid mixtures obtained in this work are discussed in terms of current theories and empirical relations in use at the present time, such as the hard-sphere theory and activation energy theory, the free volume form of equation and the Grunberg and Nissan equation. Of these the most successful theoretically-based approach is that based on the hard sphere model, and an attempt is made to correlate simultaneously the self-diffusion and viscosity coefficient data of n-alkanes (methane to n-hexane) over the wide temperature and pressure ranges and to derive a single set of Vo values. In this chapter, an outline of the different theories and various correlation methods is first given for the two properties and discussed.

2.2 HARD SPHERE MODEL.

The kinetic theory of transport properties is highly developed for dilute monatomic gases [31,32]. The transport coefficients derived from the theory depend upon the nature of the pair potential, which in the case of rare gases is now quite well known. The problems arise in trying to account theoretically for the transport coefficients of dilute polyatomic gases, and for dense fluids. In the case of dense fluids, there is at present no formal theory that allows exact calculation of transport properties in terms of the actual molecular interactions and so it is necessary to consider reasonably realistic but approximate models for which transport coefficients can be evaluated accurately. These solutions can then form the basis of correlations and prediction methods and are to be preferred over

purely empirical methods.

The model that has provided the required basis for such an approach is the van der Waals model of a fluid which pictures the molecules as having an infinitely steep repulsive interaction and a very long-range attractive interaction. At fluid densities, this becomes equivalent to the hard-sphere model for transport properties. For this model the interaction energy is given by:

$$U(r) = 0 \quad r>\sigma$$
$$U(r) = \infty \quad r<\sigma \qquad (2.1)$$

For any real system, the potential energy does have a steep repulsive part and the range of the attractive part can be considered large relative to the interparticle spacing at densities greater than the critical density. The attractive energy then forms a uniform attractive energy surface, and the molecules will move in straight lines between core collisions, providing that the kinetic energy is not too low. In applying the hard-sphere model to real fluids therefore it is to be expected that the core size will decrease as the temperature is increased, a consequence of the softness of the repulsive interaction.

2.2.1 TRANSPORT COEFFICIENTS FOR A DENSE HARD-SPHERE FLUID.

Transport coefficient for a dense hard-sphere system can be related to the dilute hard-sphere values. For a dilute gas of hard spheres, where the interparticle distance is large compared to the size of the particles, the transport coefficients, namely, diffusion coefficient

D_o, viscosity coefficient η_o and coefficient of thermal conductivity λ_o can be written as [13].

$$D_o = (3/8n_o\pi\sigma^2)(\pi kT/m)^{1/2} \qquad (2.2)$$

$$\eta_o = (5/16\pi\sigma^2)(\pi mkT)^{1/2} \qquad (2.3)$$

$$\lambda_o = (25C_v/32\pi\sigma^2)(\pi kT/m)^{1/2} \qquad (2.4)$$

where n_o is the number density, m is the mass of the particle, T is the absolute temperature, k is the Boltzmann constant and C_v is the heat capacity for monatomic species at constant volume.

The kinetic theory for transport coefficients of a dense hard sphere system has been given by Enskog [33]. In a dense system, the collision rate is higher than in a dilute system because the molecular diameter is no longer negligible compared with the interparticle distance. The Enskog theory of diffusion assumes that the high density system behaves exactly as a low density system except that the collision frequency is increased by a factor of $g(\sigma)$, where $g(\sigma)$ is the radial distribution function at contact for the spheres of diameter σ [15,34,35]. The solution of the Boltzmann equation valid at low density is merely scaled in time to give the ratio of the diffusion coefficient D_E at high number density n relative to that at low density, subscript zero.

$$nD_E/n_oD_o = 1/g(\sigma) \qquad (2.5)$$

$g(\sigma)$ can be determined from the Carnahan-Starling equation [36]:

$$g(\sigma) = (1-0.5\xi)/(1-\xi)^3 \qquad (2.6)$$

where $\xi = b/4V$ for molar volume V, and b (the second virial coefficient for hard spheres) is $2\pi N\sigma^3/3$ where N is the Avogadro constant and D_o is given by equation 2.2.

For diffusion the particles themselves must move, but for viscosity and thermal conductivity there is the additional mechanism of collisional transfer whereby momentum and energy can be passed to another molecule upon collision. The Enskog theory for viscosity η_E and the thermal conductivity λ_E in terms of the low density coefficients accordingly contain additional terms.

$$\eta_E/\eta_o = [1/g(\sigma) + 0.800b/V + 0.761g(\sigma)(b/V)^2] \qquad (2.7)$$

$$\lambda_E/\lambda_o = [1/g(\sigma) + 1.200b/V + 0.755g(\sigma)(b/V)^2] \qquad (2.8)$$

where η_o and λ_o are given by equations 2.3 and 2.4 respectively.
Since the Enskog theory is based on the molecular chaos approximation and only binary collisions are considered, the theory fails at liquid density because of neglect of correlated molecular motion, such as back scattering of a molecule surrounded by a shell of surrounding molecules. The existence of correlated molecular motion is proved by molecular dynamics calculations [37] and Alder, Gass and Wainwright [3] have computed the resulting corrections to the Enskog coefficients at different reduced volumes, V/Vo, where Vo is the volume of close packing.

For dense gases at densities up to 2.5-times the critical density, the corrections to Enskog theory for viscosity and thermal conductivity coefficients are less than 10%, but for diffusion the corrected coefficient is significantly greater than the Enskog value at densities corresponding to 1.5- to 2-times the critical density. At the highest densities, approaching the onset of solidification, the correction arising from back-scattering results in the exact hard-sphere diffusion coefficient being lower by about 40%, and viscosity coefficient being higher by a similar amount.Thus, to obtain the exact relationship for the dense hard-sphere transport coefficients in terms of the low density coefficients, equations 2.5, 2.7 and 2.8 must be multiplied by the appropriate correction factor.

2.2.2 ROUGH HARD-SPHERE THEORY.

The smooth hard-sphere theory is only applicable to the monatomic fluids (noble gases),liquid metals [38], and polyatomic spherical molecules such as methane, where the mass distribution is spherically symmetric. For polyatomic fluids generally it is necessary to take into account the effects of non-spherical shape and the possibility of coupling of translational and rotational motion. Chandler [39-41], related the diffusion and viscosity coefficients for a rough hard-sphere fluid to those for a smooth hard-sphere fluid as

$$D_{RHS} = AD_{SHS} \qquad (2.9)$$

$$\eta_{RHS} = C\eta_{SHS} \qquad (2.10)$$

where A and C are translation-rotation coupling factors, expected to

be density and temperature independent, taking into account the possibility of changes in angular momentum as well as in translational momentum upon collision, and are bounded by the condition:

$$0 < A \leqslant 1 \quad \text{and} \quad C \geqslant 1.$$

An equation for A [42] suggests that A has a value from 5/7 to 1 for polyatomic fluids, while in the case of the lower alkanes it was found that the coupling factor C could be taken to have the value unity [43].

The thermal conductivity for rough hard-sphere fluids cannot be simply related to that for a smooth hard-sphere fluid like the viscosity and diffusion coefficient because the internal energy must be taken into account in consideration of this property. In this work , attention is therefore restricted to application of the rough hard-sphere theory to the correlation of diffusion and viscosity coefficients over the wide temperature and densities ranges. The method of application, and results, are discussed below in section 2.6, using literature results for n-alkanes, and in Chapter 6 for the experimental results of toluene plus n-hexane and toluene plus acetonitrile obtained in this work.

This rough hard-sphere model can also be applied to transport properties of liquid mixtures. For example, the binary diffusion coefficient D_{12} for a dense fluid mixture is given by Eq. 2.11 [23]

$$D_{12} = \frac{3(kT)^{1/2}}{8n\sigma_{12}^2}\left[\frac{m_1 + m_2}{2m_1m_2\pi}\right]^{1/2}\frac{A_{12}}{g_{12}(\sigma)}\left[\frac{D}{D_E}\right]_{MD} \qquad (2.11)$$

where n is the total number density, $\sigma_{12}=(\sigma_1+\sigma_2)/2$ for spheres of diameter σ_1, σ_2; m_1 and m_2 are the molecular masses and $(D/D_E)_{MD}$ is the computed correction to the Enskog value. A_{12} is the translation-rotation coupling constant and $g_{12}(\sigma)$ is the unlike radial distribution function which is given in terms of the like radial distribution functions by:

$$g_{12}(\sigma) = [\ \sigma_1 g_{22}(\sigma) + \sigma_2 g_{11}(\sigma)\ ]/2\sigma_{12} \qquad (2.12)$$

where $g_{ii}(\sigma)$ is given by

$$g_{ii}(\sigma) = 1/(1-x)+3y_i/[2(1-x)^2]+y_i^2/[2(1-x)^3] \qquad (2.13)$$

where $x= x_1 + x_2$, with x_i equal to $n_i\sigma_i^3/6$
and $y_i = (\sigma_i x_j + \sigma_j x_i)/\sigma_j$

Thus mutual diffusion coefficients for binary mixtures of hard-sphere fluids can be calculated provided that the core sizes of the solvent and solute molecules are known as a function of temperature. Values for A_{12} can be derived from limiting tracer diffusion coefficient or limiting mutual diffusion coefficient measurements by using equations 2.11-2.13 with given core sizes. Corrections to the Enskog values can be determined by molecular dynamics calculations while the core sizes can be estimated from fitting the viscosity or tracer diffusion coefficient data for the pure components to a free volume form of equation [44] or from the formula presented by Protopapas et al. [38].

This approach has been used for the analysis of the mutual diffusion coefficient measurements at trace solute concentration reported in Chapter 3, to derive values for A_{12} for the organic solutes in

n-hexane and for the systems toluene + n-hexane and toluene + acetonitrile.

2.3 ACTIVATION ENERGY THEORY.

An alternative approach to the solution of the problem of transport processes has been considered in terms of an activation energy theory [45] which is based on the theory of absolute reaction rates. According to this theory, in a pure liquid at rest the individual molecules are constantly in motion. However, because of the relatively close packing of molecules the motion is largely confined to vibration of each molecule within a "cage" formed by its nearest neighbours.

Eyring [46] has suggested that a liquid at rest continually undergoes rearrangement in which one molecule at a time escapes from its "cage" into an adjoining hole. In order to "jump" into a neighbouring vacancy, a molecule must first overcome an activation energy barrier caused by the field of the neighbouring molecules. On the basis of the absolute reaction rate theory, the viscosity of a pure liquid is given as follows [47]:

$$\eta_l = (Nh/V)(\lambda/a)^2 \exp(\Delta G^*/RT) \qquad (2.14)$$

where N is the Avogadro constant, h is the Planck constant, λ is the distance between adjacent moleculer layers, V is the molar volume, a is the distance between neighbouring molecules in the layer and ΔG^* is the Gibbs free energy of activation for viscous flow, equal to the difference in the chemical potentials of the transition state and the pure liquid.

Similarly, the temperature dependence of diffusion coefficients can be expressed as an Arrhenius type of equation in terms of the activation energy of diffusion, which arises from two different mechanisms [48], one static and the other dynamic. The static contribution comes from the contact pair correlation function $g_{12}(\sigma)$ in Enskog diffusivity. The pair correlation function can be expressed in the form:

$$g_{12}(\sigma) = \exp[-w(\sigma)/RT] \qquad (2.15)$$

where $w(\sigma)$ is the potential of mean force of a pair of molecules held just at contact. $g_{12}(\sigma)$ is also a measure of the number of nearest neighbour solvent molecules around a solute molecule. This caging of a solute molecule by solvent molecules give rise to the configurational activation energy.

The other source of activation energy is dynamical, namely, the activation energy of the back scattering effect, accounted for by the factor D/D_E. The total activation energy of diffusion is the algebraic sum of the two activation energies.

Both the Arrhenius type equation for diffusion and equation 2.14 predict that ln D and ln η should be a linear function of reciprocal temperature as is found experimentally in most of the cases, with slope equal to the activation energy divided by Gas constant R. In Chapter 3, section 3.4.10, this approach is applied to the mutual diffusion coefficient data for fluorinated benzenes in n-hexane and the activation energy of diffusion is calculated.

2.4 FREE VOLUME THEORIES.

The first relationship between viscosity and the free volume, in which the molecules are free to move, of an unassociated liquid was proposed by Batschinski in 1913 [49] as follows:

$$1/\eta = (v-w)/C \qquad (2.16)$$

where v is the specific volume of the liquid, w and C are constants. w was correlated as being a nearly constant fraction of the critical volume, similar to van der Waals b, but Batschinski failed to find a correlation for C.

Doolittle [50] found that the fluidity of many simple hydrocarbon liquids could be represented by a relation having a form quite different from Batschinski's equation as follows:

$$1/\eta = A' \exp[-B'Vo/Vf] \qquad (2.17)$$

which is equivalent to

$$\ln \eta = A'' + CV^*/(V-V^*) \qquad (2.18)$$

where A" and C are constant for a given liquid and V* was defined initially as the specific volume of the liquid extrapolated to absolute zero, but later [51] was considered as an other adjustable parameter.

Cohen and Turnbull [52] derived a similar equation from consideration of the statistical redistribution of the free volume in a hard-sphere fluid. According to them:

$$\ln (\eta/T^{1/2}) = A_c + B_c/V_f \qquad (2.19)$$

where A_c and B_c are constants and V_f is the free volume, assumed to be equivalent to a thermal expansion from a reference temperature to the experimental temperature.

Recently Hildebrand [53] modified Batschinski's equation, by reasoning that fluidity should be a linear function of the ratio of free volume, V-Vo, to the volume Vo at which, as the temperature decreases, molecules become too close to permit either free flow or self diffusion. He wrote

$$1/\eta = B''(V-Vo)/Vo \qquad (2.20)$$

where B" is a constant whose value depends upon the capacity of molecules to absorb momentum because of their mass, flexibility or inertia of rotation. B" has been found to be linearly related to chain length in the case of the n-alkanes [54]. Equation 2.20 fits the data fairly well, whether the volume change is brought about by temperature change at atmospheric pressure or pressure variation at a constant temperature [55], provided the freezing point is not approached. Application of the Hildebrand equation to the viscosity data of benzene, mono-halogenated benzenes and n-alkanes such as n-heptane and n-decane [56] at temperature from 293.2 K down to their melting points, reveals that equation 2.20 is restricted to reduced

temperatures T/Tc, where Tc is the critical temperature, greater than 0.46 at which unhindered molecular rotation is possible.

A more recent approach [57] was based on the exact smooth hard-sphere results which are expressed in the form :

$$\ln \eta' = -0.762 + 1.355Vo/(V-Vo) \qquad (2.21)$$

where η' was given by $9.118X10^{7}\eta V^{2/3}/(MRT)^{1/2}$ for monatomic and simple polyatomic fluids, which can be treated as smooth hard spheres. This equation fitted the viscosity data very well. A similar form of equation was expected to hold for other polyatomic fluids, with different values for the parameters, to take into account the effects of translational rotational coupling and non-spherical molecular shape. The equation has the form:

$$\ln \eta' = A + BVo/(V-Vo) \qquad (2.22)$$

where A and B are now adjustable parameters. Dymond and Brawn [57] fitted the viscosity data for certain pseudo-spherical molecules and relatively rigid ring hydrocarbons to equation 2.22 . They found that A was temperature independent and had the same value (-1.0) for the liquids of closely similar molecular structure. This value of A also gave a good fit to the data for carbon tetrachloride and tetramethylsilane.

Dymond et al. [58-60] applied equation 2.22 to the viscosity coefficient of liquid n-alkanes and mixtures of n-alkanes as well as to mixtures of aromatic compounds with A equal to -1.0, while Vo and B

were derived from the data of the pure components as:

$$Vo = x_1 Vo_1 + x_2 Vo_2 \qquad (2.23)$$

$$B = x_1 B_1 + x_2 B_2 + x_1 x_2 a|B_1 - B_2| \qquad (2.24)$$

where a is a positive constant, obtained by fitting the data of the pure components to equation 2.24. It was observed [59] that calculated B values were significantly different from the observed B values for systems having enhanced intermolecular interactions.

Equation 2.22 is tested using the measured viscosity coefficient data of toluene, acetonitrile, three binary mixtures of toluene + n-hexane and three binary mixtures of toluene + acetonitrile in Chapter 6, section 6.4.2.

2.5 GRUNBERG AND NISSAN EQUATION.

The above methods have the disadvantage of requiring accurate information on liquid densities under the experimental conditions. The empirical Grunberg and Nissan equation [61] simply relates the viscosity coefficient of a mixture η_m to the viscosity coefficient of the pure components η_1 and η_2 according to:

of the pure components η_1 and η_2 according to:

$$\ln \eta_m = x_1 \ln \eta_1 + x_2 \ln \eta_2 + x_1 x_2 G \qquad (2.25)$$

where G is a characteristic constant for each mixture. Equation 2.25 is applicable to saturation as well as high pressure viscosity data. Grunberg and Nissan constant, G, may depend upon the pressure as well as on the composition for mixtures of n-alkanes or aromatic compounds

[60,62,63], whereas the temperature dependence in these cases is insignificant. The Grunberg and Nissan equation is applied to the viscosity data obtained in this work, in Chapter 6, section 6.4.3.

2.6 CORRELATION OF HIGH PRESSURE DIFFUSION AND VISCOSITY COEFFICIENTS FOR n-ALKANES.

Thermal conductivity coefficients and viscosity coefficients of n-alkanes over wide ranges of temperature and pressure can, separately, be successfully correlated by methods based on a consideration of the hard-sphere theory of transport properties [13,57,64]. Unfortunately, values which have been reported for the molecular parameter Vo, the volume of close packing, differ significantly. For example, for n-hexane at temperatures close to 323 K, Vo has been variously given as 71.77 [65], 73.06 [66] and $77.3X10^{-6}$ m^3/mol [67] from thermal conductivity data analysis and $72.0X10^{-6}$ m^3/mol [68] from viscosity measurements. A preliminary simultaneous fit of viscosity and thermal conductivity coefficients gave a Vo value of $83.12X10^{-6}$ m^3/mol [69] which is significantly higher than these values and also much higher than the figure of $76.32X10^{-6}$ m^3/mol given by Harris [70] from fitting self-diffusion data for n-hexane at 333 K. For a satisfactory correlation of transport properties of n-alkanes using methods based on hard-sphere models, it is essential to establish a consistent set of Vo values. This is particularly important when this approch is to be used for calculation of transport coefficients at other temperatures, or for other members of the series where data are at present limited. It is also preferable to have an agreed set of Vo parameters before embarking on the correlation of transport properties of liquid n-alkane mixtures.

Thermal conductivity coefficients and viscosity coefficients of n-alkanes have been correlated simultaneously [69] by using a single set of Vo values, derived from the viscosity coefficient data. However, since an increase in pressure has only a relatively small effect on thermal conductivity of the n-alkanes, and also because the effects of internal energy have not yet been exactly quantified, we considered it prefereble to correlate the high pressure diffusion and viscosity coefficients of n-alkanes, initially, and to consider thermal conductivity at a later stage.

2.6.1 THE CORRELATION METHOD.

Calculation of viscosity or self-diffusion coefficients for any compound on the basis of exact smooth hard-sphere theory at a given temperature and pressure requires just a value for the parameter Vo, the volume of close-packing of spheres, given by $N\sigma^3/2^{1/2}$.
This is conveniently carried out by an established curve-fitting procedure [57,71] based on reduced quantities D^* and η^* defined by the following expressions:

$$D^* = (nD_{SHS}/n_oD_o)(V/Vo)^{2/3} \qquad (2.26)$$

$$\eta^* = (\eta_{SHS}/\eta_o)(V/Vo)^{2/3} \qquad (2.27)$$

where the smooth hard-sphere coefficients are given by the product of the Enskog value and the corrections to Enskog theory, $D_{SHS}=D_E(D/D_E)_{MD}$ and $\eta_{SHS}=\eta_E(n/n_E)_{MD}$

Values for D^* and η^* are calculated from theory for different

reduced volumes, V/Vo. Values are also calculated from experiment since on substitution of the hard-sphere expressions:

$$D^* = 5.030X10^8(M/RT)^{1/2}(D/V^{1/3}) \qquad (2.28)$$

$$\eta^* = 6.035X10^8(\eta V^{2/3})/(MRT)^{1/2} \qquad (2.29)$$

To determine Vo for a given compound from self-diffusion data at a given temperature, a plot of log D^* from experiment versus log V , where V is the molar volume, is superimposed on the curve of log D^* versus log (V/Vo) by translation along the x-axis. Values for Vo can similarly be derived by curve-fitting using viscosity coefficient data. In figs. 2.1 and 2.2, the variation of log D^* and log η^* with log (V/Vo) for the hard-sphere system are shown respectively. D^* and η^* are defined by Eq. 2.26 and 2.27 respectively. Solid lines are given by smooth hard-sphere theory with corrections to Enskog theory given by Easteal et al.[72] for the diffusion coefficient and Dymond [74] in the case of the viscosity coefficient. Circles represent diffusion [71] and viscosity [73] data for methane at 140 K while vertical lines identify the range of D^* and η^* for n-hexane. Crosses represent the predicted hard-sphere values using the earlier corrections (Alder et al. [3]) to the Enskog theory, and it is important to note the significant difference in density dependence of these predictions. It is essential that all curv-fitting should be carried out with respect to the same reference curves and we therefore recommend that the solid lines given here, calculated as described above, be taken as the exact hard-sphere reference curves.

Methane at 140 K was taken as the reference smooth hard-sphere system because accurate diffusion [71] and viscosity coefficient [73] measurements have been made at this temperature, and this molecule can be expected to behave as a smooth hard-sphere with respect to transport properties at high densities. For this molecule the mass is effectively concentrated at the centre. Indeed, it is found [74] that these data can be interpreted on the basis of the smooth hard-sphere model, with the same value for Vo of 20.825×10^{-6} m^3/mol.
Methane data at other temperatures are similarly fitted to the hard-sphere curves, and the derived Vo values are found [74] to decrease smoothly with increase in temperature as expected since real molecules experience a soft repulsive interaction.

At high densities the hard-sphere system becomes metastable, but for real fluids still higher values for η^* and D^* are possible, as shown for n-hexane in figs. 2.1 and 2.2. Such molecules are generally non-spherical and also exhibit roughness, that is there is the possibility of transfer of rotational as well as translational momentum on collision. For pseudo-spherical molecules, correlation of these transport properties can be achieved on the basis of the rough hard-sphere model, by superimposing plots of log D^* versus log V, and similarly of log η^* versus log V, on respective curves given by experimental results for a selected reference temperature. This is illustrated in fig. 2.3 for the n-hexane diffusion coefficient measurements of Harris [70] which cover the temperature ranges 223 to 333 K. The 298 K isotherm was taken as reference and the required shift along the x-axis in order to superimpose the other curves gives the ratio of Vo values for the different temperatures. These vary smoothly with temperature. It should be noted that, in terms of the

model, there is no evidence of a temperature dependence for A. Similar results have been obtained from viscosity coefficient measurements for individual alkanes, and this is now an established method [60,62] for testing the consistancy of experimental viscosity measurements.

In order to determine absolute values for Vo for different n-alkanes, the correlated curves for a given compound are compared with the appropriate smooth hard-sphere curve. To allow for the fact that higher n-alkanes are non-spherical the above ideas can be extended to give:

$$D = R_D D_{SHS} \quad \text{and} \quad \eta = R_\eta \eta_{SHS} \qquad (2.30)$$

where the factors R_D and R_η account for non-spherical shape and translational- rotational coupling. Values for these parameters for a given compound are derived by simultaneously curve-fitting the correlated log D^* versus log V with the solid line in fig. 2.1, and the correlated log η^* versus log V curve with the solid line in fig. 2.2. Since horizontal and vertical adjustments are possible, there is a range of values for Vo at the reference temperature, and also for R_D and R_η.

2.6.2 APPLICATION.

The first conclusion which results from applying the above procedure to n-hexane viscosity (298 to 373 K and up to 500 MPa) and self-diffusion coefficients (223 to 333 K and up to 400 MPa) is that it is not possible to obtain a simultaneous fit of both properties with the same Vo for the reference temperature (298 K) with R_D and R_η set

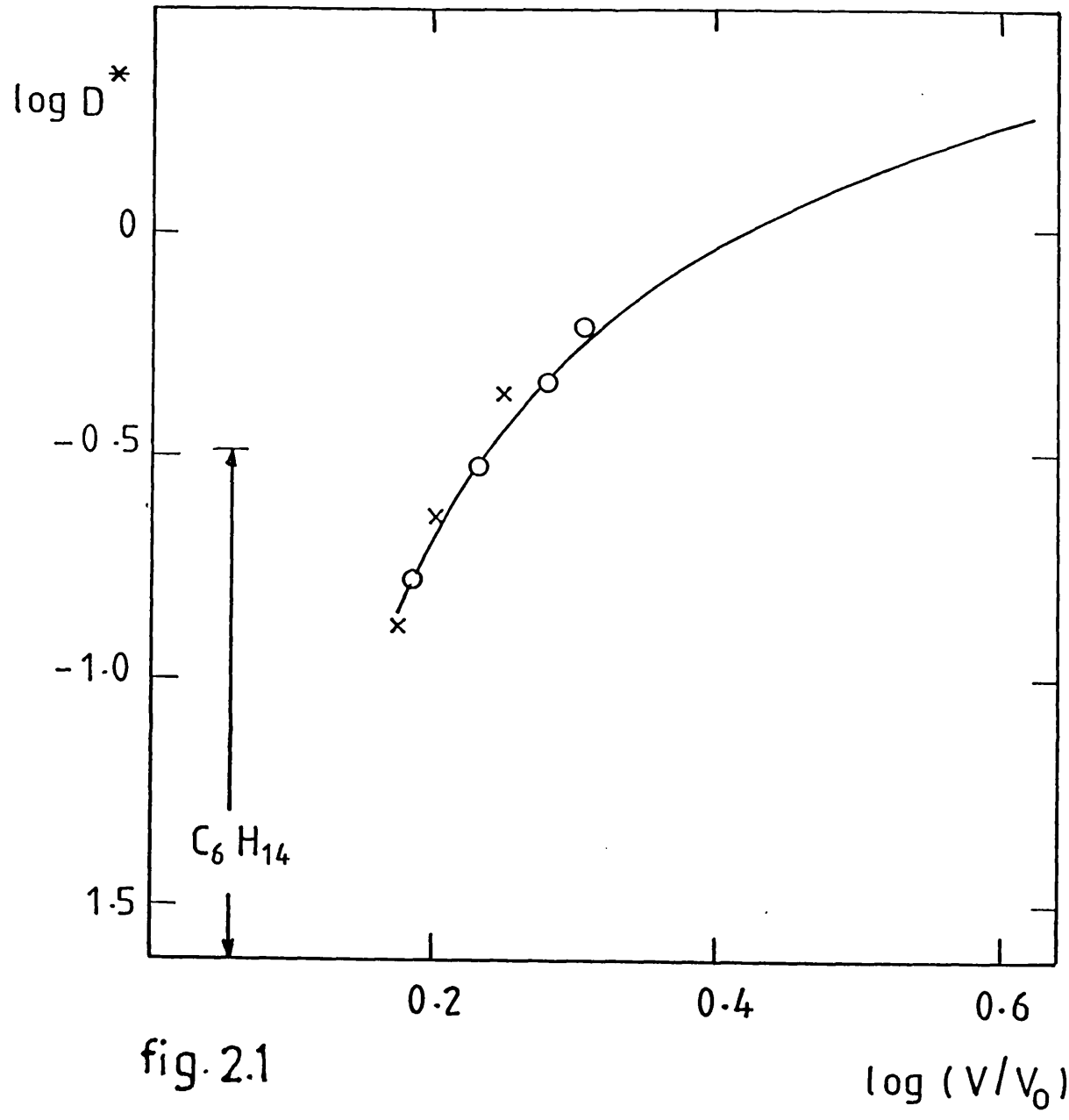

fig. 2.1

Variation of log D^* with log(V/Vo) for Hard-Sphere System. Solid lines are given by Smooth Hard-Sphere Theory with Corrections to Enskog Theory given by Easteal et al. [72]; x Corrections given by Alder et al. [3]. o Data for Methane at 140 K [71]. Vertical line identify the range of D^* for n-hexane.

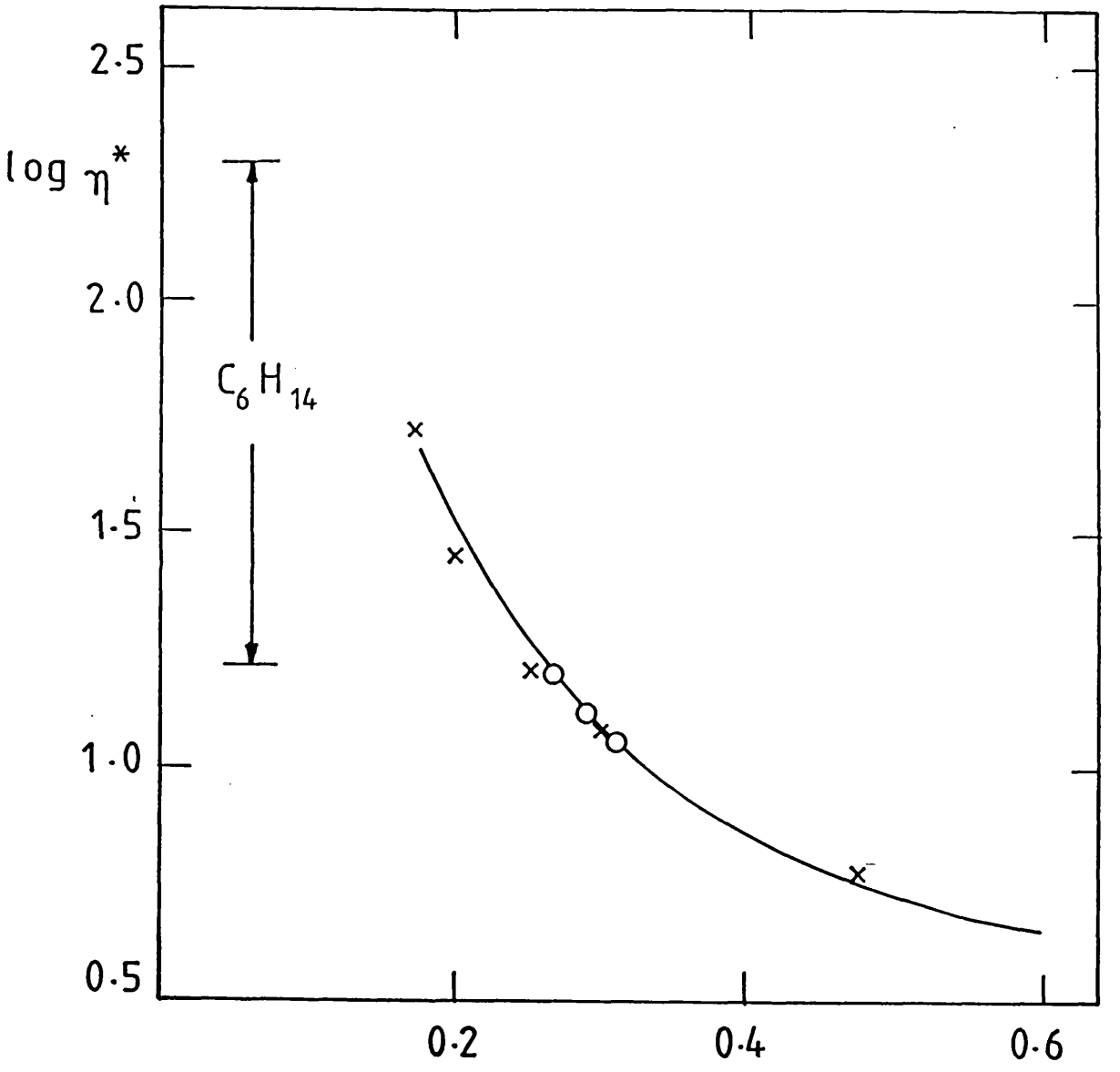

fig. 2.2

Variation of log η* with log(V/Vo) for Hard-Sphere System. Solid lines are given by Smooth Hard-Sphere Theory with Corrections to Enskog Theory given by Dymond [74]; x Corrections given by Alder et al. [3]. Data for Methane at 140 K [73]. Vertical line identify the range of η^* for n-hexane

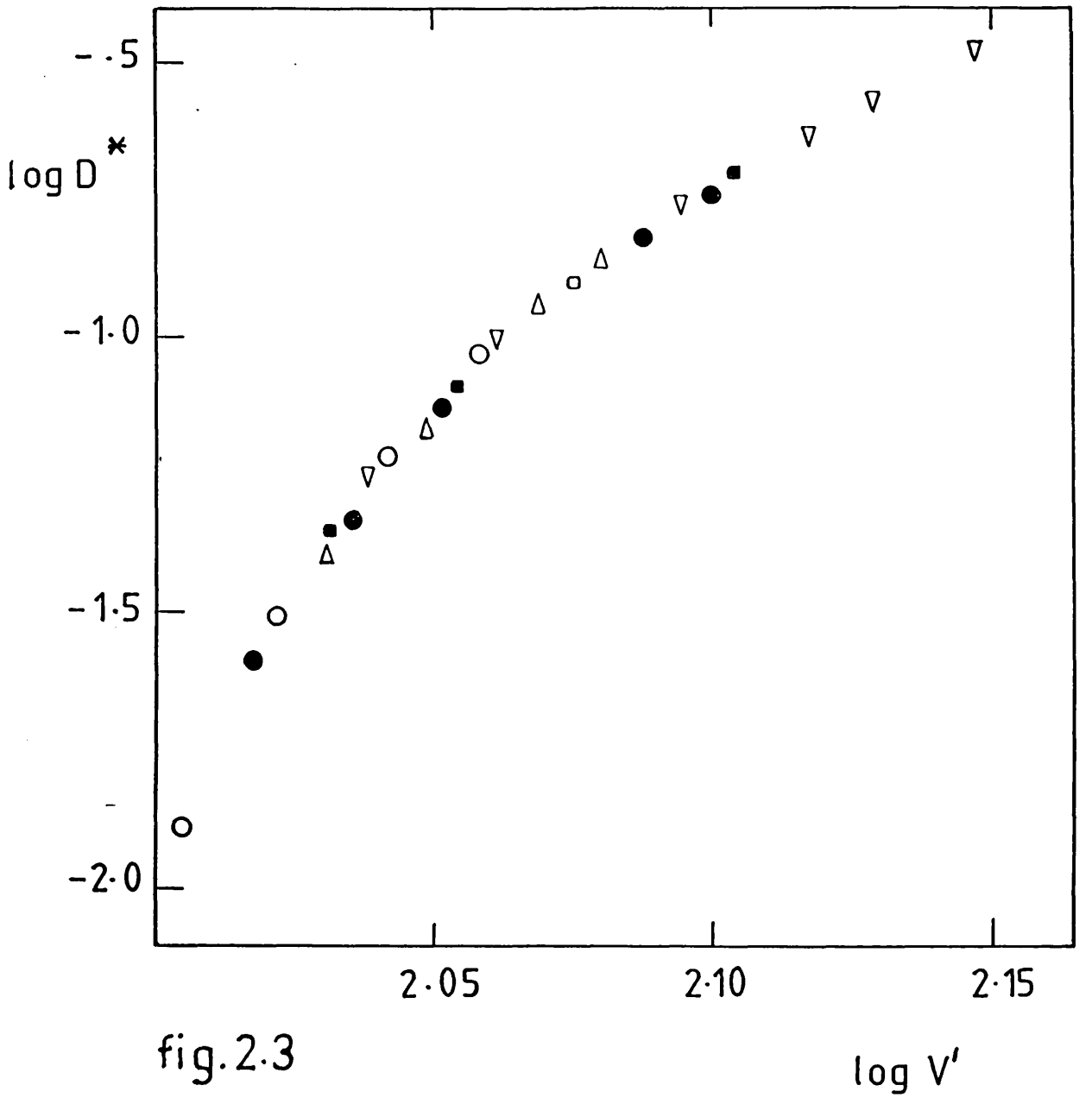

fig.2.3

Correlation of Self-Diffusion Coefficient data [70] for n-hexane, based on the 298 K isotherm.
V'=V[Vo(298)/Vo(T)], where V is molar volume.
o 223 K; △ 248 K; ● 273 K; ■ 298 K; ▽ 333 K.

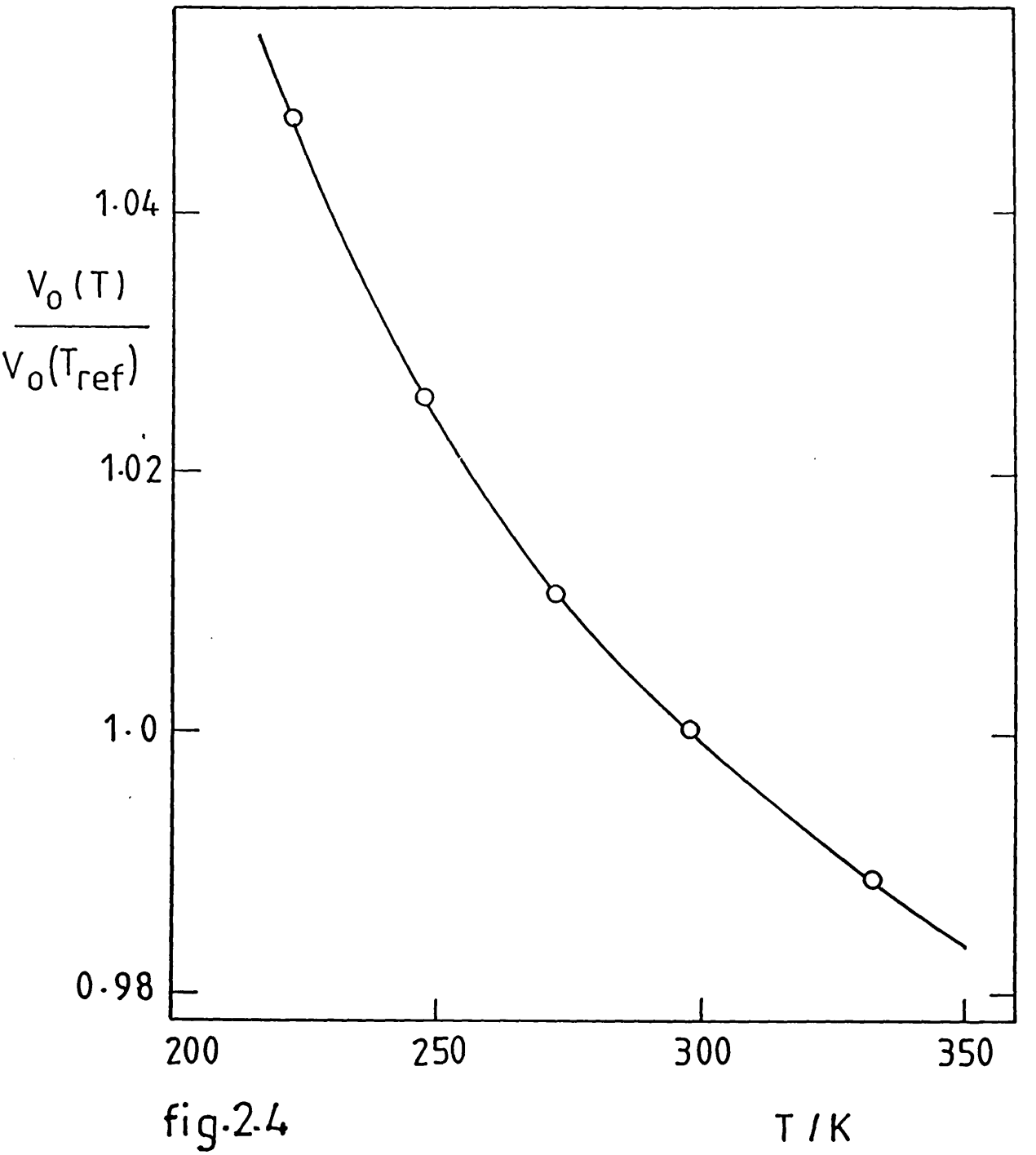

fig.2.4

Relative Vo values for n-hexane. Reference temperature is 298 K.

equal to unity.

To determine the possible range of values for Vo, conditions similar to those which pertain to the translational-rotational coupling factors have been applied, namely that $R_D \leq 1.$ and $R_\eta \geq 1.$ Matching the correlated diffusion curves for n-hexane with fig. 2.1 to give agreement within 3% leads to the conclusion that Vo at 298 K, lies between 76.9 and 80.4X10^{-6} m^3/mol with R_D between 0.77 and 1.0. From the corresponding viscosity coefficient data fit, Vo must be between 79.4 and 81.8X10^{-6} m^3/mol and R_η has the limits of 1.0 and 1.33, to fit the data within estimated experimental uncertainity. For a simultaneous fit of these two properties Vo for n-hexane at 298 K must lie between 79.4 and 80.4X10^{-6} m^3/mol with $1.33 > R_\eta > 1.16$ and $0.92 < R_D < 1.0$. Similarly, limits can be found for R_D, R_η and Vo at the reference temperature for other n-alkanes for which self-diffusion and viscosity coefficient values are available. It is found for the accurate n-hexane self-diffusion coefficient data [70] and the less accurate diffusion coefficients for other n-alkanes [75,76] that, in terms of the model, effects of the non-spherical molecular shape and roughness are very small and indeed, R_D may be set equal to unity. The corresponding Vo values lie in the middle of the range determined from a fit of viscosity data alone. Accordingly, R_D has been taken as 1.0, and the optimum Vo and R_η values that give the best simultaneous fit to the hard-sphere viscosity and diffusion curve determined by curve fitting.

Values which have been obtained in this way for Vo are given in Table 2.1. As expected, the Vo values at a given temperature vary smoothly

TABLE 2.1

VALUES FOR THE CHARACTERISTIC VOLUME Vo (10^{-6} m^3/mol)

T/K	90	95	100	110	120	130	140	150
CH_4	-	-	22.46	-	21.57	-	20.82	-
C_2H_6	-	-	34.59	34.10	33.70	33.32	-	32.69
C_3H_8	50.95	50.40	49.82	48.95	-	-	47.01	-
C_4H_{10}	-	-	-	-	-	-	61.25	60.50

T/K	160	170	180	200	250	290	300	320
CH_4	-	19.93	19.69	19.26	18.51	-	18.00	-
C_2H_6	-	-	-	31.52	30.75	30.27	-	29.94
C_3H_8	-	-	-	-	-	-	42.67	-
C_4H_{10}	59.84	-	58.86	58.17	56.59	-	55.19	-

T/K	223.2	248.2	273.2	298.2	323.2	348.3	373.2
C_6H_{14}	84.34	82.64	81.32	80.40	79.64	78.91	78.23
C_8H_{18}	-	111.7	109.0	107.1	105.5	104.4	-
$C_{12}H_{26}$	-	-	-	165.8	163.3	160.9	158.6
$C_{16}H_{34}$	-	-	-	224.4	221.1	217.6	214.2

with change in n-alkane carbon number, as shown in fig. 2.5. This makes possible an accurate estimation of Vo for the other members of this series. The factor R_{r_η} also varies smoothly with increase in carbon chain length for the n-alkanes, as shown in fig. 2.6, going from 1 for methane to 1.2 for n-octane and then rising more rapidly to just above 1.6 for n-hexadecane. Accurate interpolation is possible for other n-alkanes from the fitting equation:

$$R_{r_\eta} = 0.9855 + 0.01687C + 0.001403\ C^2 \qquad (2.31)$$

where C is the carbon number. Once Vo and R_{r_η} have been determined with R_D equal to 1, universal curves can be drawn for log D^* versus log V_r, and for log η^* versus log V_r, where V_r is the molar volume under given conditions multiplied by 20.825, the Vo value for methane at the reference temperature of 140 K, divided by Vo for the compound at the experimental temperature. log η^* and log D^* have been represented by polynomials in $(1/V_r)$:

$$\log \eta^* = 0.877 - 78.97/V_r + 7130.4/V_r^2 - 219020/V_r^3 + 3075840/V_r^4 \qquad (2.32)$$

$$\log D^* = 3.285 - 661.04/V_r + 57700/V_r^2 - 2575677/V_r^3 + 56074080/V_r^4 - 490561075/V_r^5 \qquad (2.33)$$

Although this is not the best form of representation, it is considered suitable for determining the degree to which the experimental data can be fitted. For methane, there is a very satisfactory fit of both self-diffusion coefficient and viscosity coefficient measurements, as

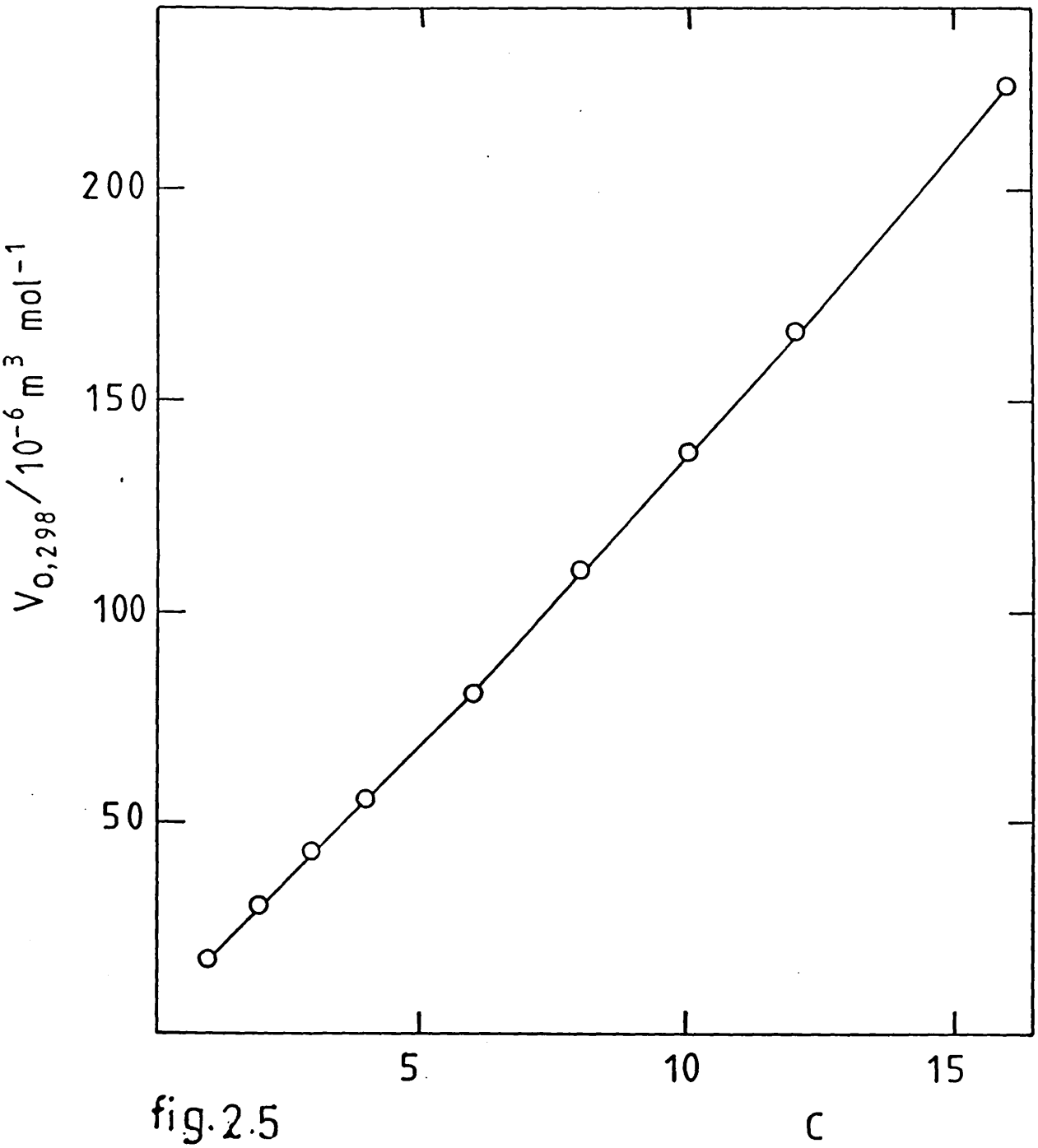

fig.2.5

Variation of Vo with carbon number of n-alkanes.

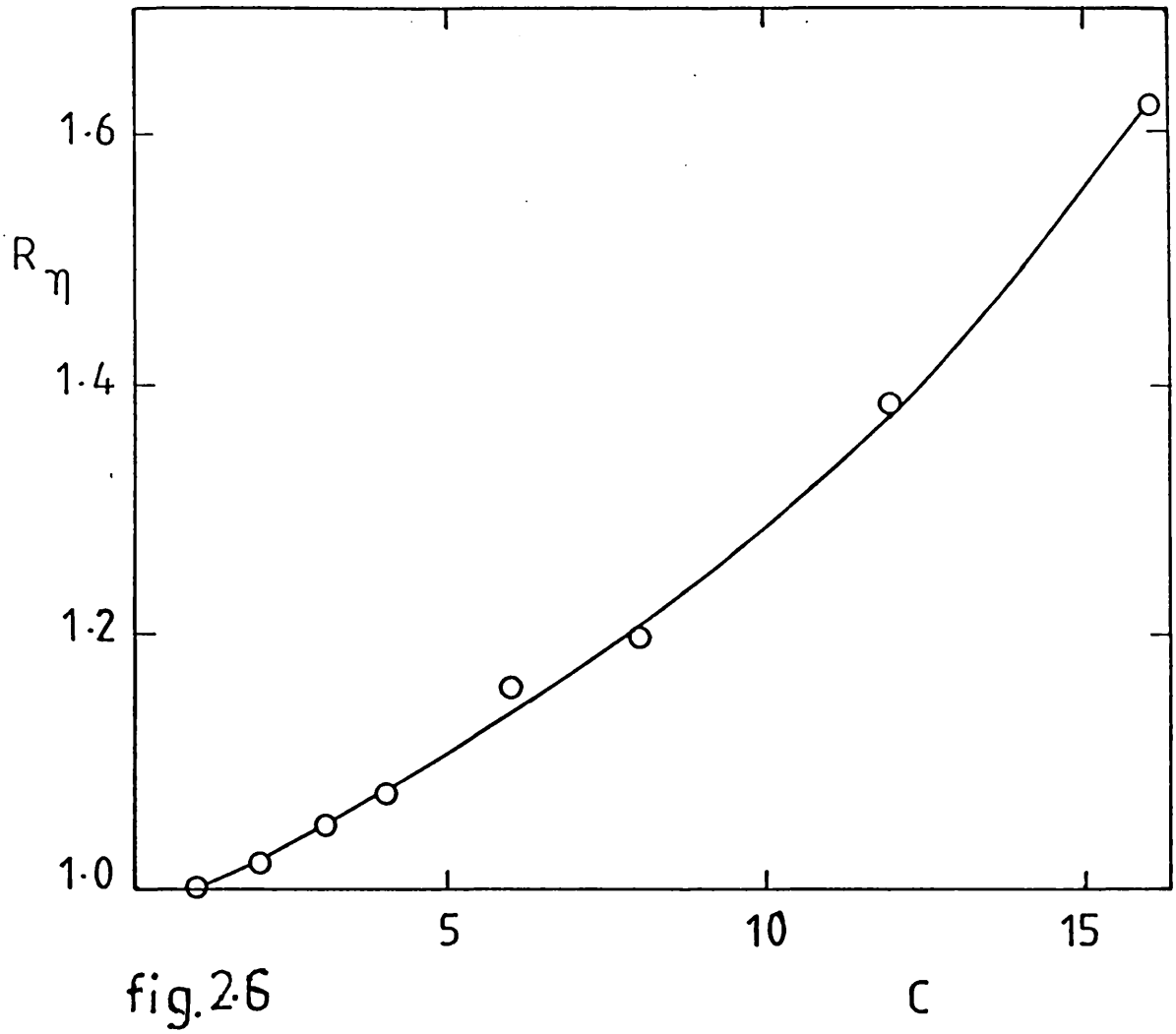

fig. 2·6

Variation of $R\eta$ with n-alkane carbon number.

shown in fig. 2.7, with agreement with experimental values generally well within 3%. The Vo values were taken from Table 2.1.

In the case of n-hexane, the other n-alkane for which extensive accurate viscosity and self-diffusion measurements have been made, the experimental values are compared with values calculated from Eqs. 2.32 and 2.33, with Vo values from Table 2.1, in figs. 2.8 and 2.9. For diffusion there is excellent agreement with results of Harris [70] and also reasonable agreement with those of Ludemann [75,76], for which the reliability is quoted as 10%, at temperatures of 240 K and above. However. at 214 K the experimental values are on average 15% higher than calculated. Since this isotherm is close to the 223 K isotherm for which Harris reported measurements, it appears that there is some inconsistency in these data.

A summary of the data fit for all the n-alkanes studied is presented in Table 2.2 for diffusion and Table 2.3 for viscosity. Some of the diffusion coefficient measurements of Ludemann show deviations of more than 10%, but part of the discrepancy may be due to the fact that the corresponding experimental densities are not available. In this case, densities were calculated from the modified Tait equation by the method of Dymond and Malhotra [77], with an estimated uncertainty of 0.2%. This method is restricted to the temperatures below the critical temperature, and higher temperature diffusion coefficient data of Ludemann were not considered.

For viscosity, the agreement between calculated and experimental coefficients is generally extremely satisfactory, with only 2 points out of 481 deviating by more than 10% from the calculated values. For

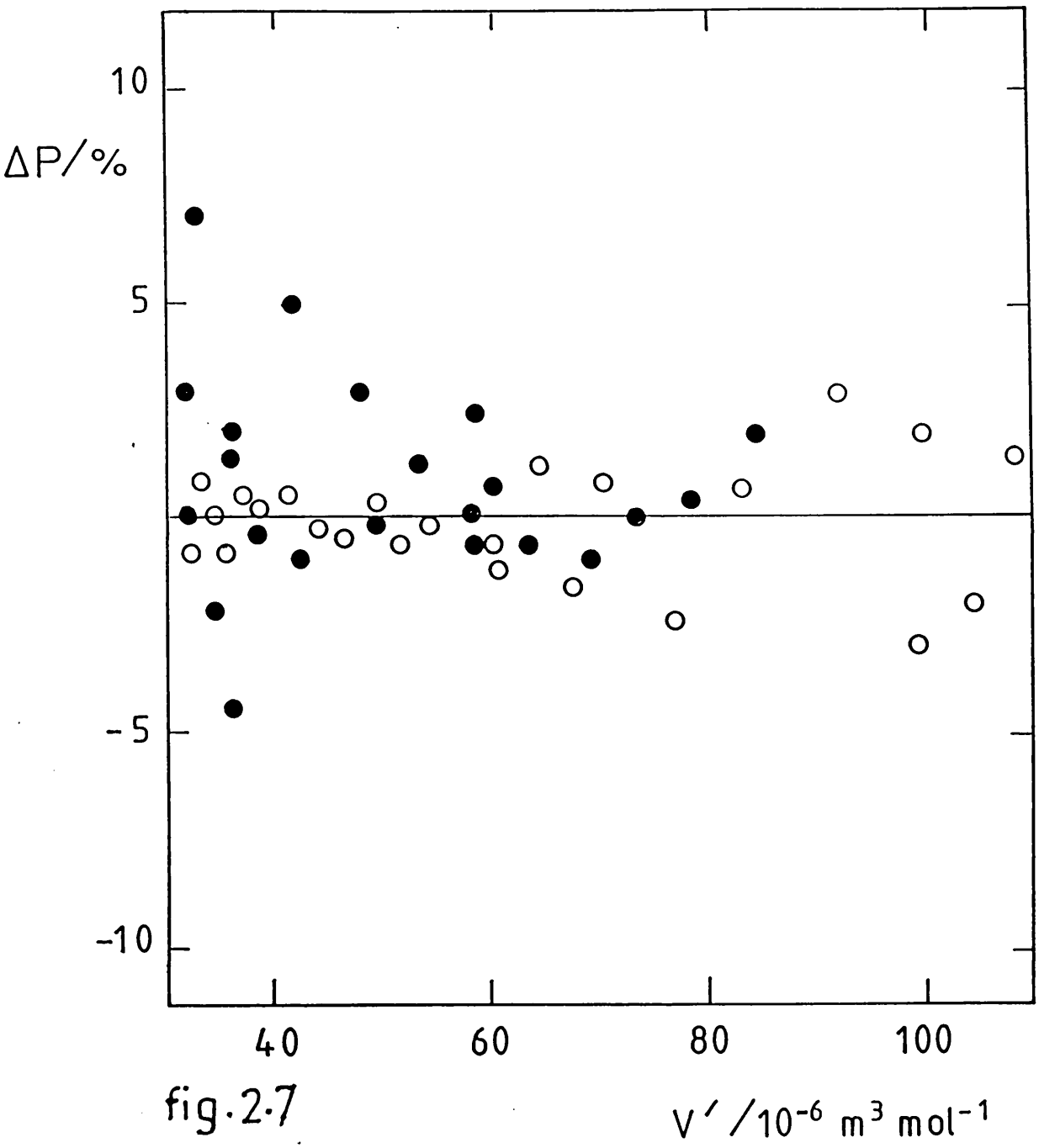

fig. 2.7

Comparison of experimental self-diffusion and viscosity coefficients for methane with values calculated on the basis of Eqs. 2.26, 2.33 and 2.27, 2.32 with Vo values from Table 2.1. ● self-diffusion data [71,78]; o viscosity coefficient data [73].

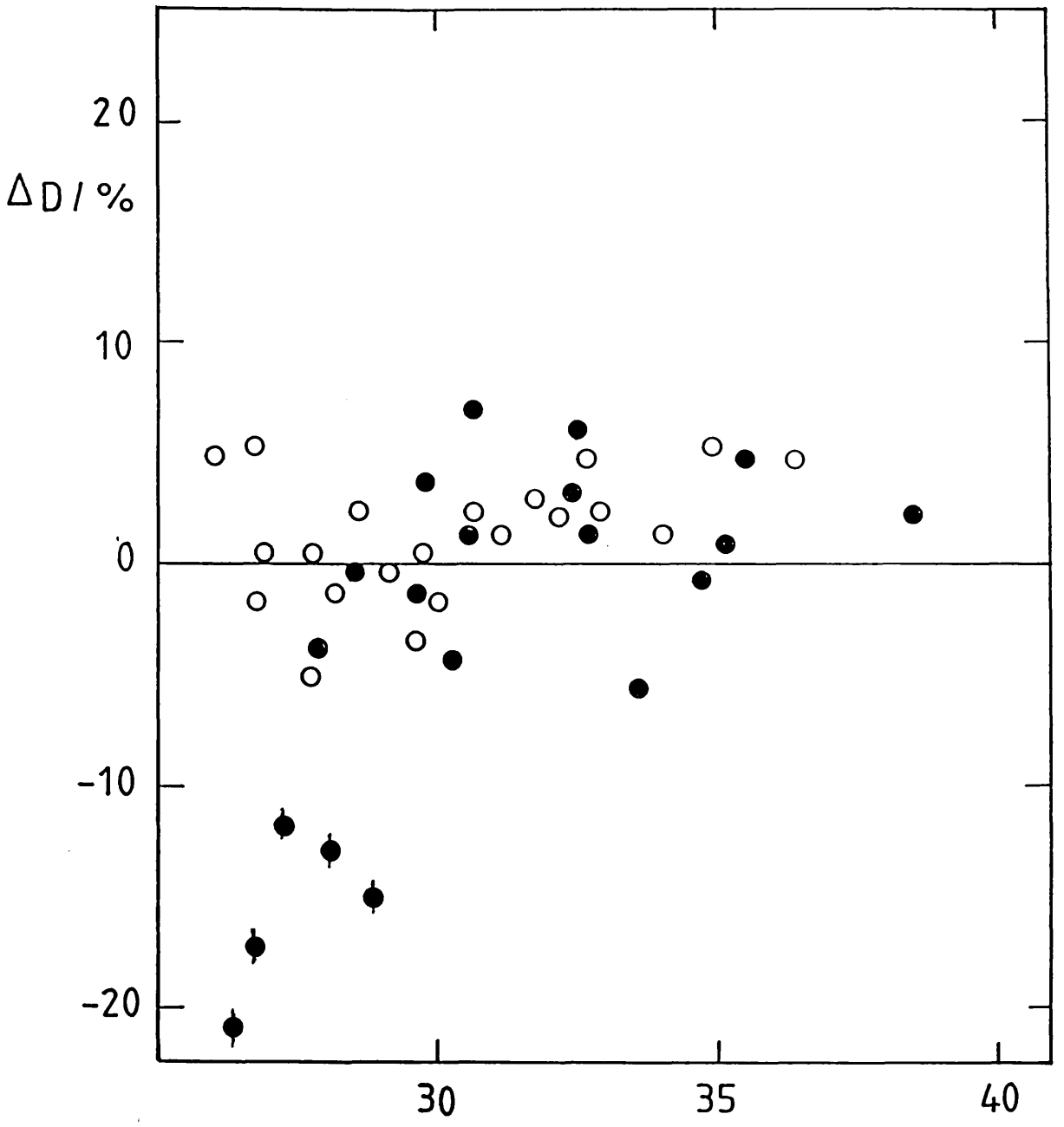

fig. 2.8

Comparison of experimental self-diffusion coefficient o [70] and • [75,76] for n-hexane with calculated on the basis of Eqs. 2.26 and 2.33 with Vo values given in Table 2.1.

214K

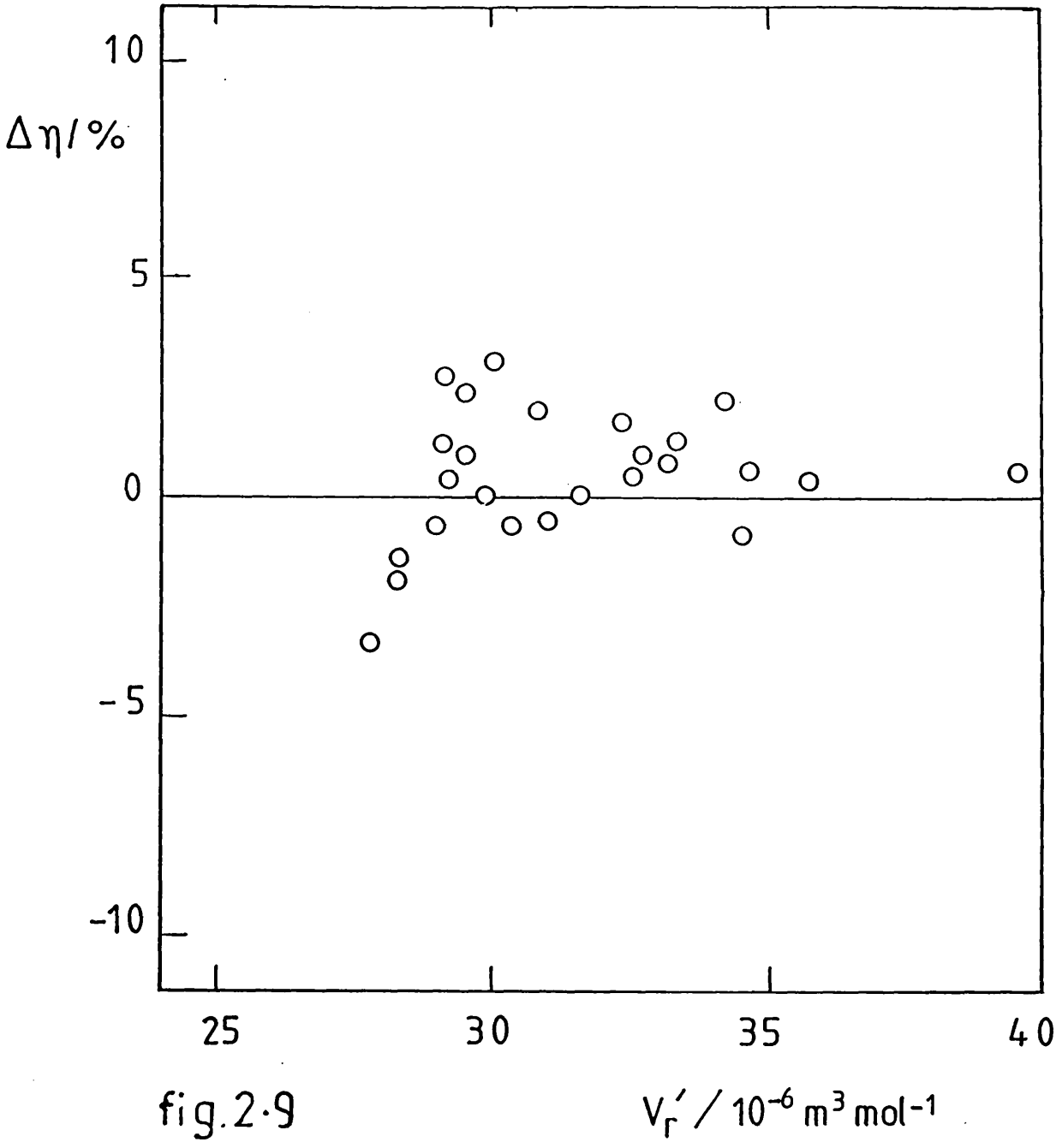

fig. 2·9

Comparison of experimental viscosity coefficient for n-hexane [62] with values calculated from Eqs. 2.27, 2.30 and 2.32, with R_η from fig 2.6 and Vo given in Table 2.1

TABLE 2.2

COMPARISON OF SELF-DIFFUSION COEFFICIENTS CALCULATED BY THE CORRELATION METHOD WITH EXPERIMENTAL VALUES.

	Total	No. of points Deviation from expt. 5-10%	>10%	Reference
CH_4	54	6	-	[71,78]
C_4H_{10}	19	6	8	[75,76]
C_6H_{14}	54	4	-	[70]
C_6H_{14}	21	3	6	[75,76]
$C_{10}H_{22}$	25	6	4	[75,76]

TABLE 2.3

COMPARISON OF VISCOSITY COEFFICIENTS CALCULATED BY THE CORRELATION METHOD WITH EXPERIMENTAL VALUES.

	Total	No. of Points Deviation from expt 5-10%	>10%	Max.Dev. (%)	Ref.
CH_4	107	-	-	3.1	[73]
C_2H_6	98	-	-	3.3	[79]
C_3H_8	60	5	-	6.5	[80]
C_4H_{10}	79	-	-	3.4	[81]
C_6H_{14}	37	-	-	3.5	[62]
C_8H_{18}	41	11	1	11.2	[58]
$C_{12}H_{26}$	31	7	1	16.6	[58]
$C_{16}H_{34}$	28	-	-	4.7	[62]

n-alkanes from methane to hexane, the agreement is better than 3% in practically all cases. For higher n-alkanes, there are larger discrepancies which may be due in part to the greater uncertainty in the measured density.

CHAPTER 3

MEASUREMENTS OF DIFFUSION COEFFICIENT

3.1 INTRODUCTION.

In 1911, Griffiths [82] found experimentally that if a patch of colouring matter is injected into a water stream flowing slowly through an impermeable cylindrical tube, the colouring matter spreads out in a symmetrical manner from a point which moves with the mean velocity of water in the tube. Later on, Taylor [83-85] found that the spreading of the colour band is due to the combined action of molecular diffusion and the variation of the velocity over the cross section of the tube and under certain conditions it is possible to calculate the diffusion coefficient from the observed distribution of concentration (Taylor Dispersion Technique).

The diffusive mixing of two solutions of the same components but with different composition is expressed in terms of an interdiffusion coefficient or mutual diffusion coefficient, designated as D_{12} for binary liquid mixtures. Self diffusion coefficient is the term used to describe the motion of molecules in an environment which consists of one chemical species only, while the term intra diffusion coefficient or tracer diffusion coefficient involves the motion of a labelled species in a homogeneous medium which may, or may not, be multicomponent, and may, or may not, contain that unlabelled species.

The SI unit for diffusion coefficients is meter^2/second (m^2/s) and for liquid diffusivity, the value is of the order of 10^{-9} m^2/s. A number of techniques are available to measure the liquid mutual diffusivity such as the diaphragm cell method [86], the stabilised inverse density gradient method [87,88]; Gouy diffusiometer method

[89]; the light absorption technique [90] and Taylor dispersion or chromatographic peak broadening technique. The polarographic method [91,92] and diaphragm cell method can be used for tracer diffusivity measurements and the NMR spin echo technique [93] used for self diffusion measurements. The chromatographic peak broadening technique was used to measure the mutual diffusion coefficients reported in this work because of its demonstrated accuracy at atmospheric pressure {Alizadeh and Wakeham (100)} and increased speed of operation over the other available methods.

The measurements were in two parts. Firstly, the mutual diffusion coefficients, D_{12} ,have been measured for benzene and eight fluorinated benzenes, at trace concentration, in n-hexane over the temperature range from 213.2 to 333.2 K at atmospheric pressure. Secondly, the D_{12} measurements were extended to higher pressures for toluene plus n-hexane binary mixtures over the whole composition range at temperatures from 299 to 348 K and pressure up to 25 MPa, with a few measurements for toluene plus acetonitrile mixtures over the temperature range 273 to 348 K and at 0, 0.2, 0.4, 0.6, 0.8 and 1.0 mole fraction of toluene. The values have an estimated uncertainty of ± 2.5%. The results are presented and discussed in section 3.5.5.

D_{12} values have been calculated theoretically on the basis of the Rough Hard Sphere theory, for the fluorobenzenes in n-hexane. It is found that experimental results for D_{12} can be reproduced to within ±10% with the translational- rotational coupling factor A_{12} equal to 0.72. The experimental results for toluene in n-hexane, acetonitrile in toluene and toluene in acetonitrile can be reproduced to within

±3% with A_{12} equal to 0.72 for toluene in n-hexane and acetonitrile in toluene and A_{12} equal to 0.69 for toluene in acetonitrile.

3.2 THEORY OF TAYLOR DISPERSION METHOD.

The ideal model for an apparatus for the measurement of diffusion coefficients by the Taylor dispersion method consists of an infinitely long straight and impermeable tube of uniform circular cross-section, through which flows the incompressible liquid in laminar regime. A mixture of the same components but with different composition is injected into the tube as a delta-function pulse that is dispersed by combined action of molecular diffusion and parabolic velocity profile. Provided certain conditions are satisfied the concentration profile at the end of the diffusion tube results in a Gaussian curve. The theory of the method has been discussed extensively in the literature [94-98]. The variance of the Gaussian curve is related to the diffusion coefficient of the liquid by the equation (3.1).

$$\sigma^2 = 2\, D_{12}\, t^3/L^2 + Ro^2.t/(24.D_{12}) \qquad (3.1)$$

where Ro is the inside radius of the diffusion tube of length L, t is the retention time of the solute in the tube and σ^2 is the variance of the eluted Gaussian peak. Equation (3.1) is valid under certain conditions (Tyrrell and Harris 1984) [99] such as

$$\text{(a)} \qquad Re = 2\, Uo\, Ro\, \rho/\eta < 2000 \qquad (3.2)$$

where Uo is the mean velosity and ρ and η are the density and

viscosity of the fluid. Re is a dimensionless group called the Reynolds number. This condition restricts the flow to be in the laminar regime.

(b) $$t >> Ro^2/(3.8)^2 D_{12} \qquad (3.3)$$

that is, retention time should be long enough for the radial variation of the concentration to die down to 1/e of its initial value and further that at time t=0 the solute distribution is given by a delta-function.

Diffusion coefficients in gases are much larger than those found in liquids and therefore the first term of right-hand side of equation 3.1 is dominant. However in liquids diffusivity is smaller by a factor of about 10^5, therefore it is possible under certain experimental conditions to reduce equation (3.1) to the working equation

$$\sigma^2 = Ro^2.t/(24.D_{12}) \qquad (3.4)$$

The diffusion tube is normally 10-20 metres in length and is wound on a former either in a U-shape [97] or in the form of a helix for isothermal measurements. This give rise to secondary flow in the curved tube and the observed diffusivity is higher than the true value. The effect of this secondary flow can be minimised to less then +0.005% if the following condition is fulfilled [100,101].

$$t > \{Ro^3.L^2\rho/(5.\eta.D_{12}\,Rc)\}^{1/2}. \qquad (3.5)$$

where Rc is the radius of curvature of the helix. The secondary flow effect also depends upon the ratio of the helix to tube radius (W) and provided 100< W <500 the effects are less than ±0.05% if the following condition is fullfilled [100].

$$De^2.Sc \leq 20 \qquad (3.6)$$

where De is the Dean number and Sc is Schmidt number defined as

$$De = Re/\sqrt{W} \quad \text{and} \quad Sc = \eta/(\rho.D_{12}) \qquad (3.7)$$

Secondary flow effects on dispersion of the solute have been considered in detail by Nunge et al. [102], Golay [103], and Tijssen [104] and a transition flow rate F_{TR} was defined as the flow rate in a curved tube at which secondary flow becomes significant compared to diffusion as the process which determines dispersion [105,106]. For a sample of given diffusion coefficient, in a liquid of density ρ and viscosity η

$$F_{TR} = (518\ Ro.Rc.D_{12}\eta/\rho)^{1/2} \qquad (3.8)$$

Provided W>>1, the effect of the curved path on the dispersion is dependent only upon the group $[De.Sc^{1/2}]^4$. Using the solution of Nunge [102] and Golay [103], Atwood and Goldstien [106] estimated the diffusion coefficient Dm that would have been obtained if the tube was straight. The observed diffusion coefficient Dx in a curved tube can be corrected by the expression

$$Dm = Dx\ \{1-a(F/F_{TR})^4\} \qquad (3.9)$$

where F is the experimental flow rate and a was found to be equal to

0.1034 . When $F/F_{TR} < 0.6$, the secondary flow effect is negligible and Dx equals Dm.

The Taylor dispersion technique is a dynamic method for measurements of liquid diffusivity and because of its simplicity and rapidity as well as rapid development of the chromatographic instrumentation this method has been used widely for diffusion studies of gases [107-110], liquids [42,111-117] and compressed fluids systems [118-120].

3.3 LIQUIDS USED

The liquids used in this work, their grades and stated purities are shown in Table 3.1. The liquids were used as received without further purification. However the solvents (n-hexane, toluene and acetonitrile) were degassed by distillation prior to use.

Refractive index was measured using a high accuracy 60/ED Abbe' refractometer (Bellingham and Stanley Ltd, England), illuminated by a sodium lamp at 293.2 K by water circulation. Densities of n-hexane, toluene and acetonitrile were measured using a vibrating tube densimeter as described in Chapter 4, section 4.3. As shown in Table 4.3, the agreement with the literature values is generally very satisfactory.

3.4 MEASUREMENT OF DIFFUSION COEFFICIENTS.

3.4.1 DESCRIPTION OF APPARATUS.

The apparatus for the measurement of diffusion coefficients by the Taylor dispersion technique consists of a constant temperature bath,

Table 3.1

LIQUIDS USED

Compound	Purity %	Refractive index Measured	Refractive index Literature	Grade and Manufacturer
n-Hexane	99.9	1.3748	1.3749	HPLC (a)
Toluene	99.9	1.4961	1.4969	HPLC (a)
Acetonitrile	99.9	1.3443	1.3440	HPLC (a)
Benzene	99.9	1.5010	1.5011	(b)
o-Difluoro-benzene	98.0	1.4431	1.4427	(a)
p-Difluoro-benzene	98.0	1.4414	1.4415	(a)
1,2,4 Trifluoro benzene	pure	1.4229	1.4140	(c)
1,2,3,5 Tetra-fluorobenzene	99 +	1.4040	1.4035	(a)
1,2,4,5 Tetra-fluorobenzene	98.0	1.4079	1.4067	(a)
Pentafluoro-benzene	98.0	1.3916	1.3905	(a)
Hexafluoro-benzene	99.0	1.3777	1.3769	(a)
Octafluoro-toluene	98.0	1.3671	1.3670	(a)

Literature values from Catalogue Handbook of Fine Chemicals, Aldrich (1986-1987)

(a) Aldrich Chemical Co. Ltd. Gillingham, Dorset, England.

(b) BDH Chemical Ltd., Poole, England.

(c) Koch-Light Laboratories Ltd. Colnbrook, England.

a metering pump, a sample injector, a long uniform, circular capillary tube, a detector and a recorder. The experimental set up is shown in fig. 3.1. The pump used was an Altex Model 110 A metering pump which delivers liquid at flow rates from 0.1 ml per minute upwards. The diffusion tubes used had lengths of approximately 20 metres (loop A) and 30 metres (loop B) of 316 stainless steel capillary with nominal 1/16 inch O.D., obtained from Phase Separation Ltd. Clwyd, U.K., wound in helical form for the ease of temperature control. The characteristics of the diffusion loops are given in Table 3.2. Sample injection was by a six port loading injector (Rheodyne Model 7125) with a 10 μl loop. Two detectors were employed in this work, an Altex Model 153 UV detector with a 254 nm filter for aromatic compounds and a LDC Refracto-Monitor Model 1107 for non aromatic compounds. The recorder was a variable speed Tekman Electronic recorder Model TE 200. A Budenberg Gauge Co Ltd. pressure gauge was employed for high pressure diffusion measurements.

3.4.2 TEMPERATURE CONTROL AND MEASUREMENT.

For the measurements of diffusion coefficients, the temperature was kept constant to within ±0.02 °C by immersion of the diffusion tube in a bridge controlled constant temperature bath (Townson and Mercer Ltd. Model E.270 series III) containing water. The temperature was controlled with a Clandon proportional temperature controller Model YSI 72. Temperatures between 298.2 and 348.2 K were measured using a mercury-in-glass thermometer (No.9566) which had a range from -5 °C to 105 °C, was subdivided in 10ths of a degree and was capable of being read to ±0.02 °C. An eye piece was used to avoid parallex errors. This thermometer was previously calibrated at the National Physical

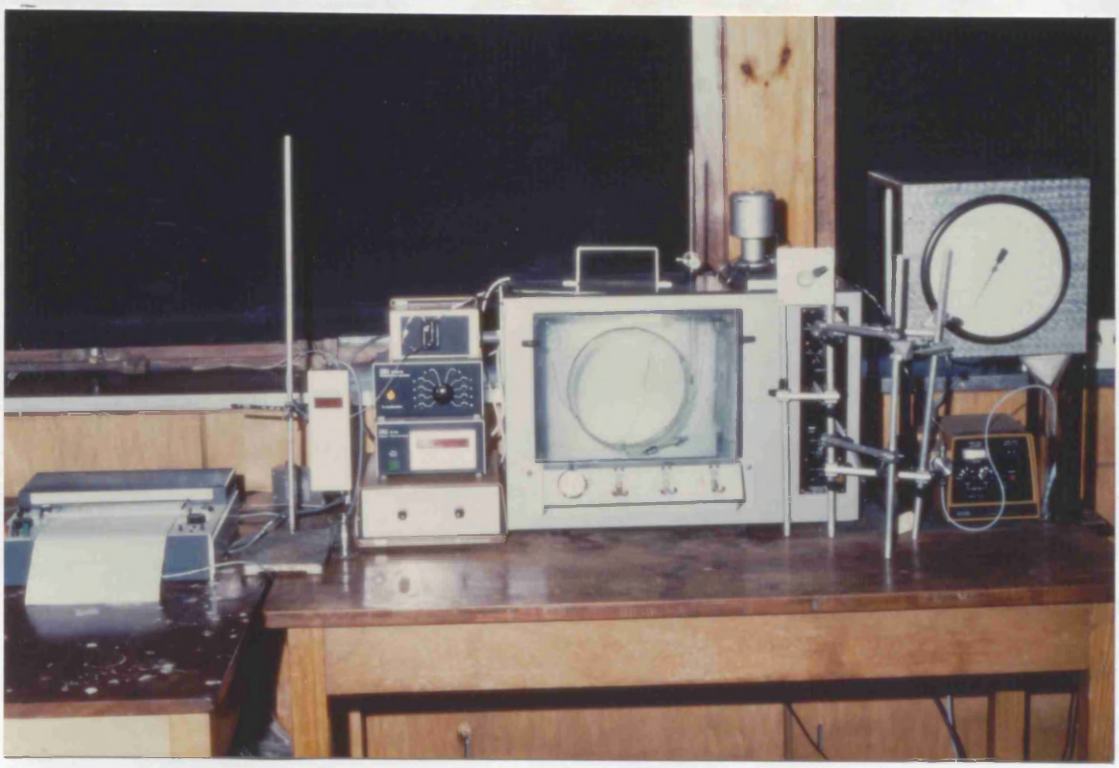

fig. 3.1

Experimental set up for diffusion coefficient measurements.

Table 3.2

CHARACTERISTICS OF DIFFUSION TUBES.

	LOOP A	LOOP B
Length/cm	2039.8	2996.2
Volume/cm^3	9.4	15.4
Radius/cm	0.0383	0.0405
Helical radius/cm	11.364	4.350
Apparatus Constant/cm^2	$7.40X10^{-5}$	$7.96X10^{-5}$

Laboratory, London. As a check, temperature was also measured using a Lauda R46 digital thermometer and was found to agree to within ±0.02 °C.

For measurements at 273.2 K the temperature bath was filled with a crushed ice-water mixture, having a six inch layer of ice on top, covered by a layer of Allplas insulating balls and stirred thoroughly for uniform temperature. Temperatures below 273.2 K were attained by a bridge controlled Minus Seventy thermostat bath (Townson amd Mercer, series III). The coolant was methylated spirit-Cardice (dry ice) mixture [121-123], and temperature was controlled to ±0.05 °C. The temperature was measured by a Lauda R46 digital thermometer.

3.4.3 PROCEDURE.

The system is brought to the required temperature and degassed solvent is pumped through the diffusion tube at low flow rate. When thermal equilibrium is established and detector response steady (steady base line on recorder), 10 µl of dilute solution is injected into the stream by means of a hyperdermic syringe through a liquid chromatographic injection valve. To fill the loop, an excess volume of sample (usually 50 µl) is used. The syringe needle is inserted into the needle port with the injector in LOAD position. The end of the needle abuts directly against one of the loop passages and the sample is injected. The handle is turned clockwise 60°. This connects the loop with the pump and column and the sample is flushed. After injection, the handle is rotated anticlockwise 60°. The solute is allowed to disperse in the mobile phase and after a sufficient time the sample is detected by the detector and an output signal is

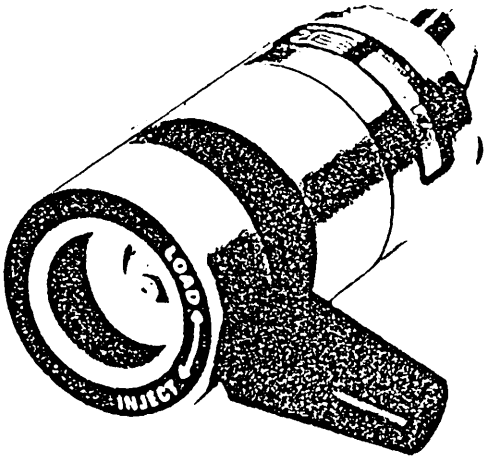

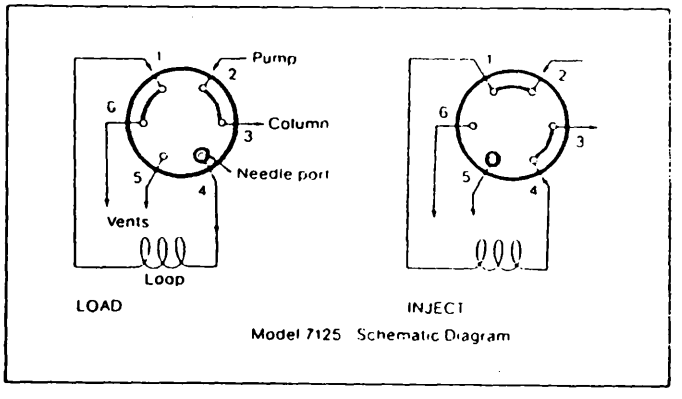

fig. 3.2 Chromatographic Sample Injector.

recorded on the recorder. The time taken from injection to the maximum of the peak is noted.

As already explained in section 3.2, provided certain conditions are satisfied, the solute is normally distributed at the end of the diffusion tube. The diffusion coefficient is determined from the dispersion time and variance of the Gaussian peak, calculated graphically as described in section 3.4.4. A typical experimental peak is shown in fig. 3.3.

The extinction coefficients of the fluorobenzenes at 254 nm are sufficient to allow measurements at low concentration (0.1% to 0.5%). However, because of excessive base line drift in the case of the Refracto-Monitor at high sensitivity, a higher concentration (5% to 10%) was employed with this detector. Base line drift can be controlled to a large extent by attaining a good thermal equilibrium between the reference and the sample cells of the Refracto-Monitor. This can be achieved by filling the thermostat of the Refracto-Monitor with water at room temperature and sealing the inlet and outlet with rubber caps.

Multiple measurements can be made by introducing a series of samples at regular intervals. A blank sample (mobile phase) was introduced between two different solutes. The whole apparatus was flushed with freshly degassed solvent everyday. The values reported here are the mean of at least 5 injections. Variation from run to run was generally less than the uncertainty of the measurement.

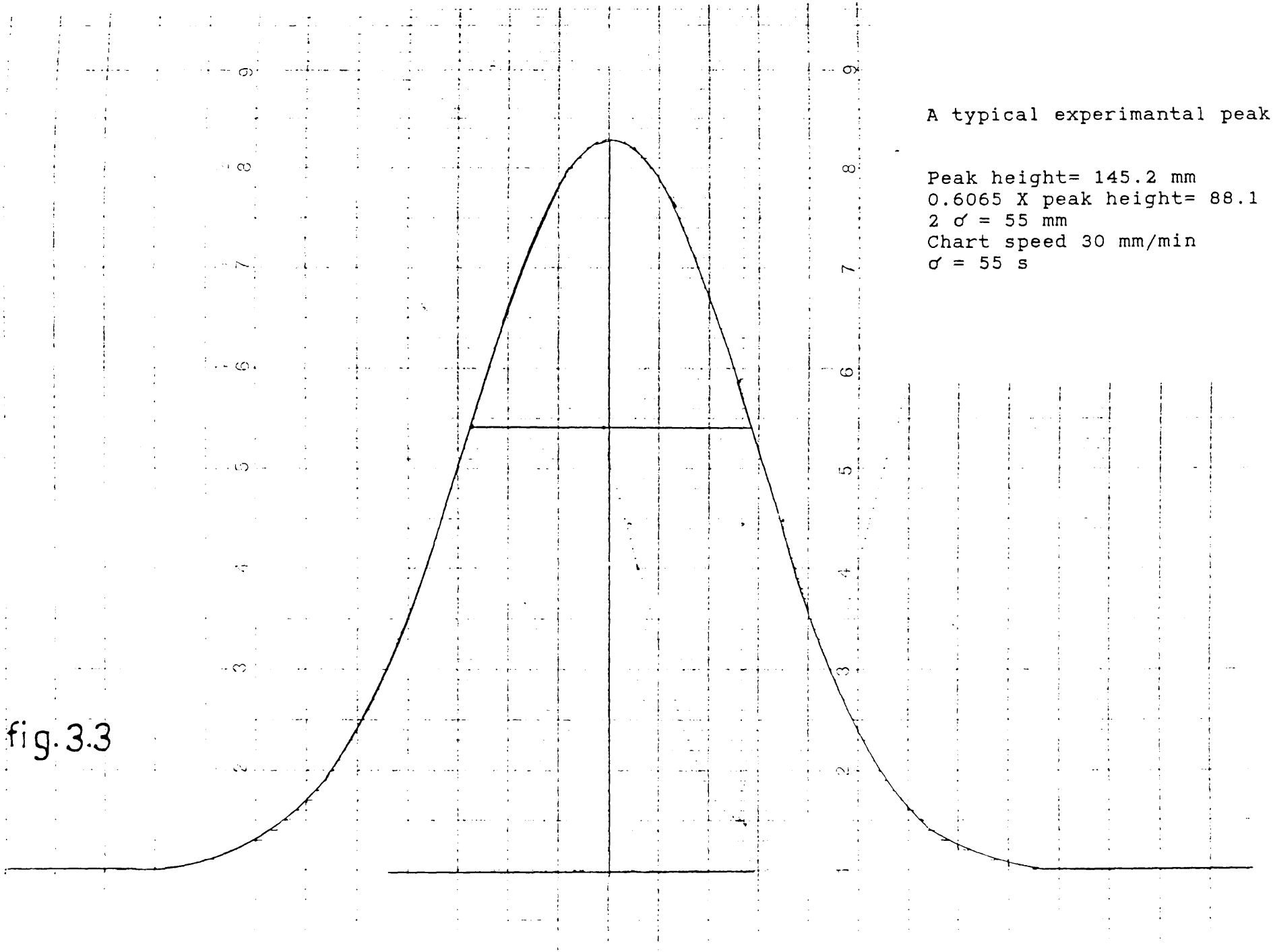

A typical experimantal peak.

Peak height= 145.2 mm
0.6065 X peak height= 88.1 mm
2 σ = 55 mm
Chart speed 30 mm/min
σ = 55 s

fig. 3.3

3.4.4 DETERMINATION OF VARIANCE.

A Normal curve is defined by the equation

$$y = 1/\{\sigma(2\pi)^{1/2}\} \exp(-(x-m)^2/2\sigma^2) \qquad (3.10)$$

where m is the mean of the data points x1, x2, x3, ... xn, having corresponding values of y, y1, y2, y3, ... yn respectively and σ^2 is the variance of the curve. The maximum of the curve occures at x = m and the corresponding value of y is $1/\{\sigma(2\pi)^{1/2}\}$. The equation 3.10 can therefore be written as

$$y = ym.\exp(-(x-m)^2/2\sigma^2) \qquad (3.11)$$

For $x-m=\sigma$, where σ is the standard deviation, equation 3.11 becomes

$$y = ym \exp(-1/2) = ym \times 0.6065 \qquad (3.12)$$

Thus the half width at 0.6065 times the maximum height of the peak gives the value for standard deviation and squaring this value gives a value for the variance of the Gaussian curve.

3.4.5 CALIBRATION OF THE APPARATUS.

The Taylor Dispersion technique can be used as an absolute method for measurements of liquid diffusivity, provided the diffusion tube is highly uniform in circularity and the dimensions of the diffusion tube as well as other components are known accurately. However, since for the purpose of isothermal measurements the diffusion tube is wound in a helix on a former and small pieces of connecting tubes with different bore size are often used to connect the diffusion tube to the detector, the apparatus is calibrated with solute/solvent systems whose diffusion coefficient is known accurately.

The residence time of the solutes from injection to the elution is measured and the variance of the peak is calculated. The working apparatus constant ($Ro^2/24$) is calculated as

$$\text{Apparatus Constant} = D_{12}\,\sigma^2\,/t \qquad (3.13)$$

The calibration was carried out with benzene at trace concentration diffusing in n-hexane at a nominal flow rate of 0.1 ml per minute at 299.2 K using the UV detector, both with low and high pressure cells and also using the Refracto-Monitor. A number of injections were made and an average value of the apparatus constant was determined. The results for the two loops are given in Table 3.2.

3.4.6 COMPARISON OF MEASURED VALUES WITH LITERATURE VALUES.

The experimentally determined mutual diffusion coefficients for a flow rate of 0.1 ml/min are compared with the literature values in Table 3.3 for benzene diffusing in pure n-hexane at 273.7 K, 299.2 K, 313.2 K and 333.2 K. The injected solution had concentrations from 0.1 to 1% (v/v) which all gave the same D_{12} values (within estimated uncertainty) using the UV detector. Values are also compared for toluene diffusing in n-hexane at 273.2 K, 299.2 K and 313.2 K. For this system, both the UV detector and Refracto-Monitor were used with toluene concentration in the same 0.1 to 1% (v/v) range. The agreement with literature values is very satisfactory. Measurements were also made for n-hexane, n-decane and n-tetradecane diffusing in toluene at 299.2 K, 323.2 K and 348.2 K. The injected solution had a concentration of solute from 5 to 10% (v/v) and the Refracto-Monitor was used for the detection of the peak. High concentration was required where solute and solvent refractive indices were comparable. The results for a flow rate of 0.1 ml/min are compared with the

literature values in Table 3.3. The values are in good agreement, generally well within the combined uncertainties.

3.4.7 EFFECT OF FLOW RATE ON CALCULATED D_{12} .

In order to establish a method to derive the correct mutual diffusion coefficients from the experimental measurements, the D_{12} values were measured for toluene diffusing in n-hexane, and vice versa, at 299.2 K as a function of flow rate at 0.1% solute concentration, using the UV detector in the former case and at 10% solute concentration using the Refracto-Monitor in the latter case. Coil B was used for these measurements as it had a smaller helix to diffusion tube diameter ratio, and will give rise to a greater secondary flow effect. The results are presented in Table 3.4 and the ratio of the observed diffusion coefficient to the limiting value (Dx/Dm) is plotted against the normalised flow rate (F/F_{TR}) in fig. 3.4.

The points for the two systems lie on a common curve, showing that it is a characteristic curve for this coil. It can be seen from fig. 3.4 that the D_{12} ratio is practically independent of flow rate up to 0.6 times the transition flow rate, and from Table 3.4 that there is an increase up to almost 4% at a normalised flow rate equal to 0.85. The Dx/Dm ratio increases linearly with normalised flow rate in the region 1.5 to 2.5.

Alizadeh et al. (1980) [124] and Atwood and Goldstien [106] found that the theoretical curve of Nunge's solution for the dispersion of solute in a mobile phase in a curved tube, lies very close to the

Table 3.3

COMPARISON OF MEASURED DIFFUSION COEFFICIENTS WITH LITERATURE VALUES.

Solute	Solvent	Temp/K	$10^9 \times D_{12}$ /(m^2/s) Literature	Measured Loop A	Loop B
Benzene	n-hexane	273.7	3.40 (a)	3.45 (1)	-
		299.2	4.66 (a)	4.71 (2)	4.66
		299.2	4.747(b)	4.69 (3)	4.72
		299.2	4.758(c)	4.74 (4)	-
		299.2	4.723(d)	4.70 (5)	-
		313.2	6.82 (a)	-	6.96
		313.2	7.01 (e)	-	-
		333.2	5.47 (a)	5.53 (6)	-
Toluene	n-hexane	273.2	3.21 (a)	3.22	-
		299.2	4.38 (a)	4.45	4.40
		299.2	4.344(f)	-	-
		299.2	4.355(f)	-	-
		313.2	5.00 (a)	4.95	-
n-hexane	toluene	299.2	2.479(f)	2.52	2.48
		300.2	2.41 (g)	-	-
		323.2	3.25 (g)	3.21	3.30
		348.2	3.99 (g)	4.17	4.33
n-decane	toluene	299.2	1.87 (g)	1.86	1.82
		323.2	2.41 (g)	2.52	2.51
		348.2	3.21 (g)	3.25	3.20
n-tetra-decane	toluene	299.2	1.45 (g)	1.47	1.45
		323.2	1.97 (g)	1.98	1.99
		348.2	2.61 (g)	2.61	2.60

(a) Dymond (1981) [23]
(b) Harris et al. (1970) [133]
(c) Shankland et al. (1977) [89]
(d) Albright et al. (1976) [134]
(e) Chen et al. (1985) [135]
(f) Ghai and Dullien (1974) [131]
(g) Chen and Chen (1985) [136]

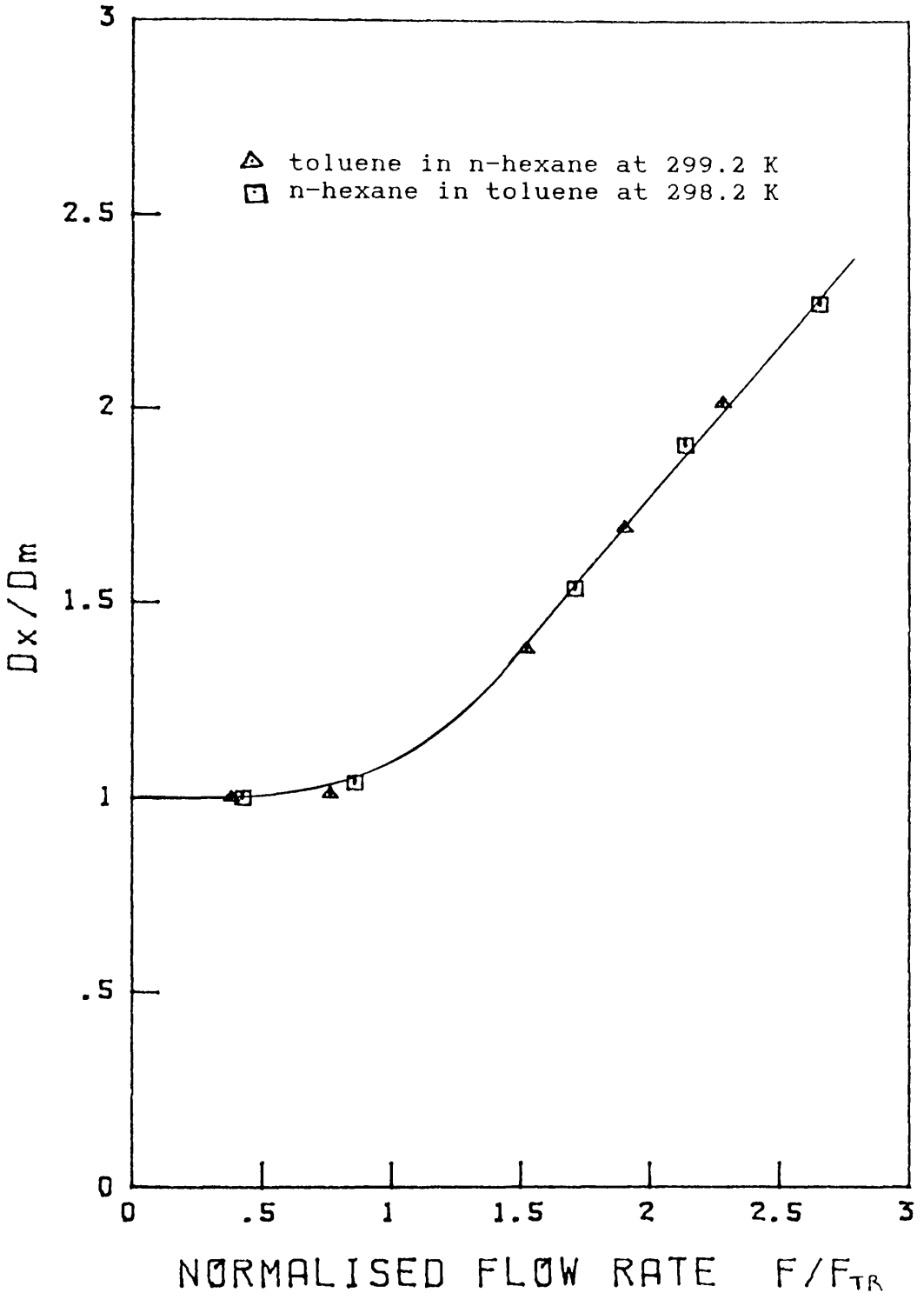

fig.3.4

Diffusion Coefficient Ratios as a Function of Flow Rate of Mobile Phase.

Table 3.4

D_{12} AS A FUNCTION OF FLOW RATE AT 299.2 K.

Flow rate ml / min.	10^9 D_{12} m^2/s	F/F_{TR}	Dx/Dm
(a)	Toluene in n-hexane		
0.1	4.40 ± 0.05	0.380	1.000
0.2	4.45 ± 0.05	0.760	1.011
0.4	6.08 ± 0.06	1.521	1.382
0.5	7.45 ± 0.01	1.901	1.693
0.6	8.87 ± 0.12	2.281	2.016
(b)	n-hexane in Toluene		
0.1	2.48 ± 0.02	0.427	1.000
0.2	2.58 ± 0.05	0.855	1.040
0.4	3.81 ± 0.04	1.709	1.536
0.5	4.73 ± 0.01	2.137	1.907
0.6	5.64 ± 0.02	2.654	2.274

Table 3.5

OBSERVED AND CORRECTED D_{12} VALUES FOR N-HEXANE, N-DECANE AND N-TETRADECANE IN TOLUENE.

Temp/ K	$10^9 D_{12}$/ m^2/s			
	n-hexane	n-decane	n-tetradecane	
299.2	2.48 ± 0.02	1.82 ± 0.01	1.45 ± 0.01	(a)
	2.58 ± 0.05	1.99 ± 0.01	1.65 ± 0.01	(b)
	2.48	1.85	1.46	(c)
323.2	3.30 ± 0.04	2.51 ± 0.02	1.99 ± 0.01	(a)
	3.51 ± 0.03	2.68 ± 0.03	2.24 ± 0.02	(b)
	3.34	2.44	1.93	(c)
348.2	4.33 ± 0.03	3.20 ± 0.02	2.60 ± 0.02	(a)
	4.57 ± 0.02	3.56 ± 0.04	3.00 ± 0.02	(b)
	4.38	3.30	2.65	(c)

(a) at 0.1 ml/min flow rate.
(b) at 0.2 ml/min flow rate
(c) gives (b) corrected for secondary flow effect.

experimental results and fits the data quite well.

In order to check their conclusion, D_{12} values were measured for n-hexane, n-decane, n-tetradecane {at concentraions of 5 to 10% (v/v)} in toluene at 299.2, 323.2 and 348.2 K at a flow rate of 0.1 ml/min and approximately 0.2 ml/min in loop B to see the effect of curvature of the tube in the region where the normalised flow rate is greater than 0.6 but less than one. The results are presented in Table 3.5.

Equation 3.9 was applied with a =0.1034 and Dm was calculated from the observed diffusion coefficient for flow rates of about 0.2 ml/min. The appropriate values of density and viscosity of the mobile phase were taken from the literature and interpolated or extrapolated where necessary. A computer programme was used to calculate the limiting values of D_{12} from observed Dx. The absolute average percentage deviation of 9 measured (0.1 ml/min flow rate) and corrected data points is 1.64%, having a rms deviation of 1.07% and maximum deviation of 3.1%, which is within the expected uncertainty. Equation 3.9 was used in all the subsequent work where the flow rate exceeded 0.1 ml/min.

3.4.8 EFFECT OF CONCENTRATION CHANGES IN INJECTED SOLUTION ON D_{12}.

In order to determine the effect of concentration changes in the injected solution on the measured mutual diffusion coefficients for fluorinated benzenes diffusing in n-hexane, measurements were made of D_{12} for hexafluorobenzene diffusing in n-hexane at 299.2 K as a function of concentration (volume percent) of the injected solution.

The results using the Refracto-Monitro as detector are presented in Table 3.6.

The results show that D_{12} is constant up to 30% v/v hexafluorobenzene solution but decreases beyond that from $4.1X10^{-9}$ m^2 /s to a value $2.49X10^{-9}$ m^2 /s when pure solute was injected into the stream. Similar behaviour was observed when using the UV detector but for this detector flat topped and non-Gaussian peaks were observed for solution as dilute as 3%(v/v). The limiting values were thus measured at trace concentration (0.05 or 0.1%) with the UV detector.

Table 3.6 also contains the D_{12} values for equimolar mixtures of toluene plus n-hexane at 299.2 K as a function of mole fraction of n-hexane in the injected solution. The values are fairly constant from 0.546 to 0.788 mole fraction of n-hexane in the injected solution. However, the D_{12} value decreases from the average value of $2.75X10^{-9}$ m^2/s [comparable to $2.75X10^{-9}$ m^2/s at 298.2 K, obtained by the diaphragm cell method {Ghai and Dullien (1974)}to a value of $2.38X10^{-9}$ m^2 /s when pure n-hexane was injected. A similar comparison for toluene diffusing in acetonitrile at 298.2 K (Table 3.13) shows that D_{12} values are constant up to 20% (v/v) concentration of the injected solution using the Refracto-Monitor.

3.4.9 D_{12} RESULTS FOR FLUORINATED BENZENES IN N-HEXANE.

D_{12} values were measured for benzene and 8 fluorinated benzenes at atmospheric pressure over the temperature range from 213.2 K to 333.2 K, using different coils and detectors. It was found that for benzene itself and partially fluorinated benzenes that a steady baseline and

Table 3.6

(a) D_{12} FOR HEXAFLUOROBENZENE AS A FUNCTION OF CONCENTRATION OF INJECTED SOLUTION.

Conc.	$10^9 . D_{12}/m^2/s$
5 %	4.00 ± 0.04
10 %	4.08 ± 0.03
30 %	4.10 ± 0.01
40 %	3.90 ± 0.02
50 %	3.60 ± 0.02
100 %	2.49 ± 0.01

(b) D_{12} FOR EQUIMOLAR MIXTURES OF TOLUENE + n-HEXANE AS A FUNCTION OF MOLE FRACTION OF THE n-HEXANE IN INJECTED SOLUTION.

Mole fraction of n-hexane	$10^9 . D_{12}/m^2/s$
0.546	2.79 ± 0.04
0.592	2.74 ± 0.01
0.688	2.74 ± 0.01
0.788	2.76 ± 0.03
1.000	2.38 ± 0.05

well defined peak were obtained using the Refracto-Monitor at concentrations much lower than had been required for hexafluorobenzene. The measurements made at a flow rate higher than 0.1 ml/min were corrected for the secondary flow effect as described earlier. The results are presented in Table 3.7, and have an estimated uncertainty of ±2.5%. D_{12} values are quoted with standard deviations. Each value is the average of at least five measurements.

3.4.10 EYRING THEORY APPLIED TO RESULTS FOR FLUORINATED BENZENES IN n-HEXANE.

Extension of the Eyring theory of reaction rates [48] leads to the interpretation of diffusion coefficient data in terms of an activation energy for diffusion which is due to the caging of the solute molecule by solvent molecules (configurational activation energy) and back scattering (back scattering activation energy). The configurational activation energy increases with solute to solvent size ratio, reflecting the fact that the larger the solute molecule, the more the nearest neighbour solvent molecules around it and therefore the greater the probability of binary collisions between the solvent and solute molecules. Thus, it is more difficult for larger molecules to escape a cage of solvent molecules. The back scattering activation energy depends upon solute to solvent mass ratio. As the solute molecule become heavier, back scattering diminishes.

The activation energy for diffusion was calculated from Arrhenius-type plots (log D against the reciprocal of the absolute temperature) which for these systems are straight lines over this

Table 3.7

MUTUAL DIFFUSION COEFFICIENTS OF ORGANIC SOLUTES IN N-HEXANE.

Compound	$10^9 D_{12}$ / $m^2.s^{-1}$			
	213.2 K	233.2 K	253.2 K	273.2 K
Benzene	1.21 ± 0.01	1.80 ± 0.03	2.57 ± 0.03	3.43 ± 0.08 (a) 3.45 ± 0.02 (a) 3.40 ± 0.04 (b)
o-difluoro -benzene	1.10 ± 0.03	1.60 ± 0.08	2.41 ± 0.02	3.35 ± 0.04 (a) 3.26 ± 0.03 (b)
p-difluoro -benzene	1.10 ± 0.03	1.72 ± 0.11	2.49 ± 0.02	3.36 ± 0.06 (a)
1,2,4 tri- fluorobenzene	1.18 ± 0.09	1.72 ± 0.03	2.33 ± 0.03	3.20 ± 0.04 (c) 3.21 ± 0.02 (b)
1,2,3,5 tetra fluorobenzene	1.05 ± 0.02	1.67 ± 0.03	2.27 ± 0.08	3.29 ± 0.06 (b) 3.42 ± 0.02 (d)
1,2,4,5 tetra fluorobenzene	1.05 ± 0.02	1.68 ± 0.05	2.22 ± 0.03	3.17 ± 0.05 (d) 3.15 ± 0.05 (b)
Pentafluoro- benzene	1.06 ± 0.04	1.70 ± 0.02	2.26 ± 0.04	2.98 ± 0.01 (b)
Hexafluoro- benzene	1.01 ± 0.02	1.62 ± 0.03	2.16 ± 0.03	2.87 ± 0.01 (e) 2.82 ± 0.09 (b)
Octafluoro- toluene	0.88 ± 0.01	1.40 ± 0.06	1.83 ± 0.02	2.51 ± 0.02 (f) 2.45 ± 0.04 (b)

(a)= (1%, R, A) (b)= (0.1%, H, A) (c)= (0.05%, L, B)
(d)= (10%, R, A) (e)= (5%, R, A) (f)= (0.05%, H, B)

where the first figure is the concentration of injected solution, R stands for Refracto-Monitor, A and B for loop A or B and H and L stand for low pressure or high pressure cell in the UV detector.

Table 3.7 (Continued)

MUTUAL DIFFUSION COEFFICIENTS OF ORGANIC SOLUTES IN N-HEXANE.

Compound	$10^9 . D_{12}$ (m^2/s)		
	299.2 K	313.2 K	333.2 K
Benzene	4.73 ± 0.06 (h) 4.66 ± 0.04 (i)	5.53 ± 0.05 (i) 5.57 ± 0.01 (a) 5.61 ± 0.01 (j)	6.96 ± 0.10
o-difluoro -benzene	4.48 ± 0.06 (h) 4.44 ± 0.03 (k)	5.23 ± 0.01 (a) 5.29 ± 0.08 (b)	6.61 ± 0.20
p-difluoro -benzene	4.63 ± 0.03 (l) 4.63 ± 0.07 (k)	5.51 ± 0.07 (a) 5.37 ± 0.06 (b)	6.62 ± 0.03
1,2,4 tri- fluorobenzene	4.43 ± 0.06 (h) 4.39 ± 0.05 (b) 4.49 ± 0.02 (m)	5.29 ± 0.04 (b) 5.16 ± 0.05 (c)	6.34 ± 0.06
1,2,3,5 tetra fluorobenzene	4.40 ± 0.05 (d) 4.41 ± 0.07 (n) 4.57 ± 0.01 (b)	5.00 ± 0.09 (b) 4.91 ± 0.07 (c)	6.48 ± 0.06
1,2,4,5 tetra fluorobenzene	4.42 ± 0.08 (d) 4.26 ± 0.04 (b) 4.49 ± 0.04 (e)	5.28 ± 0.04 (b) 5.17 ± 0.09 (c) 4.99 ± 0.06 (d)	6.20 ± 0.08
Pentafluoro- benzene	3.99 ± 0.01 (o) 4.02 ± 0.04 (p) 4.02 ± 0.04 (d) 4.06 ± 0.08 (q)	4.83 ± 0.08 (b)	5.95 ± 0.07
Hexafluoro- benzene	4.00 ± 0.04 (r) 4.08 ± 0.03 (s) 4.10 ± 0.01 (t) 4.03 ± 0.05 (m)	4.62 ± 0.09 (e)	5.81 ± 0.10
Octafluoro- toluene	3.48 ± 0.06 (u) 3.51 ± 0.03 (e) 3.52 ± 0.03 (a) 3.45 ± 0.05 (n)	4.07 ± 0.02 (j)	4.98 ± 0.01

(h)= (1%, R, B) (i)= (0.5%, R, A) (j)= (1.5%,R,A)
(k)= (0.05%, H, A) (l)=(2%, R,B) (m)= (0.1%, L, A)
(n)= (0.5%, L, B) (o)= (8%, R, A) (p)= (6%, R, A)
(q)= (0.2%, L, B) (r)= (5%, R, B) (s)= (10%, R,B)
(t)= (30%, R, B) (u)= (3%, R, A)

temperature range, with only an occasional point deviating slightly more than experimental uncertainty, and generally a very close fit to the line . The activation energy Ea, is calculated from the slope of the best straight line fitted by the method of least squares and results are presented in Table 3.8. The values are remarkably similar. These can be contrasted with the calculated activation energy for diffusion for n-hexane in toluene and for toluene in n-hexane which show that Ea is larger for the former case (12.5 kJ/mole), where m_2/m_1 is less than one and the size ratio greater than one (hence both the factors contribute to a greater activation energy), than in the latter case (7.9 kJ/mole) where the size ratio is less than one while the mass ratio is greater than unity, hence giving a smaller total activation energy.

The organic solutes studied in this work have solute to solvent mass ratios greater than one (except benzene) and core size ratios less than one, except octafluorotoluene. Their activation energy values for diffusion are comparable to that of toluene in n-hexane. The similar values for activation energies for these solutes reflect their similar dependence of diffusion coefficient on temperature.

3.4.11 APPLICATION OF ROUGH HARD SPHERE THEORY.

The Rough Hard Sphere theory is applied to the mutual diffusion coefficients of organic solutes in n-hexane at trace concentration. On the basis of the Rough Hard Sphere theory model, the mutual diffusion coefficient, D_{12} of rough hard spherical molecules diffusing into a dense fluid is given by

Table 3.8

ACTIVATION ENERGY FOR DIFFUSION OF FLUOROBENZENES IN N-HEXANE.

Compound	Activation energy (kJ/mole)
Benzene	8.55
o-Difluorobenzene	8.84
p-Difluorobenzene	8.80
1,2,4 Trifluorobenzene	8.33
1,2,3,5,Tetrafluorobenzene	8.80
1,2,4,5 Tetrafluorobenzene	8.72
Pentafluorobenzene	8.27
Hexafluorobenzene	8.42
Octafluorotoluene	8.43

$$D_{12} = D_E \cdot A_{12} (D/D_E)_{MD} \qquad (3.14)$$

where D_E is the Enskog smooth hard sphere diffusion coefficient, A_{12} is the translational-rotational coupling constant and $(D/D_E)_{MD}$ is the computed correction to the Enskog theory to take into account correlated molecular motion. Computed corrections [125-127] to Enskog theory for different solute-solvent mass and size ratios have been given for mixtures where solute is present in trace amount. A prediction method proposed for equimolar mixtures [128] is not supported by experimental results.

The $(D/D_E)_{MD}$ corrections to the Enkog theory for different size and mass ratios were calculated using the following equation [129]:

$$\begin{aligned}(D/D_E)_{MD} = {} & 0.58 + 7.08(0.6666-Vo/V)-20.2(0.6666-Vo/V)^2 \\ & + 0.29\ \log(m_2/m_1) - 0.12\{\log(m_2/m_1)\}^2 \\ & + 1.8(\sigma_2/\sigma_1)\log(m_2/m_1)(V/Vo-1.6) \\ & + 17.6(0.6666-Vo/V)^3 - 0.42(\sigma_2/\sigma_1-1) \\ & - 0.42\log(m_2/m_1)(\sigma_2/\sigma_1-1) - \log(m_2/m_1)(\sigma_2/\sigma_1)^2 \end{aligned} \qquad (3.15)$$

The V/Vo of n-hexane from 213.2 to 333.2 K was calculated using density (API tables) and core size values [70] over the region 223.2 to 333.2 K and extrapolating down to 213.2 K. The solute diameters at 298.2 K were derived from viscosity data. Since the solute core sizes were not available over the required temperature range, therefore solute-solvent diameter ratios were assumed to be constant at all temperatures. The V/Vo ratios and core sizes are tabulated in Table 3.9. The solute to solvent mass ratio, size ratio and core size of the solutes at 298.2 K are presented in Table 3.10.

Table 3.9

V/Vo RATIOS AND CORE SIZE OF N-HEXANE AS A FUNCTION OF TEMPERATURE.

Temp/K	213.15	233.15	253.15	273.15	298.15	313.15	333.15
V/Vo	1.4510	1.5090	1.5685	1.6255	1.6872	1.7540	1.8188
σ/nm	0.5763	0.5733	0.5706	0.5683	0.5660	0.5647	0.5635

Table 3.10

SOLUTE TO SOLVENT MASS AND SIZE RATIO
AND CORE SIZE OF SOLUTES AT 298.2 K

Compound	m_2/m_1	σ_2/σ_1	σ /nm
n-Hexane	1.00	1.00	0.566
Toluene	1.07	0.97	0.549
Acetonitrile	0.50	0.72	0.409
Benzene	0.91	0.90	0.905
o-Difluorobenzene	1.32	0.92	0.521
p-Difluorobenzene	1.32	0.92	0.521
1,2,4 Trifluorobenzene	1.53	0.94	0.532
1,2,3,5 Tetrafluorobenzene	1.74	0.95	0.538
1,2,4,5 Tetrafluorobenzene	1.74	0.95	0.538
Pentafluorobenzene	1.95	0.97	0.549
Hexafluorobenzene	2.16	0.98	0.555
Octafluorotoluene	2.74	1.02	0.577

The translational-rotational coupling factor A_{12} was calculated by taking the ratio of the average experimental diffusion coefficient to the Enskog value corrected for correlated molecular motions. The calculated $(D/D_E)_{MD}$ values along with the derived A_{12} values are presented in Table 3.11.

The magnitude of A_{12} is a measure of the roughness of the molecule (or the departure of a molecule from spherical shape). The average value of A_{12} over the temperature range 233.2 to 333.2 K for these organic solutes lies within the range 0.67 to 0.72 and although the mass ratio of solutes ranges from 0.9 to 2.74 and diameter ratio from 0.9 to 1.02, the A_{12} are close to the A_{11} value of n-hexane derived from self diffusion data. The A_{12} value is roughly temperature independent for benzene, ortho- and para difluorobenzene, but shows slightly irregular variation with temperature for the rest of the solutes. The average of 54 A_{12} values for 9 solutes at 6 temperatures is 0.70 ± 0.04 as expected for systems of rough polyatomic molecules [42]. This shows that D_{12} can be calculated theoretically with $A_{12}=A_{11}$ for these solutes in spite of the larger solute to solvent mass and size ratios. An attempt was made to calculate D_{12} for these solutes with A_{12} =0.72 (A_{11} for n-hexane at 298.2 K). The absolute average percentage deviation of 54 data points was 5.5%. The values were generally reproducible to better than ± 10% with only 5 points out of 54 having a deviation greater than 10%. Four of these points are of octafluorotoluene, while one corresponds to penta fluorobenzene, at 233.2 K.

In spite of the fact that (1) the experimental uncertainty of the

Table 3.11

VALUES OF $(D/D_E)_{MD}$ AND A_{12} FOR FLUOROBENZENES IN n-HEXANE.

Temp/ K	233.2	253.2	273.2	298.2	313.2	333.2
			Benzene			
$(D/D_E)_{MD}$	0.642	0.799	0.926	1.027	1.109	1.174
A_{12}	0.69	0.67	0.67	0.70	0.68	0.70
			o-Difluorobenzene			
$(D/D_E)_{MD}$	0.659	0.833	0.975	1.088	1.191	1.273
A_{12}	0.67	0.67	0.68	0.70	0.67	0.69
			p-Difluorobenzene			
$(D/D_E)_{MD}$	0.659	0.833	0.975	1.088	1.191	1.273
A_{12}	0.72	0.70	0.69	0.72	0.69	0.69
			1,2,4 Trifluorobenzene			
$(D/D_E)_{MD}$	0.658	0.838	0.687	1.106	1.217	1.306
A_{12}	0.76	0.69	0.69	0.73	0.68	0.68
			1,2,3,5 Tetrafluorobenzene			
$(D/D_E)_{MD}$	0.658	0.844	0.999	1.124	1.241	1.338
A_{12}	0.77	0.69	0.74	0.75	0.66	0.70
			1,2,4,5 Tetrafluorobenzene			
$(D/D_E)_{MD}$	0.658	0.844	0.999	1.124	1.241	1.338
A_{12}	0.77	0.68	0.71	0.74	0.71	0.67
			Pentafluorobenzene			
$(D/D_E)_{MD}$	0.651	0.843	1.004	1.134	1.258	1.360
A_{12}	0.83	0.73	0.69	0.70	0.68	0.67
			Hexafluorobenzene			
$(D/D_E)_{MD}$	0.648	0.845	1.011	1.146	1.275	1.383
A_{12}	0.82	0.71	0.68	0.72	0.67	0.66
			Octafluorotoluene			
$(D/D_E)_{MD}$	0.626	0.835	1.014	1.188	1.305	1.427
A_{12}	0.80	0.67	0.64	0.66	0.60	0.62

measurements is 2.5%, (2) the computed correction is made on the assumption that solute-solvent diameter ratios are constant at all temperatures, (3) there is uncertainty in the extrapolated or interpolated core size of n-hexane, (4) the molecules depart from spherical shape to varying extends, and (5) there is uncertainty in the computed corrections to Enskog theory, the near constancy of A_{12} is remarkable and although the molecules are non spherical in shape, the data can be reproduced satisfactorily on the basis of the rough hard sphere model with the translational-rotational coupling factor equal to that of the solvent.

3.5 HIGH PRESSURE DIFFUSION MEASUREMENTS.

3.5.1 PRESSURE GENERATION AND MEASUREMENT.

Commercially available metering valves can be used for the pressure generation in high pressure diffusivity measurements. However, since they have inlet and outlet diameters significantly different from that of the diffusion tube, this may contribute to extra band broadening. Therefore, to avoid this, small pieces of 316 stainless steel crimped capillaries were used to generate the pressure. It has been reported [130] that this method raises the mobile phase pressure in the diffusion tube without changing the flow rate. In this work it was found that a slight increase in flow rate resulted at high pressures.

Measurements with the high pressure cell were made with crimped capillary connected either directly to the diffusion tube or to the outlet side of the UV detector. In the case of the Refracto-Monitor where this capillary had to be connected before the detector, the

capillary was immersed in water at room temperature to avoid base line drift. Since the residence time in the cooling and pressure reducing section is negligible compared to the period over which the dispersion proceeds at the bath temperature, the perturbation on measured diffusivities caused by temperature and pressure reduction is expected to be negligible [48]. This also reduced the pressure fluctuations. A 2.8 cm length of crimped capillary was found to raise the pressure to about 60 bars, while pressures about 100 and 200 bars were attained using 5 cm and 8 cm lengths of capillary tube respectively at a flow rate of 0.2 ml per minute. The pressure was measured using a Budenberg Gauge Co. Ltd. Broadheath Standard Test gauge, that can be read to $\pm$ 1 bar, and had been calibrated using a primary pressure standard.

3.5.2 PROCEDURE.

The mixtures were prepared by weight, weighing the less volatile component first followed by adding the required amount of the second component. The system was brought to the required temperature and mobile phase was pumped through the loop. The system was allowed to attain a constant pressure before injections were made. The flow rate was monitored throughout the run as well as during elution of peaks using a Phase Separation flow rate meter, which had a stated accuracy of ±1%.

The effects of flow rate fluctuation on the variance of the eluted peak were considered by Atwood and Goldstien [106] and using their results it can be shown that, if there is a fluctuation in flow rate during the elution of the peak, then the ratio of the true variance

to the observed variance will be equal to the square of the ratio of the flow rate during elution to the average flow rate during the run.

The variance from the recorded trace was corrected in this way for all the high pressure measurements. When measurements were completed at one temperature, the temperature was raised and the system was allowed to attain thermal equilibrium before further injections were made.

The systems investigated were toluene plus n-hexane and tolene plus acetonitrile. The results are given in section 3.5.4., following a comparison of measured mixture D_{12} values with the literature values for the toluene plus n-hexane system at atmospheric pressure in section 3.5.3. Measured D_{12} at trace concentration for benzene in n-hexane and toluene in n-hexane at 298.2 K up to 24 MPa are compared with tracer diffusion measurements in that same section.

The D_{12} measurement was carried out for toluene in n-hexane at 299.2 K and at 7.0 MPa with the crimped capillary connected to the outlet of the detector (with high pressure cell) and then in between the diffusion tube and the detector. A comparison of the two values ($4.13X10^{-9}$ m^2/s in the former case and $4.11X10^{-9}$ m^2/s in the latter case) shows that the capillary can be connected either at the outlet of the detector (with high pressure cell) or in between the loop and detector.

3.5.3 COMPARISON WITH LITERATURE VALUES.

Mutual diffusion coefficients have been measured for toluene +

n-hexane mixtures over the whole composition range at 298.2 K and at ambient pressure {Ghai and Dullien [131]}. The present measurements at 299.2 K, at an injected solution concentration of 5% to 10% are on average 1% higher than their results, which is close to the average temperature coefficient of D_{12} of these mixtures. The maximum difference between the two sets of data is only 1.6%.

Trace diffusion coefficients have been reported for {^{14}C} benzene and {^{14}C} toluene in n-hexane at 298.2 K at pressures up to 400 MPa {Dymond and Woolf (1982) },[132]. The present high pressure D_{12} measurements were made for benzene in n-hexane at 299.2 K up to 20 MPa with injected solution from 0.5% to 1% (v/v) and for toluene in n-hexane up to 24 MPa (concentration 1%). For the purpose of comparison the literature values were interpolated for the experimental pressures from a log D_{12} against pressure (MPa) plot.

The measured D_{12} (10^{9} /m^2 s^{-1}) values for benzene in n-hexane at 5.2, 10.0 and 20.2 MPa pressure, namely 4.55 ± 0.04, 4.36 ± 0.04 and 4.07 ± 0.14 are in excellent agreement with interpolated intradiffusion coefficient values of 4.54, 4.38 and 4.07 at the same respective pressures. The measured D_{12} values for toluene at the same temperature are within the combined experimental uncertainty. A maximum deviation of 5.7% between the two sets of data is observed at 16.8 MPa pressure, infering that the present high pressure measurements have an accuracy, which at worst, is better than ±4%.

3.5.4 RESULTS.

High pressure D_{12} measurements were made for toluene + n-hexane and

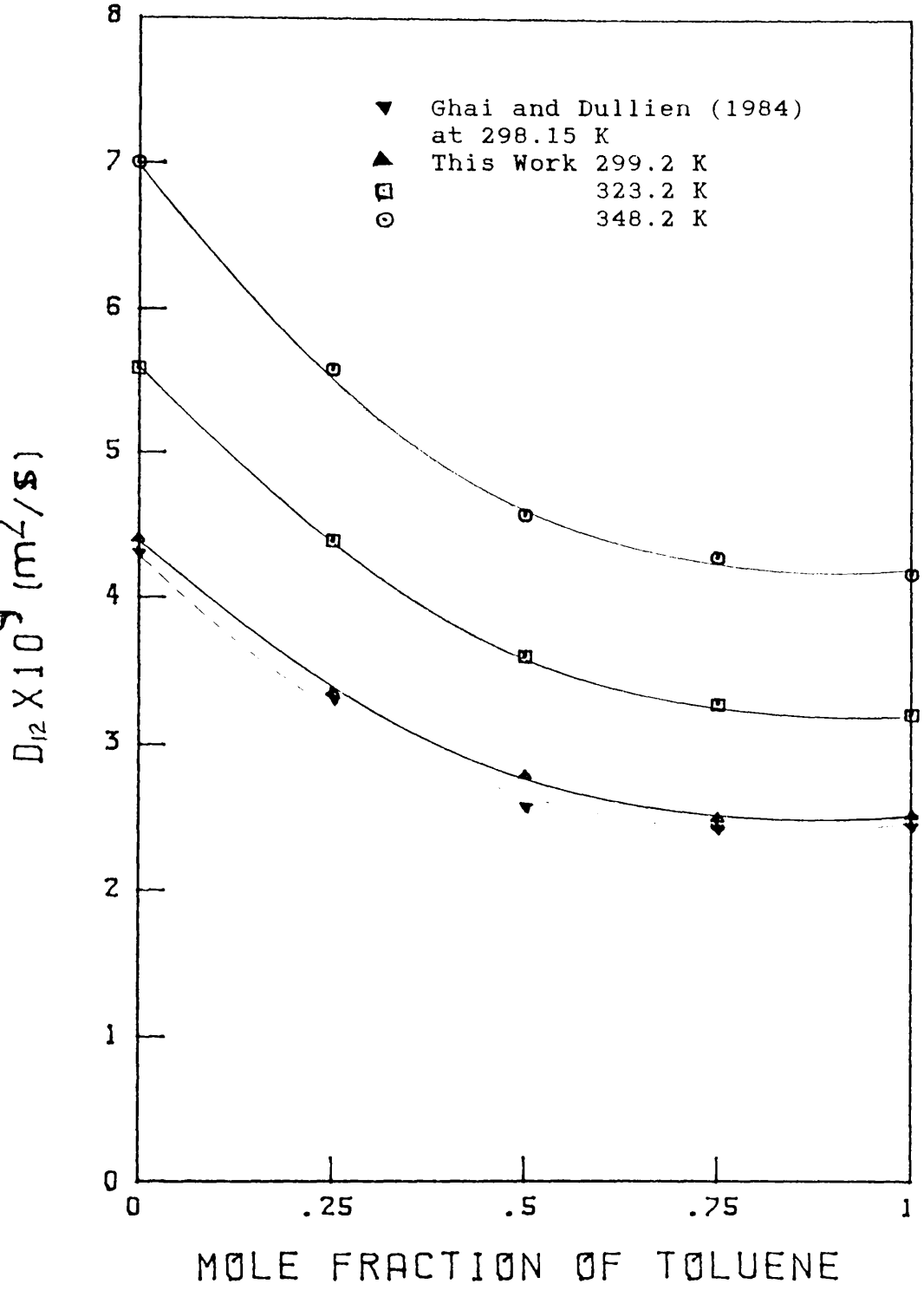

fig.3.5

Dependence of Diffusion Coefficient on Mole Fraction of Toluene for x Toluene + (1-x) n-hexane

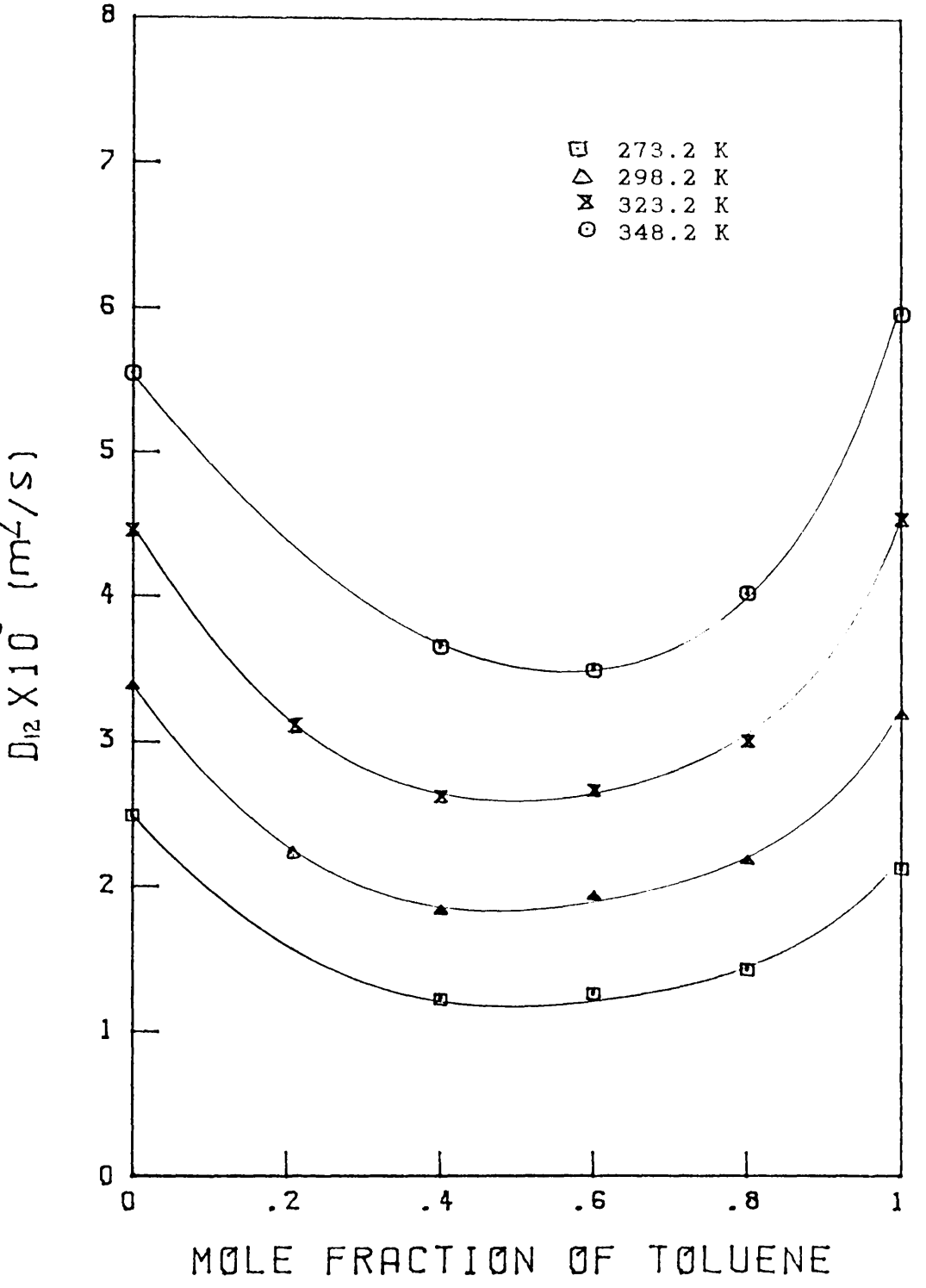

fig. 3.6

Dependence of Diffusion Coefficient on Mole Fraction of Toluene For x Toluene + (1-x) acetonitrile

toluene + acetonitrile mixtures at different mixture compositions and temperatures. For the n-hexane plus toluene system, the injected solution was richer in n-hexane. The difference in concentration between the mobile phase and the injected solution was sufficient to give a steady base line and well defined peaks. In practice, the injected solution had a mole fraction of n-hexane of 0.38, 0.74 and 1.0 where the mobile phase mole fraction was 0.25, 0.50 and 0.75 respectively. For the pure solvent (x=1) mobile phase, the injected solutions generally had a solute concentration of 10% (v/v). In the case of the toluene plus acetonitrile system, the mole fractions of acetonitrile in the injected solution were 0.32, 0.51, and 1.0 corresponding to mole fractions of acetonitrile in the mobile phase of 0.2, 0.4, and 0.8, while for the mobile phase with 0.4 mole fraction of toluene the injected solution had a 0.44 mole fraction of toluene. For toluene diffusing in pure acetonitrile and vice versa the solute concentration in the injected solution was 10%(v/v), equivalant to 0.05 mole fraction of toluene in the former case and 0.18 mole fraction of acetonitrile in the latter case. The results are presented in Tables 3.12 and 3.13 respectively. The D_{12} values are plotted as a function of the mixture composition at atmospheric pressure and at different temperatures in fig. 3.5 and 3.6, while D_{12} values at 299.2 and 348.2 K at 22 MPa are compared with atmospheric pressure values as a function of mole fraction of toluene for the toluene plus n-hexane system in fig.3.7. A similar comparison for the toluene plus acetonitrile system, at 10 MPa, is shown in fig. 3.8.

3.5.5 DISCUSSION.

To investigate the effect of pressure on diffusion tube diameter, the

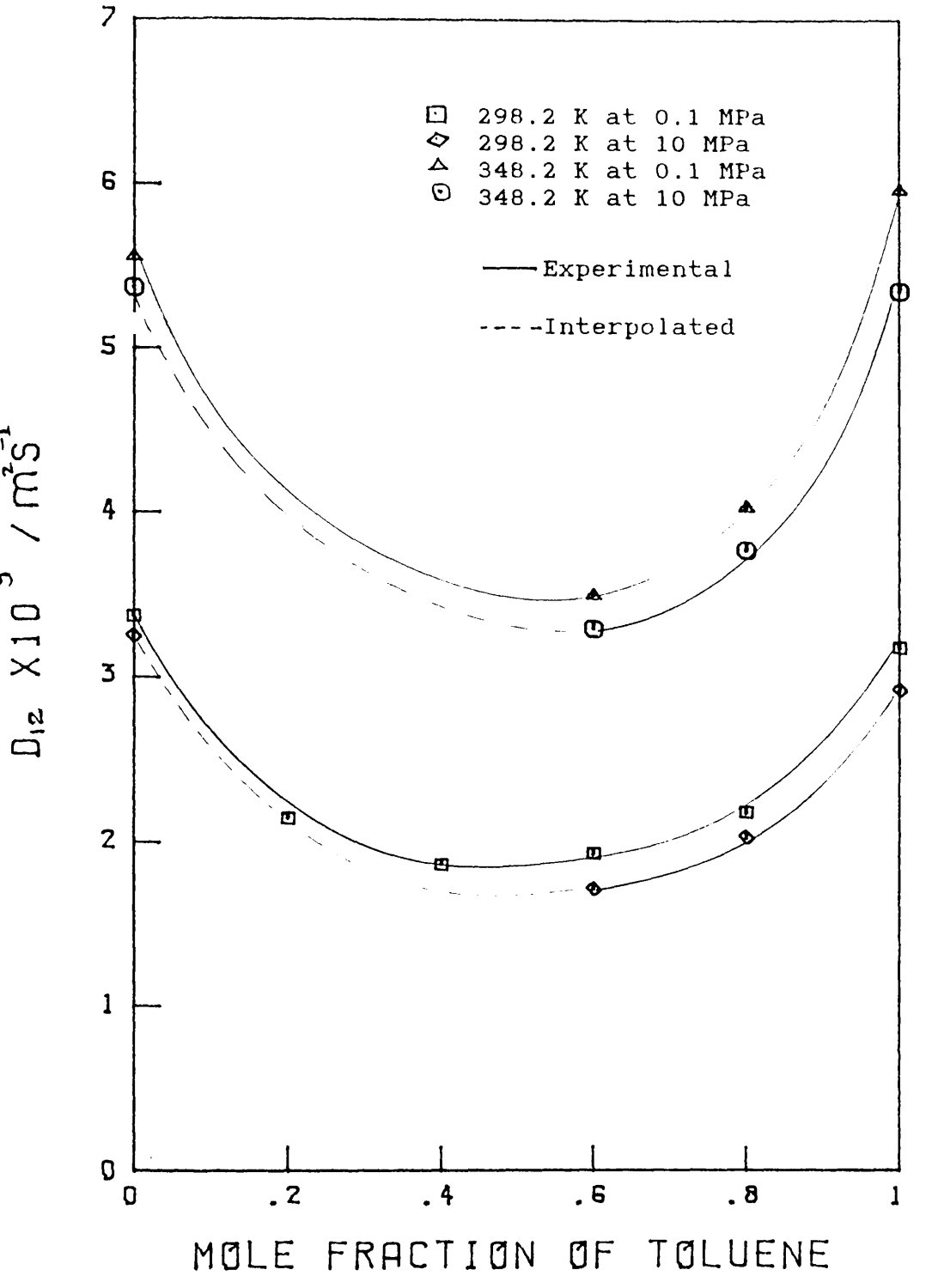

fig.38

Dependence of Diffusion Coefficient on Composition and Pressure for x toluene + (1-x) acetonitrile

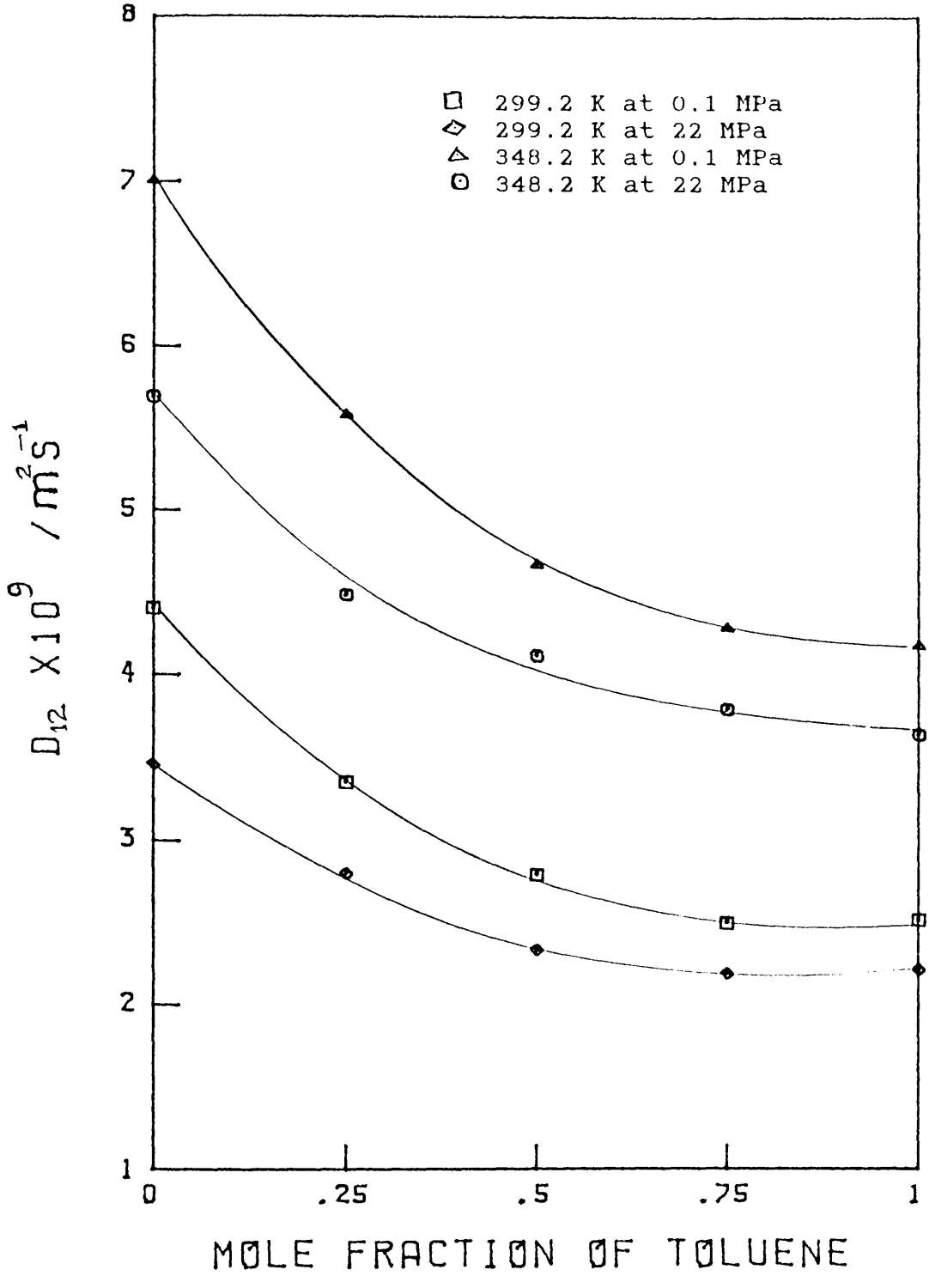

fig.3.7

Dependence of Diffusion Coefficient on Composition and Pressure for x Toluene + (1-x) n-hexane

Table 3.12

MUTUAL DIFFUSION COEFFICIENTS OF (1-x) n-HEXANE (A) + x TOLUENE (B) MIXTURES AS A FUNCTION OF TEMPERATURE, PRESSURE, AND COMPOSITION OF THE MOBILE PHASE.

	T= 299.15 K		T= 323.15 K		T= 348.15 K	
x	P/MPa	10^9 D_{12} m^2/s	P/MPa	10^9 D_{12} m^2/s	P/MPa	10^9 D_{12} m^2/s
0.00	0.1	4.40 ± 0.04	0.1	5.59 ± 0.01	0.1	7.00 ± 0.06
	10.0	4.01 ± 0.06	10.0	5.06 ± 0.08	9.9	6.29 ± 0.04
	16.8	3.67 ± 0.05	16.5	4.77 ± 0.03	16.6	5.88 ± 0.05
	24.2	3.54 ± 0.02	24.3	4.54 ± 0.03	24.2	5.57 ± 0.04
0.25	0.1	3.35 ± 0.03	0.1	4.39 ± 0.06	0.1	5.58 ± 0.03
	7.5	3.05 ± 0.06	6.7	4.15 ± 0.05	6.8	5.22 ± 0.08
	15.6	2.88 ± 0.06	15.2	3.89 ± 0.06	14.9	4.83 ± 0.06
	22.8	2.78 ± 0.02	23.7	3.65 ± 0.04	22.8	4.44 ± 0.08
0.50	0.1	2.79 ± 0.04	0.1	3.60 ± 0.03	0.1	4.57 ± 0.05
	9.8	2.56 ± 0.03	9.8	3.45 ± 0.06	8.6	4.47 ± 0.05
	16.0	2.47 ± 0.04	16.5	3.26 ± 0.07	16.6	4.18 ± 0.07
	25.4	2.26 ± 0.06	24.0	3.00 ± 0.04	23.8	3.98 ± 0.05
0.75	0.1	2.50 ± 0.04	0.1	3.28 ± 0.07	0.1	4.28 ± 0.03
	8.0	2.38 ± 0.04	8.2	3.14 ± 0.05	7.1	4.19 ± 0.08
	17.8	2.25 ± 0.06	16.5	3.02 ± 0.04	15.5	3.92 ± 0.09
	22.8	2.18 ± 0.03	23.1	2.87 ± 0.08	22.8	3.78 ± 0.08
1.00	0.1	2.52 ± 0.03	0.1	3.21 ± 0.08	0.1	4.17 ± 0.07
	7.5	2.34 ± 0.03	7.4	3.14 ± 0.02	7.7	4.01 ± 0.02
	15.9	2.23 ± 0.02	15.4	2.99 ± 0.06	15.0	3.80 ± 0.04
	24.8	1.98 ± 0.03	23.8	2.80 ± 0.07	24.0	3.59 ± 0.03

x= Mole fraction of toluene
T= Temperature

Table 3.13

MUTUAL DIFFUSION COEFFICIENTS OF (1-x) ACETONITRILE (A) + x TOLUENE (B) MIXTURES AS A FUNCTION OF TEMPERATURE, PRESSURE, AND COMPOSITION OF THE MOBILE PHASE.

	T= 273.15 K		T= 298.15 K	
x	P/MPa	$10^9 D_{12}$ m^2/s	P/MPa	$10^9 D_{12}$ m^2/s
1.00	0.1	2.13 ± 0.01	0.1	3.18 ± 0.03
	8.0	2.09 ± 0.02	8.0	2.91 ± 0.02
	16.1	1.94 ± 0.01	15.8	2.76 ± 0.04
	24.4	1.86 ± 0.01	24.0	2.67 ± 0.01
0.80	0.1	1.43 ± 0.03	0.1	2.18 ± 0.04
	8.0	1.39 ± 0.02	8.7	2.05 ± 0.02
	16.3	1.37 ± 0.02	16.2	1.94 ± 0.01
0.60	0.1	1.29 ± 0.02	0.1	1.93 ± 0.02
	8.3	1.19 ± 0.01	7.6	1.77 ± 0.03
	17.8	1.14 ± 0.02	17.8	1.55 ± 0.01
0.40	0.1	1.22 ± 0.01	0.1	1.86 ± 0.05 *
0.20		-	0.1	2.14 ± 0.04
0.00	0.1	2.49 ± 0.02	0.1	3.38 ± 0.04 (a)
				3.39 ± 0.05 (b)
				3.35 ± 0.04 (c)
				3.38 ± 0.03 (d)
	8.8	2.44 ± 0.02	9.5	3.27 ± 0.01
		2.38 ± 0.03		

* less reliable value.

(a) at 5% conc.
(b) at 10% conc.
(c) at 10% conc.
(d) at 20% conc.

Table 3.13 (Continued)

MUTUAL DIFFUSION COEFFICIENTS OF (1-x) ACETONITRILE (A) + x TOLUENE (B) MIXTURES AS A FUNCTION OF TEMPERATURE, PRESSURE, AND COMPOSITION OF THE MOBILE PHASE.

	T= 323.15 K		T= 348.15 K	
x	P/MPa	10^9 D_{12} m^2/s	P/MPa	10^9 D_{12} m^2/s
1.00	0.1	4.54 ± 0.03	0.1	5.96 ± 0.08
	7.8	3.83 ± 0.06	8.1	5.30 ± 0.05
	15.0	4.09 ± 0.05	15.8	5.04 ± 0.03
	24.2	3.64 ± 0.01	24.5	4.78 ± 0.01
0.80	0.1	3.01 ± 0.06	0.1	4.03 ± 0.07
	8.4	2.81 ± 0.01	8.7	3.74 ± 0.05
	16.3	2.69 ± 0.02	16.3	3.67 ± 0.04
0.60	0.1	2.67 ± 0.05	0.1	3.49 ± 0.07
	8.2	2.49 ± 0.03	8.4	3.32 ± 0.2
	16.3	2.38 ± 0.01	16.9	3.16 ± 0.04
0.40	0.1	2.63 ± 0.04	0.1	3.65 ± 0.03
0.20	0.1	3.16 ± 0.05		-
0.00	0.1	4.46 ± 0.07	0.1	5.55 ± 0.04
	8.1	4.29 ± 0.05	8.7	5.40 ± 0.04
		4.25 ± 0.05		

system was pressurised to approximately 30 MPa, then reduced to atmospheric pressure and D_{12} re-measured for toluene in n-hexane at 299.2 K. The constancy of the values revealed that there is no permanent effect of pressure on the diffusion tube diameter.

The D_{12} values plotted against mole fraction of toluene at ambient pressure for the two systems studied show that these mixtures are non-ideal and that the toluene plus acetonitrile system shows more deviation with respect to straight line behavior than that of toluene plus n-hexane. Similar behavior is observed at elevated pressure as shown in fig. 3.7 for toluene plus n-hexane, where D_{12} values interpolated for a pressure of 22 MPa are plotted against mole fraction of toluene and the composition dependence is compared with that for the atmospheric pressure results. For toluene plus acetonitrile, a problem arose in trying to establish a steady high pressure for the solution where the mole fraction of toluene was 0.4. Even at atmospheric pressure, there were problems with the peak height not being proportional to the sensitivity of the detector. This was more evident for the solution of mole fraction of 0.2 of toluene, where it proved impossible to obtain results at 273.2 and 348.2 K. The reason is that the refractive index for these solutions lies at the extreme end of the range for each of the two prisms in the detector. For the pure component mobile phase and solutions with mole fraction of toluene equal to 0.6 and 0.8, the results lie parallel to the atmospheric pressure curve, as shown in fig.3.8.

The activity coefficient measurements for these systems were not conducted, but Ghai and Dullien [131] have shown that the activity corrected mutual diffusion coefficients for the toluene plus n-hexane

system at 298.2 K show positive deviation.

The hard sphere theory can only be applied to these mixtures at the limiting cases where one of the constituents is present at trace amount. Using density data and V/Vo values as given in chapter 6, the $(D/D_E)_{MD}$ were calculated for the limiting cases at atmospheric pressure and values for A_{12} were derived as explained earlier.

The A_{12} values for toluene in n-hexane are fairly constant (0.72 ± .01) over the temperature range 273.2 to 348.2 K and equal to the A_{11} value for n-hexane itself. Taking $A_{12} = A_{11}$ produces a maximum difference of 3% between the calculated and experimental values.

The A_{12} value for acetonitrile in toluene from 298.2 to 348.2 K is also constant (0.72 ± 0.01). The derived value of A_{12} at 273.2 K, i.e. 0.83 is somewhat higher than the average, but this descrepency is attributed to the fact that the V/Vo value for toluene at this temperature is beyond the limit of the hard sphere theory, as the hard sphere system become metastable at V/Vo < 1.5. The A_{12} values for toluene in acetonitrile have an average value of 0.69 ± 0.06 over the temperature range 273.2 to 348.2 K, but for this system there is a definite decrease in A_{12} values with rise in temperature.

The pressure coefficient of diffusion for the two systems studied is presented in Table 3.14. The experimental accuracy does not allow a critical analysis of the dependence of diffusion coefficients on pressure at different temperature and mobile phase composition, as a ±2.5% error in atmospheric pressure values and ±4% error in high pressure measurements can add ±0.4% to the percent change in

Table 3.14

PERCENT CHANGE IN DIFFUSION COEFFICIENTS PER MPa.

(a) toluene plus n-hexane mixtures.

Mole fraction of toluene	Temperature / K		
	299.2	323.2	348.2
0.00	-0.81	-0.77	-0.85
0.25	-0.75	-0.72	-0.90
0.50	-0.75	-0.69	-0.54
0.75	-0.56	-0.54	-0.52
1.00	-0.87	-0.53	-0.58

(b) toluene + acetonitrile mixtures.

Mole fraction of toluene	Temperature / K			
	273.2	298.2	323.2	348.2
0.00	-0.28	-0.34	-0.48	-0.31
0.60	-0.65	-1.11	-0.67	-0.56
0.80	-0.26	-0.68	-0.66	-0.55
1.00	-0.52	-0.67	-0.82	-0.81

diffusion coefficient per MPa. However the values cannot be regarded as pressure independent even within this limited pressure range.

The pressure coefficient of mutual diffusion is roughly constant for the toluene plus n-hexane mixtures where the two components have comparable molecular weights. The pressure dependence is smaller for toluene in acetonitrile compared to acetonitrile in toluene over the whole temperature range, where the limiting values at infinite dilution are comparable but the solvents have significantly different molecular weights. The pressure coefficient values of these mixtures are comparable with those of other organic solutes in similar solvents [106,132].

CHAPTER 4

VISCOSITY COEFFICIENTS AND DENSITIES AT ELEVATED PRESSURE

4.1 INTRODUCTION

In 1685 Newton [137] proposed the existence of an internal resistance to the flow in liquids when relative motion exists between the particles of a liquid. This can be expressed as :

$$F = \eta A (dV/dZ) \qquad (4.1)$$

where A is the area of contact of two liquid laminae and F is the force necessary to maintain a velocity gradient (dV/dZ) between the laminae. η is a constant, characteristic of each liquid and is called the coefficient of dynamic viscosity. Fluids for which viscosity coefficient is independent of the rate of shear stress at constant temperature and pressure are said to be Newtonian. The liquids studied in this work are Newtonian.

The SI unit of viscosity is pascal second (Pa s) while the c.g.s. unit is g/cm/s or poise (P). A smaller and more convenient unit for liquid viscosity coefficient is centipoise (cP) which is equivalent to mPa s. The dynamic viscosity coefficients obtained in this work are reported as mPa s. The coefficient of kinematic viscosity is the ratio of the dynamic viscosity coefficient to the density at the same temperature and is expressed as meter^2/second (m^2/s) in SI units. The c.g.s. unit of kinematic viscosity is cm^2 / s or stokes (St) while a convenient unit for the liquid is centistokes (cSt), being equal to mm^2/s.

The viscosity coefficient of fluids can be measured using various methods but the British Standards Institution [138] recommends only

two of these methods which are based on the resistance to the motion of a liquid passing through the capillary of a glass viscometer (Poiseuille flow), or the resistance to the motion of a sphere falling through a liquid (Stokes law). The method based on Stokes law is only applicable to liquids having a kinematic viscosity coefficient of over 500 cSt and so is not suitable for the present work. Therefore, at saturation pressure, a method based on that of Poiseuille flow is used, which considers a viscous fluid flowing through a stationary tube. The fluid is assumed to be incompressible and the layer of liquid in contact with the wall of the capillary is at rest. The resulting velocity profile is parabolic and viscosity is proportional to flow time.

Modified suspended-level viscometers, described in section 4.2.1 were used for the measurement of the kinematic viscosity coefficients at saturation pressure. They have the distinctive feature that liquid is suspended in the capillary and fills it completely. The suspension ensures a uniform driving head of liquid independent of the quantity of the sample charged in to the viscometer, making viscometer constants independent of temperature. By making the diameter of the lower meniscus approximately equal to the average diameter of the upper meniscii, the surface tension correction can be reduced. Further, since the viscometer is not open to the atmosphere, it can be used for volatile liquids or mixtures even at temperatures above the normal boiling point without appreciable change in composition.

To enable the dynamic viscosity coefficient and buoyancy correction to be calculated, it is necessary to have corresponding density data . The densities were measured using a vibrating tube densimeter, as

described in section 4.3.

The densities and viscosity coefficients for toluene, acetonitrile, three binary mixtures of toluene plus acetonitrile, three binary mixtures of toluene plus n-hexane and the density of a ternary equimolar mixture of n-octane plus i-octane and oct-1-ene have been determined from 298 K to 348 K and extrapolated to 373 K.

4.2 MEASUREMENT OF KINEMATIC VISCOSITY COEFFICIENTS

4.2.1 DESCRIPTION OF VISCOMETER

Standard capillary viscometer techniques were used. The time for a definite volume of liquid to flow through a capillary tube was measured under conditions of closely controlled temperature and an accurately reproducible head of liquid. However, in order to overcome the problem of vapour loss and difficulty of repeat measurements with a conventional glass capillary viscometer a closed design was employed. The design of this instrument, a modification of the British Standard BS/IP/SL type, is shown in fig. 4.1, and has been described in detail by Young et al. [139,140] and Robertson [141].

The viscometer consisted of two reservoir bulbs A and B, of approximately 15 cm^3 capacity, connected on one side by a measuring section consisting of precision bore capillary C and a bulb D. Two circumferential marks X and Y etched on the glass above and below the bulb defined a precise volume for timing. The reservoirs A and B were also connected by a side arm and filler section, sealed by an S13 Rotaflo tap, F. To minimise surface tension effects the capillary tube opened smoothly in a bell shape into the bulbs at either end,

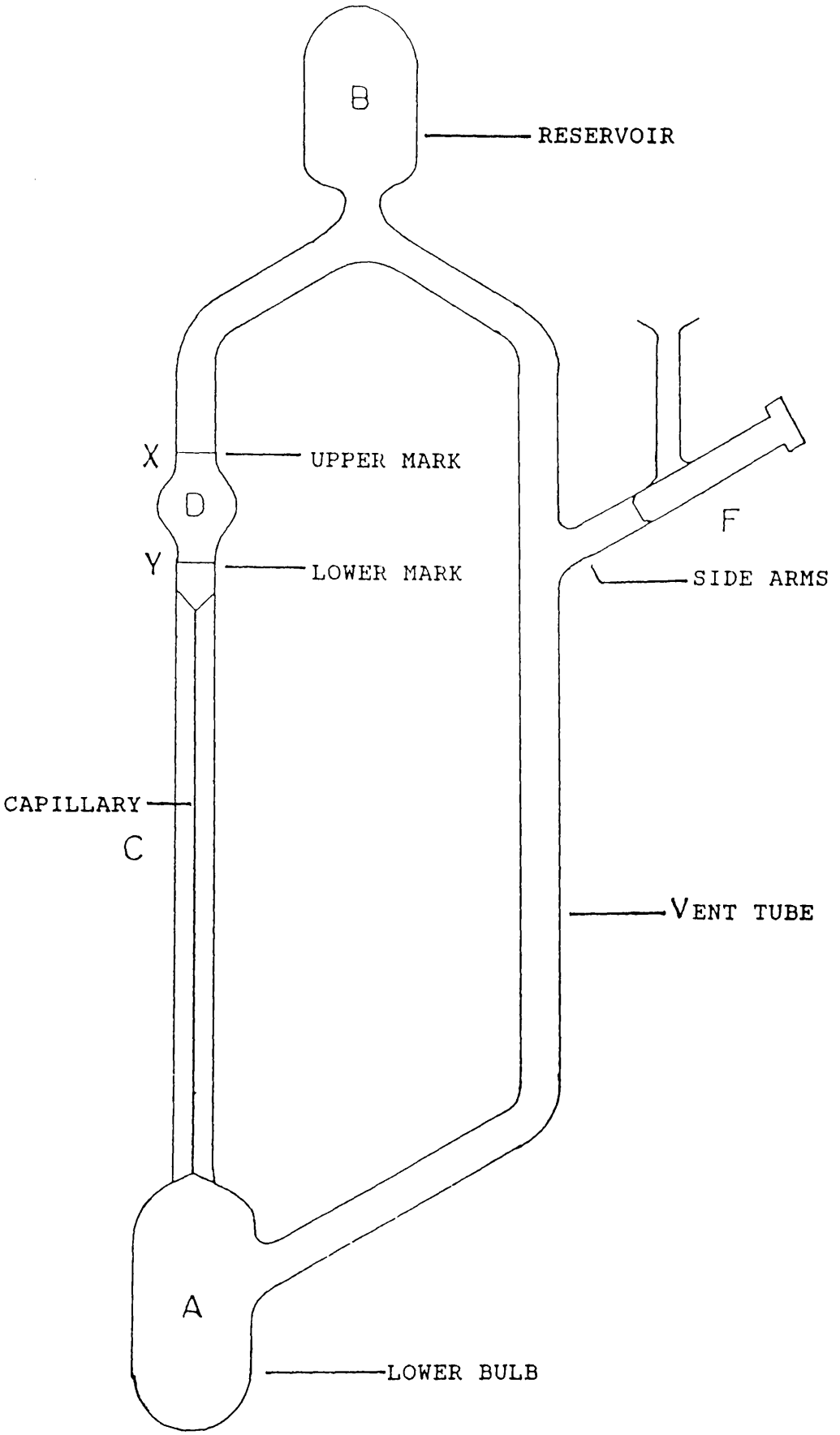

fig.4.1 Modified Suspended-Level Capillary Viscometer.

and the length of the straight section of the tube above bulb D was sufficiently long that the liquid meniscus had reached a constant velocity before passing mark X.

Measurements on each liquid were made simultaneously using two viscometers having different capillary bores and lengths to obtain a more reliable estimate of the accuracy of the viscosity coefficients. Viscometers 1 and 2 were used initially for the measurements of flow time for calibrating liquids, but as they have approximately the same bore sizes and comparable capillary lengths, viscometers 2 and 3 were used for the measurement of kinematic viscosity coefficients for the liquids and mixtures to be studied. The relevant dimensions of the viscometers are given in Table 4.1. Flow times for a given viscometer were reproducible to ±0.1% and the viscosity coefficients from the two viscometers agreed on average to within 0.3%.

4.2.2 VISCOMETER THEORY

A rigorous theory of the flow of liquids through a capillary tube was first obtained by Poiseuille [142]. If a volume V flows along a capillary of radius r and length l in time t, then Poiseuille's formula gives

$$V/t = \pi \Delta P r^4/8\eta l \qquad (4.2)$$

where ΔP is the pressure drop along the capillary. Since $P=g\rho h$ where h is the head of liquid

$$\eta/\rho = \pi g h r^4 t/8Vl \qquad (4.3)$$

Table 4.1

DIMENSIONS OF THE VISCOMETERS

Viscometer Number	Calibration Range / cSt	Capillary Bore / mm	Capillary Length/mm	Volume D / cm^3
1	0.46 - 3.97	0.50	75	9
2	0.46 - 3.97	0.50	55	9
3	0.46 - 1.82	0.30	115	2

Table 4.2

COMPARISON OF EXPERIMENTAL KINEMATIC VISCOSITY COEFFICIENTS WITH LITERATURE VALUES.

Viscometer No. 1 A= 0.002898 mm^2/s^2 B= 4.410 mm^2

Compound	Temp T/K	(η/ρ)(Exp) /cSt	(η/ρ)(Lit) /cSt	Diff. %
Cyclohexane	333.15	0.7155	0.7120 (a)	+0.49
			0.7149 (b)	-0.08
			0.7144 (c)	-0.15
			0.7168 (d)	+0.18
Benzene	333.15	0.4657	0.4660 (a)	+0.06
			0.4662 (b)	+0.11
			0.4664 (c)	+0.15
n-Dodecane	313.15	1.4463	1.4650 (a)	+1.30
			1.4450 (b)	+0.09
			1.4462 (d)	+0.01
	333.15	1.1114	1.1290 (a)	+1.60
			1.1135 (d)	+0.19

Viscometer No. 2 A= 0.002819 mm^2/s^2 B= 5.811 mm^2

Cyclohexane	298.15	1.1576	1.1570 (a)	-0.05
			1.1591 (b)	+0.13
			1.1587 (c)	+0.09
			1.1595 (d)	+0.16
	313.15	0.9273	0.9230 (a)	-0.46
			0.9250 (c)	-0.25
			0.9268 (d)	-0.05
	333.15	0.7135	0.7120 (a)	-0.21
			0.7149 (b)	+0.20
			0.7144 (c)	+0.13
			0.7168 (d)	+0.46

Table No. 4.2 (continued)

Viscometer No. 2 A= 0.002819 mm^2/s^2 B= 5.811 mm^2

Compound	Temp T/K	(η/ρ)(Exp) /cSt	(η/ρ)(Lit) /cSt	Diff. %
Benzene	298.15	0.6888	0.6878 (a)	-0.15
			0.6880 (b)	-0.12
			0.6898 (c)	+0.14
	333.15	0.4659	0.4660 (a)	+0.02
			0.4662 (b)	+0.06
			0.4664 (c)	+0.11
Toluene	298.15	0.6416	0.6378 (a)	+0.59
			0.6400 (c)	-0.25
			0.6402 (d)	-0.22
			0.6426 (e)	+0.15
	323.15	0.5023	0.4978 (a)	-0.89
			0.5036 (c)	+0.26
			0.5031 (e)	+0.16
	348.15	0.4099	0.4049 (a)	-1.21
			0.4098 (c)	-0.02
			0.4148 (e)	+1.20
n-Dodecane	298.15	1.8215	1.8430 (a)	+1.20
			1.8240 (b)	+0.14
			1.8238 (d)	+0.13
	313.15	1.4432	1.4650 (a)	+1.50
			1.4450 (b)	+0.12
			1.4462 (d)	+0.21
	333.15	1.1096	1.1290 (a)	+1.75
			1.1135 (d)	+0.35

Viscometer No. 3 A= 0.001074 mm^2/s^2 B= -2.173 mm^2

Toluene	298.15	0.6395	0.6378 (a)	-0.26
			0.6402 (c)	+0.11
			0.6426 (e)	+0.48
	323.15	0.5018	0.4978 (a)	-0.80
			0.5036 (c)	+0.36
			0.5031 (e)	+0.26
	348.15	0.4097	0.4049 (a)	-1.20
			0.4098 (c)	+0.02
			0.4148 (e)	+1.20

Literature data from:

(a) API tables [151] (b) Young (1980) [139] (c) Robertson (1983) [141] (d) Glen (1985) [152] (e) Makita (1982) [153]

where h is now the mean head of the liquid. If h were the same for every run then η/ρ would be proportional to the time for a set volume of liquid to flow through the capillary under its own pressure. This is not the case and corrections must be applied to take account of loss of effective driving head as kinetic energy is imparted to the liquid on entering the capillary. For certain geometries these correction terms can be evaluated and Kestin, Sokolov and Wakeham [143] were able to derive an equation of the form

$$\eta/\rho = (\pi r^4 gh/8V(l+\delta l))t-(mV/8\pi(l+\delta l))/t \qquad (4.4)$$

where m is a constant and δl is a correction to the length of the capillary. The factor $(l+\delta l)$ was first suggested by Couette [144] on an entirely experimental basis.

The viscometers used in this work do not correspond to those analysed by Kestin et al, but their equation can be written in a general form as

$$\eta/\rho = A(1-\rho_v/\rho)(1+a\Delta T)t-B/t \qquad (4.5)$$

where A and B are now apparatus constants for a given viscometer. The term $(1+a\Delta T)$, where a is the coefficient of linear expension of glass, takes account of change of length of viscometer between the reference temperature (taken as 313.15 K) and the experimemtal temperature while the term $(1-\rho_v/\rho)$ is a buoyancy correction term. The vapour density can be calculated from the ideal gas law and a knowledge of the vapour pressure of the liquid.

It has previously been known [145] that almost 0.5% error may occur if the viscometer is calibrated with water and used for the determination of viscosity coefficients of organic liquids. This discrepency may be attributed to surface tension effects and can be avoided by calibrating the viscometer with organic liquids.

4.2.3 USING THE VISCOMETER

Before use, the viscometers were cleaned with chromic acid solution, washed with distilled water, rinsed with Analar acetone and dried on a vacuum line. Liquid mixtures were prepared by weighing the components into a bottle with a tight fitting top, the less volatile component being added first. Mixtures were transferred to the viscometer as quickly as possible to minimise composition change. To avoid any material entering the viscometer which could block the capillaries, the viscometers were filled using a syringe fitted with a Millipore filter (type FH, pore size 0.5 micron). The liquid in the viscometers was frozen at liquid nitrogen temperature, and the air pumped out before the viscometer was sealed and mounted in the constant temperature bath.

The viscometers were mounted on stands attached to the lid of the bath, a Townson and Mercer model E270 Series III, filled with water. The experimental arrangement is shown in fig. 4.2. Temperatures were measured to ±0.02 K by an NPL calibrated Zeal total immersion mercury-in-glass thermometer (No.9566). The viscometers were first inverted to fill the top reservoir bulbs then returned to the position shown in fig. 4.1 where liquid fell under gravity into bulb

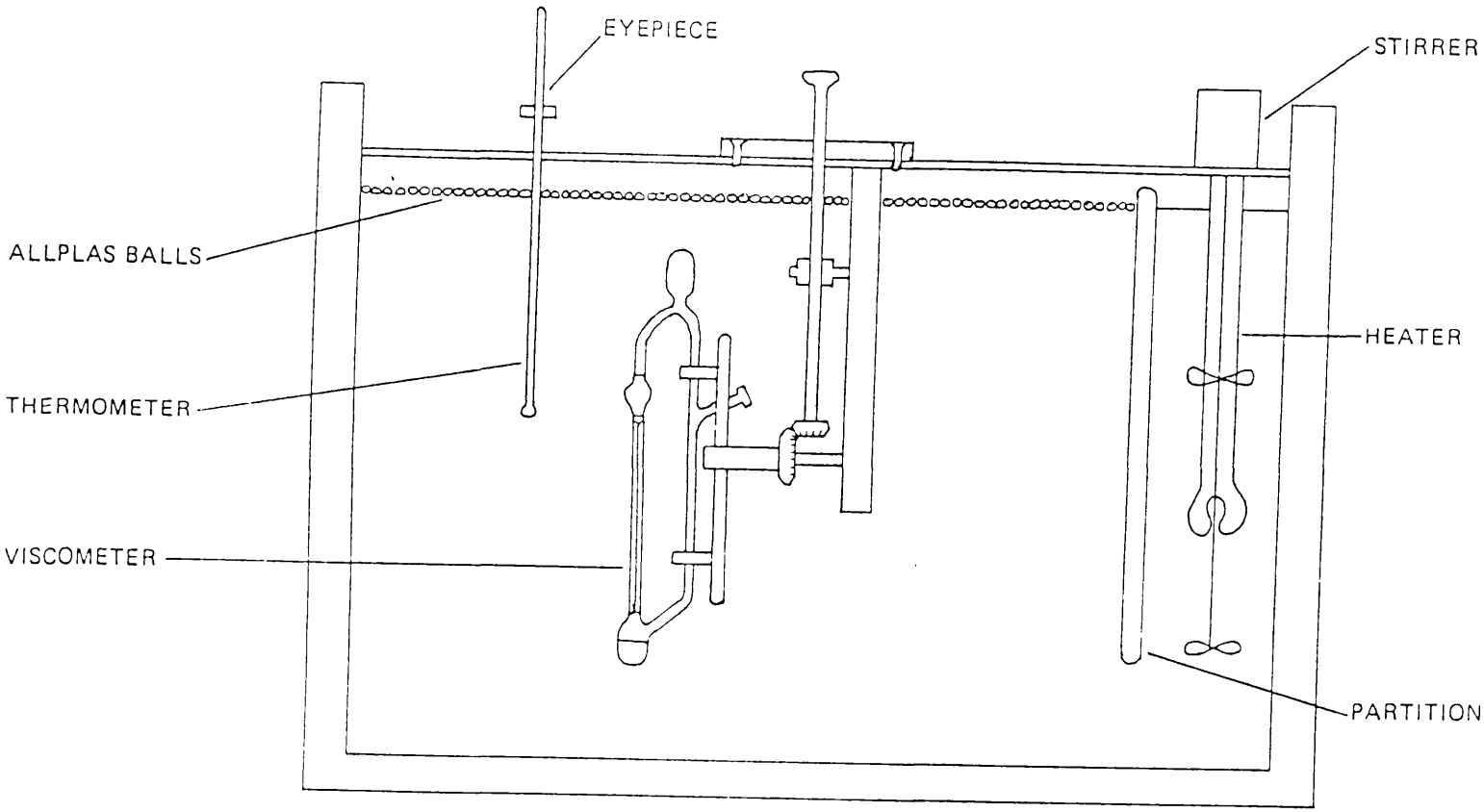

Fig 4.2 Temperature bath for capillary viscometer

D . The viscometers were aligned vertically by reference to a plumb line.

The time taken for the liquid meniscus to move from the upper mark X to the lower mark Y was measured for each viscometer to the nearest 0.1 s using a Junghans stopwatch or Racal Instrument Universal Counter 9835. Measurements could be made as often as required by inverting the viscometer and repeating the procedure outlined above. In practice readings were taken until three consecutive determinations agreed to within ±0.1% of their mean. The quoted kinematic viscosity coefficients are the average of the results of two viscometers with different capillary bore sizes.

Viscometers designated 1, 2 and 3, used in this work were calibrated by Young [139] using benzene, cyclohexane and n-dodecane. Viscometers No. 1 and 2 were calibrated in the kinematic viscosity range 0.46 to 3.97 cSt while viscometer No. 3 was calibrated up to 1.82 cSt. Flow times were measured for benzene, cyclohexane and n-dodecane and using the apparatus constants determined by Young [139] the calculated kinematic viscosity coefficients were found to be in excellent agreement with the measurements of Young and literature values within the estimated uncertainty of ±0.5% as shown in Table 4.2. No change to the apparatus constants reported by Young was therefore considered necessary. The kinematic viscosity coefficients of n-hexane and acetonitrile are less than the lower limit of the viscometer calibration range, but using the same apparatus constants, kinematic viscosity coefficients can be calculated with an uncertainty not exceeding 1%. (Young[139]).

4.3 MEASUREMENT OF DENSITY

4.3.1 DESCRIPTION OF DENSIMETER

Density measurements at saturation pressure have been made using a vibrating tube densimeter for acetonitrile, three binary mixtures of toluene plus acetonitrile, three binary mixtures of toluene plus n-hexane and the ternary equimolar mixture of n-octane plus i-octane plus oct-1-ene.

An ANTON PAAR DMA 45 Calculating Digital Densimeter was used. The measuring principle of this instrument is based on the change in the natural frequency of oscillation as a function of the total mass of the oscillator. The sample cell is a U- shaped glass tube surrounded by an outer jacket through which water could be circulated to provide temperature control. The U-tube is excited by an electro-mechanical oscillator and a signal is produced from which the period of oscillation can be determined. If the appropriate constants have been stored then density can also be displayed digitally.

4.3.2 DENSIMETER THEORY

The period of oscillation τ of a hollow body of mass M and volume V filled with fluid of density is given by [146,147]:

$$\tau = 2\pi \sqrt{(M+\rho V)/k} \qquad (4.6)$$

where k is the "spring constant". This can be rearranged to give

$$\rho = (T^2-B)/A \qquad (4.7)$$

with $A = 4\pi^2 V/k$ and $B = 4\pi^2 M/k$ (4.8)

In principle, density measurements could be on an absolute basis if k, M and V could be determined with sufficient accuracy. In practice, however, A and B are regarded as instrument constants and determined by calibration with fluids of accurately known density. The instrument constants A and B are temperature dependent due to both the temperature dependence of the modulus of elasticity and the thermal coefficient of expansion of the sample cell, and also vary with time, presumably due to slight changes in the mass of the cell and variation in the "spring constant" due to ageing.

4.3.3 USING DENSIMETER

Before using the sample cell, it was washed with distilled water, followed by Analar acetone and dried by compressed air. The cell was thermostated by circulating water from a flask in an Electrothermal bath. The bath temperature was monitored by a Lauda R46 digital thermometer. Fluid temperatures are estimated to be accurate to $\pm$0.03 K.

The sample was introduced to the cell by means of a syringe and a blanking plug used to seal the other port to prevent composition changes for mixtures due to vapour loss. Care was taken to avoid air bubbles being trapped in the system.

4.3.4 DENSIMETER CALIBRATION

The densimeter was calibrated with distilled water and air. If ρ_w and ρ_a are the densities of water and air, τ_w and τ_a are corresponding periods then equation 4.7 can be solved to give

$$A = (\tau_w^2 - \tau_a^2)/(\rho_w - \rho_a) \qquad B = \tau_w^2 - A\rho_w \qquad (4.9)$$

The density data for water and air were taken from the instruction manual of the instrument. The densimeter was calibrated at each temperature and for each liquid. There was a slight change in the apparatus constants from time to time, so the calibration was carried out prior to each set of measurements. The densities are estimated to be accurate to better than ± 0.3 kg/m^3 at temperature up to 348 K as shown in Table 4.3

4.4 RESULTS

Viscosity coefficients and density data are presented for three binary mixtures of toluene plus acetonitrile, three binary mixtures of toluene plus n-hexane and a ternary equimolar mixture of n-octane plus i-octane plus oct-1-ene at saturation pressure in the temperature range 298 to 373 K. Kinematic viscosity coefficients have been measured using modified suspended-level viscometers and density measurements are made using a vibrating tube densimeter. From these data, dynamic viscosity coefficients have been calculated.

The acetonitrile, toluene and n-hexane were Aldrich HPLC 99+% grade

Table 4.3

COMPARISON OF EXPERIMENTAL DENSITIES WITH LITERATURE VALUES.

Compound	Temp T/K	Density Exp/kg m^{-3}	Density Lit/kg m^{-3}
Acetonitrile	298.15	776.7	776.5 (b), 776.0 (c)
	323.15	749.6	749.5 (b)
	348.15	721.3	722.0 (b)
n-Hexane	298.15	655.0	655.8 (a), 655.1 (b) 655.0 (h), 655.8 (i) 655.3 (j), 655.1 (m) 654.8 (n), 654.9 (o)
	323.15	632.0	631.5 (a)
Toluene	298.15	862.0	862.3 (a),(c) and (f) 862.2 (d) and (e)
	323.15	838.8	839.3 (a), 838.9 (d)
	348.15	814.9	816.2 (a), 814.8 (d)
Cyclohexane	298.15	773.8	773.9 (a),(j) and (m) 773.8 (h), 773.6 (l)
	323.15	750.1	750.1 (a), 749.7 (h)
	348.15	725.8	726.0 (a), 724.9 (h)
Benzene	298.15	873.4	873.7 (a) and (i) 873.6 (d),(e),(f),(k) 873.8 (g)
	323.15	847.0	846.9 (a), 846.8 (d)
	348.15	819.1	819.1 (a), 819.3 (d) 818.8 (h)

Literature data from:

(a) API tables [151]
(b) Kratz and Muller (1985) [154]
(c) Ritzoulis (1986) [150]
(d) Robertson (1983) [141]
(e) Hales and Townsend (1972) [155]
(f) Timmermanns (1965) [156]
(g) Glen (1985) [152]
(h) Young (1980) [139]
(i) Diaz and Nunez (1975) [157]
(j) Letcher (1975) [158]
(k) Radojkovie et al (1977) [159]
(l) Kiyahora and Benson (1973) [160]
(m) Alcart et al (1980) [161]
(n) Int. Data Series. 1973 [162]
(o) Chen and Zwolinski (1974) [163]

and at 298.15 K measured densities are in good agreement with the literature values (Table 4.3). The n-octane and oct-1-ene were purchased from B.D.H. Chemical Ltd., and had a stated purity of > 99.5% and > 99%, while i-octane was purchased from Riedel - De Haen Ag Seelze-Hannover and had a stated purity of 99.5%. The chemicals were used without further purification.

The composition of mixtures in the viscometer will change as the temperature is increased due to differenecs in vapour pressure of the components. The change in composition can be calculated by finding the number of moles of each component in the vapour phase at each temperature and subtracting from the number of moles of each component originally present in the liquid phase. Raoult's Law was applied to calculate the number of moles of each component $n_i(G)$ in the vapour phase.

$$n_i(G) = x_i P_i V/RT \qquad (4.10)$$

where V is the volume of the vapour space, P_i is the vapour pressure of pure component i at temperature T, calculated from the Antoine equation [148], and x_i is the mole fraction of the component i in the liquid originally present. The true mole fraction of the component 1 in a binary liquid mixture is then given by

$$x_i = \frac{n_1(L) - n_1(G)}{n_1(L) - n_1(G) + n_2(L) - n_2(G)} \qquad (4.11)$$

where n_i (L) is the number of moles originally present in the liquid phase and n_i (G) is the number of moles in the vapour phase, calculated from equation 4.10.

The maximum change in the composition was observed for the toluene plus n-hexane mixture with 0.75 mole fraction of n-hexane, where a mixture with 0.7501 mole fraction of n-hexane at 298.15 K becomes a mixture with 0.7493 mole fraction of n-hexane at 348.15 K, while the maximum change in the mole fraction of acetonitrile in the toluene plus acetonitrile mixtures from 298.15 to 348.15 K was only 0.0002. Such a small change in composition has a negligible effect on the measured viscosity coefficients, hence composition corrections were not applied. Since the densimeter is a closed system with no vapour space this problem is not encountered in density measurements.

The kinematic viscosity coefficients along with density and calculated dynamic viscosity coefficients for the systems studied are tabulated in Table 4.4, and compared with literature values where available in Table 4.5.

The viscosity coefficients for acetonitrile plus toluene have been measured by Friedel and Ratzsch [149] at 293 K and Ritzoulis et al. [150] at 288, 298 and 308 K as a funtion of composition. A comparison of the present measurements with these literature values is shown in fig. 4.3. The measurements of Friedel and Ratzsch are at a low temperature of 293 K but are much as expected from consideration of our results at 298 and 323 K, however the results of Ritzoulis et al. disagree totally with the present measurements. Their results at 288 and 308 K have a similar composition dependence to the curve shown at 298 K. It seems that they have miscalculated the composition of the mixtures. This is supported by the fact that at 298 K their viscosity coefficient and density at 0.8397 mole

Table 4.4

DENSITY AND VISCOSITY COEFFICIENTS OF MIXTURES

Mole fraction of toluene	Temp T/K	(η/ρ) /cSt	Density ρ/kg m^{-3}	η /mPa s
	(a) Toluene + acetonitrile			
0.000	298.15	0.4387	776.7	0.3406
	323.15	0.3631	749.6	0.2722
	348.15	0.3091	721.3	0.2229
0.250	298.15	0.4846	812.0	0.3935
	310.65	0.4327	799.2	0.3458
	323.15	0.3918	786.1	0.3080
	335.65	0.3574	772.4	0.2761
	348.15	0.3281	759.2	0.2491
	373.15	-	734.8*	0.2076*
0.500	298.15	0.5416	835.8	0.4527
	310.65	0.4809	823.5	0.3960
	323.15	0.4310	810.9	0.3495
	335.65	0.3904	797.8	0.3114
	348.15	0.3567	784.9	0.2800
	373.15	-	760.0*	0.2311*
0.750	298.15	0.5971	851.9	0.5087
	310.65	0.5258	840.1	0.4417
	323.15	0.4682	827.9	0.3876
	335.65	0.4231	815.2	0.3449
	348.15	0.3859	802.9	0.3099
	373.15	-	780.3*	0.2538*
	(b) Toluene + n-hexane			
0.250	298.15	0.4602	699.7	0.3232
	310.65	0.4179	688.4	0.2877
	323.15	0.3801	676.9	0.2573
	335.65	0.3490	664.2	0.2318
	348.15	0.3213	651.5	0.2093
	373.15	-	623.9*	0.1766*
0.500	298.15	0.4957	748.6	0.3711
	323.15	0.4057	726.0	0.2945
	348.15	0.3431	701.9	0.2397
	373.15	-	678.8*	0.2021*
0.750	298.15	0.5497	802.2	0.4410
	310.65	0.4900	791.0	0.3876
	323.15	0.4430	778.8	0.3450
	335.65	0.4013	767.1	0.3078
	348.15	0.3668	754.9	0.2769
	373.15	-	729.9*	0.2305*

* Extrapolated values

Table 4.4 (continued)

DENSITY AND VISCOSITY COEFFICIENTS OF MIXTURES

Temp T/K	(η/ρ) /cSt	Density ρ/kg m^{-3}	η /mPa s
	Ternary Equimolar mixture of n-octane + i-octane + oct-1-ene		
298.15	0.9770	698.8	0.6827
323.15	0.7938	679.0	0.5390
348.15	0.6709	657.4	0.4411
373.15	-	634.2*	0.3672*

* Extrapolated values

Table 4.5

COMPARISON OF (TOLUENE + N-HEXANE) DENSITY AND VISCOSITY COEFFICIENTS WITH LITERATURE VALUES (a) at 298 K.

Mole fraction of toluene	ρ(Exp) /kg m^{-3}	ρ(Lit) /kg m^{-3}	η(Exp) /mPa s	η(Lit) /mPa s	Diff/ %
0.00	655.0	654.9	0.2979	0.2958	0.7
0.25	699.7	699.1	0.3232	0.3258	0.80
0.50	748.6	747.8	0.3711	0.3720	0.24
0.75	802.2	801.7	0.4410	0.4420	0.23
1.00	862.0	861.5	0.5521	0.5530	0.16

(a) Ghai and Dullien [131]

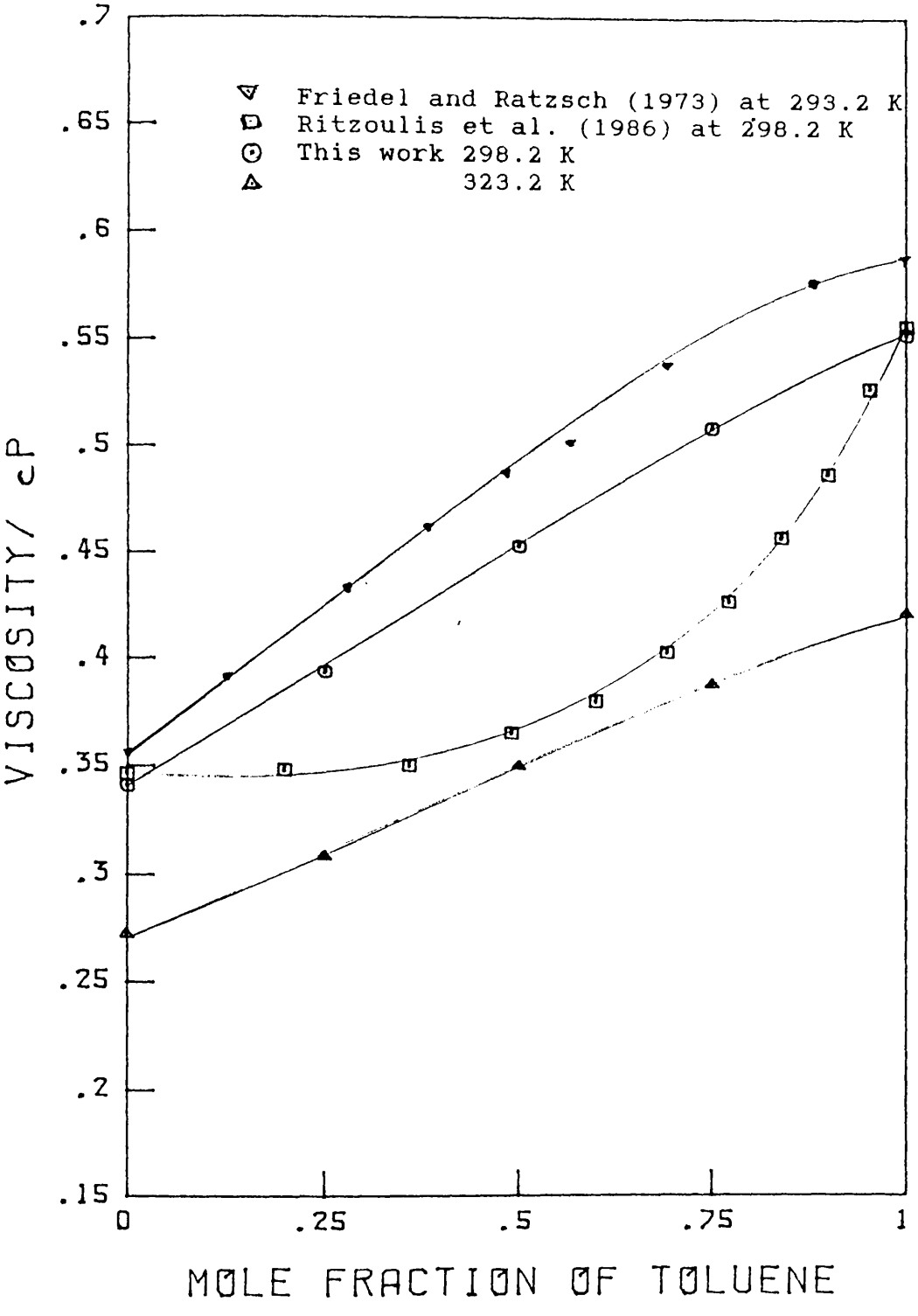

fig.4.3

Comparison of Viscosity Coefficient for x Toluene + (1-x) acetonitrile with Literature Values.

fraction of toluene are 0.457 cP and 0.8362 g/ml which are comparable to the viscosity and density determined in the present work at the equimolar mixture composition, being 0.4526 cP and 0.8358 g/ml.

The viscosity coefficients and density measurements have been reported at 298.15 K for toluene plus n-hexane mixtures as a function of composition by Ghai and Dullien [131] . The densities reported in this work are in excellent agreement with their values, the maximum difference being 0.1%. The viscosity coefficients are in good agreement within the combined uncertainty, the maximum difference being only 0.8%.

4.5 DENSITY AND VISCOSITY COEFFICIENT MEASUREMENTS AT ELEVATED PRESSURES.

Viscosity coefficients at elevated pressures were obtained using a high pressure self-centering falling body viscometer at the National Engineering Laboratory, East Kilbride, Glasgow. This apparatus was built and used by Isdale [164] for the investigation of the pressure dependence of viscosity coefficients of certain pure liquids at temperatures from 298 to 373 K up to 500 MPa and subsequently used by Young [139], Robertson [141], Glen [152] and Malhotra [63] for pure liquids as well as liquid mixtures over the same temperature and pressure range. A number of mechanical and electrical improvements, including pressure and temperature control and measurement, redesigning of the detection system and incorporating a micro processor based data logging system were made and described in detail

by Glen [152]. The corresponding density data, required for buoyancy correction, were obtained using a bellows volumometer.

4.5.1 PRESSURE GENERATION, CONTROL AND MEASUREMENT.

The pressure vessel, intensifier body and gauge block were made of En 26 steel hardened to 1.2 GPa and mounted on self-aligning bearings as shown in fig. 4.4, enabling them to be rotated through more than 180°. Further detail of design and construction of the pressure vessel is given by Isdale [164].

The pressurising system consisted of an air pump, hydraulic fluid reservoir, pressure intensifier, pressure block with release valve and pressure vessel immersed in a constant temperature bath as shown in fig. 4.5.

Pressurising fluid (1:1 mixture of paraffin and Shell Tellus 27 oil) was pumped from the reservoir using a Madan Air hydro pump, supplied by an air line. Fluid was transmitted to the gauge block and pressure vessel through two pairs of non-return valves D and E on the intensifier body, with valve B and C open and valve A closed. Pressures up to 200 MPa were generated by this method and monitored by a dial gauge and the final pressure measured by a resistance gauge.

High pressures were generated using an intensifier. The system was first primed to 200 MPa as above to return the intensifier piston to its starting position. With valves B and C now closed and valve A opened, the fluid was pumped to the low pressure side of the

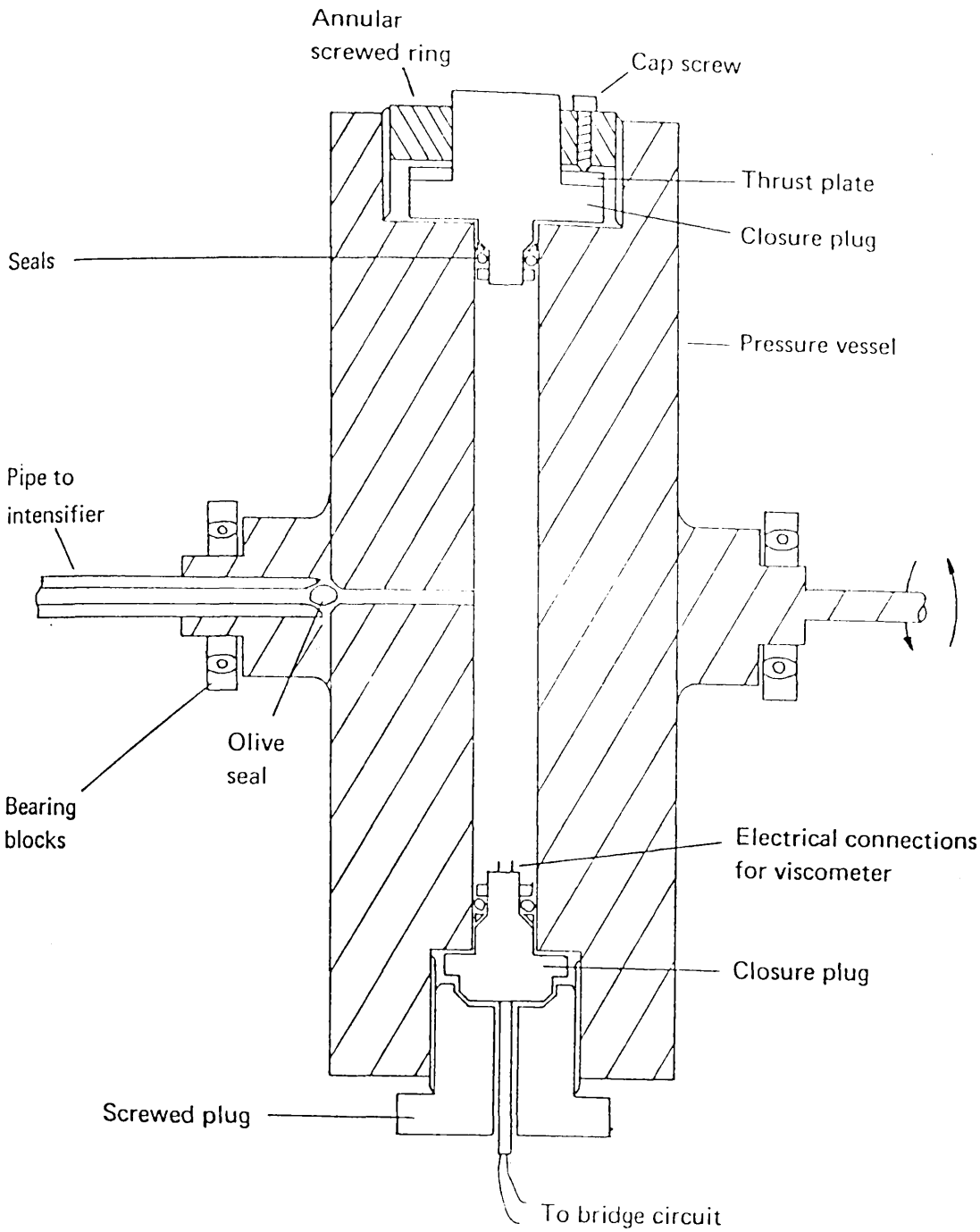

Fig 4.4 Pressure vessel

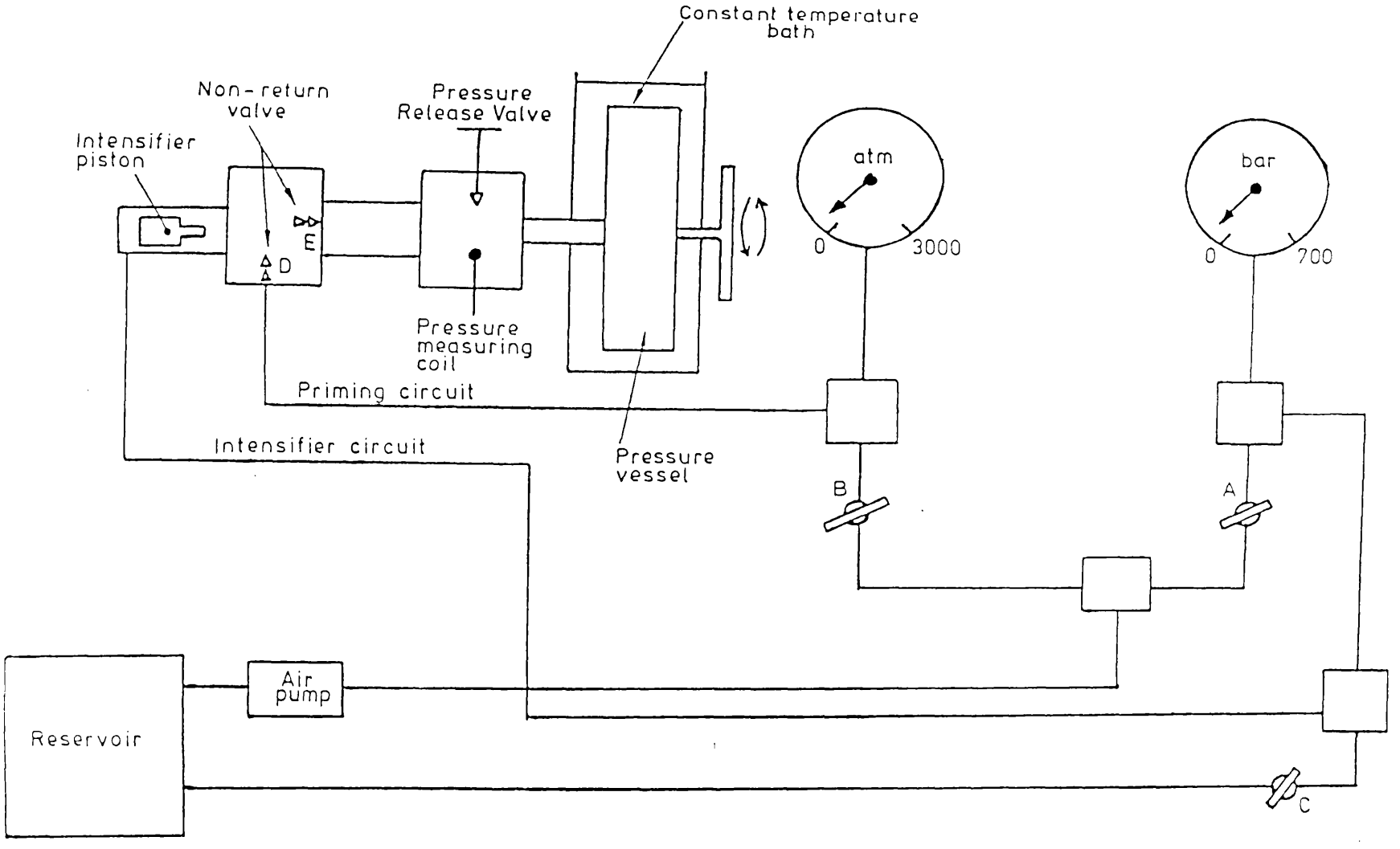

Fig 4.5 Schematic of pressurising system

intensifier piston. Each stroke of the intensifier piston raised the pressure by around 70 MPa. The piston was returned to the starting position by the priming procedure and the process repeated until the desired pressure was obtained. The pressure could be released at any time by opening the pressure release valve.

The pressure was measured by monitoring the change in the resistance of a coil of manganin wire immersed in the fluid in the pressure gauge block. The coil consisted of about 2.5 meters of 40 S.W.G. double silk covered wire, wound on a P.T.F.E. former. It had previously been stablised by subjecting it to temperature and pressure cycles and the pressure coefficient of resistance determined by Glen. Although the temperature coefficient of resistance is known to be very small in the region around room temperature [165], Glen [152] attemptted to take account of temperature variations from run to run, by incorporating a thermocouple and a platinum resistance thermometer in the gauge block. The thermocouple reference junction consisted of a well-stirred ice bath in a Dewar flask close to the gauge block. The manganin gauge was previously calibrated against a Budenberg free-piston deadweight pressure balance over the pressure range 0.1 to 600 MPa.

Since the atmospheric resistance of the manganin wire changes continually during use [164-166], possibly due to continual immersion in pressurising fluid, the atmospheric pressure resistance was measured before each pressurisation and the effect was eliminated by using an equation of the form

$$P = A + B(R-Ro-R') + C(R-Ro-R')^2 \qquad (4.12)$$

where A, B, and C are contants, R and Ro are resistances at pressure P and atmospheric pressure. R' is a correction for change in resistance due to temperature change. The overall accuracy was found to be better than ±0.2% for pressure above 100 MPa, Dymond et al. [168].

4.5.2 TEMPERATURE CONTROL AND MEASUREMENT.

The pressure vessel was immersed in heating oil, Marlotherm S oil, in the oil bath, which was insulated on all sides by a layer of fibreglass and, to minimise the heat loss from the surface, was covered by a double layer of Allplas insulating spheres. The temperature of the bath oil was maintained and controlled by six 1 kW mineral insulating heaters, four of which could be used as boosters, as shown in fig. 4.6. The oil was thoroughly mixed to keep the temperature uniform by means of four stirrers. Temperature control was found to be better than ±0.03 K but the temperature variation inside the pressure vessel would be much smallar than this due to very high thermal inertia of the pressure vessel.

The bath temperature was measured by two metal sheathed Rosemount platinum resistance thermometers immersed in the oil bath close to the pressure vessel and interfaced to a data logging system. The thermometers were previously calibrated to IPTS-68 standard by measuring their resistance at the ice point, steam point and one intermediate point and were found to give the temperature with an uncertainty not exceeding ±0.02 K, Glen [152].

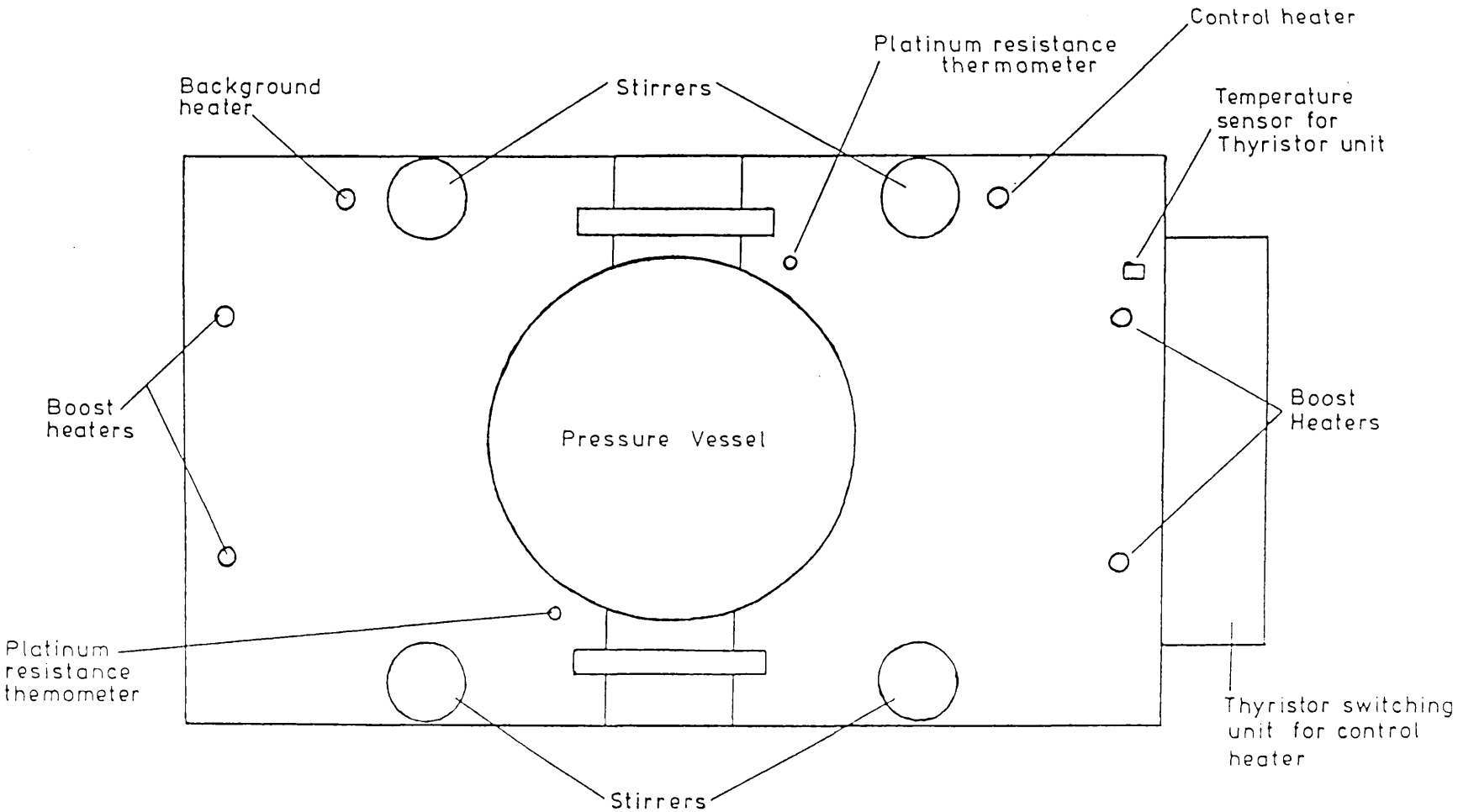

Fig 4.6 Top view of temperature bath

4.5.3 DENSITY MEASUREMENTS AT ELEVATED PRESSURE.

The simplest and the most widely used method for density measurements at high pressure is by using a bellows volumometer [169-172]. The flexible metal bellows is filled with the liquid under test with a known mass at atmospheric pressure and then its change in length as a function of pressure is measured. The bellows was made of stainless-steel, had a volume about 12 cm^3 and uncompressed length of 12 cm. Prior to filling, it was washed with Analar acetone and dried in hot air hanging upside down. After cooling and sealing with "Dowty" bounded seal it was weighed, then opened and the sample was introduced by means of a syringe, fitted with a Millipore filter (0.5 micron). The bellows was compressed and stretched for a few times to eliminate trapped air , topped up with liquid and resealed. The outer surface of bellows was cleaned and dried and the bellows re-weighed. The experimental set-up is shown in fig. 4.7.

One end of the bellows was screwed to a rigid housing which ensured linear movement. A length of non-magnetic stainless-steel rod was screwed into the free end of the bellows, with a small piece of ferrite at the tip, projected through the end cap of the pressure vessel into a length of non-magnetic high pressure tubing which was sealed at its extremity. A coil block containing a pair of coils, which could be moved along the length of the tube to detect the position of the ferrite tip, was attached to the high pressure tubing. The previously used detection system was modified by Glen [152] and later Dymond et al. (1988) incorporated a stepping-motor drive (BENTHEM, SMD3B/IEEE) controlled by a microcomputer for coil block movement, and a Capacitance Displacement Transducer (CDT) for

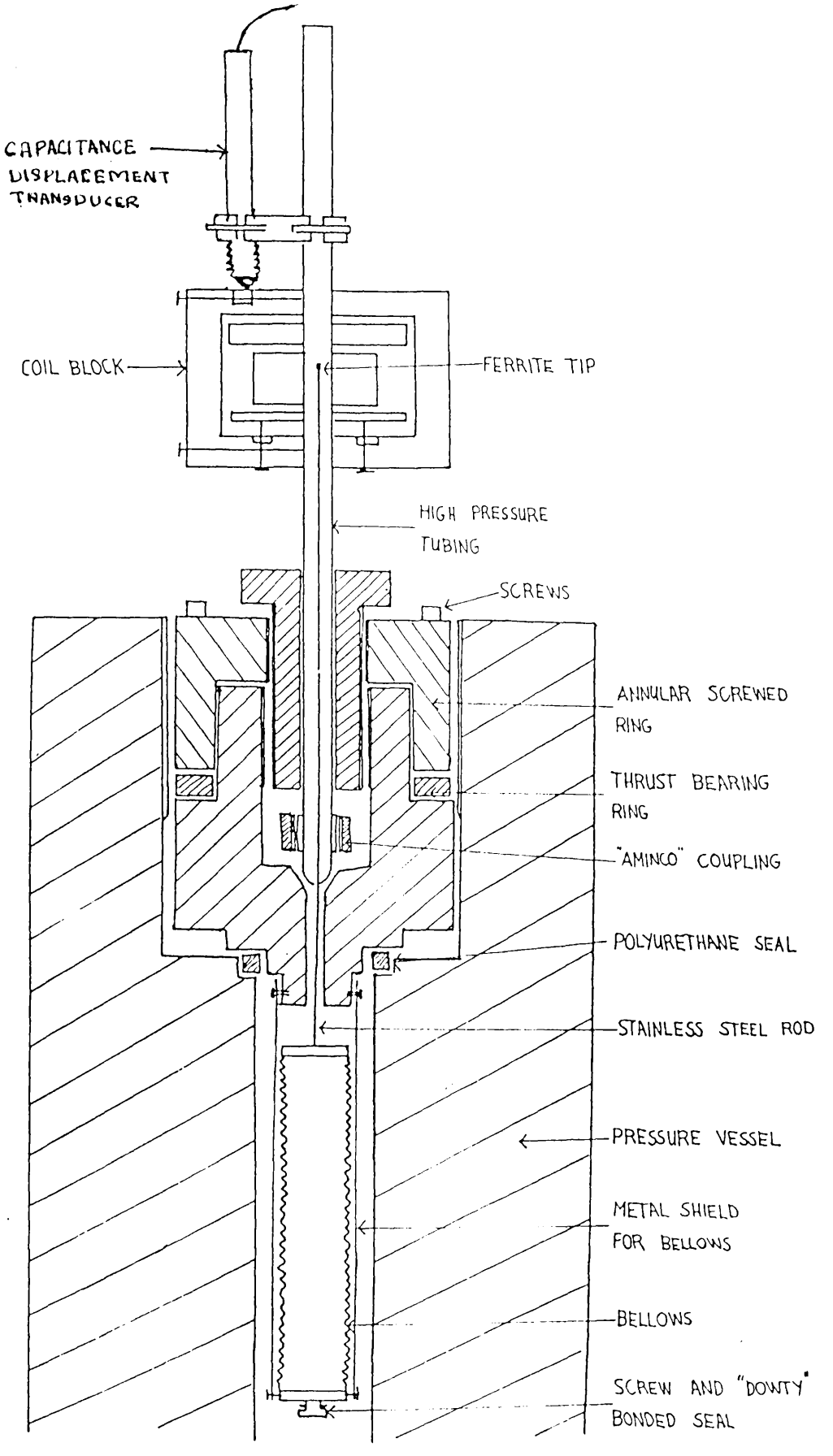

FIG. 4.7 FORM OF APPARATUS USED TO MEASURE DENSITIES AT ELEVATED PRESSURES.

more accurate measurements of the change in the length of bellows with pressure.

The bridge was initially balanced with the coil remote from the tip position. The approximate tip location was then obtained by observing the out-of-balance signal from the bridge of an oscilloscope and looking for a maximum. The coil block was moved to about 1 mm above the approximate tip position then stepped down in 15 equal steps. At each step, the bridge voltage was measured by a Digital Volt Meter (DVM). A polynomial was fitted to bridge voltage in position, from which the maximum could be obtained by differentiation. A minimum of three repeats were made at each pressure and the position of the maximum agreed to within ±0.003 mm in general. The same procedure was repeated at each pressure until the desired pressure range was covered or freezing was observed.

The bellows were initially pressurised for a few minutes to several MPa, to dissolve any air or vapour bubbles which would affect the atmospheric-pressure reading. The coil displacements were determined at approximately 20 MPa intervals from 100 to 20 MPa, with a further two determinations at about 10 and 5 MPa, to establish the coil position at atmospheric pressure by extrapolation of the CDT potential differences at higher pressures. Generally the extrapolated CDT p.d. agreed with the measured value at atmospheric pressure within ±0.01 volt.

4.5.4 CALIBRATION OF APPARATUS.

Density at pressure P can be calculated from the atmospheric pressure

density ρo and mass of the liquid M in the bellows using the equation

$$\rho(P) = M/((M/\rho o)-A.\Delta l) \qquad (4.13)$$

where A is the cross-sectional area and Δl is the change in the length of bellows from atmospheric pressure to pressure P. In term of CDT potential difference

$$\Delta l = (E(P)-E(Po))f \qquad (4.14)$$

where E(P) is CDT voltage at pressure P and f is a conversion factor obtained by calibration of CDT voltage against displacement. Full details of the calibration procedure are given by Young [1 ?]. The following equation was used to calculate the densities at high pressures.

$$\rho(P) = M/(M/\rho o-AO(1+2\alpha(T-Tr))(E(P)-E(Po))f) \qquad (4.15)$$

where AO is the bellows area at reference temperature Tr and α is the coefficient of linear expansion of the steel.

The bellows was calibrated with water at 303.15 and 343.15 K and toluene at 298.15 K, Dymond et al. [1 ?]. Density measurements for n-heptane at 298.15 K and 310.65 K at pressure up to 270 MPa were found to agree with literature values to well within the estimated uncertainty of ±0.2%.

4.5.5 ACCURACY OF DENSITY MEASUREMENTS.

The accuracy of measured density depends upon the accuracy in the measurements of temperature, pressure, liquid mass in the bellows, atmospheric pressure density and the cross sectional area of the bellows. Error in measured density can be estimated by considering the maximum uncertainty in each of these parameters. As an example, the measured density of the equimolar mixture of toluene plus n-hexane at 348.35 K and at 522.7 MPa is 917.1 kg/m^3. The mass of the liquid in the bellows was 8.3787 g, the extrapolated CDT voltage was 1.623 V at atmospheric pressure while the measured value at 522.7 MPa was 6.8383 V, and the atmospheric pressure density was 701.7 kg/m^3.

The mass of liquid could be measured to ±0.0003 g but because of possible adsorption of atmospheric moisture a better estimate is ±0.001 g, producing an uncertainty of ±0.004% in density. The extrapolated CDT voltage was within ±0.01 V of the experimental value, hence at the most, ±0.059% error would be introduced in the density using the extrapolated value. The high pressure CDT voltages were within ±0.001 V of the mean, introducing a possible error of ±0.006% in the measured density. The atmospheric pressure density was accurate to ±0.3 kg/m^3. The contribution from such a variation to the density at elevated pressure would be ±0.056%. An error of 0.002 cm^2 in the cross-sectional area of the bellows adds an error of ±0.034%. An uncertainty of 0.1 K in the reference temperature contributes ±0.00004% to density while an error of 0.03 K in experimental temperature leads to an error of ±0.00003%. Contribution of error due to error in the coefficient of linear expansion of steel would be ±0.006%. The sum of the absolute errors is thus 0.16% while the square root of the sum of the squares of the errors is ±0.09%. In addition to these, an error of ±0.02 K in the measured temperature

leads to an error of ±0.027% in absolute density, while an error of ±0.5 MPa in pressure will produce an uncertainty of ±0.09% in the measured density. The maximum error will lie somewhere in between ±0.13% to ±0.28%. It is therefore concluded that densities at elevated pressures normally should be accurate to better than ±0.2%.

4.6 DESCRIPTION OF HIGH PRESSURE VISCOMETER.

The self-centering falling-body viscometer consisted of a viscometer tube, sinker, plug and end cap. All of these components were made from the same material (En 58 J non-magnetic stainless steel) to minimise compressibility, thermal expansion and magnetic effects. The sinker was a small cylinder having a hemispherical nose at one end and a cavity at the other end into which a small piece of ferrite core could be fitted. The sinker had an approximately 1.42 cm length and 0.7465 cm outer diameter. The viscometer tube bore was 0.7620 cm in diameter and deviated from circularity by less than 0.0005 cm. The viscometer tube and sinker have their surfaces finished to 0.13 micron.

The pressure was transmitted to the liquid by means of approximately 10 cm length of collapsible P.T.F.E. tubing attached to one end of the viscometer tube. The viscometer used throughout this work was a modified version of those used earlier by Young and Robertson, redesigned and described in detail by Glen [1]. However a different tube/sinker combination was employed. The complete viscometer assembly is shown in fig.4.8.

4.6.1 EXPERIMENTAL METHOD.

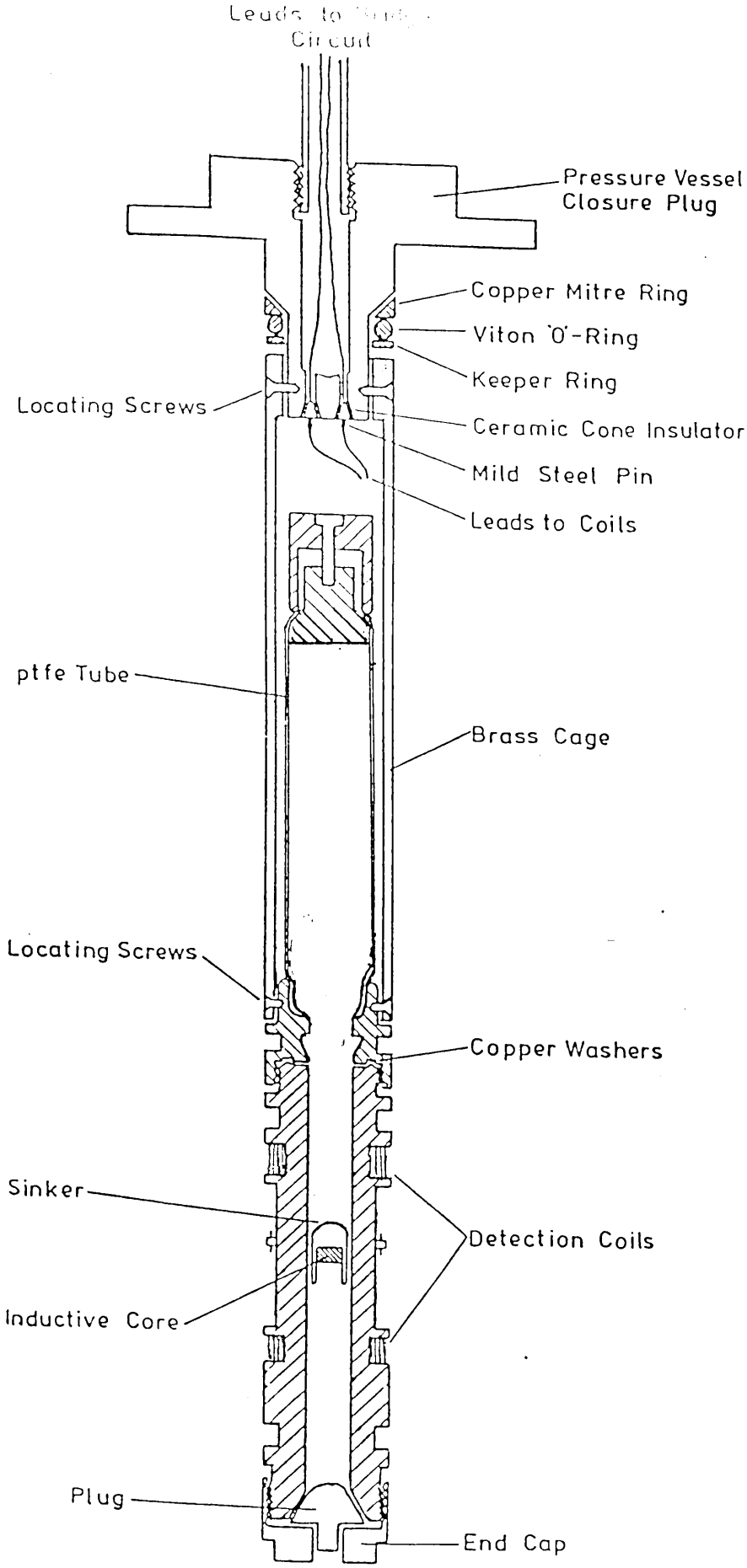

Fig 4.8 Schematic of viscometer

Prior to filling, the individual components of the viscometer were thoroughly washed with Analar acetone, followed by the liquid under test. Approximately 10 cm length of 1 cm diameter P.T.F.E. tube was straightend by heating. One end of this tube was mounted on to the viscometer and made leak tight by heating with a heat gun. On cooling the nut was tightend. The other end was sealed by means of a cap and screw. The viscometer was held vertically in a clamp and liquid under test was injected from a syringe fitted with a Millipore filter. After rinsing twice, the viscometer was filled and trapped air bubbles were expelled by agitation and squeezing the P.T.F.E. tube. The cavity of the sinker was filled with liquid under test and care was taken to have no air bubbles in the cavity. The mark on the ferrite core was aligned to the mark on the edge of the viscometer tube and the sinker was carefully dropped in to the viscometer with the hemispherical nose leading. The viscometer was sealed with an "O" ring and end plug and finally the end cap was finger-tightened. The P.T.F.E. tube was again squeezed and checked for leakage, the viscometer was opened, topped up with liquid if necessary and again sealed. Electrical connections were then made and the whole assembly lowered into the pressure vessel. The electric plug closure was tightend and checked for pressure leakage.

Pressure was generated, controlled and measured in the same manner as described in section 4.5.1. During the viscosity measurements, one of the six heaters burned out and was replaced by a 2 kW rating heater. This influenced the temperature fluctuations slightly and the largest observed fluctuation in temperature was ± 0.05 K. The temperature control and measurements are as described in section 4.5.2.

4.6.2 MEASUREMENTS OF FALL TIME.

The terminal velocity of the sinker is determined by measuring its fall time between the two coils wound on the outside of the viscometer. These two coils form the active arm of the bridge as shown in fig. 4.9. The other three arms of the bridge are remote from the viscometere. The bridge is balanced externally before any measurements were taken, with the sinker remote from either coil. As the sinker approaches the coil, an out-of-balance signal is observed due to change in induction. This out-of-balance signal is amplified and converted to a DC signal like that shown in fig. 4.10. The signal first rises and then falls then rises and falls again, triggering the timer at the maximum of the first peak and stopping it at the maximum of the second peak. The self check routines and sub-routines provided in the programme to control the data logging system eliminate false triggering caused by electronic noise. The data logging system is described in detail by Dymond et al. [1] .

The pressure vessel is inverted and time is measured for the backward fall of sinker (open end leading). Before measuring the forward fall-time again, the sinker is allowed to fall in the reverse direction for a time double the backward fall-time. This ensured that the sinker would reach its terminal velocity in the forward direction before reaching the first coil and that it would be falling centrally (Isdale and Spence [1]).

Several fall-time measurements were made at each pressure until the standard deviation of the mean, expressed as a percentage of the

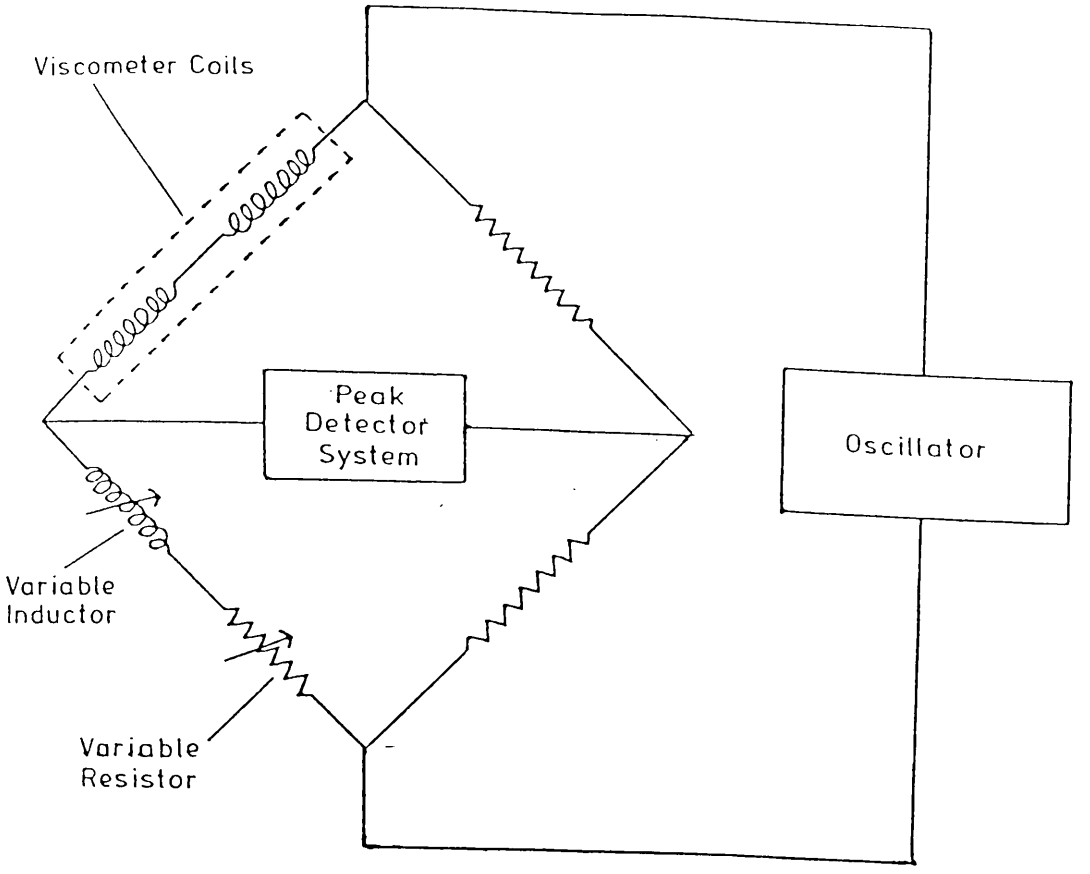

Fig 4.9 Bridge circuit

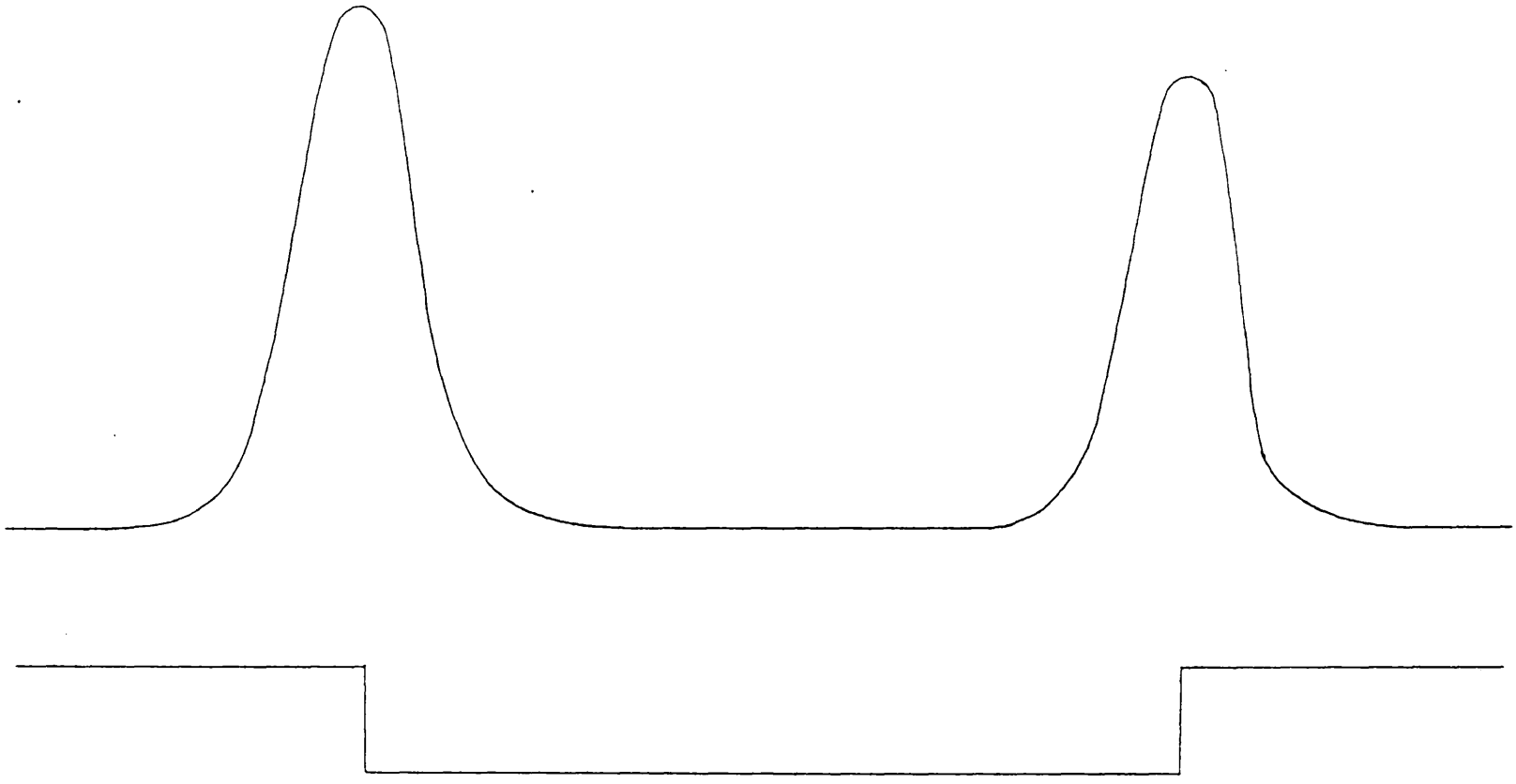

Fig 4.10 D. C. trace

mean, for the three measurements was within ±0.5%. When the required number of measurements have been taken, the pressure was changed and at least fifteen minutes allowed for equilibrium before measuring any new fall-time. The bath temperature was changed at the end of each day's measurements and allowed to stabilise overnight before measurements were made at the next temperature.

Atmospheric pressure fall time measurements were repeated for a few liquids to check the reproducibility of the fall-time. For example, for 0.25 mole fraction of toluene in toluene plus n-hexane mixture at 298.3 K fall times were reproducible to ±0.2%. For the same mixture at 323.2 K and a pressure of 25.6 MPa, the reproducibility was found to be ±0.25%, while for the equimolar mixture of the same components at atmospheric pressure the reproducibility was ±1.1% and ±1.2% at 348.2 and 373.2 K respectively. Fall time was reproducible to ±2.1% at 323.3 K for 0.75 mole fraction of toluene in toluene plus n-hexane mixture, while two sets of measurements agreed within ±0.5% at 348.4 K. Similarly, toluene plus acetonitrile mixture with 0.75 mole fraction of toluene at 348.2 K have fall-times reproducible within ±1.0%. Viscosity measurements of toluene at 298.2 K were repeated and fall-times of the two sets agreed to 1.7%. It is therefore concluded that the reproducibility of the fall-time measurements is generally better then ±1.5%.

4.6.3 CALIBRATION OF VISCOMETER.

The solution of the equations of motion of a cylindrical sinker having mass m, density ϱ_s and radius r_1 falling with laminar flow down centre of a cylindrical tube of radius r_2, filled with liquid of

density ρl and having viscosity η leads to the result given below (Isdale 1[illegible]).

$$V = \frac{mg(1 - \rho l/\rho s)}{2\pi Ls\,\eta} \left[\ln\left(\frac{r2}{r1}\right) - \left(\frac{r2^2 - r1^2}{r2^2 + r1^2}\right) \right] \qquad (4.16)$$

where Ls is the length of the sinker. If the sinker falls a distance L in time t then subtituting V=L/t and rearranging, equation 4.16 can be written as

$$\eta = \frac{mg(1 - \rho l/\rho s)t}{2\pi Ls\,L} \left[\ln\left(\frac{r2}{r1}\right) - \left(\frac{r2^2 - r1^2}{r2^2 + r1^2}\right) \right] \qquad (4.17)$$

If the sinker and tube are made of the same material (as they were in this case) then equation 4.17 can be written as

$$\eta = \frac{t(1 - \rho l/\rho s)}{A\,[1 + 2\alpha(T-To)][1-3\beta(P-Po)]} \qquad (4.18)$$

where α and β are the temperature coefficient of linear expansion and compressibility of steel and A is called the viscometer constant, given by

$$A = \frac{2\pi Lso\,Lo}{mg\,\{\ln(r2/r1) - [(r2^2 - r1^2)/(r2^2 + r1^2)]\}} \qquad (4.19)$$

Lso and Lo are the values of Ls and L at the reference temperature (295.8 K) and at atmospheric pressure.

In principle, equations 4.17 and 4.18 could be used to calculate the viscosity coefficient from the fall time and dimensions of the viscometer. However, in the derivation of equation 4.17, the entry and exit effects as the liquid passes through the annulus between the

sinker and tube have not been taken into account. Although methods of calculating these effects are available for general shapes of sinker [175,176], they could not be applied to this system due to the smaller length-to-diameter ratio of the sinker. Further, the dimensions of the instrument cannot be determined with the required accuracy. Therefore, in practice, the instrument is calibrated using liquids of accurately known density and viscosity at atmospheric pressure.

The viscometer/sinker combination used throughout this work was calibrated by Dr. Rakesh Malhotra [ ] over the viscosity range 0.227 to 16.14 cP using Shell Vitrea No. 21 oil, n-octane, i-octane and n-hexadecane. The density and viscosity coefficients of Shell Vitrea oil and n-hexadecane were measured by Young [ ]. The density and viscosity values of n-octane were those of Robertson [ ], while required data for i-octane were taken from Glen [ ]. The density of the sinker was determined by weighing it in air and water. If Ma and Mw are the mass of sinker in air and water and ρ_w is the density of water at the same temperature then the density of sinker is given by

$$\rho_s = Ma\,\rho_w/(Ma-Mw) \qquad (4.20)$$

The density of the sinker at 295.8 K was found to be 7673 kg/m^3. The density of sinker at temperature T and pressure P was calculated from the density at the reference temperature and at atmospheric pressure as

$$\rho s = \rho so/[(1 + 3\alpha(T - To))(1 - 0.666\beta(P - Po))] \qquad (4.21)$$

where α and β have the same definitions as before. The fall times were measured for the calibrating liquids at atmospheric pressure

and, using equation 4.18, the experimental viscometer constant A was calculated. The data for the calibration of the viscometer is given in Table 4.6 and the viscometer constant A is plotted against buoyancy corrected fall time t^* equal to $t(1-\rho_L/\rho_s)$ in fig. 4.11. It can be seen that A is not constant and varies about 21% over this viscosity range. As the fall time decreases A increases rapidly indicating the flow of the liquid past the sinker is becoming non-laminar at low viscosity.

The experimental viscometer constant was fitted to an equation of the form

$$A = Ao\ [1 + (B/t^*)^n] \qquad (4.22)$$

with Ao, B and n obtained by optimisation. For this tube/sinker combination Malhotra [63]. obtained the following values

Ao= 19.05 s/cP

B= 2.20 s

n= 2.00

Equation 4.22 was fitted to 19 data points. The maximum deviation from the experimental A value was 1.65% with a mean deviation 0.8%, while r.m.s. percentage deviation was 0.95%.

It was found necessary to calibrate the viscometer in the range 0.16 to 0.227 cP for the present study. The viscometer was calibrated in the same way described above using densities and viscosities of acetonitrile, 0.25 toluene + 0.75 acetonitrile, 0.25 toluene + 0.75 n-hexane reported in this chapter in Table 4.4 and the data for n-hexane from Dymond et al. [62]. Experimental viscometer constant A' was fitted by a linear equation as

Table 4.6

DATA FOR CALIBRATION OF HIGH PRESSURE VISCOMETER.

Liquid	T/K	ρ/kg m^{-3}	η/mPas	t/sec	t^*/sec	A/s cP^{-1}
n-octane	298.15	698.5	0.5088	11.12	10.11	19.865
	323.15	678.1	0.3868	8.67	7.90	20.409
	323.15	678.1	0.3868	8.64	7.88	20.348
	348.15	657.0	0.3036	7.01	6.41	21.084
i-octane	298.15	678.8	0.4718	10.56	9.61	20.375
	323.15	666.7	0.3587	8.22	7.50	20.907
	348.15	644.4	0.2818	6.73	6.16	21.840
	348.15	644.4	0.2818	6.67	6.11	21.647
	373.15	621.2	0.2270	5.56	5.11	22.464
n-hexa-	298.15	770.2	3.0670	63.47	57.10	18.616
decane	323.15	752.9	1.8350	38.49	34.71	18.901
	348.15	735.8	1.2410	26.00	23.50	18.910
Shell	313.23	852.7	16.140	348.07	309.36	19.158
Vitrea	318.16	849.5	13.380	287.12	255.30	19.069
No.21	323.28	846.2	11.130	240.45	213.90	19.204
Oil	328.11	843.1	9.476	201.15	179.02	18.875
	333.10	839.8	8.095	174.74	155.59	19.200
	342.95	833.5	6.124	131.59	117.27	19.124
	353.15	826.8	4.729	100.91	90.01	19.004
Aceto-	348.16	721.3	0.2229	5.487	4.970	22.264
nitrile	373.18	693.8	0.1885	4.557	4.144	21.936
Mixture (a)	373.15	734.8	0.2076	5.127	4.635	22.278
Mixture	348.20	651.5	0.2092	5.200	4.758	22.710
(b)	373.20	623.9	0.1765	4.248	3.902	22.059
n-hexane	348.23	606.7	0.1912	4.705	4.332	22.624
	373.29	580.8	0.1602	3.823	3.533	22.006

(a) 0.25 toluene + 0.75 acetonitrile
(b) 0.25 toluene + 0.75 n-hexane

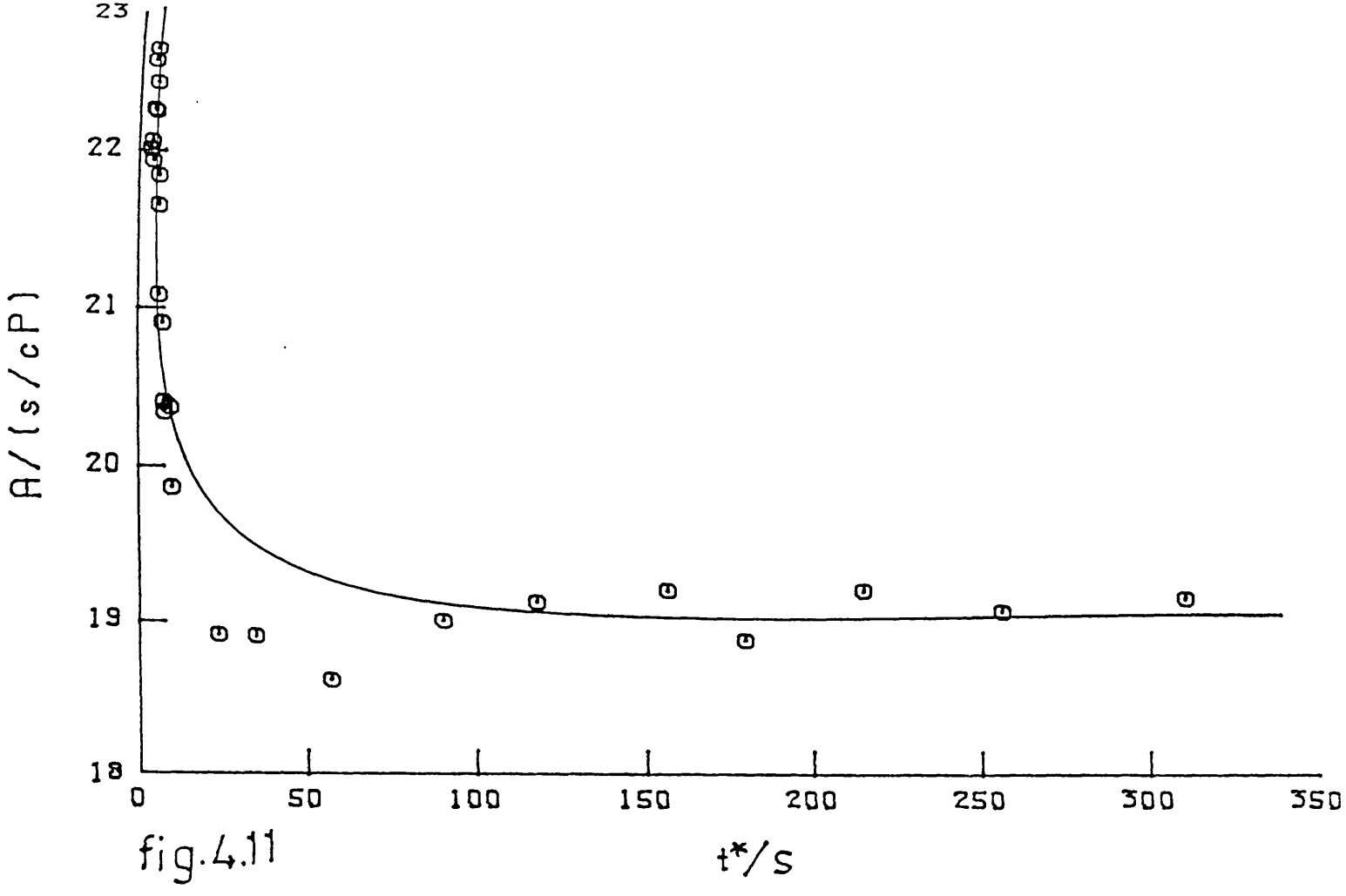

fig.4.11

Viscometer Calibration Curve

$$A' = 20.155 + 0.454t \qquad (4.23)$$

where t is now the actual fall-time. 7 points were fitted to equation 4.23, with a maximum deviation of 1.72%, the mean deviation being 1.0% while the r.m.s. deviation was ±1.2%. The experimental viscometer constant is compared with the fitted one in Table 4.7 over the whole viscosity range. This tube/sinker combination was thus calibrated over the viscosity range 0.16 to 16.14 cP.

4.6.4 CALCULATION OF VISCOSITY COEFFICIENTS.

There are two methods for calculating the viscosity coefficients from the measured fall time. The first method, the "direct" method uses equation 4.18 with the value of A from equation 4.22 or 4.23 depending upon the value of viscosity coefficient at atmospheric pressure. The second method or "ratio" method is applied when viscosity at atmospheric pressure is accurately known. Generally the ratio method is prefered because of less errors associated with it compared to the direct method. On some occasions, serious disagreements were observed between the atmospheric pressure viscosity obtained using the suspended-level viscometer and the falling body viscometer, therefore the direct method has been used in calculating high pressure viscosity coefficients reported in this work.

4.6.5 ERRORS IN MEASURED VISCOSITY COEFFICIENTS.

Errors in the measured viscosity coefficients can be estimated by considering the errors in each parameter of equation 4.18. The major contribution to the error was from the fall-time measurements and

Table 4.7

COMPARISON OF EXPERIMENTAL AND CALCULATED VISCOMETER CONTANTS FROM EQUATION 4.22 WITH Ao=19.05, B=2.2 and n=2.0

Liquid	A(exp) s/cP	A(fitted) s/cP	Deviation %
n-octane	19.87	19.95	+0.41
	20.41	20.53	+0.58
	20.35	20.53	+0.91
	21.08	21.29	+1.02
	21.17	21.28	+0.52
i-octane	20.38	20.05	-1.63
	20.91	20.69	-1.06
	21.84	21.48	-1.65
	21.65	21.52	-0.60
	22.46	22.58	+0.54
n-hexadecane	18.90	19.13	+1.19
	18.91	19.22	+1.62
Shell Vitrea No.21 oil	19.16	19.05	+0.54
	19.07	19.05	-0.10
	19.20	19.05	-0.77
	18.88	19.05	+0.92
	19.20	19.05	-0.76
	19.12	19.06	-0.33
	19.00	19.06	+0.32

Rms deviation=0.95%

COMPARISON OF EXPERIMENTAL AND CALCULATED VISCOMETER CONSTANTS FROM EQUATION 4.23

Acetonitrile	22.264	22.646	+1.72
	21.936	22.224	+1.31
0.25 toluene + 0.75 acetonitrile	22.278	22.483	+0.92
0.25 toluene + 0.75 n-hexane	22.710	22.516	-0.85
	22.059	22.083	+0.11
n-hexane	22.624	22.291	-1.47
	22.006	21.891	-0.52

Rms deviation= 1.20%

viscometer contant A. The factor containing the thermal expansion and compressibility term in equation 4.18 has a small value and the resultant error is negligible. It can be shown that the errors from uncertainty in densities are also very small. The overall contribution to uncertainty in the viscosity coefficient from all the parameters except fall time and viscometer constant is ±0.06%. The standard deviation of the fall time from the mean was generally within ±0.5%, contributing an uncertainty of ±0.5%. Similarly the contribution of uncertainty in the viscometer constant would be ±0.95% on the basis of the r.m.s. deviation of the fitted viscometer constant. The maximum contribution due to temperature fluctuations (±0.05 K) was observed for 0.25 toluene + 0.75 n-hexane mixture and was ±0.06%. For the same mixture, the pressure fluction at low temperature and pressure contributed ±0.62% uncertainty on the basis that the presure fluctuation was ±0.5 MPa during the measurements.

In addition to these, the measured pressure has an uncertainty of ±1 MPa, contributing a possible ±1.24% error in viscosity. The sum of the absolute errors is thus 3.43%. As stated in section 4.6.2 the reproducibility of fall time was found to be better than ±1.5%, hence the maximum error in measured viscosity coefficients could lie between 3.43% to 4.93%, and it is therefore concluded that viscosity coefficients reported here would be accurate to ±5.0%, and generally better than this.

CHAPTER 5

DENSITIES AND VISCOSITY COEFFICIENTS RESULTS FOR THE LIQUIDS AND BINARY LIQUID MIXTURES

5.1 DENSITIES AND VISCOSITY COEFFICIENTS AT ELEVATED PRESSURES.

Densities for one pure liquid, acetonitrile, three binary mixtures of toluene + acetonitrile, three binary mixtures of toluene + n-hexane, and one ternary equimolar mixture of n-octane + i-octane + oct-1-ene, and values of the isothermal secant bulk modulus at the same pressures and temperatures are presented in Tables 5.1 to 5.9.

Viscosity coefficients and densities at corresponding temperatures calculated using the Tait equation, are presented for acetonitrile, toluene, three binary mixtures of toluene + acetonitrile and three binary mixtures of toluene + n-hexane, in Tables 5.10 to 5.25

5.2 COMPARISON OF MEASURED DENSITIES OF ACETONITRILE WITH LITERATURE VALUES.

Densities, volume ratios, specific volumes and values of the isothermal secant bulk modulus have been reported in the literature at elevated pressures and temperatures for acetonitrile by Francesconi [177], Srinivasan and Kay [178], Schroeder [179], Landau and Wurflinger [180], Easteal and Woolf [181], [182], and Kratzke [154].The literature data have been converted to volume ratios in order to make a comparison with the present values, shown in fig. 5.17. The agreement is generally satisfactory. At 298 K, the present values are smaller than those of Srinivasan and Kay [178] with the difference increasing to 0.93% at 250 MPa, but the maximum difference with the measurements of Easteal and Woolf [182] is only 0.36%. Similarly the results of Landau and Wurflinger [180] shows a

difference of 0.13% at 0.1 MPa and 0.99% at 300 MPa. At 323 K the measurements of Easteal and Woolf [182] agree with the present values to within 0.2% up to 200 MPa, and differ by only 0.32% at their highest pressure of 250 MPa. The measurements of Schroeder et al. [174] which cover a temperature range slightly greater than the present work show the same temperature dependence of the volume ratios at the constant pressure, and are in close agreement. The measurements reported by Kratzke and Muller [154] have not been used for comparison because they have been made at significantly different pressures. The results of Franceseoni [177] appear to be seriously in error.

In conclusion, of all the previous measurements, those of Easteal and Woolf are considered the most reliable. The present measurements agree with these to within the combined estimated uncertainities.

5.3 DENSITY AT ROUNDED TEMPERATURES AND PRESSURES.

For the calculation of the molar excess volume, V_m^E of the mixtures, densities of the mixtures and the individual components are required at the rounded temperatures and pressures. Experimental densities were measured at slightly different temperatures and pressures. Rounded pressure densities can be obtained by fitting a polynomial equation to the experimental densities. An equation of the form

$$\rho = A + BP + CP^2 + DP^3 + \ldots \qquad (5.1)$$

can be used, but this equation requires at least five or more terms in order to reproduce the high pressure densities to the required accuracy. Since the number of data points on each isotherm were not

sufficient to fit a six degree polynomial therefore to avoid overfitting, rounded pressure densities were obtained from some form of the secant bulk modulus equation, suggested by Hayward [124], and used by Young [139], Robertson [141] and Glen [152].

Isothermal compressibility is defined as the fractional volume change per unit pressure at constant temperature and its reciprocal, the bulk modulus, is defined as

$$K = -V.(\partial P/\partial V)_T \qquad (5.2)$$

Secant bulk modulus, defined as the average value of the bulk modulus from saturation pressure, Po to P is given by

$$\bar{K} = -Vo.(P-Po)/(V-Vo) \qquad (5.3)$$

where V is the volume of liquid or mixture at pressure P. Equation 5.3 is equivalent to

$$\bar{K} = \rho(P-Po)/(\rho - \rho_o) \qquad (5.4)$$

in term of densities, where ρ and ρ_o are the densities at pressure P and Po respectively. Experimentally derived values of K, obtained by application of equation 5.4, were fitted to the equation

$$\bar{K} = Ko+K1P+K2P^2+.... \qquad (5.5)$$

where Ko, K1, K2, are the coefficients of the least squares fit. Equation 5.4 can be rearranged to

$$\rho = \bar{K}.\rho_o/(\bar{K}-(P-Po)) \qquad (5.6)$$

Equation 5.6 was used along with equation 5.5 to calculate the densities at rounded pressures of 50 or 100 MPa intervals up to the maximum experimental pressure at each temperature. Rounded pressure densities at the experimental temperature were converted to the rounded temperature assuming linear variation of density with temperature along the isobars.

Table 5.26 list the coefficients derived using equation 5.5 for all the liquids and mixtures studied. It is found that up to a pressure of 100 MPa, $\bar{K}$ varies linearly with pressure while at higher pressure a quadratic equation fits the experimental data for most of the measurements, however a cubic equation improved the fitting where deviations were more than ±0.2 %. The coefficients of the cubic equation have been presented in Table 5.26. The advantage of using equation 5.5 over 5.1 is that fewer terms are required, furthermore equation 5.5 fits the experimental density data to within the experimental uncertainity of ±0.2 % . For acetonitrile at 298.15 K, the freezing pressure lies between 320 and 360 MPa. Both equations 5.1 and 5.6 can only be used for interpolation of densities within the limit of the experimental pressures. Rounded pressure densities beyond the experimental pressure range were calculated from the Tait equation.

5.4 COMPARISON OF MEASURED VISCOSITY COEFFICIENTS WITH THE LITERATURE VALUES.

The viscosity ratio has been reported in the literature for n-hexane by Bridgman [184] at 303 and 348 K up to 980 MPa, Ageav and Golubev [185] at 298 and 348 K up to 50 MPa, Brazier and Freeman [186] at 303, 323 and 333 K up to 400 MPa, by Isdale et al. [187] at 298, 323, 348 and 373 K up to 400 MPa and by Dymond et al. [62] over the same temperature and pressure range, and by Kashiwagi and Makita [153] at 298 to 333 K up to 110 MPa. The viscosity coefficients measured for n-hexane were converted to viscosity ratios and a comparison made. The relative viscosity is plotted against pressure in fig. 5.18 along with the literature values. The measured viscosity ratios at 298, 323, 348 and 373 K are in general agreement with Isdale [187] and Dymond [62] within the combined uncertainity of 8 % . The results of Brazier and Freeman are not shown in fig. 5.18, as there is serious disagreement between their results and those of Isdale et al., as earlier pointed out by Young [139].

For toluene, viscosity coefficients at elevated temperatures and pressures have been measured by Bridgman [184] at 303 and 348 K up to 1200 MPa, by Kashiwagi and Makita [153] at 298, 303, 323 and 348 K up to 110 MPa, by Krall et al. [188] from 298 to 398 K, up to 30 MPa and by Malhotra [189] at 298.2 K up to 110 MPa.

The viscosity ratios for toluene are compared with values given by Kashiwagi and Makita in fig. 5.19. At 298 K the two sets of data

agree very satisfactory up to 110 MPa, the maximum deviation being 1.6% . At 323 K the agreement is within 1.5 %. and at 348 K the present measurement are slightly higher but are still within the combined uncertainity of 8% except the highest pressure value of Kashiwagi and Makita which is as much as 11% lower than this work. The reason for this significant difference is not known. The results of Malhotra at 298 K and up to 110 MPa agree with this work within 4%. His results are slightly higher then the present work and the results of Kashiwagi and Makita. Generally the results for three isotherms agree with the literature values within the estimated combined accuracy of the measurements.

The viscosity coefficients at saturation pressure and at 298.15 K have been reported for x toluene + (1-x) n-hexane by Ghai and Dullien [131] and x toluene + (1-x) acetonitrile at 288, 298 and 308 K by Ritzoulis et al. [150]. A comparison with the present measurements is made in section 4.4. No high pressure viscosity data was found in the literature for these mixtures.

5.5 VISCOSITY COEFFICIENTS AT ROUNDED TEMPERATURES AND PRESSURES.

Viscosity coefficients at rounded temperatures and pressures were obtained in two steps. Firstly, the viscosity coefficients were obtained at rounded pressures at experimental temperatures. Secondly these values were interpolated for exact temperatures. Viscosity data were fitted to an equation of the form

$$\ln \eta = a + bP \qquad (5.7)$$

over a small pressure range, where a, b are contants and P is pressure. If Pi is pressure close to the rounded pressure Pr and Pl and Ph are the the pressures below and above Pi respectively, then

$$\ln \eta i = a + bPi \qquad (5.8a)$$

$$\ln \eta l = a + bPl \qquad (5.8b)$$

$$\ln \eta h = a + bPh \qquad (5.8c)$$

$$\ln \eta r' = a + bPr \qquad (5.8d)$$

where $\eta r'$ is the rounded pressure viscosity coefficient at rounded pressure Pr at the experimental temperature. Solving these equations simultaneously for $\eta r'$, it can be shown that

$$\eta r' = \eta i \left(\frac{\eta h}{\eta l}\right)^{\left[\frac{Pr - Pi}{Ph - Pl}\right]} \qquad (5.9)$$

Generally the rounded and experimental pressures are close together, hence additional uncertainity in the rounded pressure viscosity coefficient is small. The viscosity coefficients so obtained were converted to the rounded temperatures, by fitting ln η against 1/T, where T is the absolute temperature.

If ηr is the viscosity coefficient at rounded pressure and rounded temperature Tr, T3 is the temperature close to Tr and T2, T1 are experimental temperatures above and below T3, while corresponding rounded pressure viscosity coefficients are $\eta 3$, $\eta 2$ and $\eta 1$ respectively,then solving a set of equations like

$$\ln \eta_i = a + b/Ti \qquad (5.10)$$

where i=1, 2, 3 or r, and a and b are the coefficients of the least square fit, yields

$$\eta_r = \eta_3 \left(\frac{\eta_1}{\eta_2}\right)^{\left(\frac{T1\ T2\ (T3 - Tr)}{Tr\ T3\ (T2 - T1)}\right)} \qquad (5.11)$$

At 298.15 K, T1 was taken to be equal to T3, while at 373.15 K T2 was taken to be equal to T3, as there are no measurements carried out beyond this temperature range. The experimental temperature differed only slightly from the rounded temperature, hence the additional uncertainity in the derived viscosity coefficients is small. It is estimated that the total uncertainity in the rounded temperature and pressure viscosity coefficient is less than ±6%.

5.6 RESULTS

5.6.1 ACETONITRILE

The density of acetonitrile is presented in Table 5.1 at 298, 323, 348 and 373 K and up to 500 MPa, or the freezing pressure where this is lower and plotted against pressure in fig. 5.1. At 298.16 K, a sharp increase in density was observed at approximately 400 MPa, indicating the solidification of the liquid. No attempt was made to determine the exact freezing pressure. However fall-time measurements at the same temperature revealed that the freezing pressure lies between 320 MPa and 360 MPa. The viscosity coefficient at 298, 323, 348 and 373 K at pressures up to 500 MPa, or to the freezing pressure if lower, is presented in Table 5.10 and plotted in fig. 5.2. Rounded

pressure values of density and viscosity coefficient are tabulated in Table 5.11.

5.6.2 TOLUENE

The viscosity coefficients for toluene are presented from 298 to 373 K and pressures up to 500 MPa in Table 5.12 and plotted in fig. 5.3. Density measurement for this liquid was not undertaken as Dymond and Malhotra [198] have measured the density over this temperature and pressure range, in the same laboratory, using the same apparatus. The rounded temperature and pressure values of density and viscosity coefficients are tabulated in Table 5.13

5.6.3 x TOLUENE + (1- x) ACETONITRILE SYSTEM.

The densities of (x Toluene + (1-x) Acetonitrile) in the range 298 to 373 K and 0.1 to 500 MPa with x equal to 0.25, 0.50, and 0.75 are presented in Tables 5.2, 5.3, and 5.4 respectively and plotted against pressure in figs. 5.4, 5.6 and 5.8 respectively. The viscosities of the same mixtures are presented in Tables 5.14, 5.16 and 5.18 and plotted in figs. 5.5, 5.7 and 5.9 respectively. Rounded temperature and pressure values are presented in Tables 5.15, 5.17 and 5.19.

5.6.4 x TOLUENE + (1-x) n-HEXANE SYSTEM.

The densities of (x Toluene + (1-x) n-Hexane) with x equal to 0.25, 0.50, 0.75 are given in Tables 5.5, 5.6, 5.7 and plotted in figs. 5.10, 5.12 and 5.14. Corresponding viscosity coefficients are

tabulated in Tables 5.20, 5.22 and 5.24 and plotted in figs. 5.11, 5.13 and 5.15. The rounded temperature and pressure values are presented in Tables 5.21, 5.23 and 5.25.

5.6.5 TERNARY EQUIMOLAR MIXTURE OF n-OCTANE + i-OCTANE + OCT-1-ENE

Only density measurements were made for this mixture. The density from 298 to 373 K at pressures up to 400 MPa is presented in Table 5.8 and plotted in fig. 5.16. The rounded temperature and pressure densities are presented in Table 5.9

Table 5.1

DENSITY AND ISOTHERMAL SECANT BULK MODULUS FOR ACETONITRILE

Temperature T/K	Pressure P/MPa	Density ϱ/kg m^{-3}	Isothermal Secant Bulk Modulus $\bar{K}$/GPa
298.26	0.1	776.6	-
	5.0	780.9	0.8899
	10.3	785.3	0.9207
	20.9	793.5	0.9766
	40.7	807.8	1.0512
	60.2	820.0	1.1355
	79.7	830.6	1.2244
	102.9	842.5	1.3142
	200.4	885.4	1.6300
	313.6	925.5	1.9486
	399.3	1070.2	1.4551
323.21	0.1	749.5	-
	4.7	754.1	0.7541
	10.0	759.5	0.7519
	20.9	769.0	0.8203
	40.0	784.6	0.8919
	60.6	799.5	0.9674
	79.9	811.3	1.0450
	100.6	823.1	1.1239
	199.0	868.4	1.4527
	300.4	905.7	1.7412
	395.9	935.6	1.9898
	448.7	949.0	2.1339
	469.0	954.1	2.1866
348.26	0.1	721.2	-
	4.7	726.6	0.6190
	10.2	732.7	0.6435
	20.7	743.9	0.6751
	39.8	761.1	0.7573
	60.4	777.1	0.8383
	80.1	790.7	0.9102
	99.5	802.7	0.9790
	200.9	852.5	1.3037
	298.6	892.5	1.5552
	385.5	919.1	1.7899
	450.8	936.5	1.9604
	476.7	943.6	2.0221
373.27	0.1	693.7	-
	10.4	708.6	0.4898
	20.7	722.0	0.5256
	40.4	742.7	0.6108
	59.8	760.2	0.6825
	79.5	775.4	0.7536
	100.5	789.6	0.8267
	200.3	842.5	1.1335
	300.0	885.2	1.3863
	401.2	917.6	1.6438
	467.8	936.3	1.8051

Table 5.2

DENSITY AND ISOTHERMAL SECANT BULK MODULUS FOR (0.25 TOLUENE + 0.75 ACETONITRILE)

Temperature T/K	Pressure P/MPa	Density ϱ/kg m^{-3}	Isothermal Secant Bulk Modulus $\bar{K}$/GPa
298.28	0.1	811.8	-
	7.0	818.0	0.9253
	15.0	824.5	0.9750
	30.5	836.2	1.0461
	50.3	849.1	1.1458
	70.1	861.0	1.2275
	90.6	871.8	1.3172
	112.3	883.1	1.3916
	204.2	921.9	1.7105
	306.0	954.8	2.0439
	402.8	986.2	2.2785
	507.7	1010.2	2.5859
323.18	0.1	786.1	-
	10.0	795.9	0.8040
	20.2	805.0	0.8561
	40.0	820.9	0.9412
	60.0	835.1	1.0209
	80.4	848.0	1.1001
	100.6	859.3	1.1798
	198.0	904.6	1.5107
	299.1	942.1	1.8057
	398.0	972.1	2.0796
	492.9	997.4	2.3262
348.23	0.1	759.2	-
	9.6	770.4	0.6535
	20.2	781.2	0.7137
	39.8	798.8	0.8008
	59.2	814.1	0.8764
	80.2	828.5	0.9576
	100.6	841.6	1.0265
	200.3	890.3	1.3596
	296.6	927.6	1.6332
	386.3	956.4	1.8730
	449.9	974.1	2.0389
	472.2	979.6	2.0983
373.35	0.1	734.6	-
	10.1	748.3	0.5462
	21.2	762.0	0.5868
	39.9	781.5	0.6632
	58.7	797.8	0.7397
	79.7	814.3	0.8133
	99.5	827.7	0.8837
	200.9	881.8	1.2029
	309.9	923.4	1.5152
	400.9	956.6	1.7271
	490.0	978.5	1.9654
	515.6	988.2	2.0087

Table 5.3

DENSITY AND ISOTHERMAL SECANT BULK MODULUS FOR (0.50 TOLUENE + 0.50 ACETONITRILE)

Temperature T/K	Pressure P/MPa	Density ϱ/kg m^{-3}	Isothermal Secant Bulk Modulus $\bar{K}$/GPa
298.40	0.1	835.5	-
	10.8	842.9	1.2188
	21.0	851.5	1.1123
	40.3	864.7	1.1904
	60.0	874.5	1.3431
	79.6	885.4	1.4106
	100.8	895.9	1.4937
	200.4	939.7	1.8064
	299.1	975.3	2.0859
	349.9	991.1	2.2281
	415.2	1006.6	2.4421
323.36	0.1	810.6	-
	10.1	819.9	0.8816
	20.4	828.9	0.9195
	40.5	844.8	0.9980
	60.3	857.9	1.0919
	80.6	870.5	1.1699
	100.0	881.4	1.2437
	200.4	926.7	1.5988
	304.2	963.1	1.9205
	407.3	994.4	2.2030
348.43	0.1	784.6	-
	10.9	794.6	0.8582
	20.1	805.0	0.7892
	40.2	822.4	0.8724
	60.7	837.0	0.9680
	80.8	851.0	1.0343
	101.5	863.4	1.1110
	201.3	910.9	1.4511
	288.1	944.7	1.6994
	348.4	965.1	1.8623
	402.5	980.4	2.0149
373.31	0.1	759.8	-
	9.6	773.0	0.5563
	20.3	785.7	0.6128
	40.7	805.0	0.7231
	59.8	822.0	0.7890
	79.8	836.7	0.8672
	101.6	850.6	0.9508
	200.9	901.5	1.2775
	301.0	943.2	1.5475
	404.8	974.8	1.8349

Table 5.4

DENSITY AND ISOTHERMAL SECANT BULK MODULUS FOR (0.75 TOLUENE + 0.25 ACETONITRILE)

Temperature T/K	Pressure P/MPa	Density ϱ/kg m^{-3}	Isothermal Secant Bulk Modulus $\bar{K}$/GPa
298.27	0.1	851.8	-
	10.3	859.5	1.1386
	22.3	868.2	1.1752
	41.6	879.6	1.3131
	61.7	891.4	1.3866
	80.3	902.3	1.4330
	100.3	911.5	1.5299
	202.9	952.4	1.9199
	300.7	986.1	2.2072
	379.3	1006.4	2.4685
	415.8	1015.8	2.5748
323.32	0.1	827.6	-
	4.7	831.8	0.9110
	9.6	836.3	0.9132
	20.8	845.4	0.9831
	40.4	858.5	1.1197
	60.0	872.3	1.1689
	79.4	883.3	1.2576
	100.2	894.2	1.3440
	203.0	937.5	1.7308
	293.6	970.0	1.9993
	354.8	987.3	2.1928
	394.7	997.2	2.3201
348.33	0.1	802.7	-
	4.6	807.6	0.7417
	9.8	813.1	0.7584
	19.7	822.5	0.8142
	40.2	839.1	0.9244
	60.8	852.9	1.0313
	80.4	866.4	1.0922
	100.4	876.8	1.1868
	199.1	922.8	1.5290
	255.4	942.7	1.7191
	304.5	960.0	1.8577
	342.8	972.3	1.9647
	396.1	986.5	2.1254
373.26	0.1	780.2	-
	10.1	792.3	0.6292
	21.1	804.7	0.6897
	40.5	822.6	0.7838
	60.9	837.7	0.8858
	78.9	851.0	0.9472
	102.2	865.4	1.0371
	201.4	912.8	1.3857
	300.4	950.3	1.6777
	401.2	980.4	1.9642
	494.8	1003.2	2.2255

Table 5.5

DENSITY AND ISOTHERMAL SECANT BULK MODULUS OF (0.25 TOLUENE + 0.75 n-HEXANE)

Temperature T/K	Pressure P/MPa	Density ϱ/kg m^{-3}	Isothermal Secant Bulk Modulus $\bar{K}$/GPa
298.27	0.1	699.6	-
	10.6	710.3	0.6970
	19.7	717.3	0.7943
	41.7	733.8	0.8926
	60.1	747.2	0.9418
	79.5	758.8	1.0177
	101.3	769.2	1.1184
	200.6	812.2	1.4462
	300.3	845.5	1.7397
	381.6	867.9	1.9673
	446.7	882.7	2.1530
	473.6	887.8	2.2337
323.33	0.1	676.5	-
	4.7	682.0	0.5704
	10.1	688.2	0.5882
	20.5	698.6	0.6449
	39.7	716.0	0.7178
	59.8	730.8	0.8035
	81.3	743.7	0.8986
	100.7	754.9	0.9687
	202.8	800.3	1.3103
	304.0	835.8	1.5945
	381.9	859.2	1.7955
348.40	0.1	651.2	-
	9.9	664.6	0.4861
	20.1	677.1	0.5229
	40.0	696.5	0.6135
	60.4	713.1	0.6947
	78.9	726.1	0.7639
	101.1	739.4	0.8467
	200.6	785.7	1.1712
	300.2	822.1	1.4436
	378.9	846.0	1.6451
	429.8	856.7	1.7914
	465.0	865.1	1.8802
373.36	0.1	623.6	-
	10.2	642.2	0.3487
	21.1	656.7	0.4166
	42.1	680.0	0.5064
	60.6	696.9	0.5752
	80.8	711.8	0.6513
	100.6	724.4	0.7222
	200.1	773.1	1.0342
	311.9	812.6	1.3406
	417.1	842.4	1.6055
	493.9	861.2	1.7898

Table 5.6

DENSITY AND ISOTHERMAL SECANT BULK MODULUS OF (0.50 TOLUENE + 0.50 n-HEXANE)

Temperature T/K	Pressure P/MPa	Density ϱ/kg m^{-3}	Isothermal Secant Bulk Modulus $\bar{K}$/GPa
298.22	0.1	748.5	-
	9.1	756.3	0.8727
	20.2	765.0	0.9319
	39.3	778.5	1.0172
	59.9	791.3	1.1056
	80.2	801.8	1.2050
	101.6	812.6	1.2867
	199.7	851.5	1.6501
	300.7	883.4	1.9685
	399.9	909.2	2.2620
	460.0	921.6	2.4485
323.26	0.1	725.9	-
	10.3	736.7	0.6958
	21.0	746.5	0.7574
	40.5	761.8	0.8573
	60.4	775.3	0.9464
	80.5	787.3	1.0309
	101.5	798.6	1.1139
	200.9	840.1	1.4772
	300.5	873.9	1.7738
	397.3	899.5	2.0581
	447.9	910.3	2.2106
348.35	0.1	701.7	-
	10.8	715.4	0.5587
	20.2	725.9	0.6029
	41.1	744.8	0.7085
	60.7	759.3	0.7988
	86.2	775.6	0.9036
	102.0	784.8	0.9623
	201.4	828.9	1.3118
	301.8	863.6	1.6093
	410.4	893.1	1.9145
	522.7	917.1	2.2251
373.35	0.1	676.1	-
	8.2	689.6	0.4138
	21.3	707.7	0.4748
	44.5	730.8	0.5932
	58.7	739.4	0.6845
	79.6	754.6	0.7642
	100.6	767.5	0.8439
	201.7	816.0	1.1759
	301.2	852.9	1.4525
	414.0	883.5	1.7632
	522.3	909.9	2.0323

Table 5.7

DENSITY AND ISOTHERMAL SECANT BULK MODULUS OF (0.75 TOLUENE + 0.25 n-HEXANE)

Temperature T/K	Pressure P/MPa	Density ϱ/kg m^{-3}	Isothermal Secant Bulk Modulus $\bar{K}$/GPa
298.22	0.1	802.2	-
	9.5	809.6	1.0284
	20.2	817.8	1.0537
	40.6	831.3	1.1570
	58.1	840.5	1.2728
	78.6	852.4	1.3329
	101.2	863.1	1.4328
	201.4	901.6	1.8259
	301.4	933.5	2.1421
	402.9	958.2	2.4741
	490.6	976.0	2.7545
323.31	0.1	778.6	-
	10.2	788.7	0.7887
	20.0	797.0	0.8620
	40.3	811.1	1.0033
	60.1	824.4	1.0800
	80.0	835.6	1.1713
	101.1	846.4	1.2609
	201.8	886.7	1.6545
	301.3	919.4	1.9668
	399.6	944.3	2.2767
	466.5	959.4	2.4749
348.32	0.1	754.7	-
	10.1	765.6	0.7024
	20.3	775.1	0.7675
	41.0	792.0	0.8684
	59.3	804.9	0.9492
	81.2	818.8	1.0360
	100.7	829.2	1.1197
	199.6	871.7	1.4864
	299.6	905.6	1.7974
	404.2	932.7	2.1174
	515.3	957.2	2.4353
373.49	0.1	729.5	-
	10.0	741.2	0.6272
	20.4	752.6	0.6614
	40.5	772.1	0.7322
	59.6	786.6	0.8197
	80.9	800.5	0.9110
	99.2	811.1	0.9850
	200.8	857.1	1.3481
	295.8	890.9	1.6322
	371.6	911.8	1.8581
	442.1	928.8	2.0599
	498.3	940.7	2.2190

Table 5.8

DENSITY AND ISOTHERMAL SECANT BULK MODULUS FOR (0.333 n-OCTANE + 0.333 i-OCTANE + 0.333 OCT-1-ENE)

Temperature T/K	Pressure P/MPa	Density ϱ/kg m^{-3}	Isothermal Secant Bulk Modulus $\bar{K}$/GPa
298.15	0.1	698.8	-
	4.4	702.7	0.7748
	10.3	707.9	0.7935
	21.1	716.4	0.8548
	39.2	728.8	0.9499
	61.3	741.3	1.0675
	79.5	751.2	1.1383
	108.9	763.9	1.2767
	202.1	797.8	1.6278
	281.0	821.0	1.8872
323.15	0.1	679.0	-
	4.6	683.5	0.6835
	10.2	689.2	0.6824
	22.4	699.3	0.7682
	39.9	712.3	0.8513
	59.4	725.7	0.9215
	81.7	738.0	1.0207
	110.8	751.4	1.1489
	223.6	792.4	1.5617
	299.7	815.7	1.7877
	411.9	841.0	2.1378
348.15	0.1	657.4	-
	4.6	663.0	0.5328
	9.4	668.7	0.5503
	20.8	680.4	0.6124
	41.8	697.5	0.7253
	59.9	710.7	0.7974
	62.3	711.7	0.8152
	81.4	722.8	0.8985
	99.0	732.4	0.9658
	210.1	777.3	1.3614
	297.6	803.9	1.6325
	414.6	832.0	1.9752
373.15	0.1	634.2	-
	4.4	640.8	0.4175
	9.5	648.1	0.4383
	20.1	661.0	0.4933
	40.6	680.8	0.5858
	63.6	697.8	0.6967
	81.9	709.8	0.7680
	98.7	720.0	0.8274
	214.4	767.1	1.2369
	305.6	794.9	1.5112
	397.4	818.9	1.7615

Table 5.9

DENSITIES AT ROUNDED PRESSURE FOR THE TERNARY EQUIMOLAR MIXTURE OF n-OCTANE + I-OCTANE + OCT-1-ENE

Pressure	Temperature/K			
MPa	298.15	323.15	348.15	373.15
		Density/kg m^{-3}		
0.1	698.8	679.0	657.4	634.2
25.0	719.2	701.6	684.2	666.3
50.0	735.3	719.4	703.9	688.7
100.0	760.3	746.6	732.6	720.0
150.0	780.1	785.5	754.6	742.8
200.0	797.1	801.2	773.4	761.8
250.0	812.3	815.1	790.0	778.5
300.0		827.7	805.0	793.7
350.0		838.7	818.1	807.3
400.0			829.1	

Table 5.10

VISCOSITY AND DENSITY OF ACETONITRILE

Temperature T/K	Pressure P/MPa	Fall time t/sec	Density ϱ/kg m^{-3}	Viscosity η/cP
298.25	0.1	8.249	776.6	0.3404
	25.8	9.918	796.7	0.440
	50.8	10.371	813.6	0.461
	73.2	11.297	827.1	0.505
	118.7	13.071	850.9	0.589
	150.9	14.169	865.7	0.640
	201.4	16.834	886.3	0.765
	260.7	19.039	907.6	0.867
	326.7	23.233	928.5	1.060
323.13	0.1	6.595	749.58	0.2722
	23.0	7.371	770.5	0.313
	49.2	8.219	790.7	0.355
	75.5	9.141	808.1	0.400
	101.2	9.924	823.2	0.438
	151.7	12.001	848.8	0.537
	200.5	13.567	869.9	0.611
	280.6	17.107	899.6	0.776
	345.7	20.956	920.4	0.954
	399.6	21.616	935.9	0.983
	511.7	26.830	964.7	1.221
348.16	0.1	5.487	721.30	0.2229
	24.0	6.246	746.2	0.256
	49.4	6.938	767.9	0.291
	75.4	7.673	786.8	0.328
	99.8	8.589	802.4	0.373
	150.6	10.676	830.2	0.474
	202.2	11.695	853.7	0.522
	300.3	14.581	891.7	0.656
	402.7	18.116	924.1	0.820
	512.4	22.296	953.5	1.021
373.18	0.1	4.557	693.80	0.1885
	24.5	5.327	725.1	0.213
	50.2	5.996	750.7	0.243
	75.2	6.600	771.4	0.273
	99.2	7.182	788.5	0.302
	150.2	8.384	819.1	0.361
	201.4	9.720	844.7	0.426
	299.7	12.441	884.7	0.555
	398.5	15.246	917.6	0.685
	502.4	18.307	947.2	0.826

Table 5.11

VISCOSITY AND DENSITY OF ACETONITRILE

AT ROUNDED TEMPERATURES AND PRESSURES

Temperature	Pressure	Density	Viscosity
T/K	P/MPa	ϱ/kg m^{-3}	η/cP
298.15	0.1	776.7	0.3406
	25.0	796.9	0.438
	50.0	813.8	0.460
	100.0	841.6	0.557
	150.0	864.8	0.639
	200.0	885.4	0.763
	250.0	904.2	0.844
	300.0	921.4	0.961
323.15	0.1	749.6	0.2721
	25.0	772.8	0.317
	50.0	792.1	0.356
	100.0	823.1	0.436
	150.0	848.1	0.534
	200.0	869.5	0.610
	300.0	905.8	0.813
	350.0	921.6	0.916
	400.0	936.2	0.984
	500.0	961.9	1.193
348.15	0.1	721.3	0.2229
	25.0	748.1	0.258
	50.0	769.6	0.292
	100.0	803.4	0.373
	150.0	830.2	0.473
	200.0	853.2	0.511
	300.0	892.3	0.656
	400.0	924.3	0.816
	500.0	950.4	0.996
373.15	0.1	693.8	0.1885
	25.0	727.1	0.214
	50.0	752.2	0.243
	100.0	789.7	0.303
	150.0	818.5	0.360
	200.0	843.0	0.424
	300.0	884.7	0.556
	400.0	918.5	0.687
	500.0	946.1	0.822

Table 5.12

VISCOSITY AND DENSITY OF TOLUENE

Temperature T/K	Pressure P/MPa	Fall time t/sec	Density ϱ/kg m^{-3}	Viscosity η/cP
298.23	0.1	12.636	862.10	0.5516
	25.5	14.585	880.2	0.659
	50.6	17.249	895.6	0.784
	76.3	20.470	909.5	0.933
	101.3	23.320	921.6	1.065
	146.8	30.194	941.0	1.381
	200.5	39.096	960.7	1.789
	299.1	66.339	990.9	3.030
	400.7	107.690	1016.6	4.905
	502.2	176.520	1038.5	8.019
323.14	0.1	9.700	838.80	0.4211
	25.9	11.581	860.8	0.516
	50.2	13.541	877.9	0.609
	75.8	15.508	893.3	0.701
	101.1	17.603	906.6	0.798
	150.2	23.913	928.7	1.091
	195.8	28.198	946.5	1.287
	294.8	42.464	977.0	1.938
	394.9	66.510	1002.3	3.031
	487.7	96.248	1022.2	4.377
348.24	0.1	8.038	814.70	0.3336
	27.2	9.828	839.7	0.431
	50.1	11.261	856.9	0.500
	74.0	13.353	872.4	0.600
	101.9	16.009	888.0	0.725
	152.6	19.377	912.1	0.880
	202.5	24.415	932.0	1.113
	298.9	36.294	963.4	1.656
	398.1	52.875	989.8	2.410
	502.1	81.063	1013.3	3.687
373.27	0.1	6.683	790.00	0.2730
	25.1	8.000	817.4	0.342
	49.8	9.467	838.6	0.413
	73.3	10.731	855.3	0.474
	101.8	12.472	872.6	0.557
	149.5	15.239	896.6	0.687
	200.7	19.903	918.0	0.904
	307.8	29.677	953.6	1.352
	412.0	42.988	981.1	1.958
	518.8	59.534	1004.8	2.707

Table 5.13

VISCOSITY AND DENSITY OF TOLUENE

AT ROUNDED TEMPERATURES AND PRESSURES

Temperature T/K	Pressure P/MPa	Density ϱ/kg m^{-3}	Viscosity η/cP
298.15	0.1	862.2	0.5521
	25.0	880.8	0.657
	50.0	896.1	0.781
	100.0	920.8	1.054
	150.0	940.8	1.406
	200.0	958.1	1.786
	300.0	991.2	3.049
	400.0	1016.5	4.895
	500.0	1038.2	7.947
323.15	0.1	838.8	0.4211
	25.0	860.4	0.512
	50.0	877.8	0.608
	100.0	905.2	0.793
	150.0	926.6	1.089
	200.0	944.4	1.308
	300.0	975.1	1.982
	400.0	1003.4	3.096
	450.0	1014.4	3.825
348.15	0.1	814.8	0.3338
	25.0	838.4	0.424
	50.0	857.6	0.500
	100.0	887.9	0.718
	150.0	911.3	0.871
	200.0	930.7	1.101
	300.0	962.9	1.665
	400.0	991.2	2.431
	500.0	1012.9	3.684
373.15	0.1	790.1	0.2732
	25.0	817.6	0.342
	50.0	839.3	0.414
	100.0	872.1	0.553
	150.0	896.6	0.689
	200.0	916.6	0.902
	300.0	949.4	1.315
	400.0	978.2	1.884
	500.0	1001.0	2.561

Table 5.14

VISCOSITY AND DENSITY OF
(0.25 TOLUENE + 0.75 ACETONITRILE)

Temperature T/K	Pressure P/MPa	Fall time t/sec	Density ϱ/kg m^{-3}	Viscosity η/cP
298.10	0.1	9.410	812.05	0.3937
	23.9	10.555	831.3	0.468
	51.0	12.731	850.0	0.573
	78.0	14.249	866.2	0.644
	102.4	16.209	879.2	0.736
	150.8	19.955	901.8	0.910
	201.4	23.380	922.2	1.068
	302.9	32.977	956.3	1.508
	414.2	46.234	986.9	2.110
323.05	0.1	7.440	786.20	0.3083
	25.0	8.547	808.6	0.370
	50.3	10.011	827.8	0.442
	77.0	11.491	845.3	0.513
	100.3	12.733	859.0	0.572
	151.2	15.031	885.0	0.679
	198.3	17.939	905.6	0.814
	301.4	24.617	943.2	1.121
	401.9	32.775	973.5	1.493
	505.1	42.115	1000.2	1.916
348.18	0.1	6.063	759.20	0.2490
	27.6	7.086	787.4	0.298
	49.9	8.061	806.2	0.346
	74.9	9.148	824.4	0.399
	101.4	10.268	841.2	0.453
	149.5	12.135	867.4	0.542
	200.2	14.594	890.8	0.657
	300.3	19.921	928.8	0.904
	400.9	25.600	960.1	1.163
	509.8	32.956	989.0	1.497
373.15	0.1	5.127	734.80	0.2076
	24.4	6.038	764.9	0.245
	50.1	6.748	789.9	0.280
	75.4	7.564	810.4	0.320
	103.2	8.338	829.8	0.358
	149.9	10.063	857.3	0.441
	200.3	11.835	882.2	0.525
	309.4	15.402	925.9	0.691
	411.4	19.550	958.8	0.882
	520.7	25.717	988.9	1.163

Table 5.15

VISCOSITY AND DENSITY OF
(0.25 TOLUENE + 0.75 ACETONITRILE)

AT ROUNDED TEMPERATURES AND PRESSURES

Temperature	Pressure	Density	Viscosity
T/K	P/MPa	ϱ/kg m^{-3}	η/cP
298.15	0.1	812.0	0.3935
	25.0	833.1	0.472
	50.0	850.1	0.569
	100.0	877.4	0.727
	150.0	899.7	0.907
	200.0	919.4	1.062
	300.0	954.5	1.493
	400.0	985.1	2.021
323.15	0.1	786.1	0.3080
	25.0	809.3	0.370
	50.0	828.4	0.440
	100.0	859.3	0.570
	150.0	884.2	0.675
	200.0	905.5	0.818
	300.0	942.1	1.116
	400.0	973.2	1.484
	500.0	998.9	1.890
348.15	0.1	759.3	0.2490
	25.0	784.9	0.293
	50.0	805.6	0.346
	100.0	838.5	0.450
	150.0	864.9	0.543
	200.0	887.8	0.657
	300.0	927.3	0.903
	400.0	960.4	1.161
	500.0	986.7	1.464
373.15	0.1	734.8	0.2076
	25.0	766.5	0.245
	50.0	791.1	0.280
	100.0	828.6	0.353
	150.0	857.3	0.442
	200.0	881.3	0.525
	300.0	921.3	0.676
	400.0	955.0	0.857
	500.0	983.4	1.104

Table 5.16

VISCOSIY AND DENSITY OF
(0.50 TOLUENE + 0.50 ACETONITRILE)

Temperature T/K	Pressure P/MPa	Fall time t/sec	Density ϱ/kg m^{-3}	Viscosity η/cP
298.17	0.1	10.975	835.50	0.4526
	26.1	13.235	855.1	0.596
	50.2	15.289	870.8	0.693
	75.0	17.248	885.2	0.785
	101.4	19.791	898.9	0.903
	150.6	25.092	921.4	1.148
	201.1	30.729	941.2	1.406
	304.3	46.601	975.3	2.130
	401.0	67.604	1001.8	3.084
	510.7	100.780	1027.7	4.584
323.09	0.1	7.980	810.95	0.3497
	25.3	9.820	833.0	0.432
	49.9	11.377	851.1	0.507
	77.4	13.417	868.7	0.604
	99.2	14.075	881.1	0.634
	150.1	17.642	906.4	0.800
	201.7	22.687	928.2	1.034
	297.9	31.881	962.1	1.454
	392.3	44.560	989.8	2.031
	440.2	51.524	1002.4	2.346
	497.1	61.184	1016.2	2.782
348.23	0.1	6.780	784.84	0.2798
	24.0	7.888	808.0	0.337
	49.2	9.090	828.5	0.396
	75.9	10.556	847.0	0.467
	100.7	12.132	862.4	0.542
	149.5	14.640	888.5	0.660
	200.3	17.843	911.6	0.808
	299.8	25.161	949.2	1.145
	405.9	33.572	982.1	1.527
	516.5	45.069	1011.4	2.046
373.10	0.1	5.634	760.04	0.2312
	26.5	7.052	791.1	0.295
	48.0	7.600	811.5	0.322
	74.8	8.720	832.8	0.377
	100.1	9.683	850.1	0.423
	152.1	12.116	880.1	0.539
	200.6	14.360	903.4	0.644
	300.8	19.624	942.8	0.887
	401.4	27.361	974.9	1.241
	515.5	35.769	1005.8	1.621

Table 5.17

VISCOSITY AND DENSITY OF
(0.50 TOLUENE + 0.50 ACETONITRILE)

AT ROUNDED TEMPERATURES AND PRESSURES

Temperature	Pressure	Density	Viscosity
T/K	P/MPa	ϱ/kg m^{-3}	η/cP
298.15	0.1	835.7	0.4527
	25.0	853.5	0.591
	50.0	869.4	0.693
	100.0	896.8	0.897
	150.0	920.1	1.145
	200.0	940.7	1.401
	300.0	975.5	2.095
	400.0	1003.9	3.074
	500.0	1025.6	4.412
323.15	0.1	810.8	0.3495
	25.0	832.8	0.431
	50.0	851.4	0.507
	100.0	881.6	0.639
	150.0	905.9	0.991
	200.0	926.6	1.028
	300.0	961.9	1.464
	400.0	991.7	2.080
	450.0	1004.6	2.448
348.15	0.1	784.8	0.2800
	25.0	808.4	0.340
	50.0	829.2	0.398
	100.0	863.3	0.540
	150.0	890.2	0.661
	200.0	912.2	0.808
	300.0	948.1	1.146
	400.0	980.7	1.504
	500.0	1007.2	1.961
373.15	0.1	759.9	0.2311
	25.0	791.1	0.292
	50.0	814.3	0.325
	100.0	849.1	0.423
	150.0	876.9	0.534
	200.0	901.2	0.643
	300.0	943.2	0.885
	400.0	973.9	1.236
	500.0	1001.7	1.563

Table 5.18

VISCOSITY AND DENSITY OF
(0.75 TOLUENE + 0.25 ACETONITRILE)

Temperature T/K	Pressure P/MPa	Fall time t/sec	Density ϱ/kg m^{-3}	Viscosity η/cP
298.19	0.1	12.064	851.86	0.5085
	51.0	16.281	886.4	0.739
	75.5	18.830	900.0	0.858
	99.9	22.122	912.2	1.011
	150.8	29.530	934.5	1.352
	202.1	37.752	953.7	1.728
	298.0	55.447	984.0	2.534
	400.6	84.554	1010.8	3.854
	467.5	109.950	1026.2	5.002
323.08	0.1	9.331	827.95	0.3879
	25.2	11.229	848.2	0.500
	48.5	12.398	864.2	0.555
	74.7	14.366	880.1	0.648
	102.7	16.530	895.2	0.749
	149.7	21.856	917.3	0.997
	200.4	25.802	937.9	1.177
	249.5	31.968	955.4	1.460
	308.2	40.349	974.0	1.842
	411.8	59.079	1002.6	2.691
348.23	0.1	7.579	802.85	0.3097
	25.2	8.962	826.3	0.390
	49.2	10.507	844.9	0.464
	75.2	11.714	862.2	0.522
	102.3	13.802	878.1	0.621
	150.2	16.198	902.2	0.732
	200.9	20.050	923.8	0.910
	245.9	23.893	940.7	1.087
	301.1	29.222	959.1	1.331
	406.9	42.753	989.6	1.946
373.22	0.1	6.209	780.25	0.2537
	25.2	7.444	807.7	0.314
	50.1	8.689	829.5	0.376
	74.1	9.879	847.2	0.433
	99.9	11.433	863.7	0.508
	150.6	14.235	891.1	0.639
	201.3	16.384	913.9	0.739
	300.2	23.700	950.1	1.076
	367.7	29.688	970.8	1.349
	436.4	35.919	989.6	1.632

Table 5.19

VISCOSITY AND DENSITY OF
(0.75 TOLUENE + 0.25 ACETONITRILE)

AT ROUNDED TEMPERATURES AND PRESSURES

Temperature	Pressure	Density	Viscosity
T/K	P/MPa	ϱ/kg m^{-3}	η/cP
298.15	0.1	851.9	0.5087
	50.0	885.5	0.7340
	100.0	911.8	1.0114
	150.0	934.0	1.3469
	200.0	953.5	1.7144
	300.0	987.1	2.5555
	400.0	1014.9	3.8468
	450.0	1022.3	4.7018
323.15	0.1	827.7	0.3876
	25.0	848.8	0.4984
	50.0	866.0	0.5590
	100.0	893.9	0.7369
	150.0	916.9	0.9968
	200.0	937.1	1.1744
	300.0	971.8	1.7981
	400.0	999.3	2.5998
348.15	0.1	802.8	0.3101
	25.0	827.4	0.3895
	50.0	846.7	0.4672
	100.0	876.9	0.6147
	150.0	901.3	0.7322
	200.0	922.5	0.9085
	300.0	959.0	1.3279
	400.0	987.6	1.9069
373.15	0.1	780.3	0.2538
	25.0	809.0	0.3142
	50.0	830.8	0.3755
	100.0	864.0	0.5079
	150.0	889.7	0.6381
	200.0	911.7	0.7358
	300.0	948.9	1.0757
	400.0	978.6	1.4762

Table 5.20

VISCOSITY AND DENSITY OF
(0.25 TOLUENE + 0.75 n-HEXANE)

Temperature T/K	Pressure P/MPa	Fall time t/sec	Density ϱ/kg m^{-3}	Viscosity η/cP
298.30	0.1	7.592	699.60	0.3227
	24.8	9.453	721.8	0.422
	49.4	11.323	739.8	0.513
	77.1	13.500	757.1	0.619
	100.4	15.657	769.8	0.722
	151.3	20.367	793.5	0.945
	200.3	26.052	812.7	1.212
	301.0	42.697	845.2	1.989
	401.4	65.707	871.6	3.055
	506.6	87.721	895.2	4.068
323.25	0.1	6.137	676.80	0.2568
	25.7	7.774	702.9	0.338
	50.1	9.325	722.8	0.415
	74.9	11.105	739.8	0.502
	98.8	12.088	754.1	0.549
	149.8	15.508	779.9	0.713
	200.0	20.684	801.0	0.958
	300.0	31.402	835.4	1.460
	400.5	46.434	863.6	2.157
	504.5	67.515	888.3	3.130
348.20	0.1	5.200	651.45	0.2092
	25.4	6.540	681.9	0.275
	49.9	7.783	704.3	0.338
	75.5	9.022	723.3	0.399
	99.5	10.307	738.6	0.462
	150.7	13.284	765.8	0.606
	201.0	16.807	787.7	0.774
	300.1	23.796	822.7	1.102
	399.5	35.713	850.9	1.657
	508.4	50.173	887.1	2.325
373.20	0.1	4.248	623.90	0.1765
	26.0	5.688	662.9	0.231
	49.4	6.582	687.4	0.277
	73.5	7.670	707.3	0.332
	101.0	9.006	726.0	0.398
	150.3	11.256	753.0	0.508
	200.2	14.565	775.2	0.667
	303.3	21.559	811.3	0.997
	399.6	28.856	838.2	1.337
	501.4	38.733	862.1	1.795

Table 5.21

VISCOSITY AND DENSITY OF
(0.25 TOLUENE + 0.75 n-HEXANE)

AT ROUNDED TEMPERATURES AND PRESSURES

Temperature T/K	Pressure P/MPa	Density ϱ/kg m^{-3}	Viscosity η/cP
298.15	0.1	699.7	0.3232
	25.0	722.5	0.423
	50.0	740.6	0.516
	100.0	769.2	0.722
	150.0	792.0	0.941
	200.0	811.8	1.212
	300.0	845.7	1.983
	400.0	872.9	3.047
	500.0	893.9	4.002
323.15	0.1	676.6	0.2570
	25.0	703.4	0.336
	50.0	723.9	0.415
	100.0	754.9	0.553
	150.0	779.0	0.715
	200.0	799.5	0.959
	300.0	834.7	1.461
	400.0	863.2	2.155
	500.0	887.0	3.084
348.15	0.1	651.4	0.2093
	25.0	682.4	0.274
	50.0	705.4	0.338
	100.0	739.3	0.464
	150.0	764.9	0.604
	200.0	786.4	0.771
	300.0	822.3	1.102
	400.0	850.9	1.661
	500.0	875.1	2.267
373.15	0.1	623.8	0.1766
	25.0	662.8	0.229
	50.0	688.9	0.278
	100.0	724.5	0.389
	150.0	750.4	0.507
	200.0	772.1	0.667
	300.0	808.9	0.986
	400.0	839.5	1.339
	500.0	861.6	1.788

Table 5.22

VISCOSITY AND DENSITY OF
(0.50 TOLUENE + 0.50 n-HEXANE)

Temperature T/K	Pressure P/MPa	Fall time t/sec	Density ρ/kg m^{-3}	Viscosity η/cP
298.23	0.1	9.334	748.55	0.3708
	24.2	11.180	767.7	0.504
	49.9	13.371	784.8	0.610
	75.0	15.514	799.2	0.712
	99.7	18.241	811.7	0.841
	151.8	23.947	834.6	1.109
	200.7	30.527	852.7	1.416
	299.9	49.158	883.3	2.279
	399.8	76.537	908.6	3.541
	503.2	114.440	931.0	5.281
323.24	0.1	6.675	725.90	0.2943
	25.9	9.160	749.8	0.405
	50.0	10.822	767.9	0.486
	75.3	12.557	784.0	0.570
	100.7	14.522	798.1	0.664
	150.9	18.808	821.7	0.866
	200.8	23.296	841.5	1.076
	300.5	36.298	873.7	1.680
	400.2	54.050	900.0	2.499
	495.7	73.331	921.4	3.384
348.32	0.1	5.764	701.75	0.2394
	25.4	7.057	729.8	0.299
	49.9	8.916	750.8	0.392
	75.2	10.523	768.6	0.471
	101.2	11.840	784.3	0.534
	151.5	15.567	809.4	0.712
	201.2	19.373	829.9	0.891
	301.8	29.079	863.4	1.343
	401.4	41.137	890.0	1.900
	508.9	57.103	914.2	2.634
373.23	0.1	4.638	676.20	0.2020
	24.9	6.066	709.3	0.249
	50.0	7.396	733.6	0.316
	75.5	8.512	753.4	0.372
	100.4	10.004	769.6	0.445
	150.7	13.136	796.5	0.596
	200.4	15.990	818.1	0.731
	300.8	23.617	853.0	1.088
	400.8	32.463	880.7	1.497
	510.3	44.821	906.0	2.066

Table 5.23

VISCOSITY AND DENSITY OF
(0.50 TOLUENE + 0.50 n-HEXANE)

AT ROUNDED TEMPERATURES AND PRESSURES

Temperature	Pressure	Density	Viscosity
T/K	P/MPa	ϱ/kg m^{-3}	η/cP
298.15	0.1	748.6	0.3711
	25.0	768.9	0.508
	50.0	785.4	0.610
	100.0	812.0	0.843
	150.0	833.5	1.100
	200.0	851.9	1.412
	300.0	883.4	2.282
	400.0	909.3	3.548
	500.0	930.4	5.224
323.15	0.1	726.0	0.2945
	25.0	750.2	0.402
	50.0	768.9	0.486
	100.0	797.8	0.662
	150.0	820.7	0.863
	200.0	840.3	1.073
	300.0	873.7	1.678
	400.0	900.5	2.499
	500.0	922.5	3.435
348.15	0.1	701.9	0.2397
	25.0	730.9	0.299
	50.0	752.4	0.400
	100.0	784.1	0.532
	150.0	808.1	0.708
	200.0	828.4	0.888
	300.0	877.9	1.337
	400.0	891.5	1.895
	500.0	913.4	2.568
373.15	0.1	676.3	0.2021
	25.0	711.6	0.249
	50.0	735.3	0.316
	100.0	768.1	0.444
	150.0	792.7	0.594
	200.0	813.8	0.730
	300.0	851.1	1.086
	400.0	882.8	1.494
	500.0	905.8	2.006

Table 5.24

VISCOSITY AND DENSITY OF
(0.75 TOLUENE + 0.25 n-HEXANE)

Temperature T/K	Pressure P/MPa	Fall time t/sec	Density ϱ/kg m^{-3}	Viscosity η/cP
298.28	0.1	11.245	802.10	0.4404
	25.1	13.401	820.5	0.608
	50.3	16.210	836.3	0.741
	74.9	18.286	849.9	0.838
	100.0	21.142	862.2	0.972
	149.8	26.852	883.5	1.237
	198.4	35.481	901.3	1.636
	300.1	58.687	932.2	2.703
	396.5	94.838	956.4	4.358
	499.4	140.220	978.6	6.426
323.27	0.1	8.647	778.70	0.3446
	25.2	10.547	799.9	0.470
	51.0	12.536	818.0	0.566
	74.7	14.400	832.2	0.654
	100.2	16.886	845.7	0.772
	150.8	21.569	868.6	0.990
	199.9	27.476	887.4	1.265
	300.4	43.038	919.0	1.981
	400.2	63.624	944.5	2.924
	499.1	90.631	966.1	4.156
348.35	0.1	6.650	754.70	0.2765
	25.2	8.346	778.8	0.362
	47.0	10.093	795.8	0.448
	75.6	12.099	814.6	0.544
	103.9	14.133	830.5	0.641
	150.5	17.287	852.7	0.789
	199.7	21.515	872.4	0.987
	299.5	31.685	905.1	1.456
	391.6	44.920	929.1	2.064
	499.7	61.999	954.2	2.843
373.35	0.1	5.672	729.70	0.2302
	26.9	6.989	759.2	0.294
	51.7	8.386	780.3	0.364
	74.6	10.021	796.6	0.444
	98.9	11.193	811.3	0.500
	149.0	14.499	836.9	0.658
	202.6	18.266	859.2	0.834
	299.6	26.500	891.9	1.216
	400.1	36.789	919.1	1.689
	505.5	48.775	942.0	2.237

Table 5.25

VISCOSITY AND DENSITY OF
(0.75 TOLUENE + 0.25 n-HEXANE)

AT ROUNDED TEMPERATURES AND PRESSURES

Temperature T/K	Pressure P/MPa	Density ϱ/kg m^{-3}	Viscosity η/cP
298.15	0.1	802.2	0.4410
	25.0	820.9	0.608
	50.0	836.7	0.741
	100.0	862.4	0.973
	150.0	883.5	1.240
	200.0	901.6	1.652
	300.0	932.6	2.706
	400.0	957.9	4.436
	500.0	978.8	6.456
323.15	0.1	778.7	0.3450
	25.0	801.2	0.470
	50.0	818.7	0.563
	100.0	845.7	0.772
	150.0	867.3	0.988
	200.0	886.1	1.266
	300.0	918.8	1.981
	400.0	945.6	2.926
	500.0	966.3	4.178
348.15	0.1	754.8	0.2769
	25.0	779.5	0.362
	50.0	799.0	0.459
	100.0	829.0	0.630
	150.0	852.2	0.789
	200.0	871.9	0.990
	300.0	905.1	1.462
	400.0	932.6	2.127
	500.0	954.4	2.853
373.15	0.1	729.8	0.2305
	25.0	757.4	0.290
	50.0	779.2	0.359
	100.0	812.3	0.504
	150.0	837.4	0.661
	200.0	858.1	0.826
	300.0	891.8	1.220
	400.0	919.2	1.691
	500.0	942.0	2.237

Table 5.26 COEFFICIENTS FOR EQUATION 5.5

Liquid/mixture	Temp. T/K	Dens. /kg m^{-3}	K0 MPa	K1 -	$-K2.10^{3}$ MPa^{-1}	$K3.10^{6}$ MPa^{-2}
Acetonitrile	298.26	776.6	875.25	4.5710	3.7011	-
	323.21	749.5	730.62	4.2484	3.8443	2.9828
	348.26	721.2	596.16	4.2758	4.7909	4.4327
	373.27	693.7	443.76	4.2820	5.2122	4.8927
Toluene (a)	298.15	862.2	1051.78	5.698	4.818	-
	323.15	838.8	873.6	5.241	3.314	-
	348.15	814.8	778.51	4.618	2.360	-
	373.15	790.1	633.1	4.553	2.331	-
n-Hexane (b)	298.15	655.0	668.2	4.156	1.580	-
	323.15	631.6	531.2	4.016	1.442	-
	348.15	606.7	454.8	3.636	1.156	-
	373.15	580.5	332.4	3.731	1.636	-
0.25 Toluene	298.28	811.9	895.54	5.1335	6.4447	5.6793
+	323.20	786.1	765.92	4.5058	4.4625	3.5461
0.75 Aceto-	348.23	759.2	622.08	4.5414	5.1854	4.6460
nitrile	373.35	734.6	506.99	4.1088	3.6534	2.6374
0.50 Toluene	298.40	835.5	1104.69	3.9139	2.9333	2.9346
+	323.36	810.6	831.64	4.4417	3.4267	1.9353
0.50 Aceto-	348.43	784.6	770.26	3.1592	-1.6204	-4.5645
nitrile	373.31	759.8	505.60	5.2736	9.3176	1.0885
0.75 Toluene	298.27	851.8	1099.45	4.7603	4.8286	4.6208
+	323.32	827.6	878.14	5.4691	8.3841	9.5869
0.25 Aceto-	348.33	802.7	713.61	5.4458	8.3213	9.0271
nitrile	373.26	780.2	584.64	5.0934	6.6978	6.3004
0.25 Toluene	298.27	699.6	677.01	4.8984	6.5022	6.5619
+	323.33	676.5	545.25	4.7060	5.5578	4.7280
0.75 n-Hexane	348.40	651.2	443.43	4.4610	5.2390	4.9437
	373.36	623.6	316.48	4.5396	5.5355	4.8536
0.50 Toluene	298.22	748.5	829.45	5.0482	5.8262	5.4311
+	323.26	725.9	653.12	5.2193	7.0595	7.0838
0.50 n-Hexane	348.35	701.7	512.35	4.9694	5.9430	5.1856
	373.35	676.1	377.90	5.2965	7.7340	7.0466
0.75 Toluene	298.2	802.2	696.24	5.1311	5.5918	5.2080
+	323.31	778.6	751.61	5.9059	8.7794	8.7087
0.25 n-Hexane	348.32	754.7	663.38	5.0422	5.5169	4.6841
	373.49	729.5	574.39	4.4200	3.5858	2.6821
0.333 n-Octane	298.15	698.8	742.78	5.6155	7.6320	7.6086
+	232.15	679.0	649.59	5.0506	5.7201	5.3945
0.333 i-Octane	348.15	657.4	506.13	5.3656	7.7950	8.2108
+	373.15	634.2	395.03	4.9919	6.1062	5.5427
0.333 Octa-1-ene						

(a)-data from J.H.Dymond and R.Malhotra (1988) [173]
(b)-data from J.H.Dymond and K.J.Young (1979) [62]

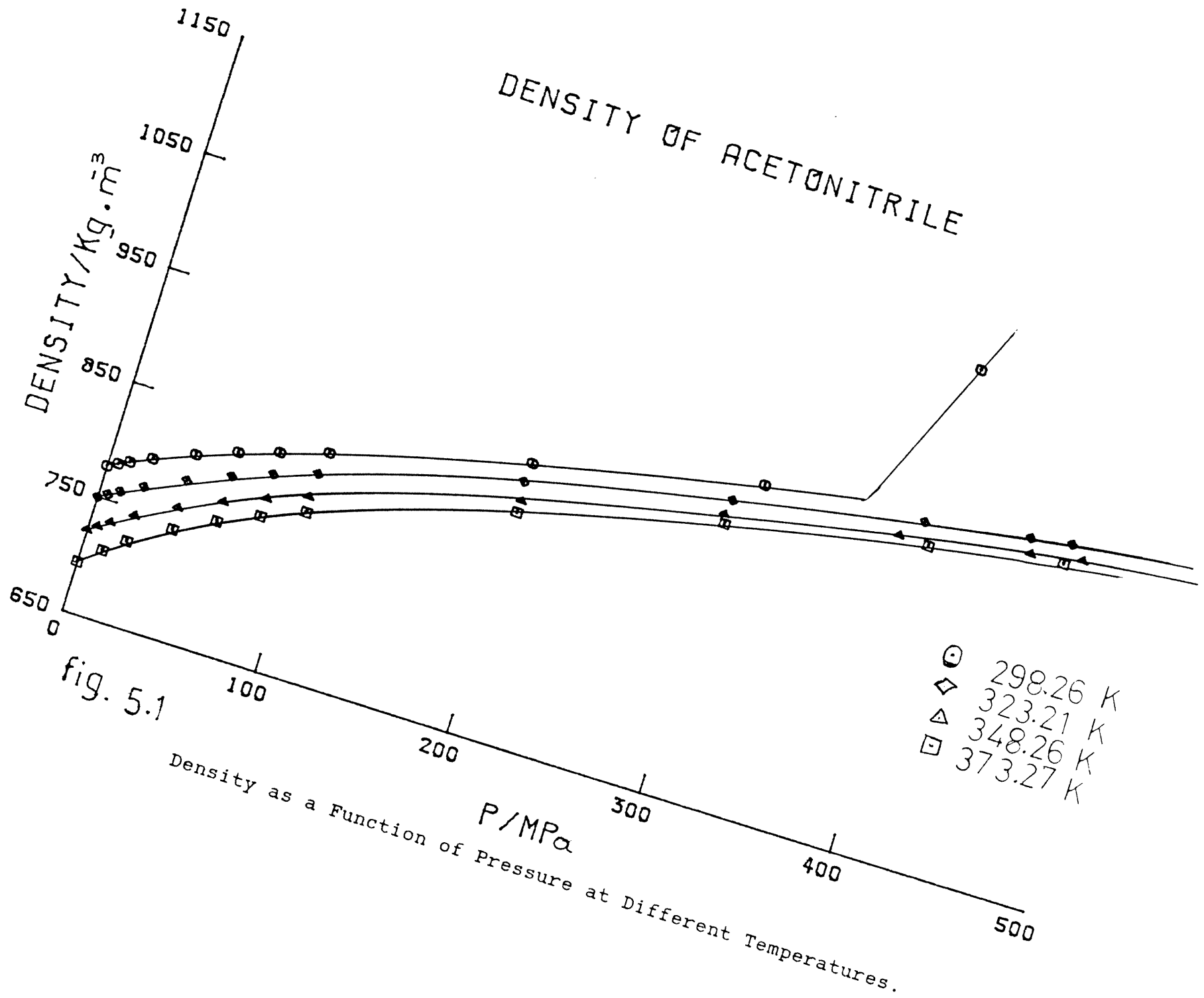

fig. 5.1

Density as a Function of Pressure at Different Temperatures.

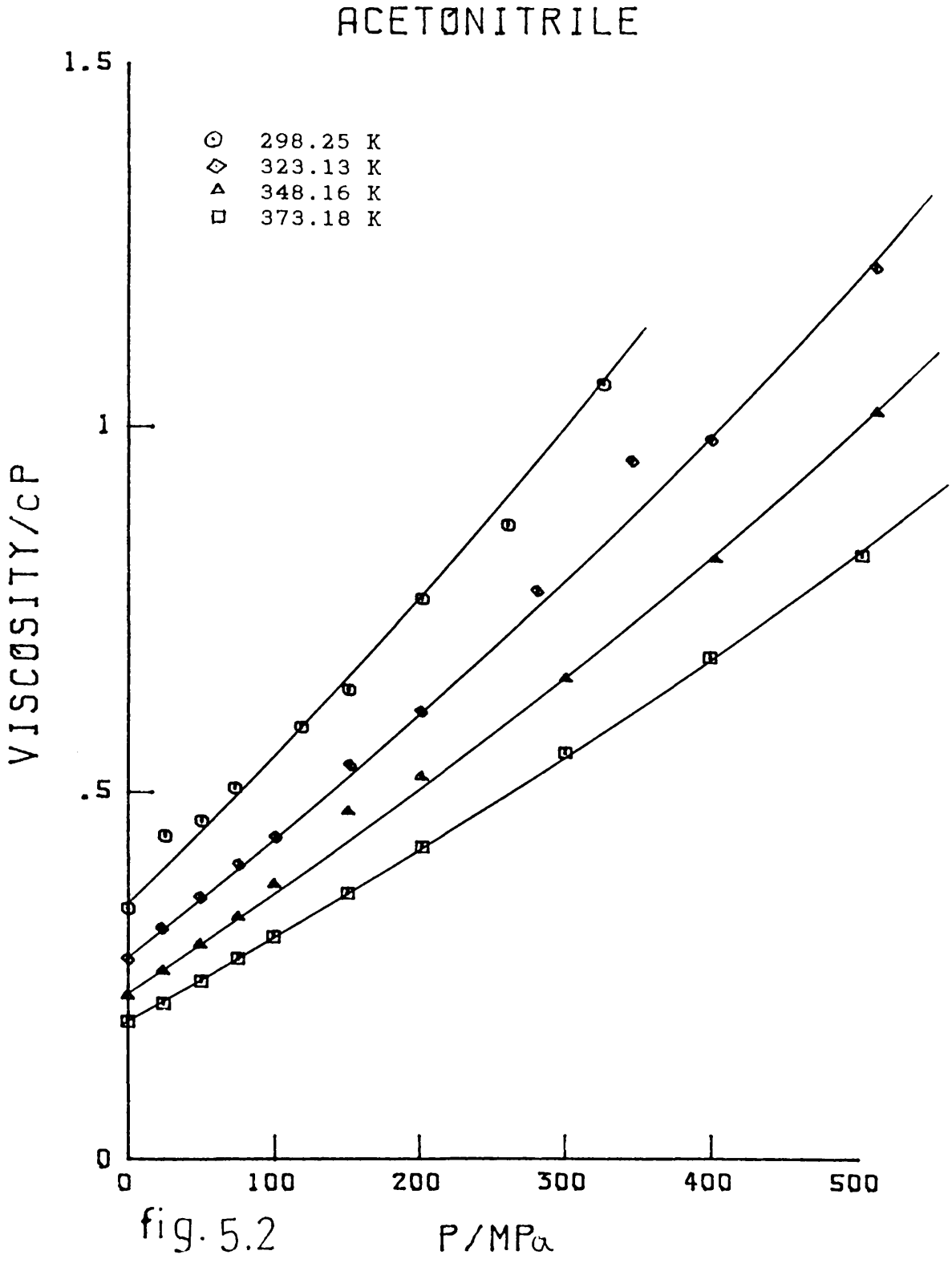

fig. 5.2

VISCOSITY COEFFICIENT AS A FUNCTION OF PRESSURE

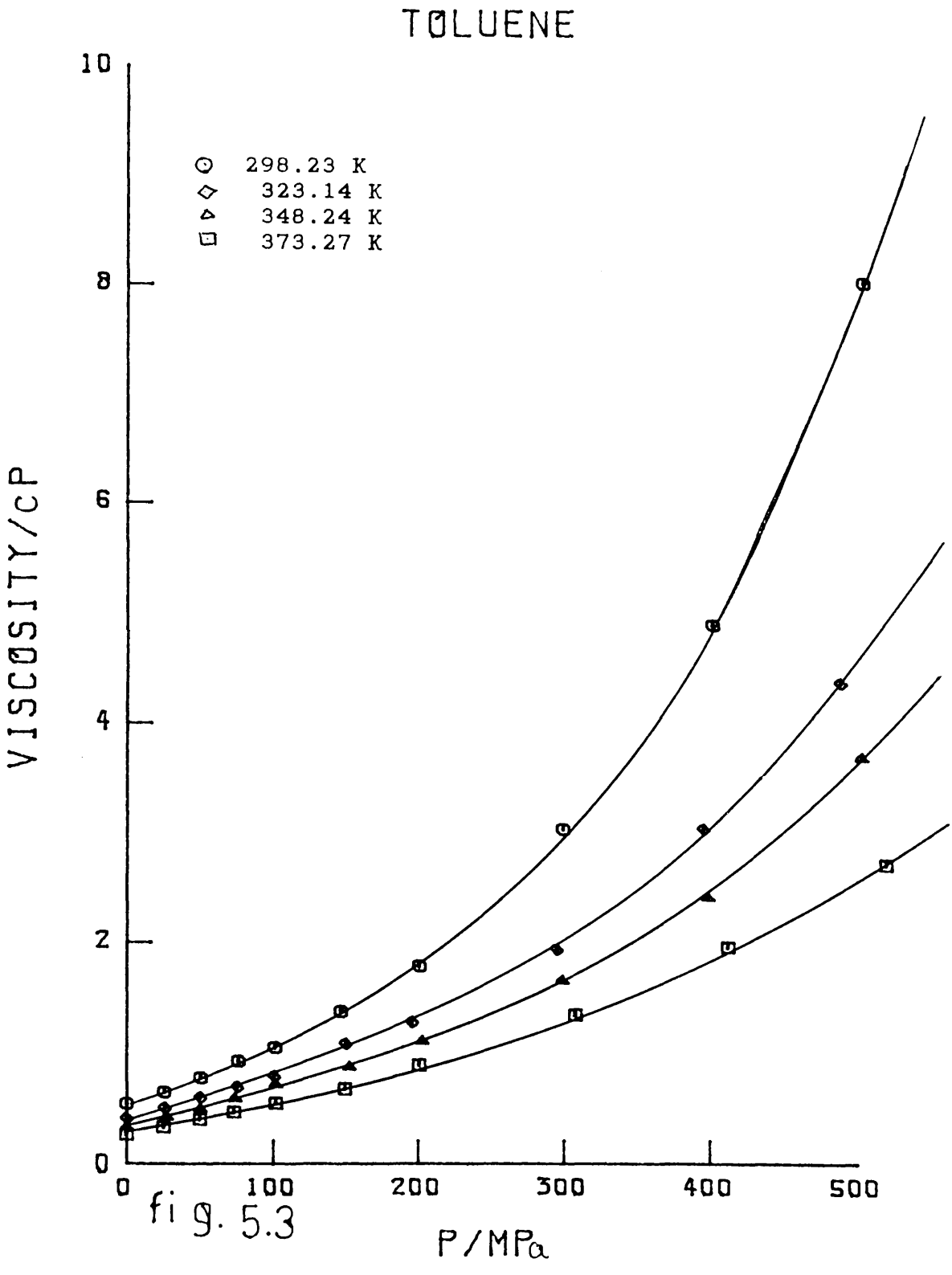

fig. 5.3

VISCOSITY COEFFICIENT AS A FUNCTION OF PRESSURE

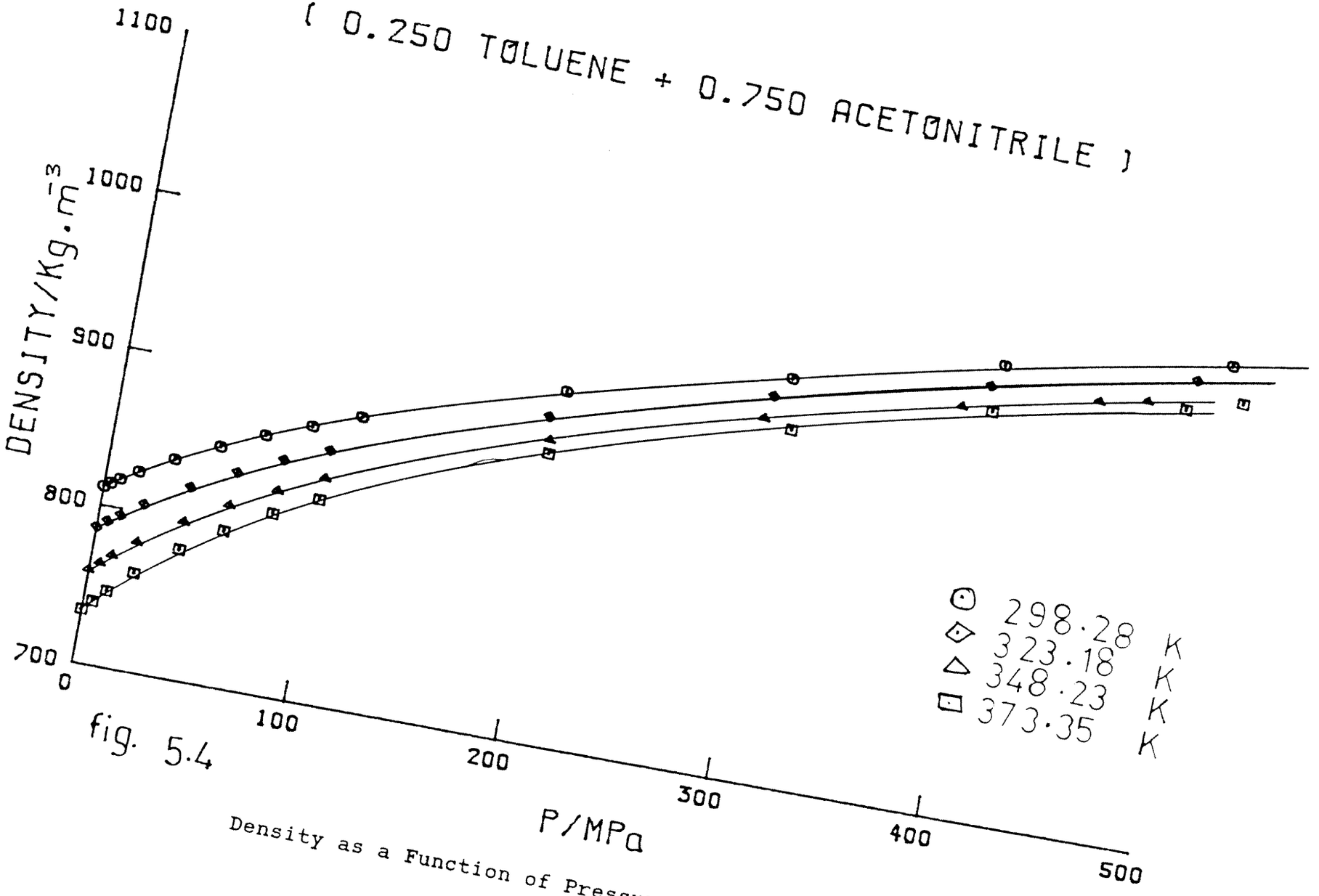

fig. 5.4

Density as a Function of Pressure at Different Temperatures.

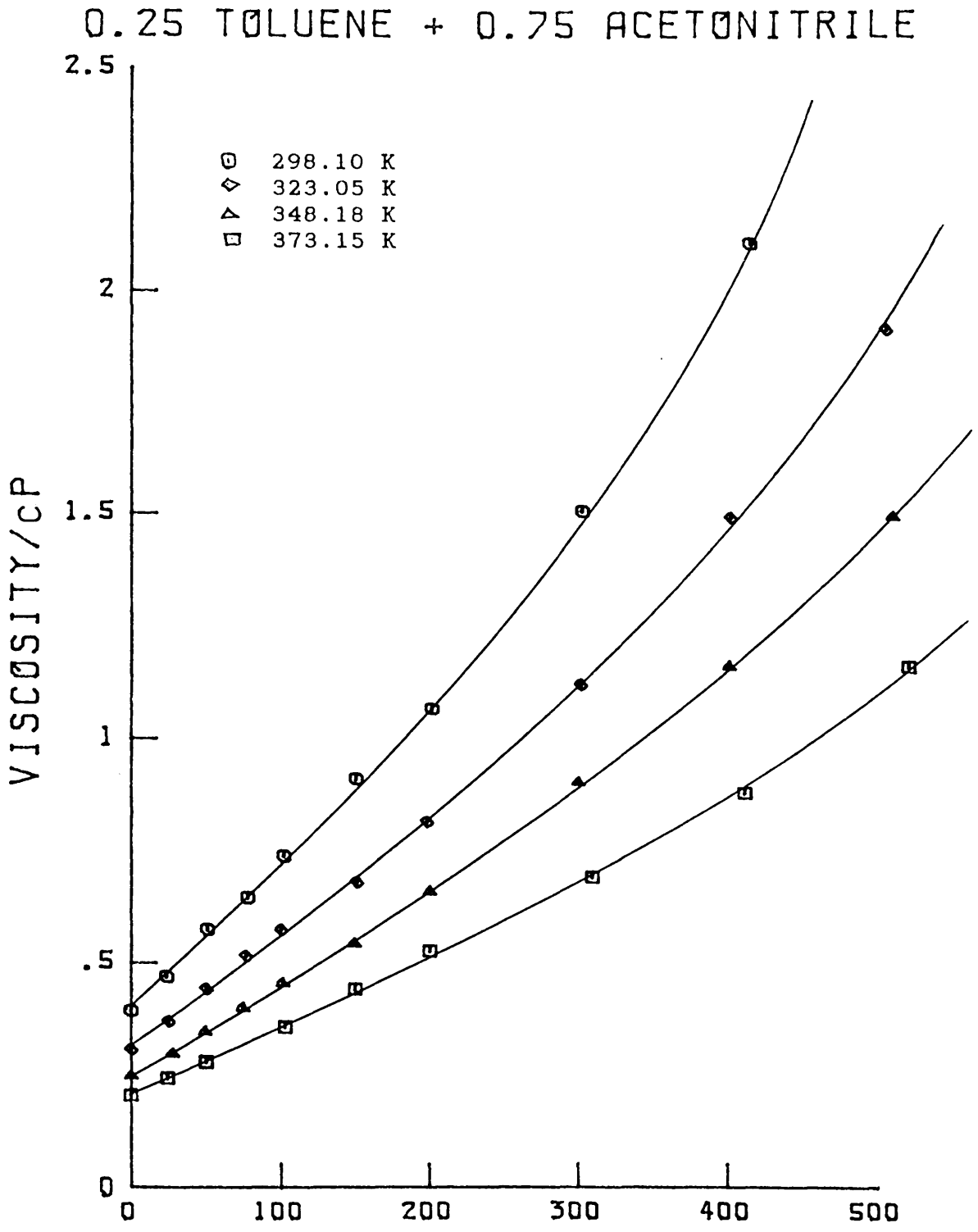

fig. 5.5 VISCOSITY COEFFICIENT AS A FUNCTION OF PRESSURE

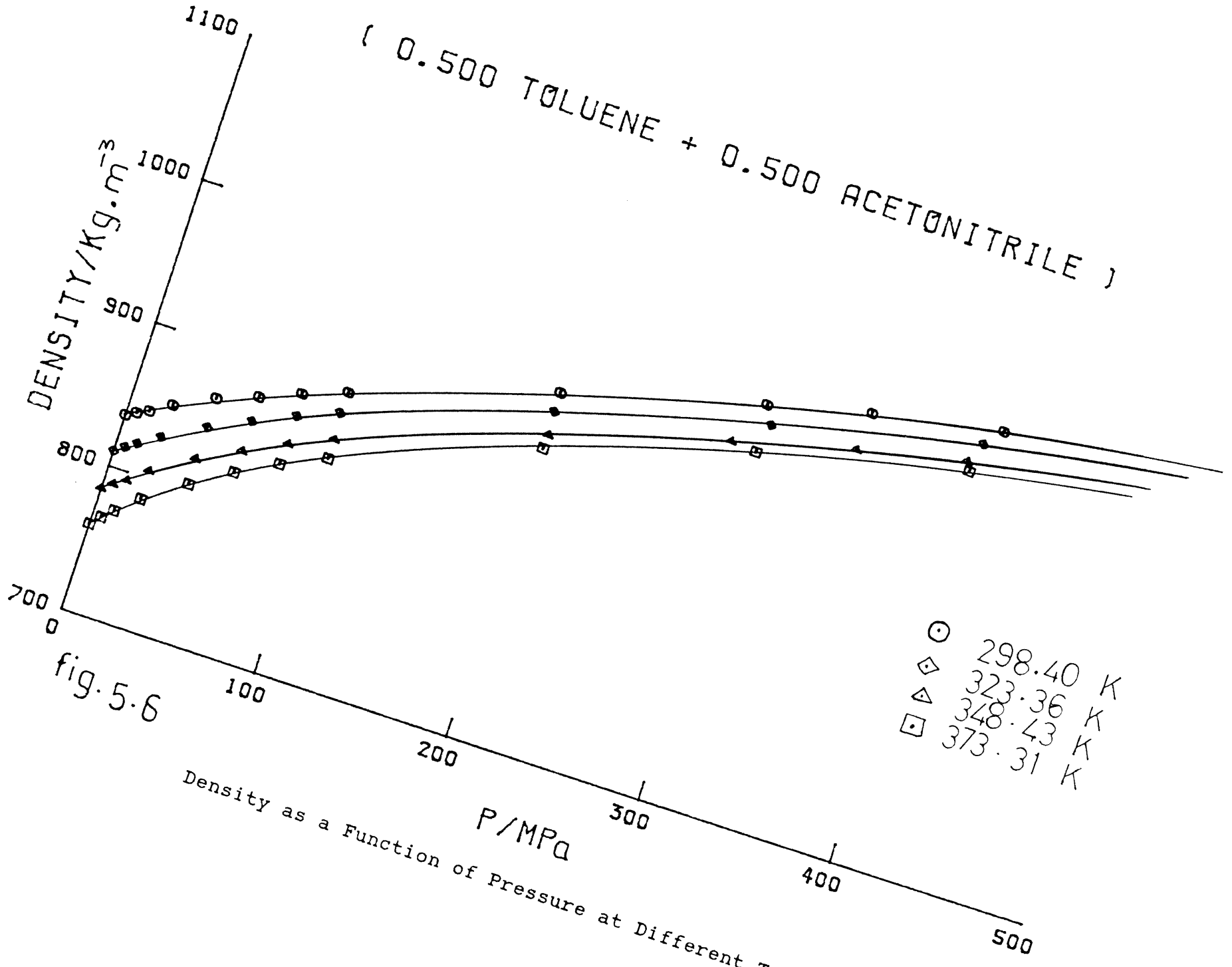

fig. 5.6

Density as a Function of Pressure at Different Temperatures.

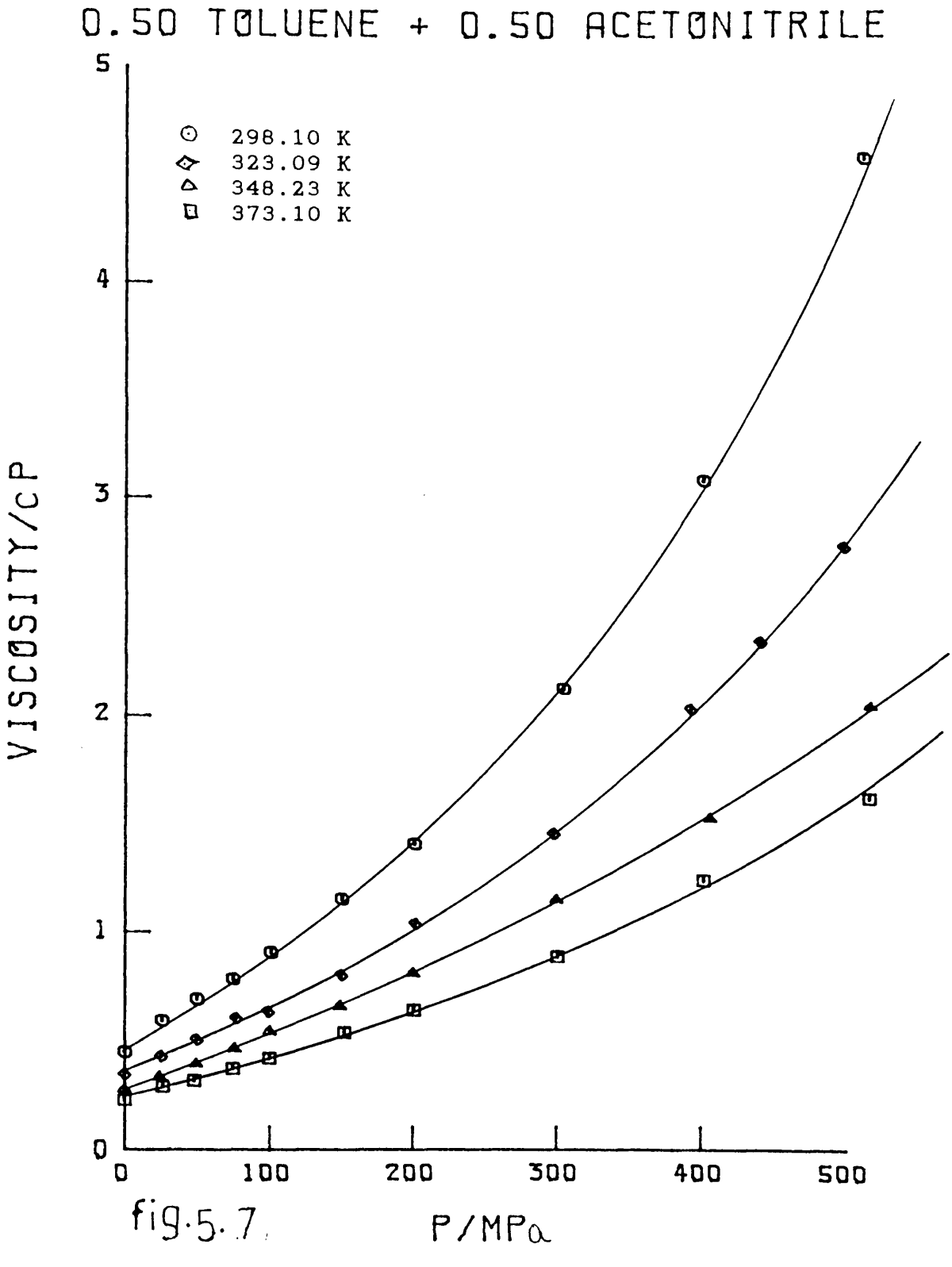

fig.5.7

VISCOSITY COEFFICIENT AS A FUNCTION OF PRESSURE

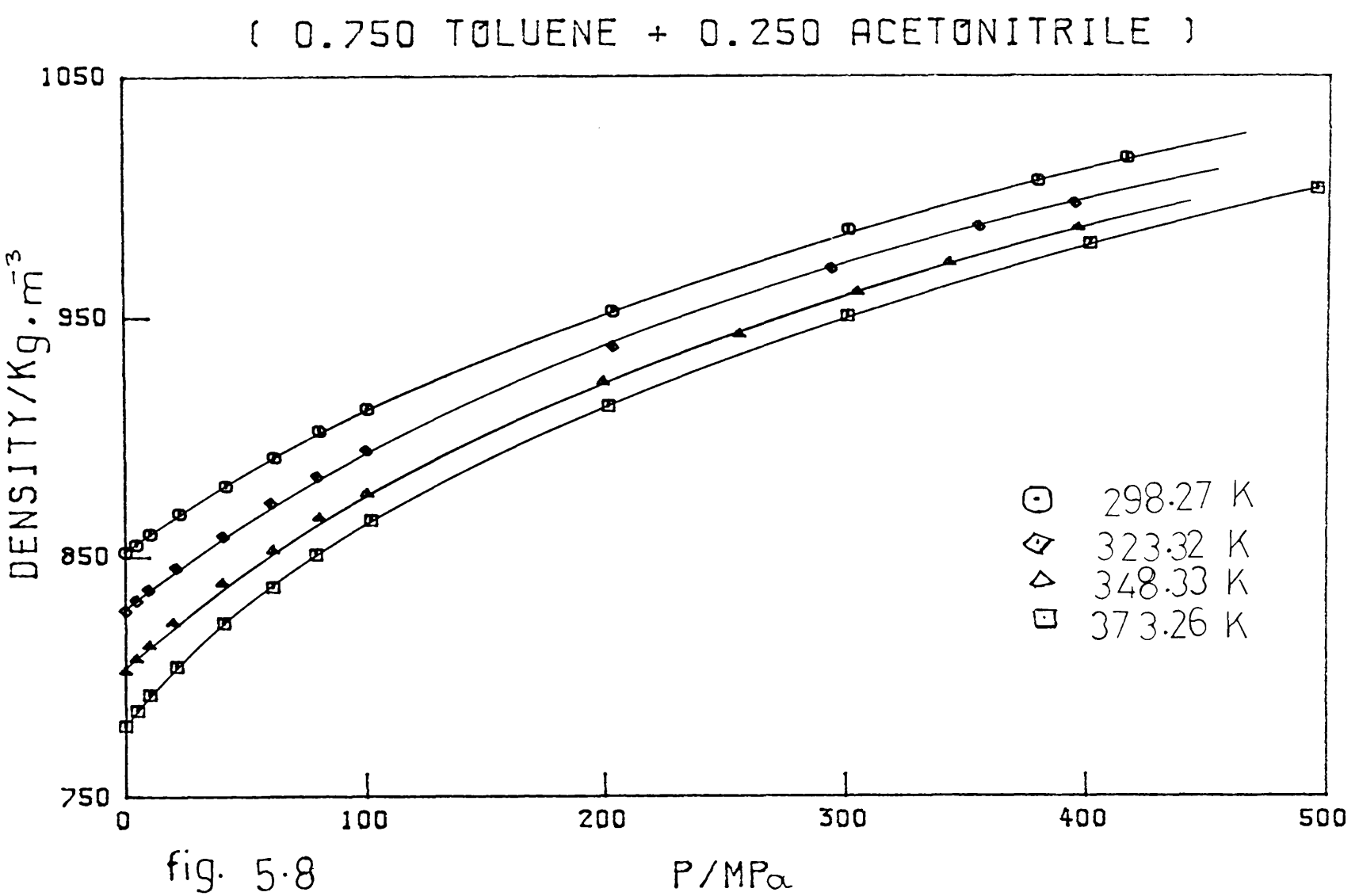

fig. 5·8

Density as a Function of Pressure at Different Temperatures.

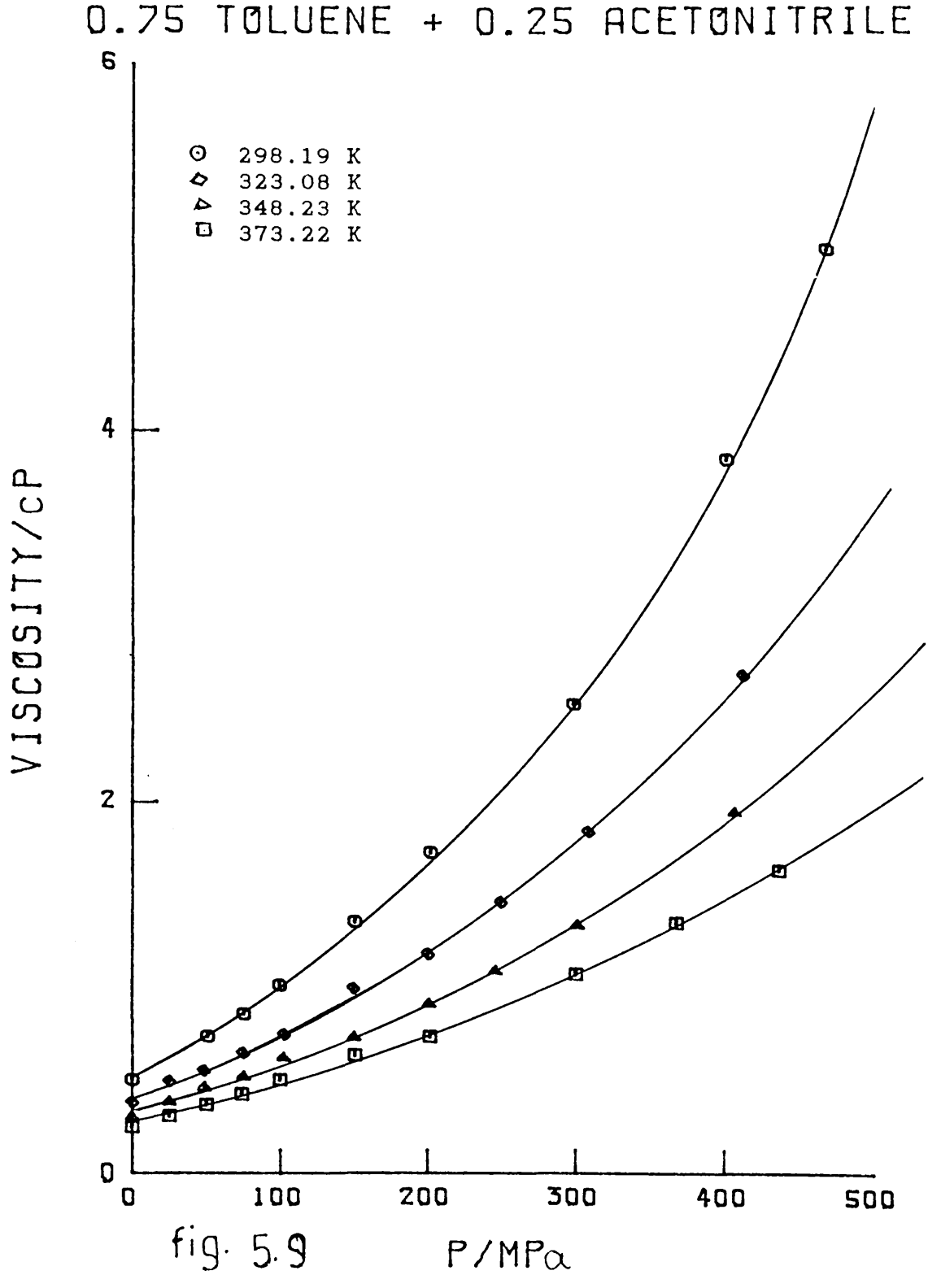

fig. 5.9

VISCOSITY COEFFICIENT AS A FUNCTION OF PRESSURE

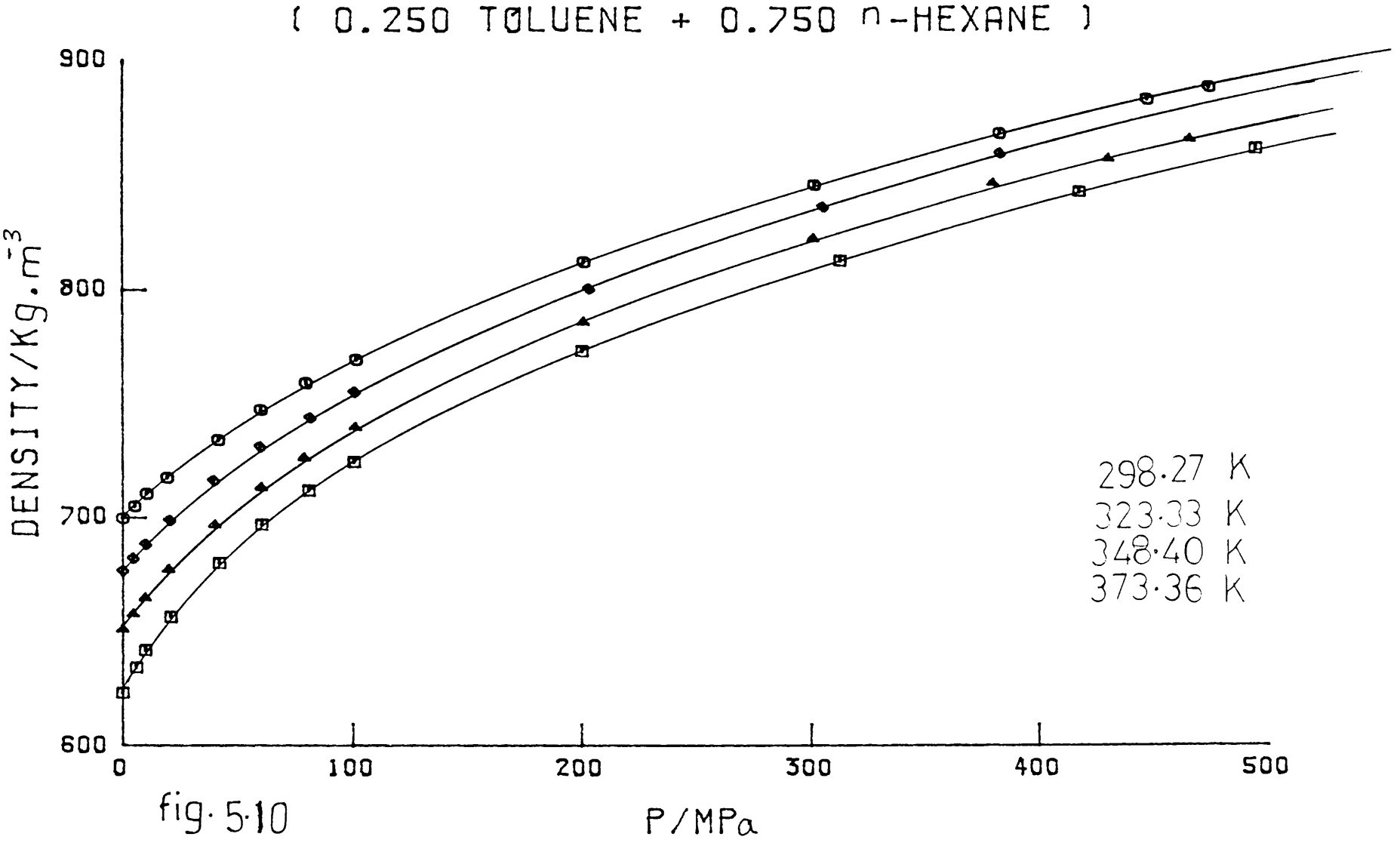

fig. 5.10

Density as a Function of Pressure at Different Temperatures.

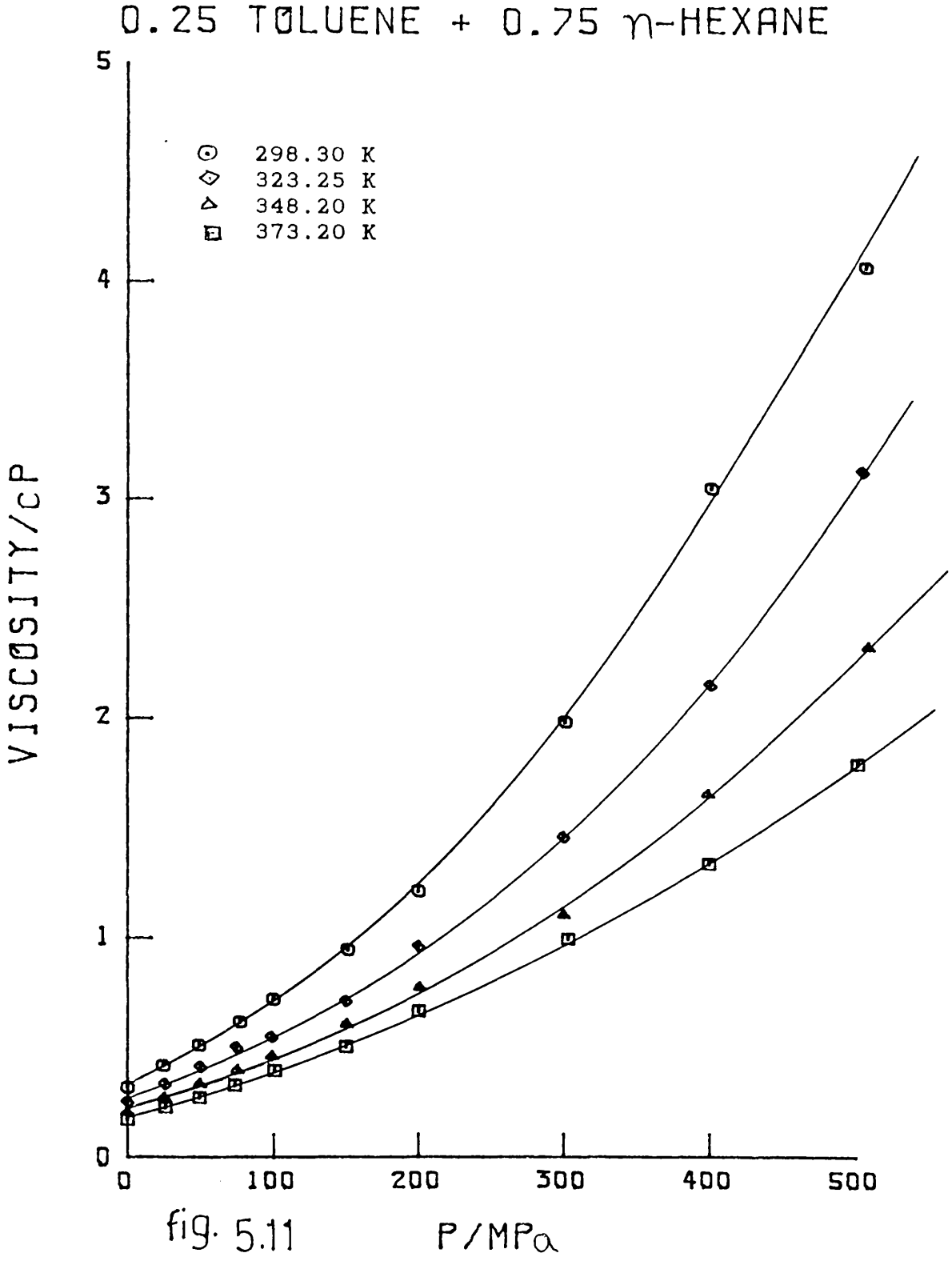

fig. 5.11

VISCOSITY COEFFICIENT AS A FUNCTION OF PRESSURE

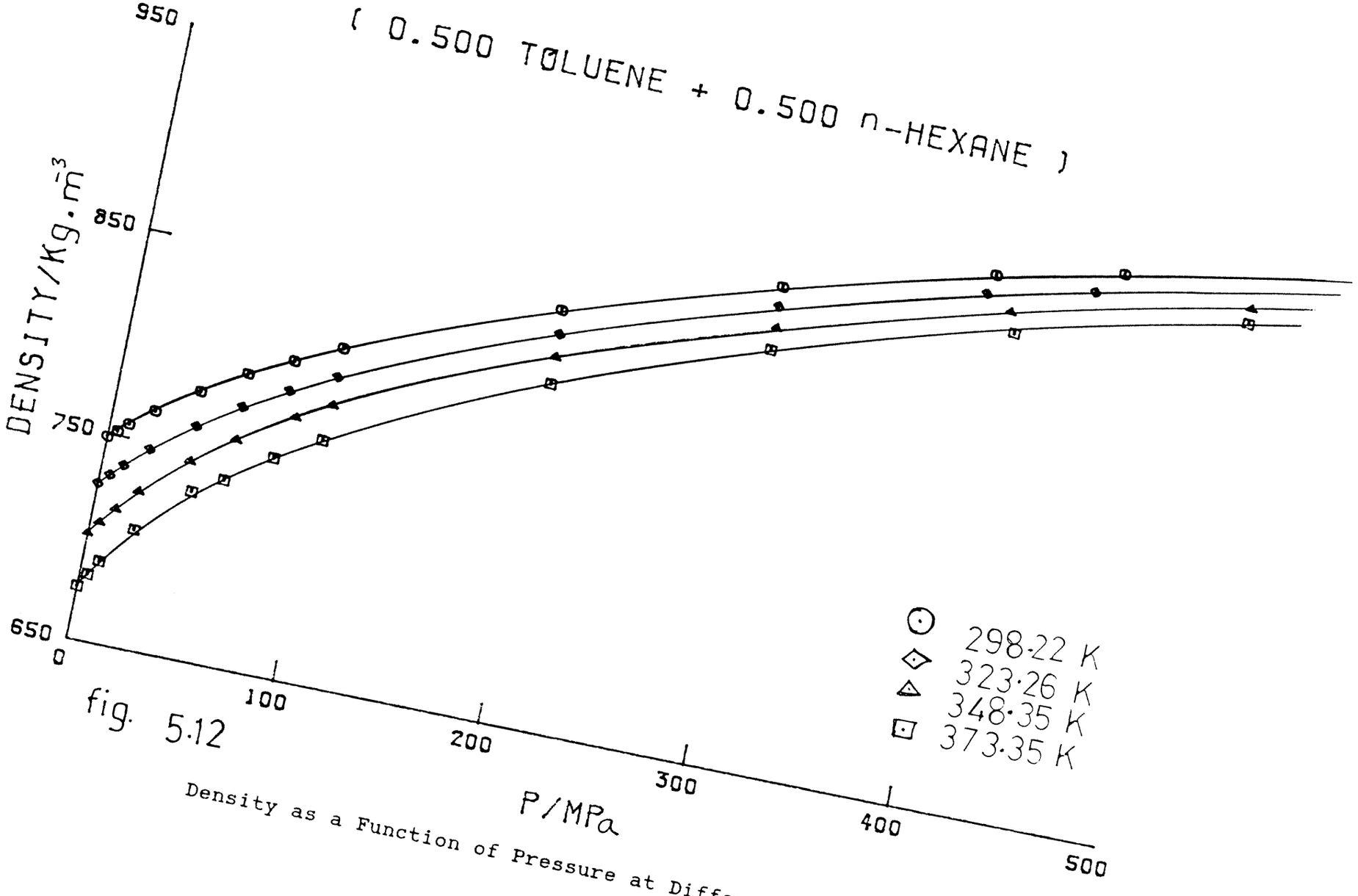

fig. 5.12

Density as a Function of Pressure at Different Temperatures.

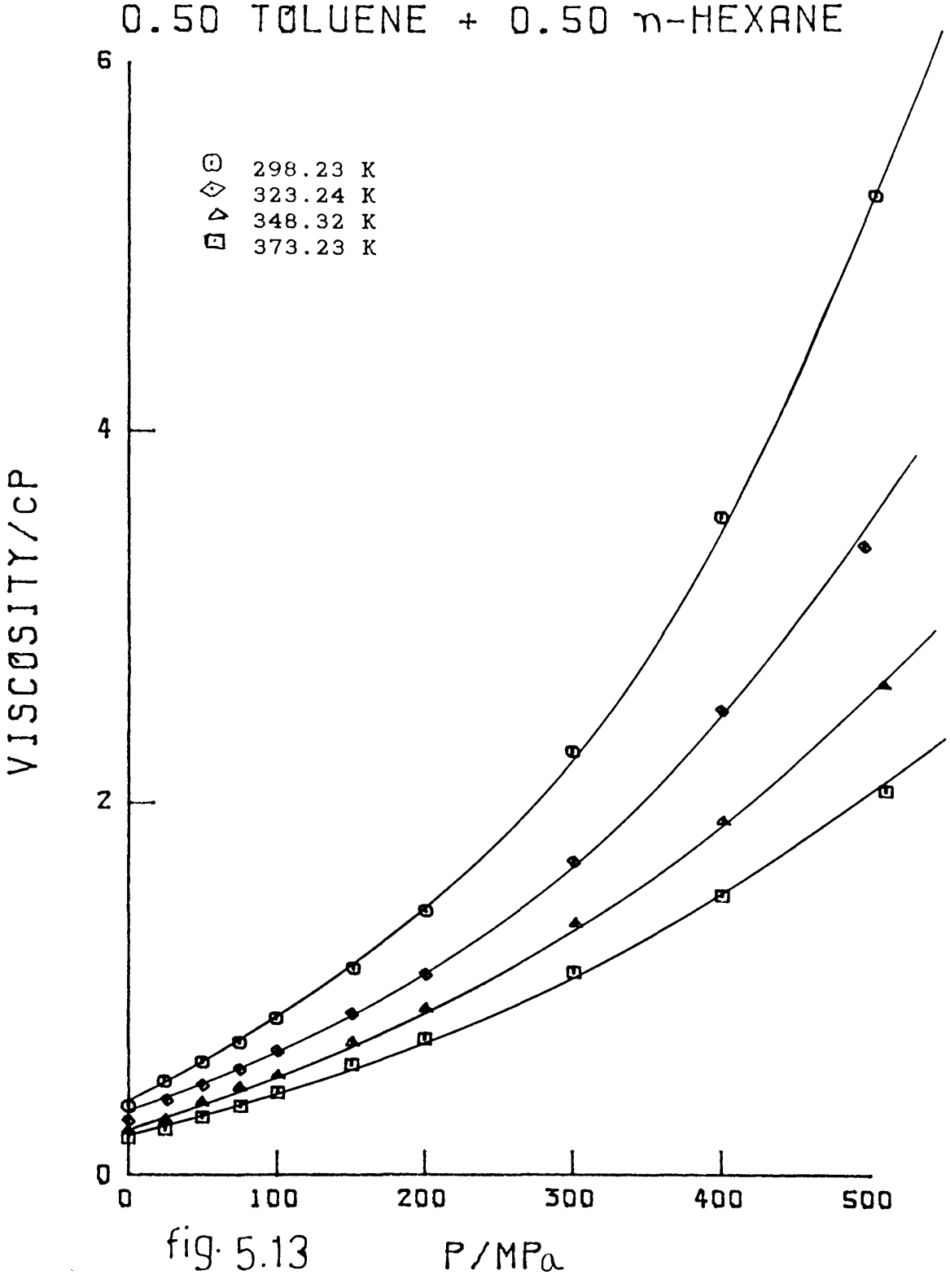

fig. 5.13

VISCOSITY COEFFICIENT AS A FUNCTION OF PRESSURE

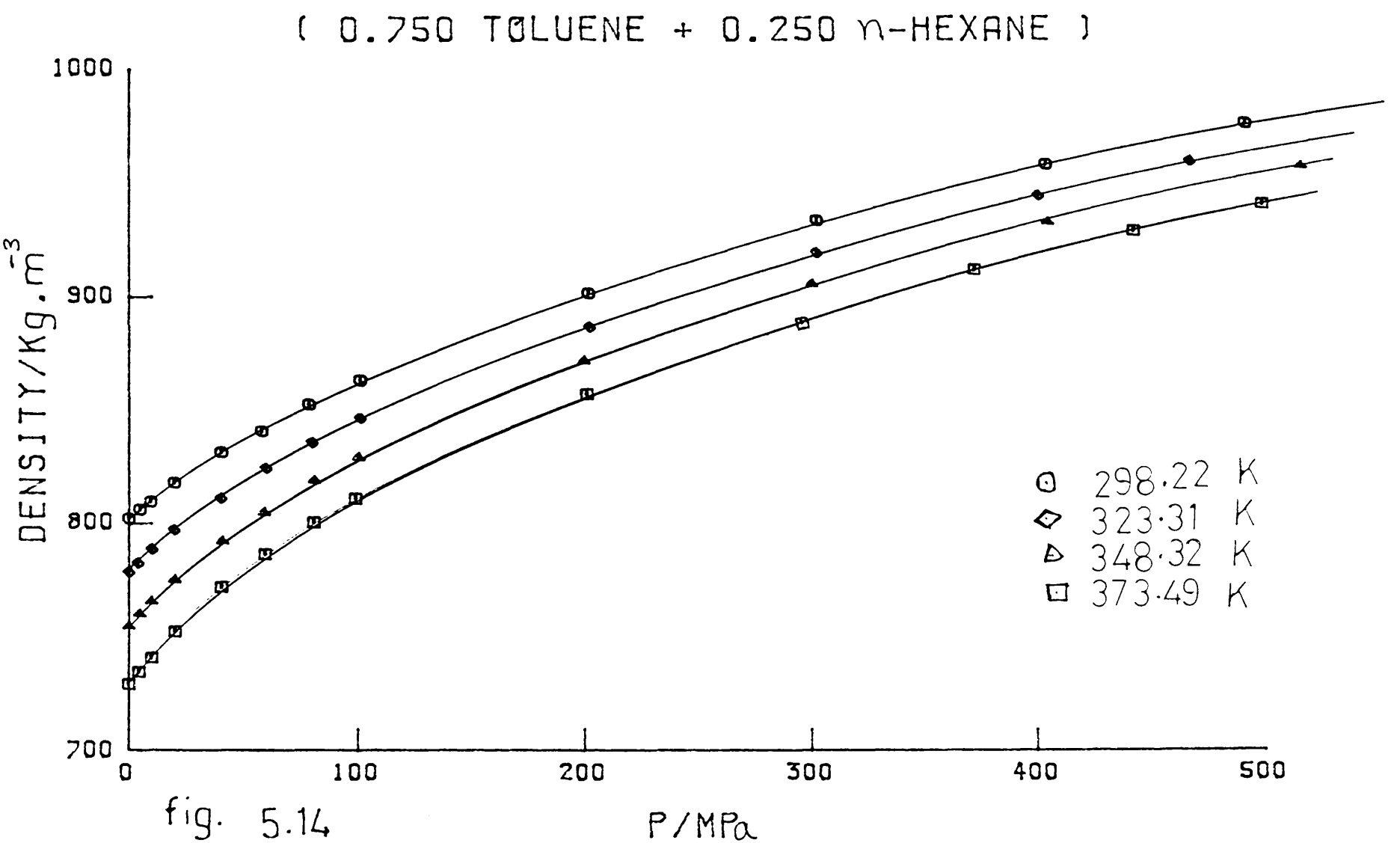

fig. 5.14

Density as a Function of Pressure at Different Temperatures.

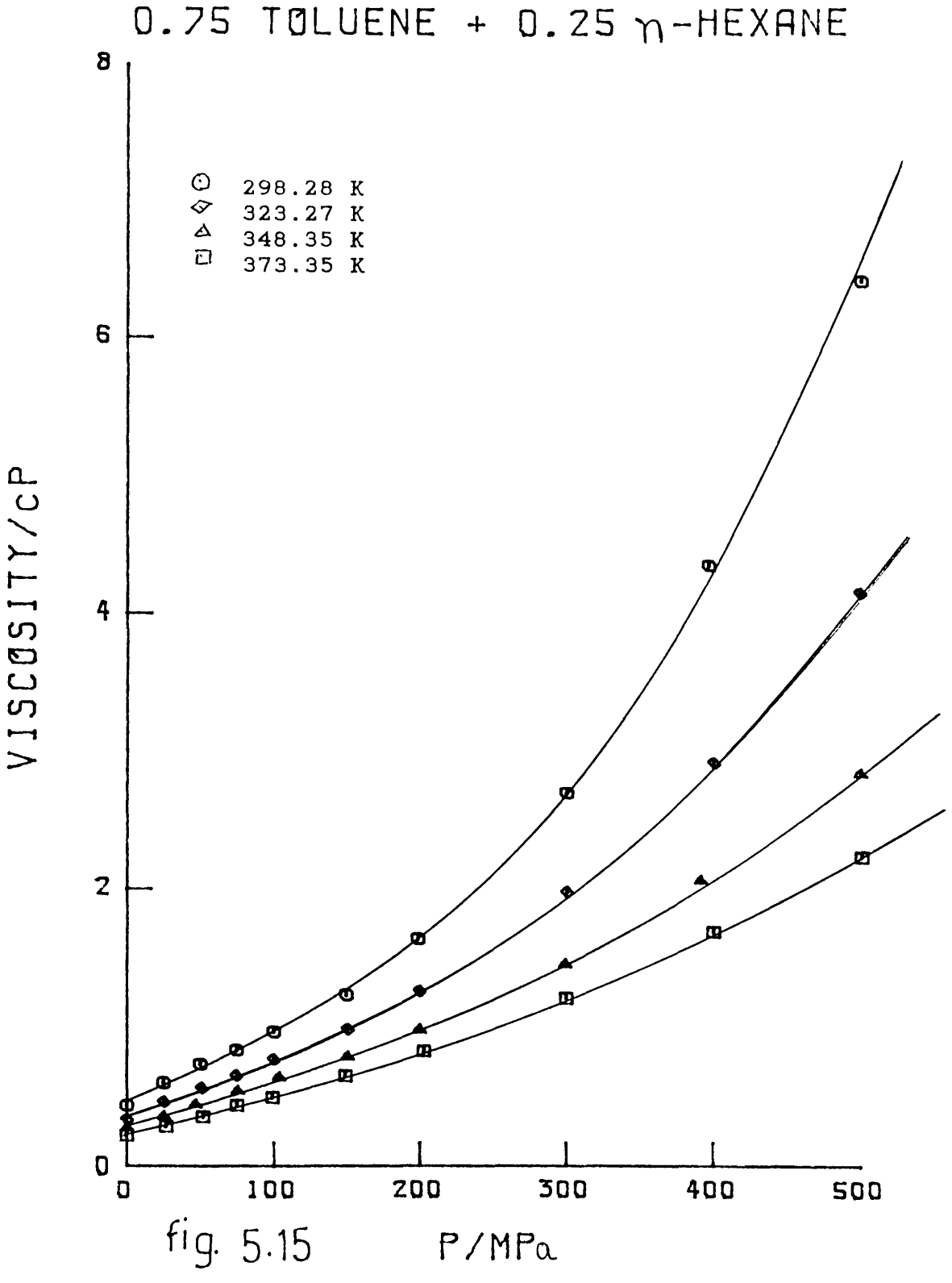

fig. 5.15

VISCOSITY COEFFICIENT AS A FUNCTION OF PRESSURE

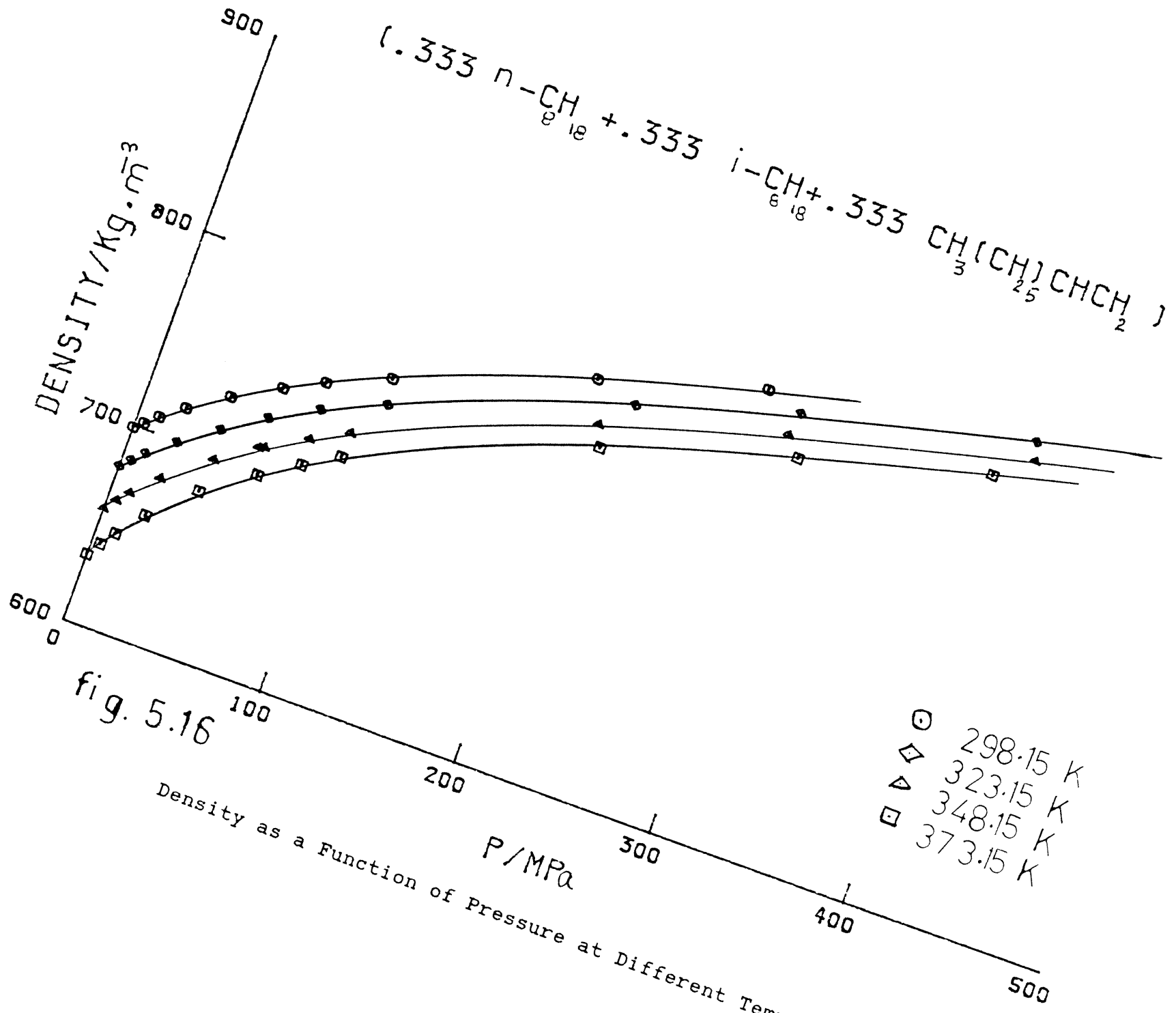

fig. 5.16

Density as a Function of Pressure at Different Temperatures.

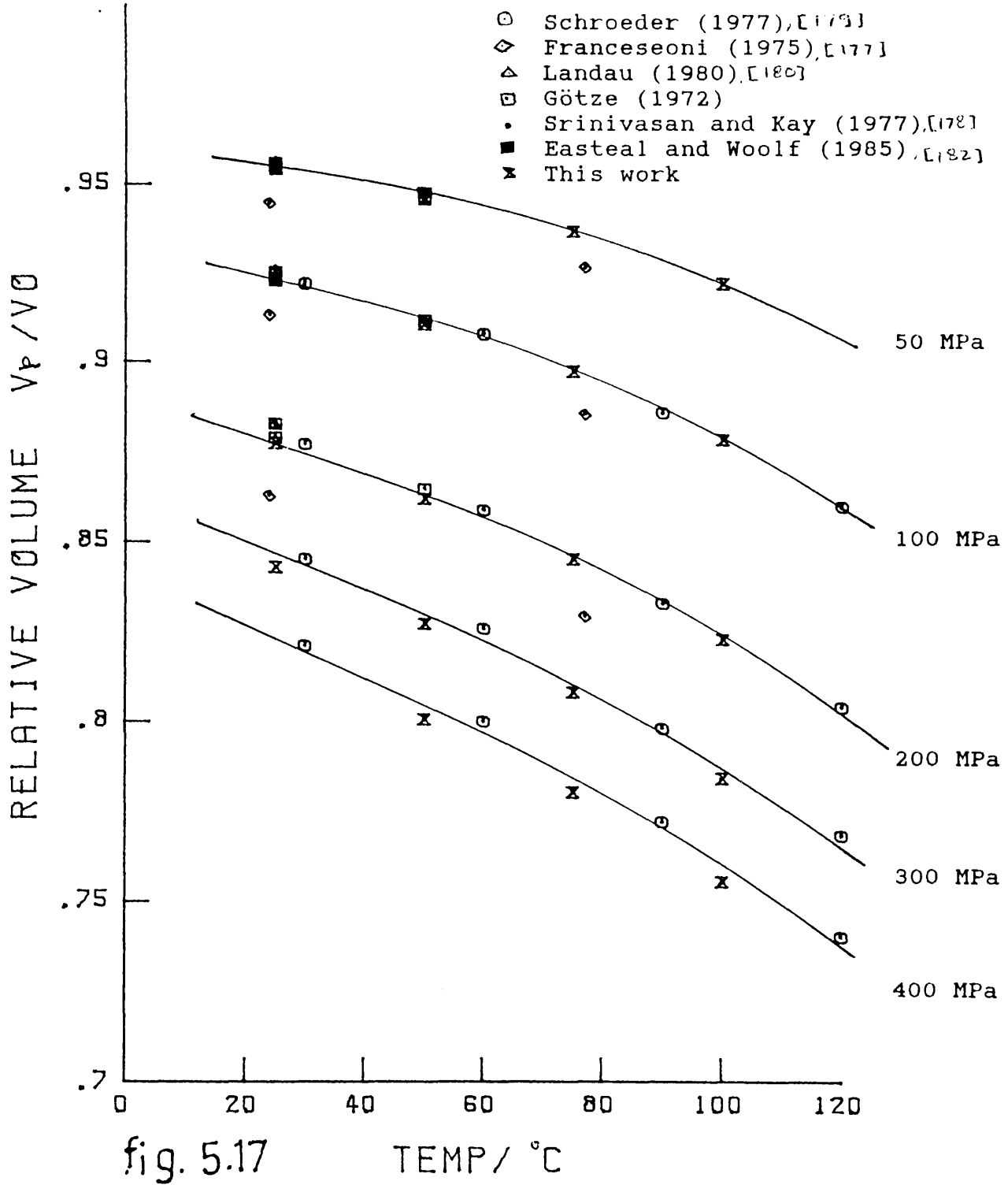

fig. 5.17

COMPARISON OF ACETONITRILE RELATIVE VOLUME WITH LITERATURE VALUES.

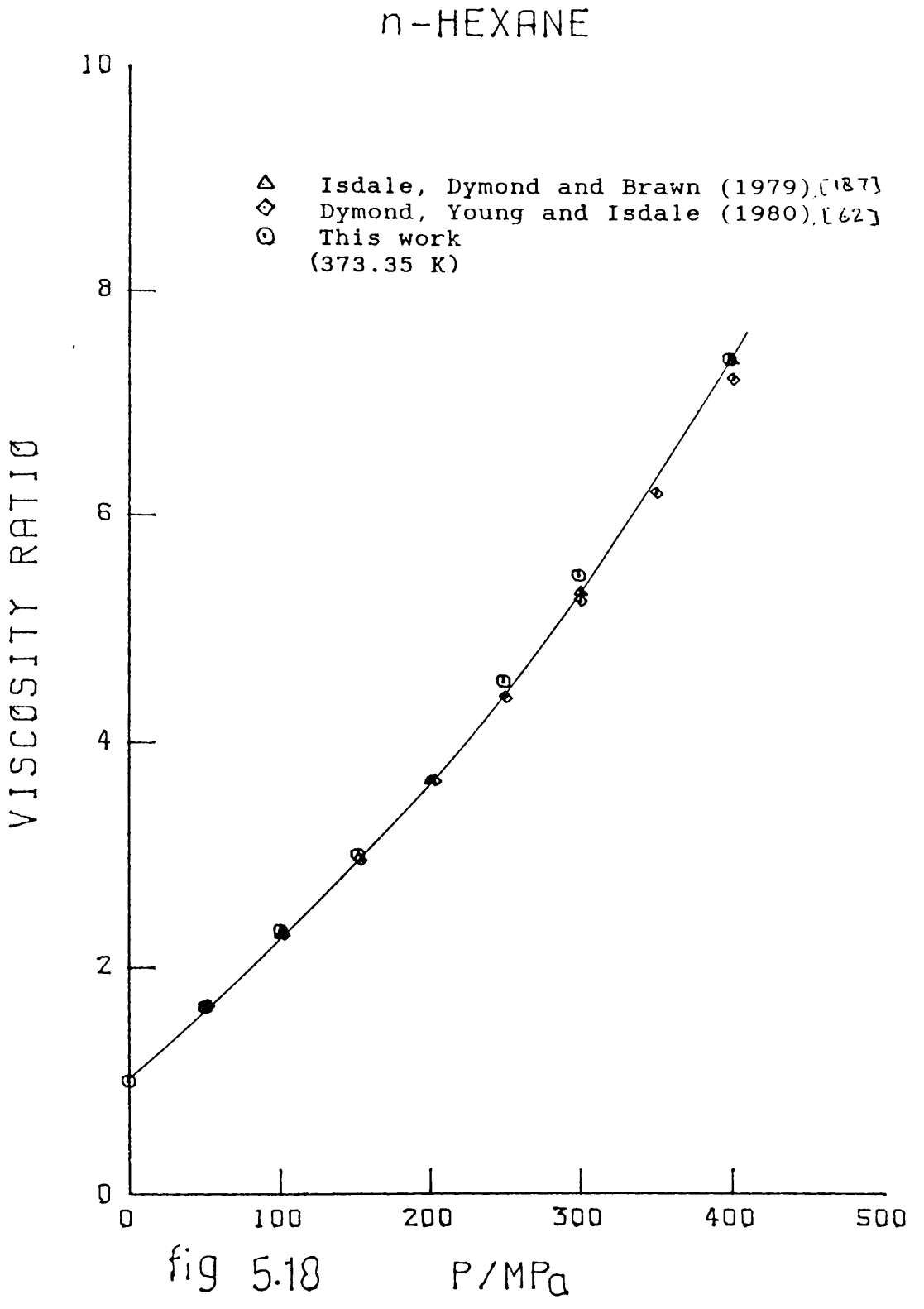

fig 5.18

COMPARISON OF MEASURED VISCOSITY COEFFICIENT WITH LITERATURE VALUES.

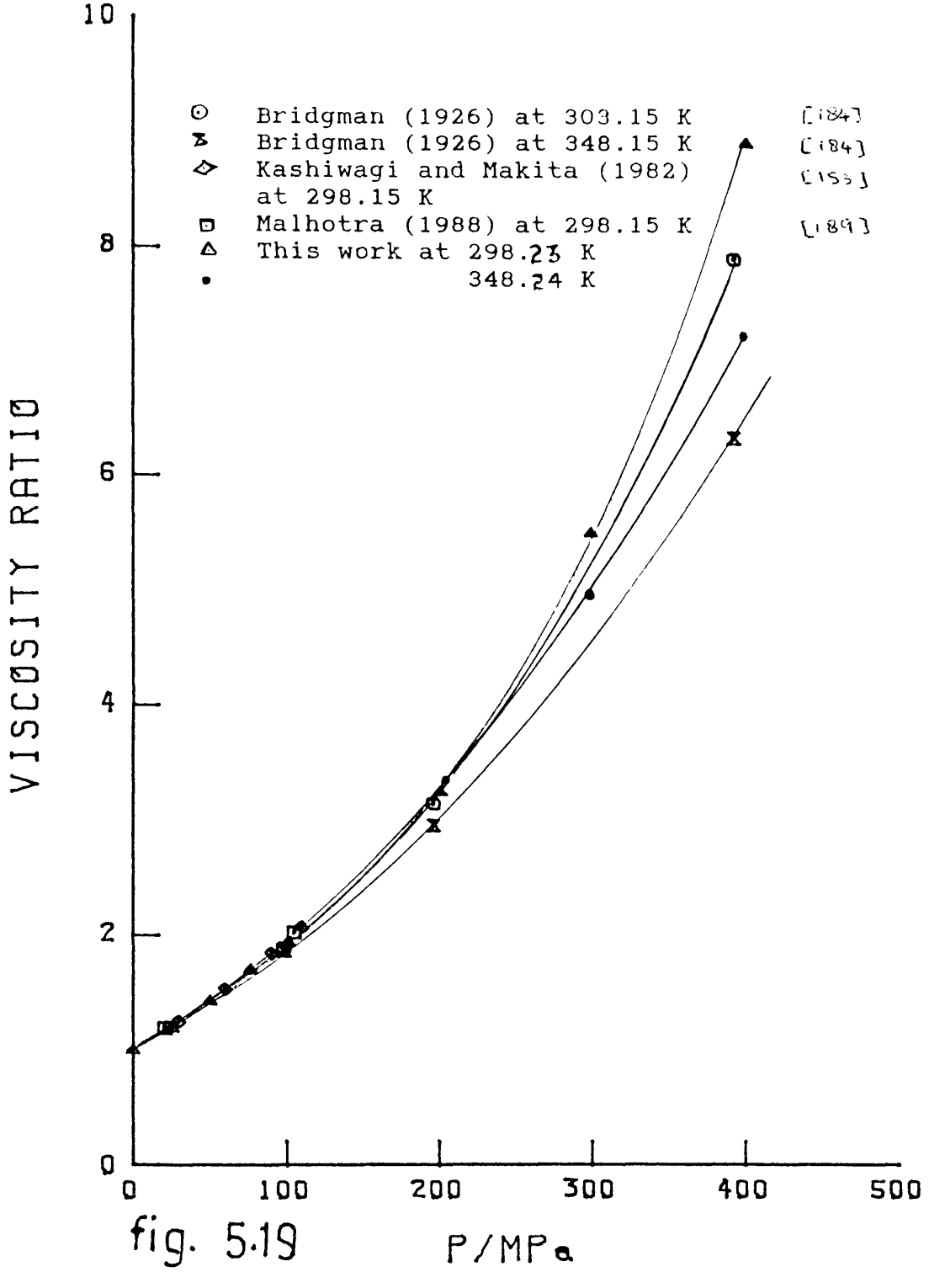

fig. 5.19

Comparison of Experimental Viscosity coefficient For Toluene with Literature Values at Different Temperatures and Pressures.

CHAPTER 6

DISCUSSION

6.1 INTRODUCTION

The density and viscosity coefficient data obtained in this work, which cover a wide range of temperature and pressure, are used in the following sections to test the various existing theories and empirical relations. The main aim of the density measurements at elevated pressures was to be able to calculate the dynamic viscosity coefficients, but measured densities obtained are sufficiently accurate to calculate the molar excess volume, V_M^E. The density data are successfully fitted to the Tait equation. The viscosity coefficient data are discussed in terms of hard sphere theory, free volume theory and the Grunberg and Nissan equation.

6.2 DISCUSSION OF DENSITY DATA

6.2.1 MOLAR EXCESS VOLUME.

When two miscible liquids are combined to form a binary mixture, the final volume is not usually the sum of the volumes of the pure components. The difference is called excess volume, mathematically

$$V_M^E = V_M - (x_1M_1/\rho_1 + x_1M_2/\rho_2) \qquad (6.1)$$

where x, M, ρ are the mole fraction, molar mass and density respectively. There are currently two general methods employed in determination of V_M^E for binary mixtures. First of these is an indirect method involving the measurement of density of the pure components and a series of mixtures at the same temperature. Density has normally been measured by using vibrating tube densimeter

[192-194] or by pyknometry [195] and V_M^E is calculated from equation 6.1 The second general method determines the change in volume directly using a dilatometric technique and is highly precise and accurate, but density of the individual components can not be obtained. Although determination of V_M^E was not the main aim of this research, the density obtained using a vibrating tube densitimeter at saturation pressure and with a bellows volumeter at elevated pressures was used to calculate V_M^E.

6.2.2 MOLAR EXCESS VOLUME OF BINARY MIXTURES AT SATURATION PRESSURE.

As shown in fig. 6.1, molar excess volumes for the toluene plus acetonitrile binary mixtures are small and negative, in accordance with the general trend for mixtures of lower nitriles plus aromatics (Rowlinson and Swinton, [198]). The curve is asymmetric and the minimum lies more towards toluene rich mixtures. The values of V_M^E at 323 K are practically identical to those at 298 K, but at 348 K the curve lies above the 298 and 323 K curve. Considering the uncertainties in the density measurements obtained using the vibrating tube densitimeter, and the calculated uncertainty in the derived V_M^E , the V_M^E values seems to be to a good approximation temperature independent for this system. V_M^E was not calculated at 373 K, as the densities at this temperature were extrapolated values, and will have higher uncertainty.

Molar excess volumes for toluene plus n-hexane binary mixtures are more negative and are in agreement with published values (Int. Data Series 1980 p 141). The V_M^E against mole fraction of toluene curve, fig. 6.2, is not truely symmetric but the minimum lies at equimolar

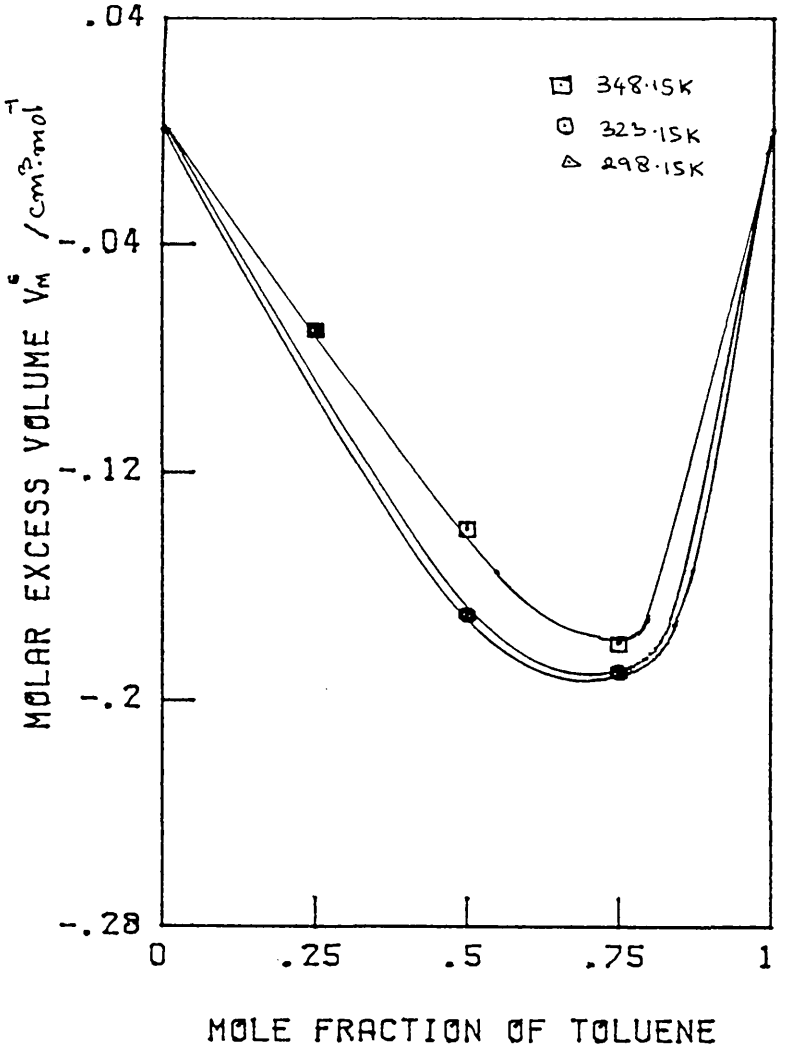

fig 6.1

toluene + acetonitrile

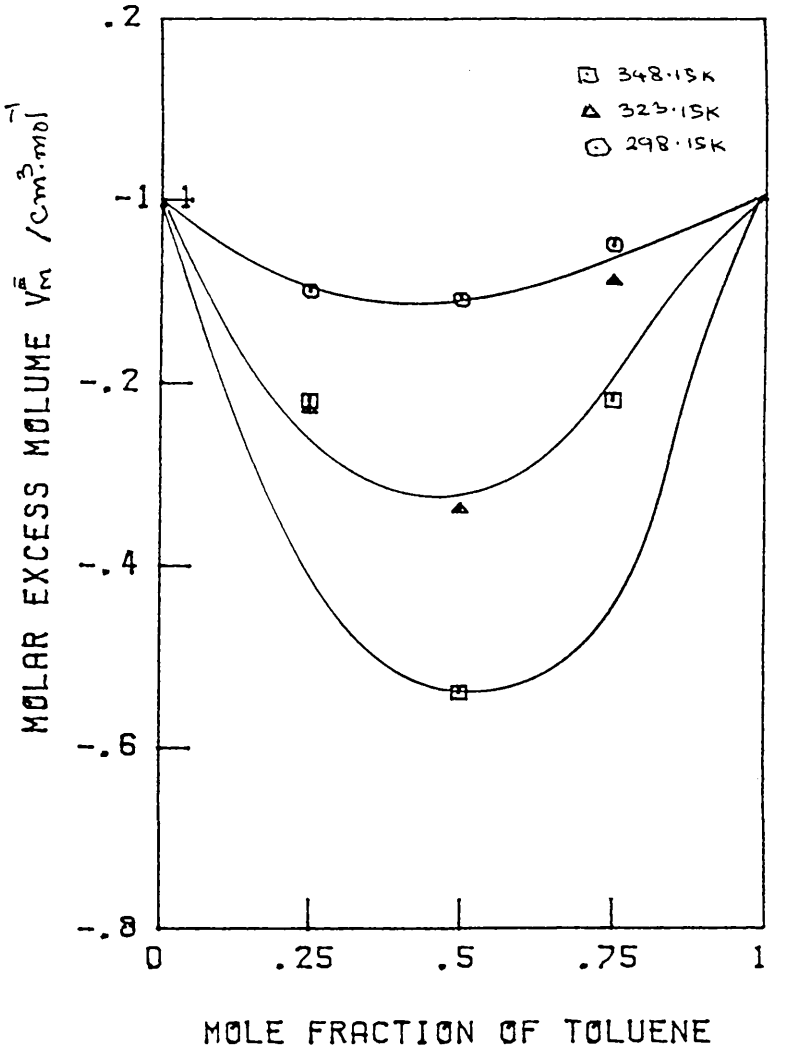

fig 6·2

toluene + n-hexane

composition. This system shows dependence of V_M^E on the temperature, becoming more negative as the temperature increases.

6.2.3 MOLAR EXCESS VOLUME OF BINARY MIXTURES AT ELEVATED PRESSURES

Molar excess volumes at elevated pressure for the six binary mixtures studied, have been calculated using densities measured by a bellows volumeter. Since the densities have an uncertainty of 0.2%, hence only a general trend of variation of V_M^E with composition, temperature and pressure can be considered. V_M^E for the equimolar toluene plus acetonitrile system has been plotted as a function of temperature and pressure in fig. 6.3. It can be seen that V_M^E increases slightly up to a pressure of 50 MPa at 298 and 323 K and then decreases with increase in pressure. For 348 and 373 K, V_M^E decreases with increases in pressure. This trend is less pronounced for the 0.75 mole fraction of toluene mixture and for the 0.25 mole fraction of toluene mixture. The variation of V_M^E with the composition of the mixture has been shown in fig. 6.4 at 323 K. The isobars follow a regular pattern of becoming more negative up to 0.5 mole fraction of toluene and then become less negative. Similar behaviour has been observed at other temperatures, and in all the cases the minimum lies close to 0.5 mole fraction of toluene in the mixture.

The variation of V_M^E for the two mixtures of toluene plus n-hexane with 0.25 and 0.5 mole fraction of toluene have been shown in fig. 6.5 The four isotherms of each mixture follow a regular pattern of variation within the uncertainty of density measurements. The V_M^E for mixture with 0.25 mole fraction of toluene are all negative and decrease with increasing pressure at constant temperature, while for

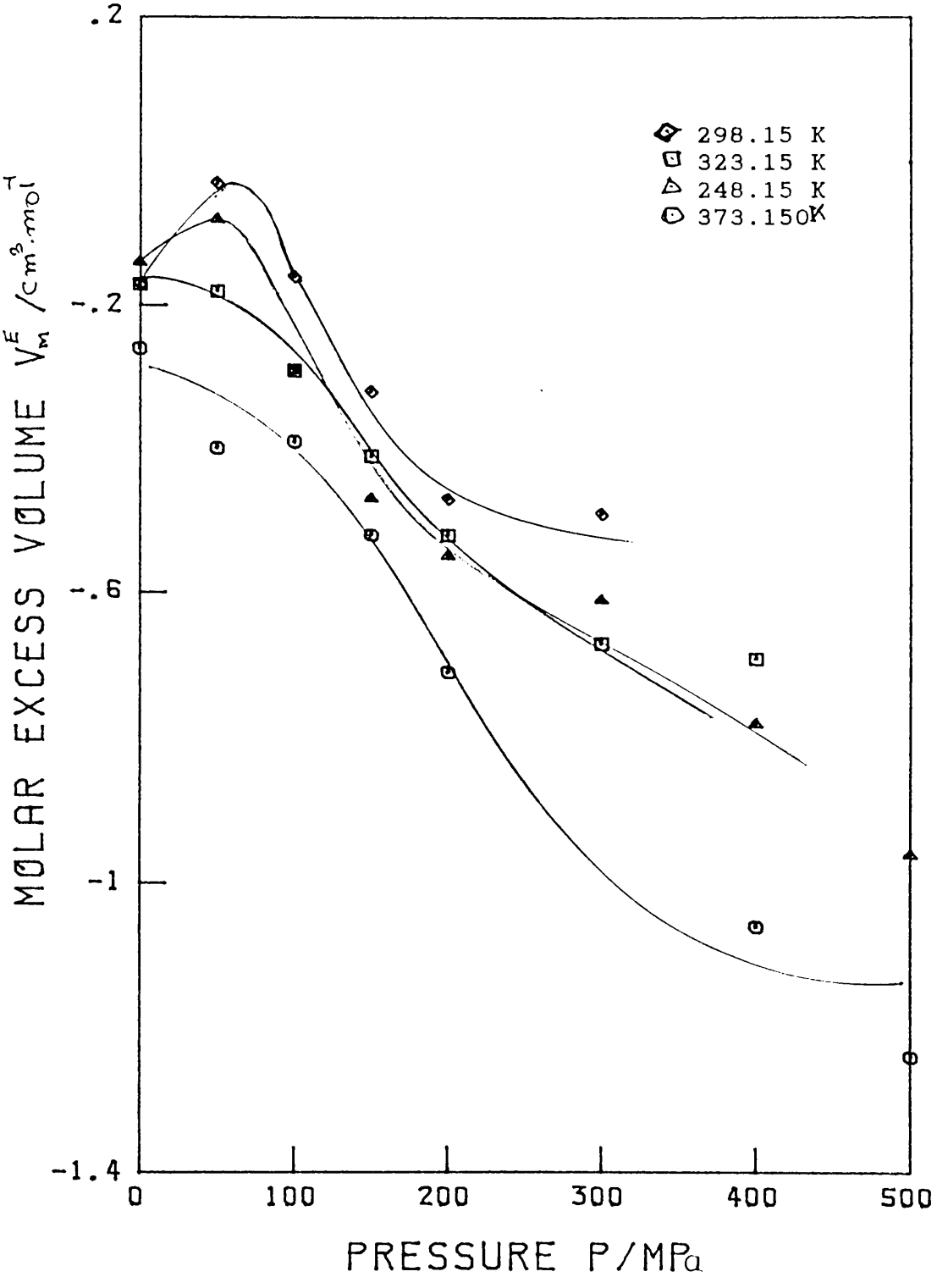

fig 6.3

Molar Excess Volume for equimolar mixture of toluene + acetonitrile, as a function of pressure

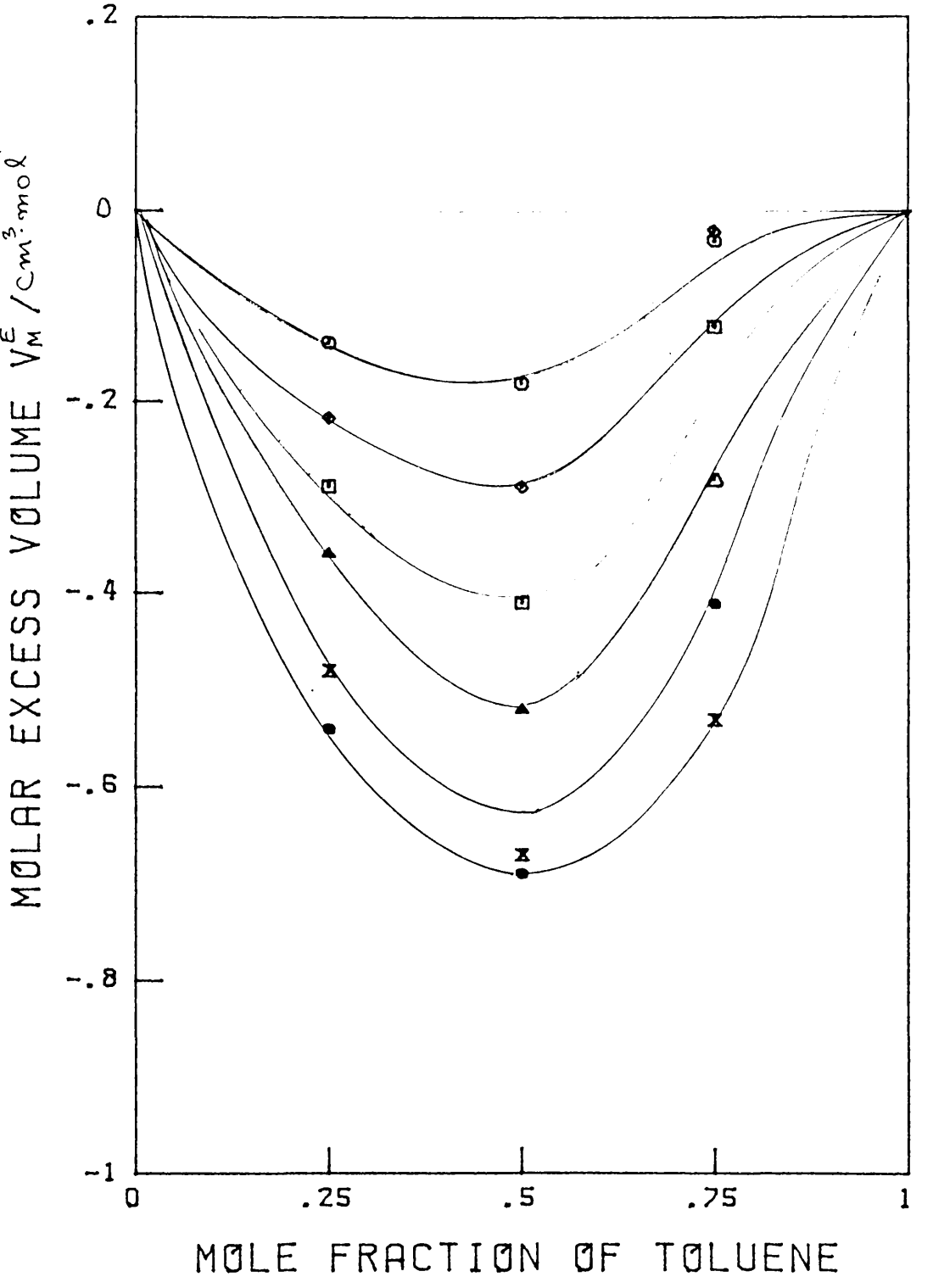

fig 6.4

Molar Excess Volume for mixtures of toluene + acetonitrile: ⊙ 50 Mpa, ◇ 100 MPa, ⊡ 150 Mpa, △ 200 MPa, ⧗ 300 MPa and ● 400 MPa at 323.15 K

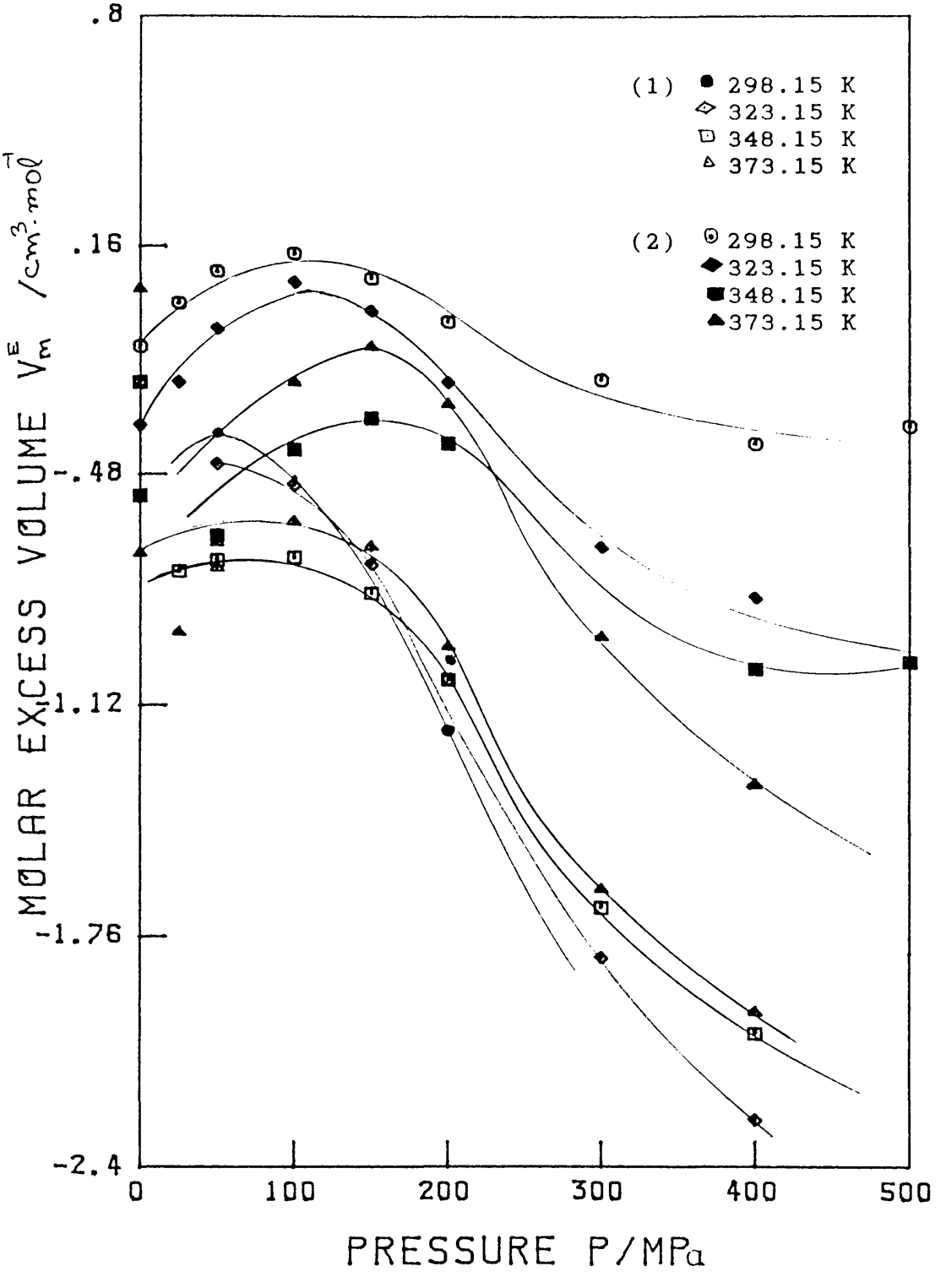

fig 6.5

Molar Excess Volume as a function of pressure
(1) 0.25 toluene + 0.75 n-hexane
(2) 0.50 toluene + o.50 n-hexane

the equimolar mixture the values first becomes less negative and eventually positive up to a pressure of 100 to 150 MPa and then decrease down to negative values. This behaviour is more pronounced for the 0.75 mole fraction of toluene mixture, where the V_M^E at saturation pressure is negative, but becomes positive, increases to a maximum and then decreases, as shown in fig. 6.6, for 323.15 K. At this temperature V_M^E at saturation pressure is -0.23 cm^3/mole, rises to 0.49 cm^3/mole at a pressure of 150 MPa and then decreases smoothly to 0.19 cm^3 /mole at 500 MPa. The other isotherms behave similarly. The V_M^E at constant pressure and at 0.25 mole fraction of toluene is negative , becomes less negative at equimolar composition and eventually positive at toluene richer mixture. Similar variation in V_M^E has been observed at other temperatures.

6.3 TAIT EQUATION

One of the disadvantages of the isothermal secant bulk modulus fitting of density data is that it can neither be used for extrapolation of density beyond the experimental pressure range nor for the interpolation within the experimental temperature range. An excellent correlation method is fitting the data to the Tait equation [77, 198-201]

$$\frac{(\rho - \rho_0)}{\rho} = C \log\left[(B+P)/(B+Po)\right] \qquad (6.2)$$

where B and C are adjustable parameters which can be optimised to provide the best fit of the isothermal densities while other symbols have their usual meanings. The Tait equation has an advantage of being more accurate for extrapolation of densities to higher

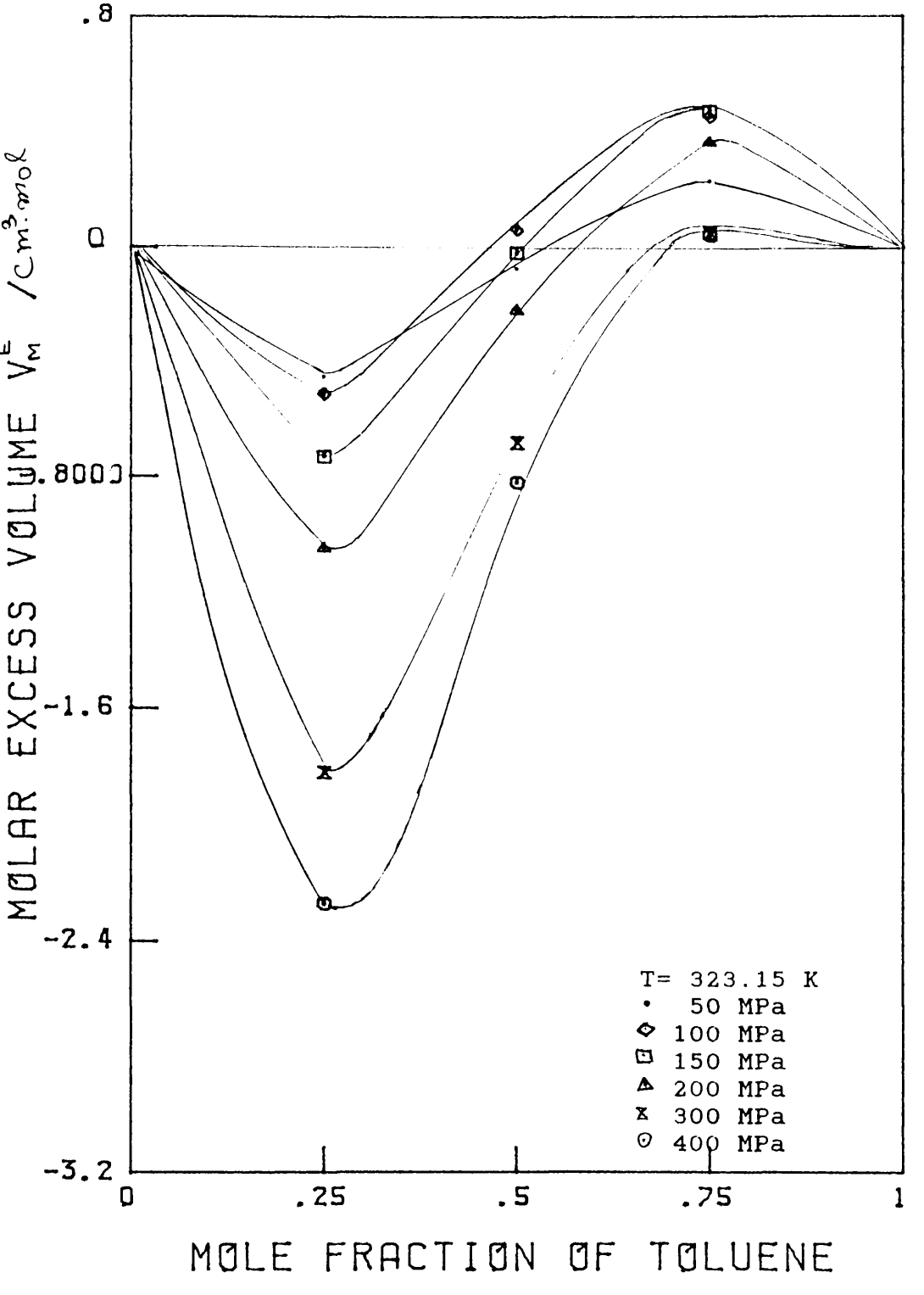

fig 6.6

Molar Excess Volume for toluene + n-hexane as a function of composition

pressure, outside the actual experminental range [173]. Equation (6.2) with the values of B and C given in Table 6.1. fits the present density data for all the liquids and mixtures. Only 12 points out of 368 shows a deviation more than 0.2% , 9 of these have deviations not more than 0.3% while 3 points have deviation between 0.3 to 0.4%.

It has previously been observed that C may be taken as constant for a given compound, independent of temperature [202,203] and may have the same value for a series of compounds [173,199,200]. For example Gibson and Loeffler [202], have suggested that for all aromatic compounds and their derivatives C may be taken equal to 0.216. This research reveals that the C value for acetonitrile (0.260 - 0.262) and the six binary mixtures are higher than 0.216 and an attempt to take C equal to 0.216 and optimise B does not reproduce the densities within experimental uncertainty. However C values seem to be roughly temperature independent and it is possible to select a common value for C, from the range of C at four temperatures, that fit the data at all temperatures for that particular liquid or mixture provided that B is optimised. For example, C equal to 0.260 for acetonitrile and optimised B, slightly different from that given in Table 6.1, reproduces the experimental densities to within experimental accuracy. The values of C seem to be composition dependent for these mixtures in contrast to the conclusion of Gibson and Loeffler [202] for sodium bromide solution in glycol. The C value decreases as the concentration of the toluene increases in both the systems studied and seem to be converging on the value of C for toluene (0.211 - 0.228). If the common value of C, selected from the range, is taken at each composition and optimised for B, the fit is marginally inferior compared to that obtained with an optimised B and C [30].

Table 6.1

COEFFICIENTS OF THE TAIT EQUATION

Liquid/Mixture	Temp T/K	Density Kg m^{-3}	B MPa	C -
acetonitrile	298.26	776.6	106.0	0.268
	323.21	749.5	86.0	0.265
	348.26	721.2	72.0	0.268
	373.27	693.7	52.8	0.262
toluene (a)	298.23	862.1	110.0	0.228
	323.14	838.8	80.0	0.211
	348.23	814.7	74.0	0.220
	373.27	790.0	57.0	0.213
n-hexane (b)	298.15	655.0	66.7	0.230
	323.15	631.6	47.5	0.217
	348.15	606.7	37.0	0.217
	373.15	580.5	26.0	0.211
0.25 toluene	298.28	811.9	99.0	0.248
+	323.18	786.1	90.0	0.261
0.75 acetonitrile	348.23	759.2	72.5	0.257
	373.35	734.6	57.2	0.256
0.50 toluene	298.40	835.5	110.0	0.249
+	323.36	810.6	91.5	0.250
0.50 acetonitrile	348.43	784.6	83.0	0.261
	373.31	759.8	60.0	0.249
0.75 toluene	298.27	851.8	110.0	0.236
+	323.32	827.6	101.0	0.247
0.25 acetonitrile	348.33	802.7	81.0	0.242
	373.26	780.2	64.0	0.237
0.25 toluene	298.27	699.6	73.0	0.243
+	323.33	676.5	62.0	0.248
0.75 n-hexane	348.40	651.2	47.5	0.241
	373.36	623.6	31.0	0.224
0.50 toluene	298.22	748.5	88.0	0.237
+	323.26	725.9	70.0	0.234
0.50 n-hexane	348.35	701.7	52.5	0.226
	373.35	676.1	40.0	0.223
0.75 toluene	298.22	802.2	100.0	0.232
+	323.31	778.6	81.0	0.227
0.25 n-hexane	348.32	754.7	68.0	0.227
	373.49	729.5	54.0	0.223

(a) data from ref: Dymond and Malhotra (1988) [173]
(b) data from ref: Dymond and Young (1979) [190]

6.4 VISCOSITY COEFFICIENT CORRELATION AND PREDICTION FOR BINARY MIXTURES

6.4.1 HARD SPHERE THEORIES

The hard sphere theory has recently been applied for the correlation and prediction of the viscosity coefficient of spherical and pseudo-spherical polyatomic molecules. Dymond and Brawn [57] defined a dimensionless quantity η' as

$$\eta' = 9.118 \times 10^{7}\, \eta\, V^{2/3}/(MRT)^{1/2} \qquad (6.3)$$

where η, V, M are viscosity, volume and molecular weight. η' calculated from the experimental data and plotted against log V for the pure liquids and their mixtures forms a family of curves, superimposible on a reference curve, to form a single curve. The lateral adjustment along the log V axis required to superimpose the particular isotherms on the reference curve gives the Vo(T)/Vo(Tr) values, where Vo(T) is the close packed volume at temperature T.

This approach has been applied to the viscosity coefficient of all the liquids studied and the values of Vo(T)/Vo(Tr) determined. Table 6.2 lists the Vo ratios for the liquid studied. 298 K was chosen as the reference isotherm for all the liquids and mixtures.

Plots of η' against log V', where V' is V.Vo(Tr)/Vo(T) and Tr is the temperature of the reference curve, are shown in fig. 6.7 to 6.10 for toluene, acetonitrile and equimolar mixtures of toluene plus

Table 6.2

VALUES OF Vo(T)/Vo(Tr) FOR HARD SPHERE CORRELATION

Liquid/Mixture	Temperature/K			
	298.2	323.2	348.2	373.2
acetonitrile	1.000	0.978	0.956	0.928
toluene	1.000	0.985	0.981	0.975
n-hexane (a)	1.000	0.989	0.982	0.974
0.25 toluene + 0.75 acetonitrile	1.000	0.983	0.960	0.930
0.50 toluene + 0.50 acetonitrile	1.000	0.973	0.960	0.937
0.75 toluene + 0.25 acetonitrile	1.000	0.983	0.972	0.956
0.25 toluene + 0.75 n-hexane	1.000	0.986	0.974	0.967
0.50 toluene + 0.50 n-hexane	1.000	0.987	0.976	0.962
0.75 toluene + 0.25 n-hexane	1.000	0.988	0.979	0.971

(a) data from ref: Dymond; Young and Isdale (1980) [62]

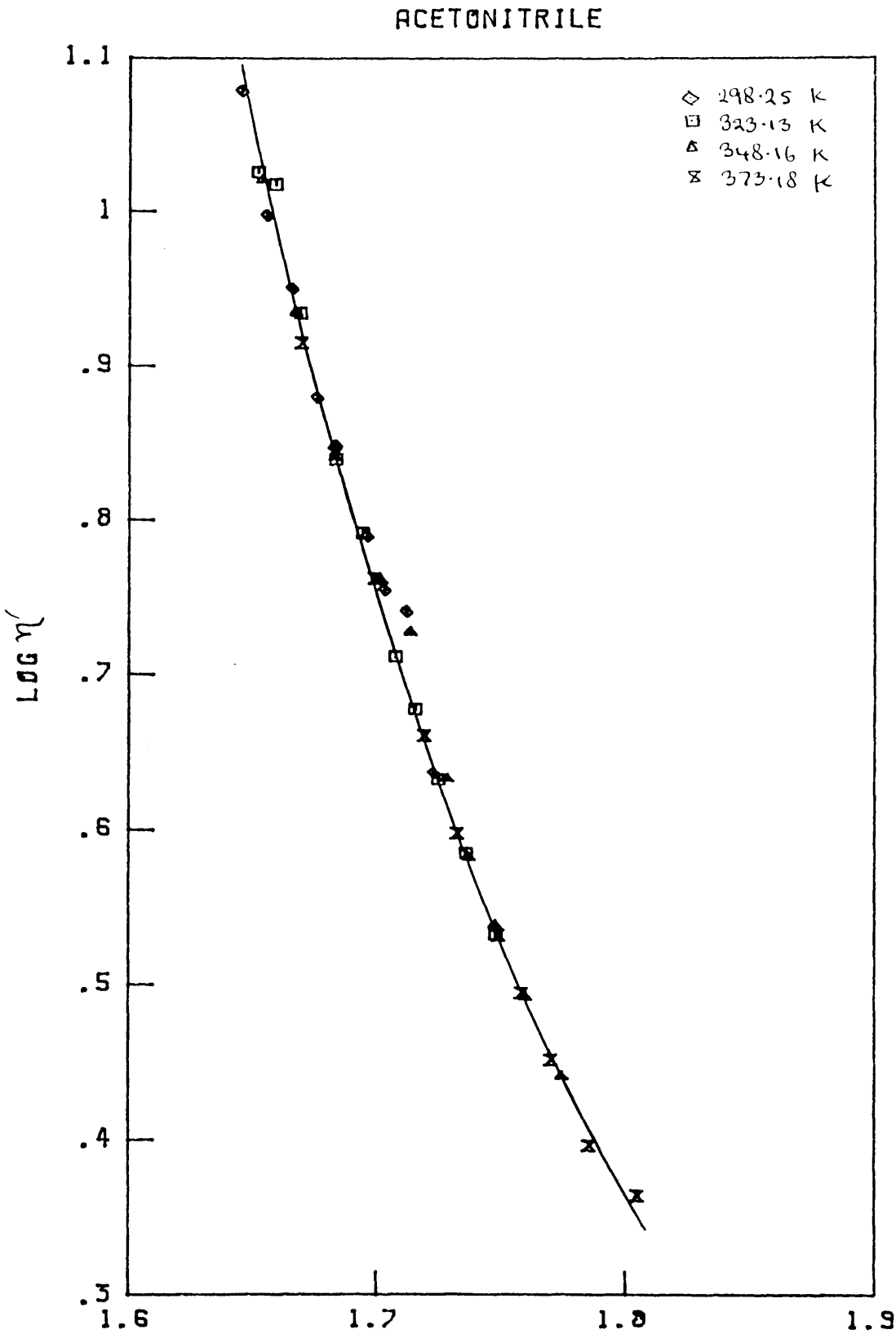

fig. 6.7

Correlation of Experimental Viscosity coefficient Data at different temperatures and pressures.

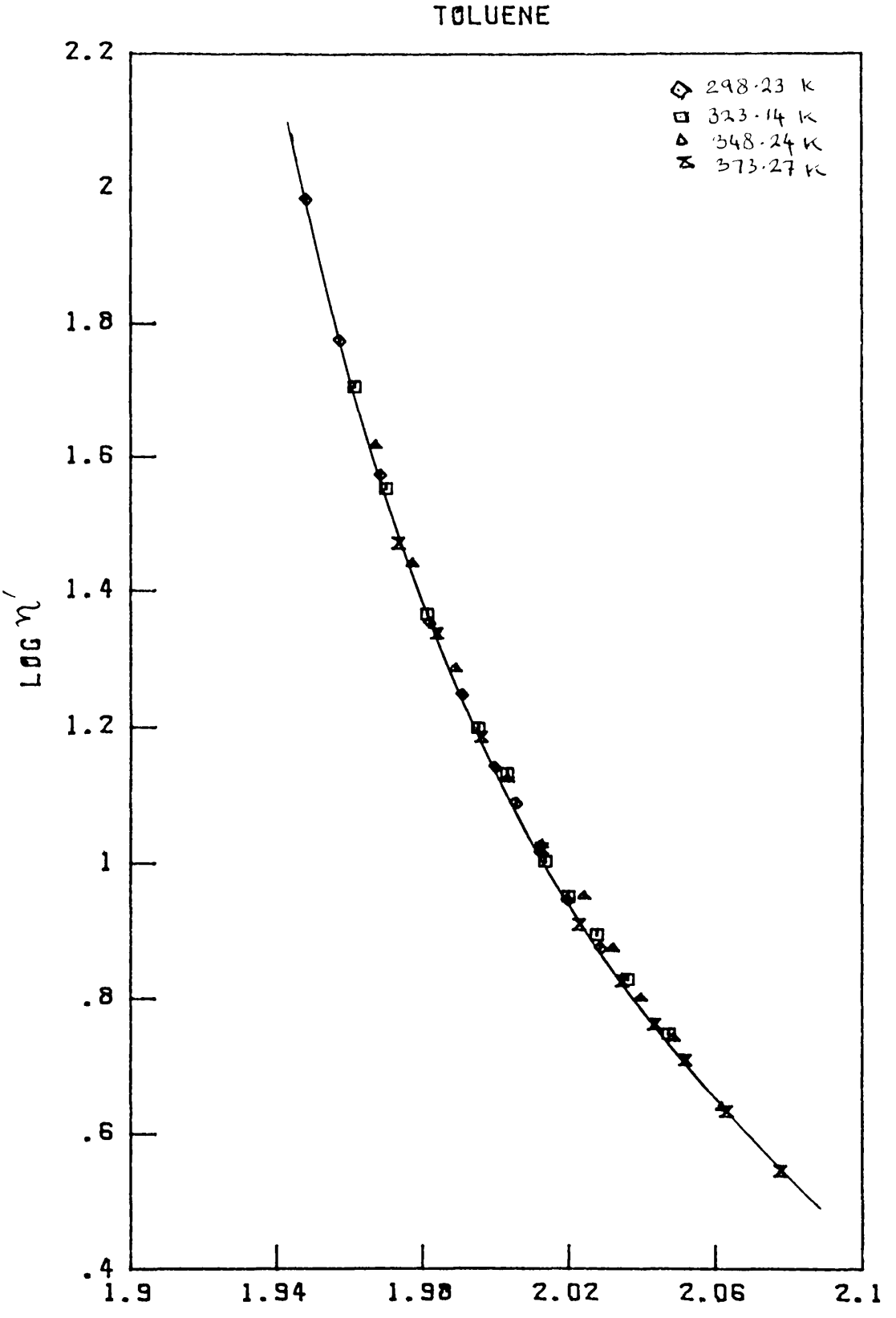

fig 6.8

Correlation of Experimental Viscosity coefficient Data at different temperatures and pressures.

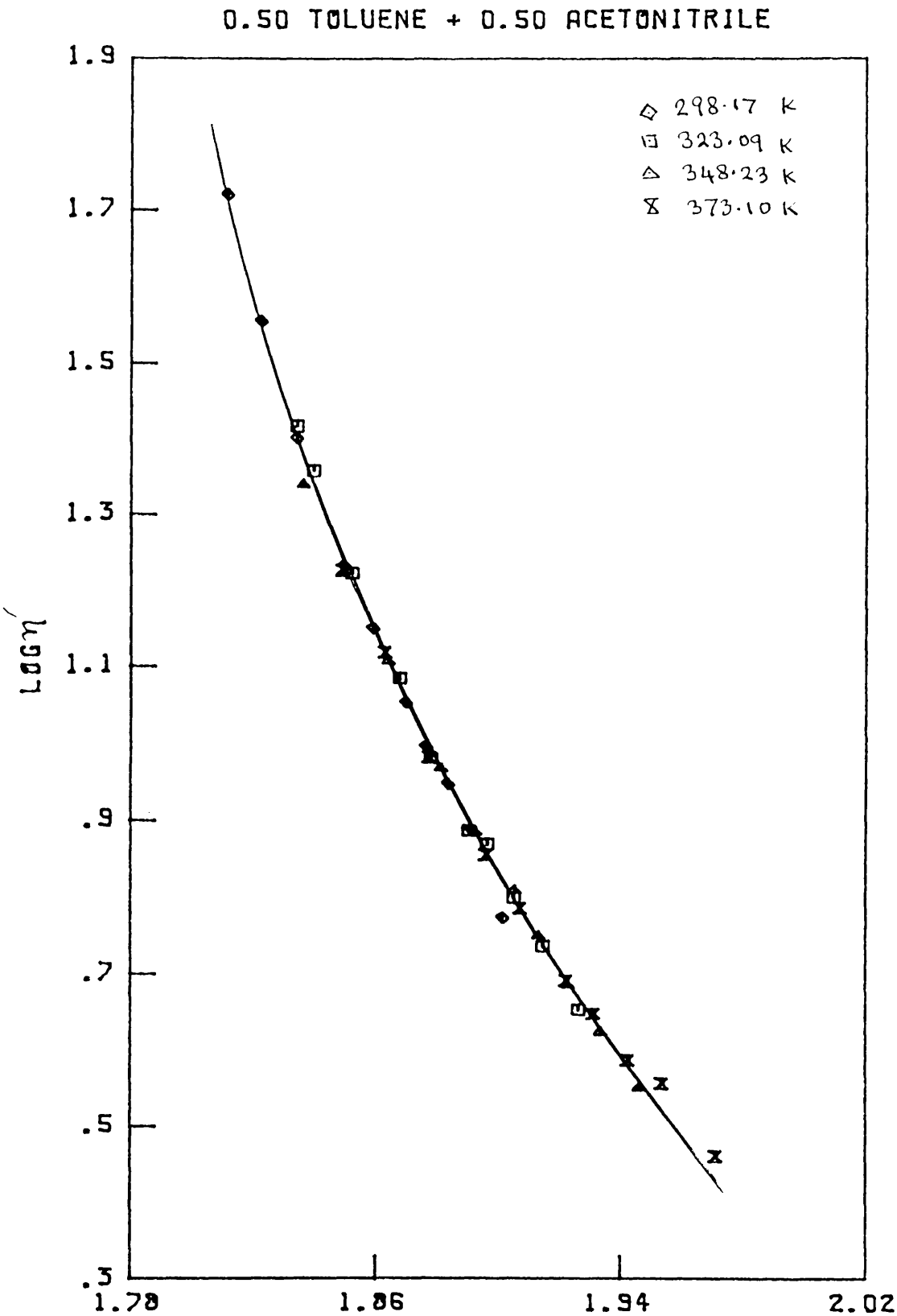

fig 6.9

Correlation of Experimental Viscosity coefficient Data at different temperatures and pressures.

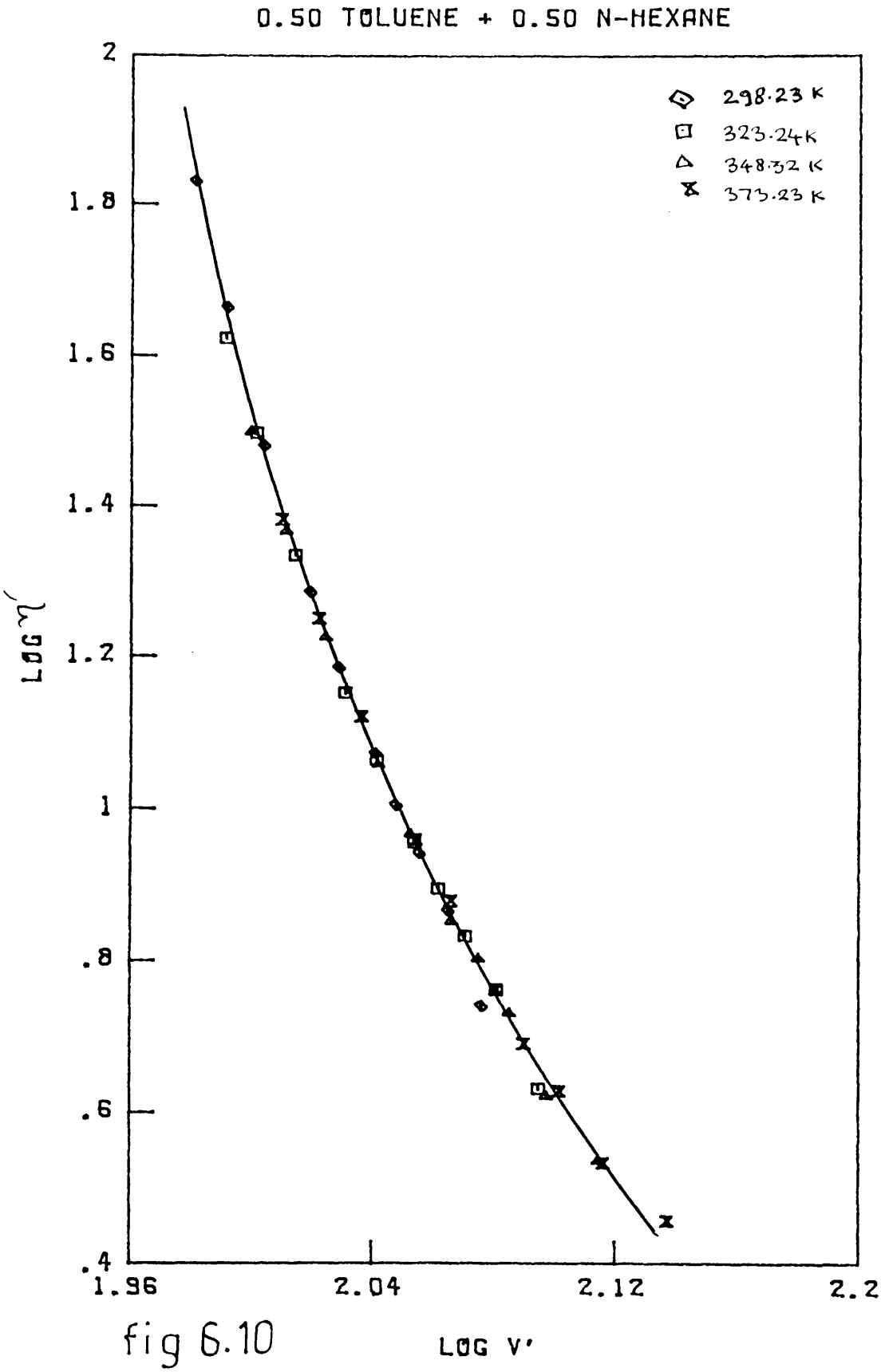

fig 6.10

Correlation of Experimental Viscosity coefficient Data at different temperatures and pressures.

acetonitrile and toluene plus n-hexane.

The viscosity coefficient measurements of n-hexane were conducted at the very end of the experimental work and values obtained for initial measurements at 348 and 373 K gave an average deviation of 3-4% from results previously obtained by Young et al. [62] . However at 298 and 323 K the values were all higher by about 5 to 6 %. The agreement at the higher temperatures confirms the Young values which are used at all temperartures in subsequent analysis. It has been found that n-hexane is prone to leakage. At 298K measurements were repeated thrice, but every time leakage was observed. Young himself came across this problem, but since he used a viscometer of different design, he manage to overcome the problem by tightening up the screws holding the viscometer tube.

As can be seen from Table 6.2, Vo ratios for acetonitrile and 0.75 mole fraction of acetonitrile mixture show stronger temperature dependence than for the other liquids. Values of Vo decrease as the temperature increases, in accordance with the fact that the repulsive interactions of real molecules are not infinitely steep. The ratios for all the acetonitrile mixtures lie in between the ratios for the pure components, while for toluene plus n-hexane mixtures, the variation of Vo(T)/Vo(Tr) is practically identical with each of the pure components.

These results suggest that there is a definite relationship between the viscosity coefficient of a dense fluid and the molar volume, specifically the molar volume relative to the close packing volume. Hence it is possible to predict the pressure dependence of viscosity

coefficient at other temperatures provided density is known along the entire pressure range. The hard sphere based correlation method can thus be successfully applied to the systems studied in this work, not only in the density range of the hard sphere theory but over the entire density range. The disadvantage of this method is that it requires volume data over the whole pressure range.

6.4.2 FREE VOLUME THEORY

Free volume theory has successfully been applied for the correlation of the viscosity coefficients of the binary mixtures of n-alkanes [58], branched hydrocarbons [60] and aromatic compounds [59]. The equation has the form

$$\ln \eta' = A + B.Vo/(V-Vo) \qquad (6.4)$$

where η' is $9.118X10^{-7}\ \eta\ V^{2/3}/(MRT)^{1/2}$, V is volume, Vo is volume of close packing and A, B are adjustable parameters, to take account of the effects of non spherical molecular shape and of translational rotational coupling. For the liquids studied by Dymond and Brawn (1977), A and B were found to be temperature independent, and with A equal to -1.0 the experimental viscosity coefficients were reproduced generally within 5%.

Equation 6.4 was applied to the viscosities of the liquids and mixtures studied, with A equal to -1.0 and optimised for Vo and B to give the best fit at each temperature. Vo values so obtained were then adjusted to give a smooth temperature variation and B was optimised. The Vo and B values for the liquids and mixtures studied

are listed in Table 6.3. The Vo values for toluene plus acetonitrile mixtures vary smoothly with composition, as shown in fig. 6.11. An attempt was made to set Vo equal to $Vo_1 x_1 + Vo_2 x_2$ at each temperature and to optimise for B to reproduce viscosity coefficients to within 5% as has previously been done successfully for n-alkane mixtures [58], but this approach failed in this case and significantly higher deviations were observed for some points. The values of B for acetonitrile are larger than for any other liquid and decrease with increase in temperature in contrast to the general trend. Similarly the 0.75 mole fraction of acetonitrile plus toluene mixture also shows a decrease in value of B with rising temperature. This is shown in fig. 6.12, where B seems to increase with acetonitrile mole fraction at all temperatures.

The Vo values for toluene plus n-hexane system do not vary smoothly with composition, values at equimolar composition are the same as for the 0.75 mole fraction of toluene mixture, while values for 0.75 mole fraction of n-hexane mixture are somewhat lower, as shown in fig. 6.14. The B values increase with rise in temperature.

Tables 6.4 lists the deviations in the calculated viscosity coefficients using optimised Vo and B values, and also using linearly varing Vo and optimised B. Although the number of points having deviations in between 5-10% is 46 in the latter case, 27 of these points have deviations in between 5-6%.

In general equation 6.4 with the values of Vo anb B given in Table 6.3 fits the viscosity data to within 6%. Large deviations were found for toluene plus n-hexane system at saturation pressure. In light of

Table 6.3

COEFFICIENTS FOR THE FREE VOLUME EQUATION, Vo AND B

Liquid/Mixture	Temp T/K	Viscosity mPa s	Vo cm^3/mol	B -
acetonitrile	298.25	0.3403	22.4	3.411
	323.13	0.2722	22.1	3.345
	348.16	0.2229	21.8	3.284
	373.18	0.1885	21.5	3.181
toluene	298.23	0.5516	68.0	1.700
	323.14	0.4211	67.0	1.709
	348.23	0.3336	66.0	1.787
	373.27	0.2730	65.0	1.800
n-hexane (a)	298.15	0.2980	73.0	2.064
	323.15	0.2357	72.0	2.084
	348.15	0.1915	71.0	2.115
	373.15	0.1603	70.0	2.144
0.25 toluene	298.10	0.3937	33.8	2.566
+	323.05	0.3083	33.3	2.521
0.75 acetonitrile	348.18	0.2490	32.8	2.500
	373.15	0.2076	32.3	2.405
0.50 toluene	298.17	0.4526	44.0	2.340
+	323.09	0.3497	43.0	2.318
0.50 acetonitrile	348.23	0.2798	42.0	2.351
	373.10	0.2312	41.0	2.355
0.75 toluene	298.19	0.5085	55.0	2.057
+	323.08	0.3879	54.0	2.065
0.25 acetonitrile	348.23	0.3097	53.0	2.095
	373.22	0.2537	52.0	2.111
0.25 toluene	298.30	0.3227	67.0	2.325
+	323.25	0.2568	66.0	2.323
0.75 n-hexane	348.20	0.2092	65.0	2.340
	373.20	0.1765	64.0	2.389
0.50 toluene	298.23	0.3708	69.0	2.034
+	323.24	0.2943	68.0	2.024
0.50 n-hexane	348.32	0.2394	67.0	2.044
	373.23	0.2020	66.0	2.066
0.75 toluene	298.28	0.4404	69.0	1.863
+	323.27	0.3446	68.0	1.885
0.25 n-hexane	348.35	0.2765	67.0	1.910
	373.35	0.2302	66.0	1.951

(a) data from ref: Dymond; Young and Isdale (1980) [62]

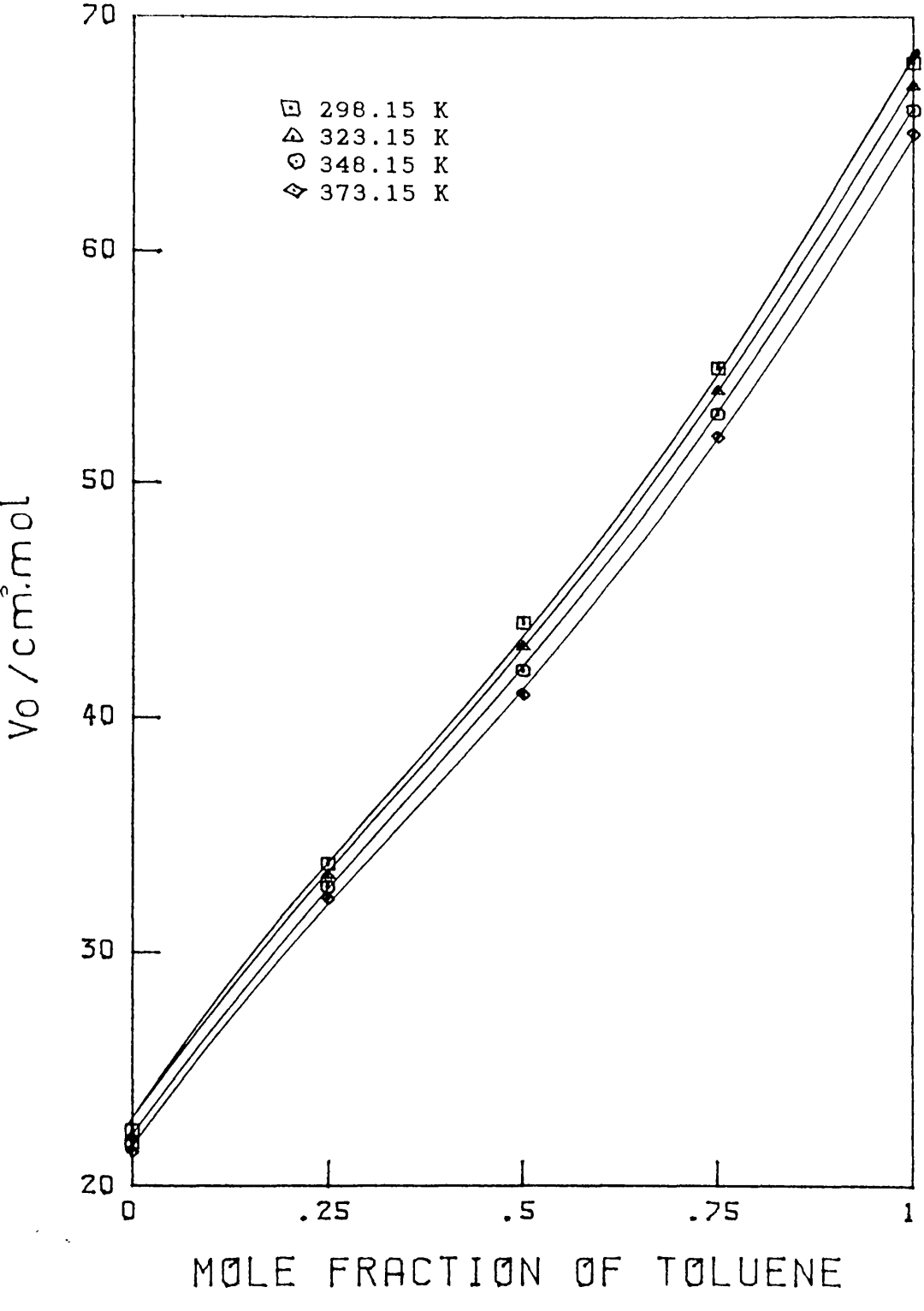

fig 6.11

Dependence of Vo on Mole Fraction and Temperatures
For toluene + acetonitrile

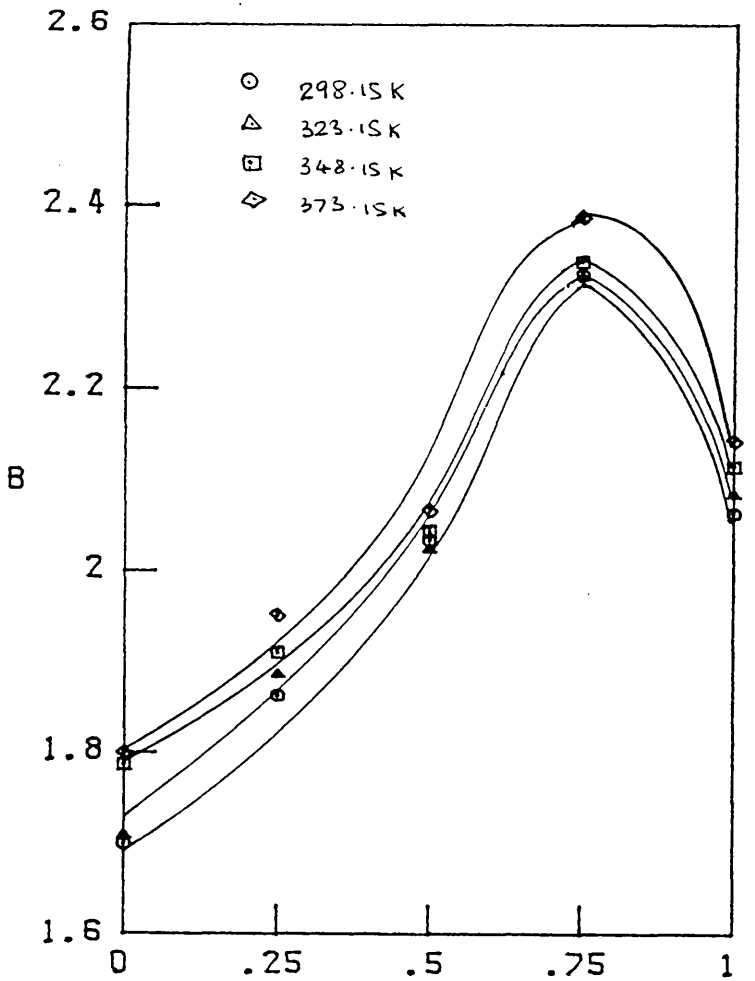

fig.6.13

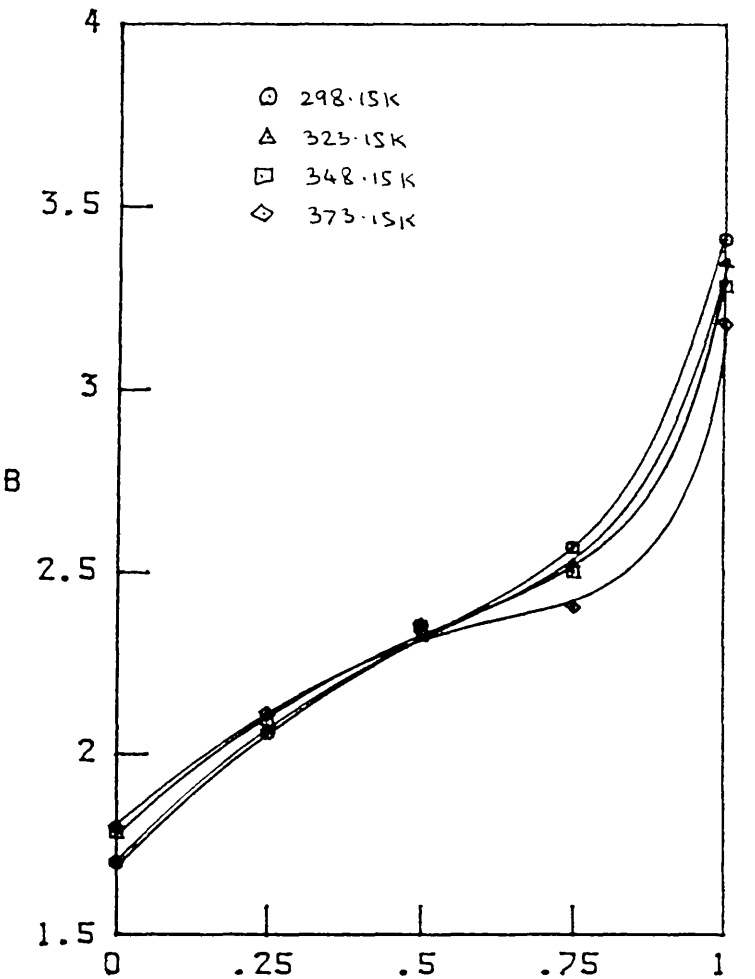

fig.6.12

Dependence of B on mole Fraction and Temperatures.

(toluene +n-hexane)

(toluene + acetonitrile)

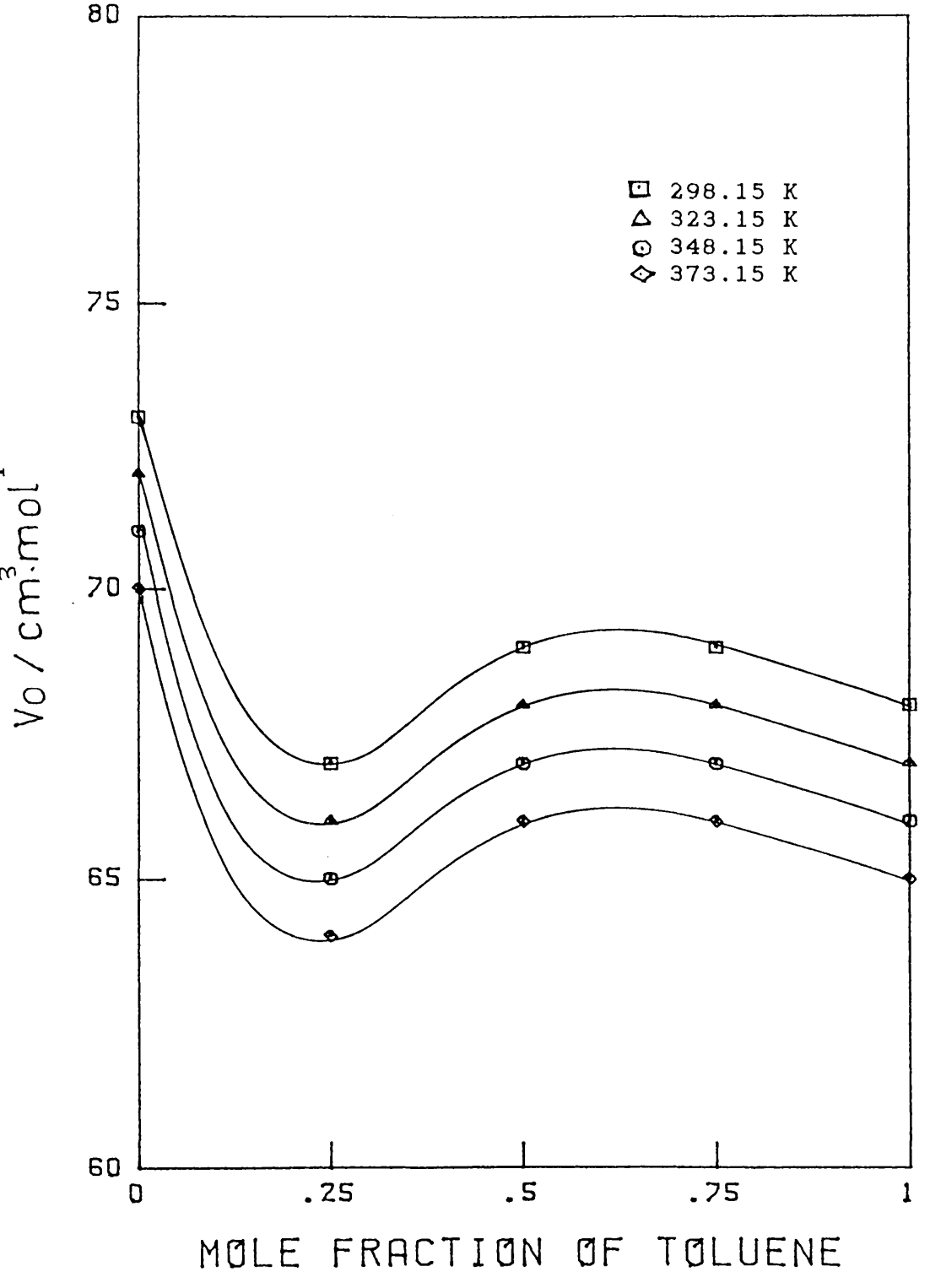

fig.6.14

Dependence of Vo on Mole Fraction and Temperatures For toluene + n-hexane

Table 6.4

DEVIATION OF CALCULATED VISCOSITY USING FREE VOLUME EQUATION

Deviation %	No. of data points: Optimised Vo and B	Optimised B
0-3 %	230	194
3-5 %	58	74
5-10 %	24	46
> 10 %	4	2

the fact that measured high pressure viscosity coefficients are 5% accurate and an uncertainity of 0.2% in the density at moderate pressure produces 1.5% error in the calculated viscosity, increasing to 4.5% at 500 MPa, the free volume equation seems to provide a reasonable fit of the data. Although Vo and B values can not be simply fitted to an equation, they can be interpolated graphically at other compositions and temperatures, and provided that molar volumes are known the viscosity coefficient can be estimated under other conditions of composition, temperature, and pressure. It is estimated that viscosiy coefficients so obtained would have an uncertainty of 6%.

6.4.3 GRUNBERG AND NISSAN EQUATION:

The Grunberg and Nissan equation, originally proposed in 1949 [61] has been recommended by Irving [204] after a study of more than 25 equations, as being the most effective equation in presenting viscosity coefficient data for binary mixtures. The empirical expression may be written as

$$\ln \eta_m = x_1 \ln \eta_1 + x_2 \ln \eta_2 + x_1 x_2 G \qquad (6.5)$$

where η_M is the viscosity coefficient of mixture of components having mole fractions x_1 , x_2 and viscosity coefficients η_1 and η_2 respectively. G is the Grunberg and Nissan constant, which Irving (1977) recommended should be considered as a single disposable parameter even though, for the few systems for which viscosity coefficients data were available at elevated temperature, G was found to be temperature dependent.

The Grunberg and Nissan equation has been applied to the viscosity coefficients data, obtained in this work. The effects of temperature and composition on G are shown in fig. 6.15 for toluene plus acetonitrile, and plus n-hexane, systems at saturation pressure. A 1% uncertainity in the measured viscosity coefficient of the mixture at equimolar composition leads to an uncertainity of 0.05 in G value, rising to 0.07 for the mixture having 0.75 mole fraction of any component. In general G is not constant for these systems, but varies with temperature. The saturation pressure G value for toluene plus acetonitrile system is positive and increases slightly with increasing mole fraction of toluene and decreases with rising temperature. At constant temperature, G can be calculated at other mole fractions from the equimolar G value, using the equation

$$G = G^{0.5}(1.343 - 0.685\ x) \qquad (6.6)$$

where x is mole fraction of acetonitrile. Using equation 6.6, saturation pressure viscosity coefficients for 12 data points were reproduced with a rms deviation of 0.23% and having a maximum deviation of 0.8%.

The G values for toluene plus n-hexane system at saturation pressure are negative, practically independent of composition and become less negative as temperature increases. Taking G at any composition equal to the equimolar G value, the 12 experimental viscosity coefficients were reproduced with a rms deviation of 0.3%, the maximum deviation being only 1%.

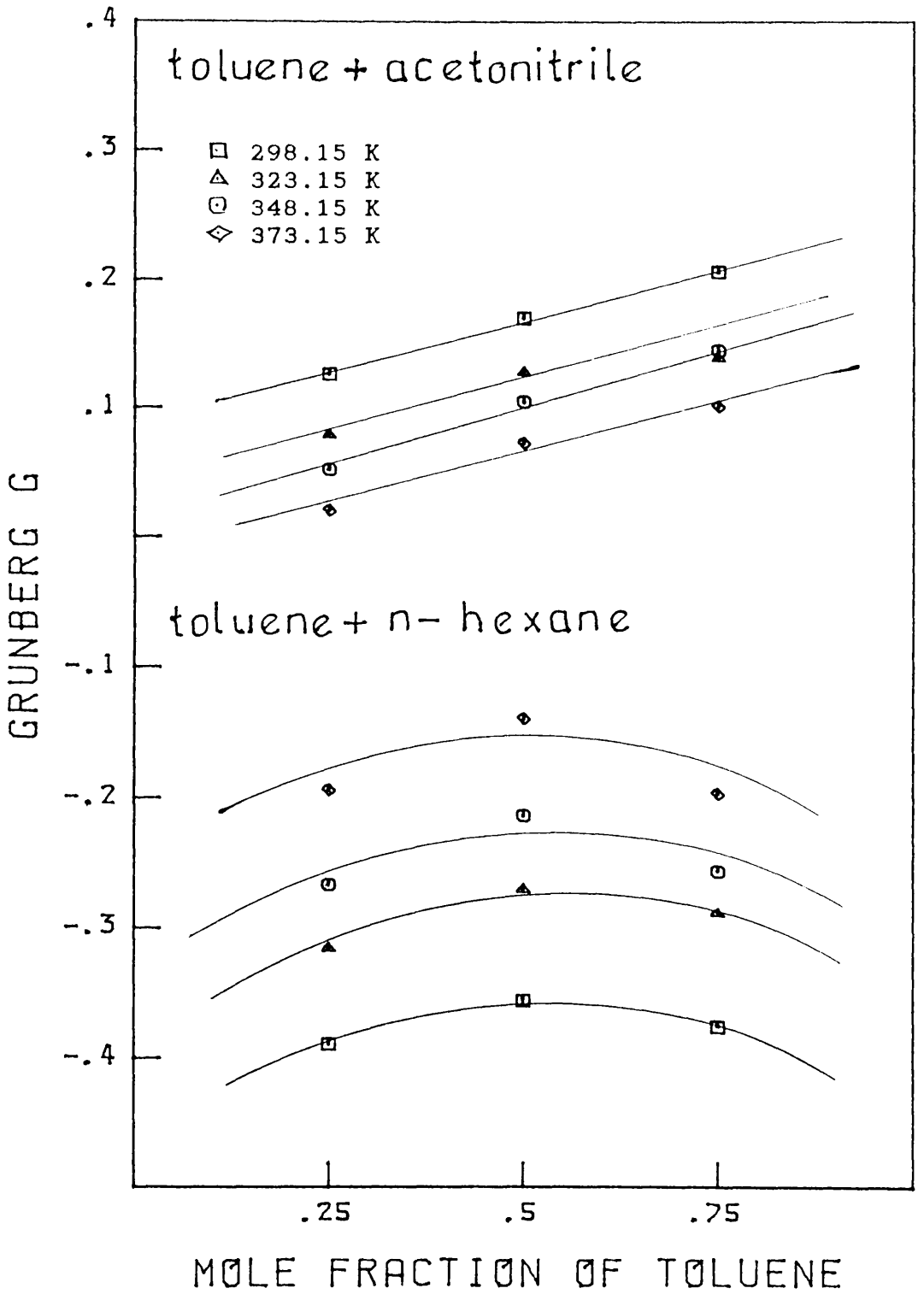

fig 6.15

Dependence of G on Composition at Saturation Pressure.

The value of G for the equimolar mixture as a function of pressure and temperature is shown in fig. 6.16 for toluene plus acetonitrile. At constant temperature, the G values in general increase with increasing pressure and then decrease. At contant pressure, G increases with mole fraction of toluene, up to a mole fraction of 0.5 and than decreases. The slope of the G versus pressure curve also varies with temperature, being 0.001 per MPa at 298 and 323 K and reducing to 0.0002 per MPa at 373 K, where G becomes nearly independent of pressure and a value of G equal to 0.1 reproduces the 24 rounded pressure viscosity coefficients with a rms deviation of 1.9%. Only one point had a deviation more than 5%.

Values for G for the equimolar toluene plus n-hexane mixture are plotted against pressure in fig. 6.17. The saturation pressure G values are negative but become less negative and eventually positive at high pressure. At 323 K there is evidence of a maximum in the curve. For any given temperature and pressure, G generally increases with an increase in the mole fraction of toluene.

Because of the dependency of G on composition of mixture, temperature and pressure, it is not a simple matter to reproduce high pressure G value for the mixtures studied, by simple empirical equations. However there is a definite trend of variation of G with the three experimental variables, and G can be estimated from the appropriate graphs.

Makita and Kashiwagi [153] proposed a modified form of Tait equation, found to give a good representation of viscosity coefficient data for n-alkanes and aromatic hydrocarbons at pressure

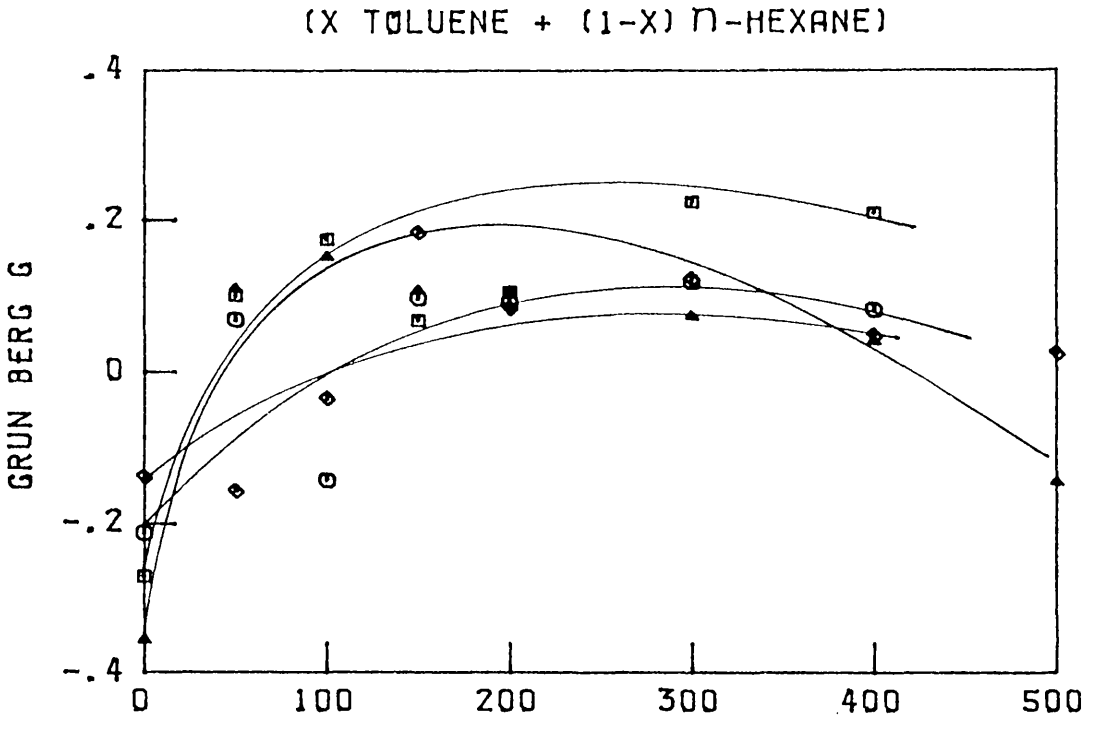

fig6.17

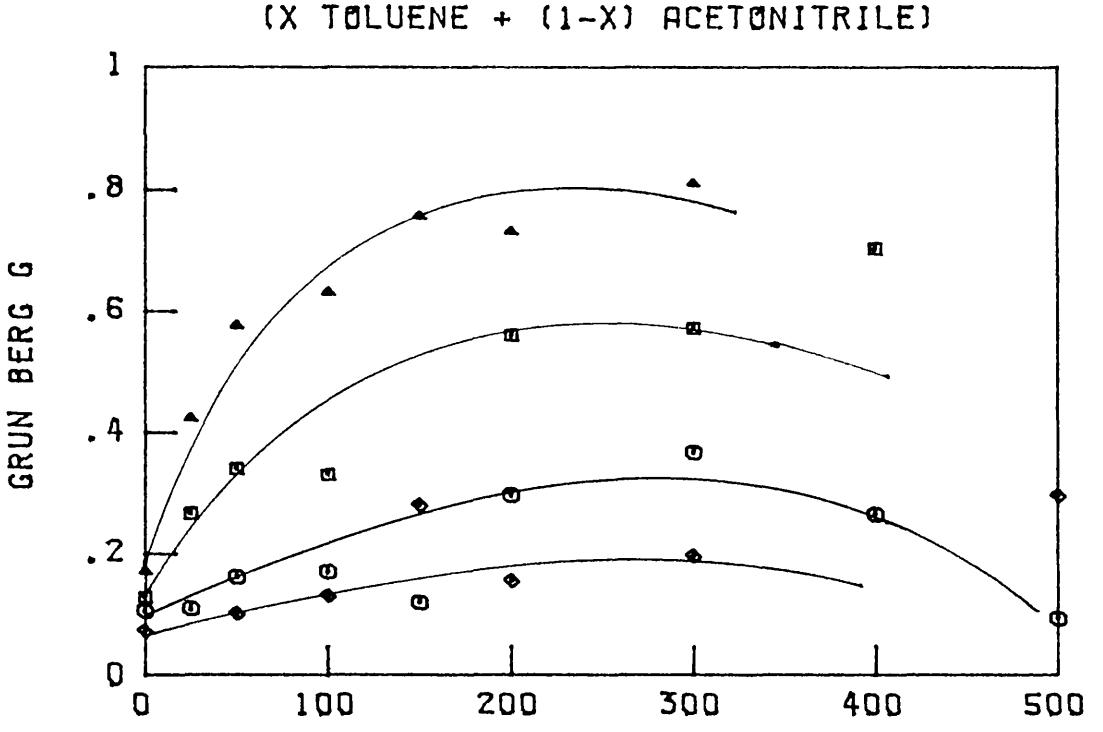

fig 6.16

Dependence of G on Pressure For Equimolar mixtures.
△ 298.15 K, □ 323.15 K, ○ 348.15 K and ◇ 373.15 K.

up to 110 MPa. The equation has the form

$$\ln \eta_P / \eta_0 = E \ln[(D+P)/(D+Po)] \qquad (6.7)$$

where D and E are adjustable parameters. Glen [152] applied this equation to the viscosity coefficients of n-octane, i-octane, n-dodecane and three equimolar mixtures of n-octane + i-octane, n-octane + i-octane and i-octane + n-dodecane up to a pressure of 500 MPa and found systematic deviations like that of the free volume equation, but of opposite sign. Futhermore D and E do not vary smoothly with temperature. Therefore the present data were not fitted to this equation.

CHAPTER 7

CONCLUSIONS

CONCLUSIONS.

The main objectives which have been achieved in this research project are:

- to apply the Taylor Dispersion Technique successfully to the measurement of mutual diffusion coefficients of liquid mixtures at elevated pressures,

- to obtain accurate mutual diffusion coefficient measurements, and density and viscosity measurements, over a wide temperature and pressure range for mixtures of two non-dipolar liquids and a non-dipolar + a highly dipolar liquid.

- to test current theories of transport properties and empirical relationships using these measured values.

- to develop a method of correlation of dense fluid transport properties based on the hard-sphere model by considering diffusion and viscosity coefficients simultaneously and to derive a consistent set of parameters for n-alkanes.

The Taylor Dispersion Technique has been applied at pressure up to 25 MPa using a UV detector with pressure reduction through crimped capillaries placed (a) before and (b) after the detector. No changes in the peak broadening were detected.

The high pressure mutual diffusion coefficient measurements have been made up to 25 MPa for binary mixtures of toluene with (i) n-hexane and

(ii) acetonitrile over the whole concentration range and at temperature in the range of 299 to 348 K in case (i) and 273 to 348 K in case (ii). Since the uncertainty in these measurements is 2.5 - 4%, only a general trend of variation of diffusion coefficient with the variation in pressure can be considered. The two systems behave non-ideally, while the toluene - acetonitrile system shows more deviation with respect to straight line behavior. In terms of the rough hard-sphere theory, the value of the translation-rotation coupling factor, A_{12}, for acetonitrile in toluene (0.72 ± 0.01), which is a typical value for a system of polyatomic molecules, suggests that there is no effect of molecular interactions between a highly dipolar molecule (acetonitrile, $\mu = 11.3 \times 10^{-30}$ Cm) and a non-polar (toluene) molecule, on the experimental diffusion coefficient. A similar conclusion had been reached earlier [205] in the case of a non dipolar liquid plus chlorinated alkanes which possess smaller dipole moments. Significantly lower values of A_{12} have been observed for systems where strong dipole - dipole interactions (for example, acetonitrile-methanol) or quadrupole-dipole interactions (for example, carbon disulphide-acetonitrile) exist [206].

Mutual diffusion coefficients have been measured for benzene and eight fluorinated benzenes in n-hexane at atmospheric pressure over the temperature range 213 - 333 K using the chromatographic peak broadening technique, with an estimated accuracy of 2.5%. An Arrhenius-type equation (which predicts that the logarithm of diffusion coefficient is a linear function of reciprocal of absolute temperature) gives a reasonable fit to the temperature dependence of the mutual diffusion coefficient data for each mixture, with some occasional points showing

deviation slightly more than experimental accuracy. The position of the fluorine atoms affects the diffusion coefficient values. For example, the D_{12} values for o-difluorobenzene in n-hexane are lower than the values for p-difluorobenzene at the corresponding temperatures. Similarly, 1,2,3,5 tetrafluorobenzene diffuses faster than 1,2,4,5 tetrafluorobenzene. Although the solute to solvent mass and size ratios for these solutes vary significantly, these solutes have similar activation energy on the basis of the Eyring "jump" model of diffusion. The solute molecules can be considered to behave as rough hard-spheres and the values derived for the translational rotational coupling constant are again typical of those for pseudo-spherical polyatomic molecules and close to the translational- rotational coupling factor derived for the solvent (n-hexane) itself. In spite of the fact that certain approximations are made in calculating the corrections to the Enskog theory of diffusivity, the mutual diffusion coefficients at trace concentration for these solutes can be reproduced to within 10%, with the roughness factor for these solutes with n-hexane equal to that of the solvent.

The saturation pressure viscosity coefficient and density have been measured for toluene, acetonitrile and the binary mixtures of toluene with n-hexane, and with acetonitrile, over the temperature range 298 to 348 K. The kinematic viscosity coefficients have been measured using a modified suspended-level capillary viscometer with an estimated accuracy of 0.5%. The densities have been measured using a vibrating tube densimeter and have an uncertainty of no more than 0.3 kg/m^3 at the highest temperature.

The high pressure viscosity coefficient and densities have been

measured for binary mixtures of toluene with n-hexane, and with acetonitrile, in the temperature range 298 to 373 K and pressure up to 500 MPa. The viscosity coefficients have been measured using the self-centering free falling body viscometer at the National Engineering Laboratory, and are accurate to 5%, while densities, measured using a bellows volumometer have an uncertainty of 0.2%.

The atmospheric pressure values of molar excess volumes for these mixtures are small and negative. Since the accuracy of high pressure density measurements is 0.2% only a general trend of variation of molar excess volume V with temperature, pressure and composition can be considered. The high pressure values show a clear trend of becoming more negative as the pressure increases for both the mixtures of toluene with n-hexane, and with acetonitrile.

For the purposes of interpolation and slight extrapolation, the density values have been fitted to the modified Tait equation. The fit is excellent and data can be interpolated or slightly extrapolated with an accuracy of 0.2%. Optimised values for C and B are reported. However, it is possible to select a single value for C in the Tait equation from the range of C determined for a given liquid or liquid mixture at the different temperatures. The parameter B in this case will then have to be optimised to fit the data within the experimental uncertainty.

The viscosity data obtained in this work have been correlated successfully using a method based on the rough hard sphere model. The dimensionless quantity η', proportional to $\eta V^{2/3}/(MRT)^{1/2}$ plotted against log V at constant temperature gives curves which for a given

composition can be superimposed. This enables the calculation of the viscosity coefficient at any temperature and pressure to be made with an estimated accuracy of 5%, provided the saturation pressure viscosity coefficient and molar volume at that pressure and temperature are known. This approach shows that viscosity coefficients depend upon the molar volume and especially on the volume relative to some reference which, in the case of the hard-sphere model is the volume of close packing.

The viscosity data have also been interpreted in terms of a free volume form of equation. The fit is very satisfactory. Although the parameters B and Vo for mixtures in the free volume equation cannot be simply related to those of the pure components, graphical interpolation is possible. The values of Vo are a decreasing function of temperature. Viscosity coefficient values can be predicted with an accuracy of 6% for other pressures provided the molar volume is known.

The empirical Grunberg and Nissan equation, which relates the viscosity coefficient for mixtures to the viscosities of pure components, and has the advantage of not requiring knowledge of the molar volume, fits the present viscosity data very well. The dependence of the values of G, the Grunberg and Nissan constant, for these mixtures upon pressure, temperature and composition of the mixture, has been determined.

Self-diffusion coefficient and viscosity coefficient data for liquid n-alkanes over the whole pressure range at different temperatures have been satisfactorily correlated simultaneously by a method based on

consideration of the exact hard-sphere theory of transport properties. Universal curves are developed for reduced quantities D^* and η^*, by extension of the hard-sphere results. Values for the equivalent hard-sphere close-packed volume Vo and factors R_D and R_η which are introduced to account for the effects of non-spherical molecular shape and molecular roughness on diffusion and viscosity respectively are determined by graphical curve fitting. It is found that both R_D and R_η can be considered temperature independent as well as density independent. While it is not possible to establish unique sets of values for these parameters, they can be fairly closely defined. R_D is very close to unity for the n-alkanes and has been taken as 1.0. On this basis, values are given for R_η, and Vo at various temperatures. It is found that R_η increases smoothly from 1.0 for methane up to slightly higher than 1.6 for n-hexadecane. Vo values for n-alkanes at a given temperature show a smooth variation with length of carbon chain.

A consistent set of parameters has been provided which, together with the equations for universal curves, will allow accurate prediction of these transport properties at elevated pressure for other n-alkanes from methane to hexadecane for which data are at present not available.

SUGGESTION FOR FUTURE WORK.

A. EXPERIMENTAL

For the mutual diffusion coefficient measurements:

(i) further work needs to be carried out on making crimped capillaries for generation of steady pressures above 25 MPa within the apparatus at low flow rates.

(ii) extension to pressures above 40 MPa, the upper limit of the present pump, needs to be considered. Steady liquid flow might be maintained by an automatic displacement method with the sample flushed out of a side tube into the mobile phase. Capillary tubing would need to have thicker walls to withstand the higher pressures.

(iii) with the present set-up, a significant improvement would be automated injection of samples. This work is in progress. A block diagram of different parts is shown in Appendix 1.

(iv) a further improvement would be to record and analyse the detector output by computer.

For the density measurements:

(i) the present method has reached the limits of its accuracy. It is therefore timely to consider the vibrating tube method, which is established as an accurate technique in general use for density measurements at atmospheric pressure. A commercial high pressure cell

allows extension to high pressures, but apparatus for measurements above 100 MPa is only now being developed [207].

For the high pressure viscosity:

(i) the falling body method is probably also at the limits of its accuracy, although a better theoretical description of the dynamics of the sinker might extend the range and lead to improved accuracy.

(ii) further consideration should be given to the vibrating wire method which has the potential for giving more reliable measurements [208].

B. CORRELATION AND PREDICTION

Methods based on the consideration of the hard sphere model of transport properties should be developed:

(i) by replacing the graphical curve-fitting techniques used until now with numerical methods, with appropriate weighting of the experimental points,

(ii) by simultaneous fitting of all three transport properties for the members of n-alkanes series with a consistent set of parameters,

(iii) by application to mixtures of n-alkanes using the previously determined parameters,

(iv) by consideration of compounds in other homologous series.

REFERENCES

REFERENCES

1. Maitland, G. C., Rigby, M., Smith, E. B. and Wakeham, W. A.,"Intermolecular Forces", (Clarendon Press, Oxford), 1981

2. Alder, B. J., and Wainwright, T. E., J. Chem. Phys., 31 (1959), 459

3. Alder, B. J., Gass, M. D. and Wainwright, T. E., J. Chem. Phys., 53 (1970), 3813

4. Cheung, P. S. Y. and Powles, J. G., Mol. Phys., 30 (1975), 921

5. Ashurst, W. T. and Hoover, W. G., Phys. Rev. A, 11 (1975), 658

6. Kushick, J. and Berne, B. J., J. Chem. Phys., 64 (1976), 1362

7. Robert, D. W. and Sando, K. M., J. Chem. Phys., 67 (1977), 2585

8. Streett, W. B. and Tildesley, D. G., Proc. Roy. Soc. London, A 355 (1977), 239.

9. Schoen, M. and Hoheisel, C., Mol. Phys., 52 (1984), 33

10. Pyckart, J. P. and Bellemans, A., Chem. Phys. Lett., 30 (1975), 123

11. Nakanishi, K., Toukubo, K. and Watanabe, N., J. Chem. Phys., 68 (1978), 2041

12. Singer, K., Singer, J. V. L. and Taylor, A. J., Mol. Phys., 37 (1979), 1239

13. Dymond, J. H., Chem. Soc. Rev., 14 (1985), 317

14. Dymond, J. H. and Alder, B. J., J. Chem. Phys., 45 (1966), 2061

15. Dymond, J. H. and Alder, B. J., J. Chem. Phys., 48 (1968), 343

16. Ascarelli, P. and Paskin, A., Phys. Rev., 165 (1968), 222

17. Parkhurst, H. J., Jr., and Jonas, J., J. Chem. Phys., 63 (1975), 2698

18. Parkhurst, H. J., Jr., and Jonas, J., J. Chem. Phys., 63 (1975), 2705

19. Harris, K. R., Physica, 93 A (1978), 593

20. Jonas, J., Hasha, D. and Huang, S. G., J. Chem. Phys., 71 (1979), 3996

21. Trappeniers, N. J., Van der Gulik, P. S. and Van den Hooff, H., Physica, 70 (1980), 438

22. Krynicki, K., Changdar, S. N. and Powles, J. G., Mol. Phys., 39

23. Dymond, J. H., J. Phys. Chem., 85 (1981), 3291

24. Chen, S. H., Davis, H. T. and Evan, D. F., J. Chem. Phys., 77 (1982), 2540

25. McLaughlin, E., J. Chem. Phys., 56 (1972), 3952

26. Sanchez, V. and Clifton, M., Ind. Eng. Chem., Fundam., 16 (1977), 318

27. Barrie, J. A., Dawonson, R. B. and Sheppard, R. N., J. Chem. Soc. Faraday Trans.1, 74 (1978), 490

28. R. F. Fedors, AIChE J., 25 (1979), 716

29. Dullien, F. A. L. and Asfour, A. F. A., Ind. Eng. Chem. Fundam., 24 (1985), 1

30. Dymond, J. H., Malhotra, R., Awan, M. A., Glen, N. F. and Isdale, J. D., J. Chem. Thermodyn., 20 (1988), 1217

31. Hirschfelder, J.O., Curtiss, C. F. and Bird,R.B., "Molecular Theory of Gases and Liquids", (John Wiley, New York, 1954).

32. Chapman, S. and Cowling, T. G. "The Mathematical Theory of Non-Uniform Gases", (Cambridge University Press, New York), 1939, Ch. 16

33. Enskog, D., Kungl. Svenska Vet. -Ak. Handl., 63 (1922).

34. Dymond, J. H. and Alder, B. J., J. Chem. Phys., 40 (1964), 939

35. Dymond, J. H. and Alder, B. J., J. Chem. Phys., 52 (1970), 923

36. Carnahan, N. F. and Starling, K. E., J. Chem. Phys. 51 (1969), 635

37. Alder, B. J. and Wainwright, T. E., Phys. Rev. Lett., 18 (1967), 898

38. Protopapas, P., Andersen, H. C. and Parlee, N. A. D., J. Chem. Phys., 59 (1973), 15

39. Chandler, D., J. Chem. Phys., 60 (1974), 3500

40. Chandler, D., J. Chem. Phys., 60 (1974), 3508

41. Chandler, D., J. Chem. Phys., 62 (1975), 1358

42. Evan, D. F., Tominaga, T. and Davis, H. T., J. Chem. Phys., 74 (1981), 1298

43. Dymond, J. H., Chem. Phys., 17 (1976), 101

44. Dymond, J. H., J. Chem. Phys., 60 (1974), 696

45. Bird, R. B., Stewart, W. E., and Lightfoot, E. N., "Transport Phenomena", (John Wiley and Sons. Inc. 1960, London), Ch. 1

46. Glasstone, S., Laidler, K. J. and Eyring, H., "Theory of Rate Processes", (McGraw Hill, New York, 1941), Ch. 9.

47. Kincaid, J. F., Eyring, H. and Stearn, A. E., Chem. Rev., 28 (1941), 301

48. Chen, S. H., Davis, H. T. and Evan, D. F., J. Chem. Phys., 75 (1981), 1422

49. Batschinski, A. Z., Z. Physik. Chem., 84 (1913), 643

50. Doolittle, A. K., J. Appl. Phys., 22 (1951), 1471

51. Doolittle, A. K. and Doolittle , B. D., J. Appl. Phys., 28 (1957), 901

52. Cohen, M. H. and Turnbull, D., J. Chem. Phys., 31 (1959), 1164

53. Hildebrand, J. H., Science, 174 (1971), 490

54. Hildebrand, J. H. and Lamoraux, R. H., Proc. Nat. Acad. Sci. U.S., 69 (1972), 3428

55. Van Cauwelaert, F. H., Jacob, P. A. and Uytterhoeven, J. B., J. Phys. Chem., 77 (1973), 1471

56. Ertl, H. and Dullien, F. A. L., J. Phys. Chem., 77 (1973), 3007

57. Dymond, J. H. and Brawn, T. A., Proc. 7th. Symp. Thermophys. Props., Amer. Soc. Mech. Engr., (New York) 1977, p 660

58. Dymond, J. H., Robertson, J. and Isdale, J. D., Int. J. Thermophys., 2 (1981), 133

59. Dymond, J. H., Robertson, J. and Isdale, J. D., Int. J. Thermophys., 2 (1981), 223

60. Dymond, J. H., Glen, N. F. and Isdale J. D., Int. J. Thermophys., 6 (1985), 233

61. Grunberg, L. and Nissan, A. H., Nature (London), 164 (1949), 799

62. Dymond, J. H., Young, K. J. and Isdale, J. D., Int. J. Thermophys., 1 (1980), 345

63. Dymond, J. H., Malhotra, R., Glen, N. F. and Isdale, J. D., Int. J. Thermophys., (to be submitted).

64. Menashe, J., Mustafa, M., Sage, M. and Wakeham, W. A., Proc. 8th. Symp. Thermophys. Props. (ASME, New York), 1982, p.254

65. Li, S. F. Y., Maitland, G. C. and Wakeham, W. A., High Temp. High Press., 17 (1985), 241

66. Assael, M. J., Charitidou, E., Nieto de Castro, C. A. and Wakeham, W. A., Int. J. Thermophys., 8 (1987), 663

67. Calado, J. C. G., Fareleira, J. M. N. A., Mardolcar, U. V. and Nieto de Castro, C. A., Paper presented at AIChE Meeting, Texas, March 1987

68. Dymond, J. H., Paper presented at AIChE Meeting, Florida, Nov 1987

69. Li, S. F. Y., Trengove, R. D., Wakeham, W. A. and Zalaf, M., Int. J. Thermophys., 7 (1986), 273

70. Harris, K. R., J. Chem. Soc. Faraday Trans.1, 78 (1982), 2265

71. Harris, K. R. and Trappeniers, N. J., Physica, 104A (1980), 262

72. Easteal, A. J., Woolf, L. A. and Jolly, D. L., Physica, 121A (1983), 286

73. Diller, D. E., Physica, 104A (1980), 417

74. Dymond, J. H., Physica, 144B (1987), 267

75. Bachl, F. and Ludemann, H. D., Physica, 139 & 140B (1986), 100

76. Bachl, F. and Ludemann, H. D., Personal Communication.

77. Dymond, J. H. and Malhotra, R., Int. J. Thermophys., 8 (1987), 541

78. Harris, K. R., Physica, 94A (1978), 448

79. Diller, D. E. and Saber, J. M., Physica, 108A (1981), 143

80. Diller, D. E., J. Chem. Eng. Data, 27 (1982), 240

81. Diller, D. E. and Van Poolen, L. J., Int. J. Thermophys., 6 (1985), 43

82. Griffiths, A., Proc. Phys. Soc., 23 (1911), 190

83. Taylor, G., Proc. Roy. Soc. A, 219 (1953), 186

84. Taylor, G., Proc. Roy. Soc. A, 223 (1954), 446

85. Taylor, G., Proc. Roy. Soc. A, 225 (1954), 473

86. Sanni, S. A. and Huchison, P., J. Chem. Eng. Data, 18 (1973), 317

87. Taylor, G. I., Proc. Phys. Soc., B67 (1954), 857

88. Anderson, J. L., Rauh, F. and Morales A., J. Phys. Chem., 82 (1978), 608

89. Shankland, I. R., Arrora, P. S. and Dunlop, P. J., J. Phys. Chem., 81 (1977), 1518

90. Mathad, R. D. and Umakantha, N., J. Chem. Phys., 84 (1986), 2295

91. Wang, J. H., J. Am. Chem. Soc., 76 (1954), 1528

92. Wang, J. H. and Polestra, F. M., J. Am. Chem. Soc., 76 (1954), 1584

93. Oosting, P. H. and Trappeniers, N. J., Physica, 51 (1971), 418

94. Grushka, E. and Kikta Jr., E. J., J. Phys. Chem., 78 (1974), 2297

95. Pratt, K. C. and Wakeham, W. A., Proc. Roy. Soc. Lond. A, 336 (1974), 393

96. Aris, R., Proc. Roy. Soc. Lond. A, 235 (1956), 67

97. Ouano, A. C., Ind. Eng. Chem. Fundam., 11 (1972), 268

98. Wakeham, W. A., Faraday Symp. of the Chem. Soc., No. 15 (1981), 145

99. Tyrrell, H. J. V. and Harris, K. R., "Diffusion in Liquids", (Butterworths, London), 1984, p. 193-198

100. Alizadeh, A. and Wakeham, W. A., Int. J. Thermophys., 3 (1982), 307

101. Manuel Matos Lopes, L. S. and Nieto de Castro, C. A., High Temp. High Press., 17 (1985) 599

102. Nunge, R. J., Lin, T. S. and Gill, W. N., J. Fluid Mech., 51 (1972), 363

103. Golay, M. J. E., J. Chromatogr., 186 (1979), 341

104. Tijssen, R., Sep. Sci. Technol., 13 (1978), 681

105. Atwood, J. G. and Golay, M. J. E., J. Chromatogr., 218 (1981), 97

106. Atwood, J. G. and Goldstein, J., J. Phys. Chem., 88 (1984), 1875

107. Gidding, J. C. and Seager, S. L., J. Chem. Phys., 33 (1960), 1579

108. Balenovic, Z., Mayers, M. N. and Gidding, J. C., J. Chem. Phys., 52 (1970), 915

109. Grushka, E. and Maynard, V. R., J. Phys. Chem., 77 (1973), 1437

110. Grushka, E. and Schmipelsky, P., J. Phys. Chem., 78 (1974), 1428

111. Komiyana, H. and Smith, J. M., J. Chem. Eng. Data, 19 (1974), 384

112. Pratt, K. C. and Wakeham, W. A., Proc. Roy. Soc. A, 342 (1975), 401

113. Ouano, A. C. and Carother, J. A., J. Phys. Chem., 79 (1975), 1314

114. Pratt, K. C. and Wakeham, W. A., J. Phys. Chem., 79 (1975), 2198

115. Grushka, E. and Kikta, E., J. Phys. Chem., 79 (1975), 2199

116. Grushka, E. and Kikta, E., J. Am. Chem. Soc., 98 (1976), 643

117. Tominaga, T. and Matsumoto, S. I., J. Phys. Chem., 90 (1986), 139

118. Wilsch, A., Fiest, R. and Schneider, G. M., Fluid Phase Equilib., 10 (1983), 299

119. Lauer, H. H., McManigill, D. and Board, R. D., Anal. Chem., 55 (1983), 1370

120. Springton, S. R. and Novotny, M., Anal. Chem., 56 (1984), 1762

121. Vogel, A., "Text Book of Practical Organic Chemistry", (Longman, London, 4th. Ed. 1978), p. 44

122. Phipps, A. M. and Hume David, N., J. Chem. Ed., 45 (1968), 664

123. Rondea, R. E., J. Chem. Eng. Data, 11 (1966), 124

124. Alizadeh, A., Nieto de Castro, C. A. and Wakeham, W. A., Int. J. Thermophys., 1 (1980), 243

125. Alder, B. J., Alley, W. E. and Dymond, J. H., J. Chem. Phys., 61 (1974), 1415

126. Herman, P. T. and Alder, B. J., J. Chem. Phys., 56 (1972), 987

127. Czworniak K. J., Andersen, H. C. and Pecora, R., Chem. Phys., 11 (1975), 451

128. Easteal, A. J. and Woolf, L. A., Chem. Phys. 88 (1984), 110

129. Dymond. J. H., Personal Communication.

130. Katz, E., Ogan, K. and Scott, R. P. W., J. Chromatogr., 260 (1983), 277

131. Ghai, R. K. and Dullien, F. A. L., J. Phys. Chem., 78 (1974), 2283

132. Dymond, J. H. and Woolf, L. A., J. Chem. Soc. Faraday Trans.1, 78 (1982), 990

133. Harris, K. R., Pau, C. K. N. and Dunlop, P. J., J. Phys. Chem., 74 (1970), 3518

134. Albright, J. G. and Aoyagi, K., J. Chem. Phys., 64 (1976), 81

135. Chen, B. H. C., Sun, C. K. J. and Chen, S. H., J. Chem. Phys., 82 (1985), 2052

136. Chen, H. C. and Chen, S. H., Chem. Eng. Sci., 40 (1985), 521

137. Newton, I., Principia Lib II, Sect. IX, (1685)

138. B. S. 188: 1977 (British Standards Institution, British Standards House, 2 Park Street London)

139. Young, K. J., Ph.D. Thesis, University of Glasgow, 1980

140. Dymond, J. H. and Young K. J., Int. J. Thermophys. 1 (1980), 27

141. Robertson, J., Ph.D. Thesis, University of Glasgow, 1983

142. Poiseuille, J. L. E., Ann. Chim., 3 Series 7 (1843), 50

143. Kestin, J., Sokolov, M. and Wakeham, W., Appl. Sci. Res., 27 (1973), 241

144. Couette, M. M., Ann. de Chim. et Phys., 21 (1980), 433

145. Wedlake, G. D., Vera, J. H. and Ratcliff, G. A., Rev. Sci. Instrum., 50 (1979), 93

146. Kratky, O., Leopold, H. and Stabinger H., Z. Angew. Phys., 27 (1969), 273

147. Picker, P., Tremblay, E. and Jolicoeur, C., J. Soln. Chem., 3 (1974), 377

148. Reid, R. C., Prausnitz, J. M. and Sherwood, T. K., "The Properties of Gases and Liquids", (McGraw Hill Book Co.) 3rd. Ed.

149. Friedel, B. and Ratzsch, M. T., Wissenschaftl. Zeitschr., 15 (1973), 333

150. Ritzoulis, G., Papadopoulus, N. and Jannakoudakis, D., J. Chem. Eng. Data, 31 (1986), 146

151. A. P. I. Tables, American Petroleum Research Project 44, Thermodynymics Research Centre, Texas, A.and M. University (1952)

152. Glen, N. F., Ph.D. Thesis, University of Glasgow, 1985

153. Kashiwagi, H. and Makita, T., Int. J. Thermophys., 3 (1982), 289

154. Kratzke, H. and Muller, S., J. Chem. Thermodyn., 17 (1985), 151

155. Hales, J. L. and Townsend, R., J. Chem. Thermodyn., 4 (1972), 763

156. Timmermans, J., "Physico-Chemical Constants of Pure Organic Compounds" Vol. II, Elsevier Publishing Co. London, 1965

157. Diaz Pena, M. and Nunez Delgado, J., J. Chem. Thermodyn. 7 (1975), 201

158. Letcher, T. M., J. Chem. Thermodyn., 7 (1975), 205

159. Radojkovic, N., Tasic, A., Grozdanic, D., Jorjevic, B. D. and Malic, D. J. Chem. Thermodyn., 9 (1977), 349

160. Kiyohora, O. and Benson, G. C., Can. J. Chem., 51 (1973), 2489

161. Alcart, E., Taradajos, G. and Diaz Pena, M., J. Chem. Eng. Data, 25 (1980), 140

162. Int. Data Series, Selected Data on Mixtures, Ser A., 1973, p 100

163. Chen, S. S. and Zwolinski, B. J., J. Chem. Soc. Faraday Trans.II, 70 (1974), 1133

164. Isdale, J. D., Ph.D. Thesis, University of Strathclyde, 1976

165. Decker, D. L., Bassett, W. A., Merrill, L., Hall, H. T. and Barnett, J. D., J. Phys. Chem., Ref. Data, 1 (1972), 773

166. Johnson, D. P., "High Pressure Measurements", (Eds. A. A. Giargini and E. C. LLoyd, Butterworths, Washington,) 1963, p 123

167. Boren, M. D., Babb, S. E. and Scott, G. J., Rev. Sci. Instrum., 36 (1965), 1456

168. Dymond, J. H., Isdale, J. D. and Glen, N. F., Fluid Phase Equilib., 20 (1985), 305

169. Lowitz, D. A., Spencer, J. W., Webb, W. and Schiessler, R. W., J. Chem. Phys., 30 (1959), 73

170. Hogenboom, D. L., Webb, W. and Dixon, J. A., J. Phys. Chem., 46 (1967), 2856

171. Snyder, P. S., Benson, M. S., Huang, H. S. and Winnick, J., J. Chem. Eng. Data, 19 (1974), 157

172. Back, P. J., Easteal, A. J., Hurle, R. L. and Woolf, L. A., J. Phys. E: Scientific Instruments, 15 (1982), 360

173. Dymond, J. H., Malhotra, R., Isdale, J. D. and Glen, N. F., J. Chem. Thermodyn., 20 (1988), 603

174. Isdale, J. D. and Spence, C. M., N. E. L. Report No. 92, National Engineering Laboratory, East Kilbride, Glasgow (1975)

175. Chen, M. C. S. and Swift, W. G., AIChE J., 18 (1972), 146

176. Etson, I, and Pinkus, D., J. Lub. Tech., 98 (1976), 433

177. Francesconi, A. Z., Frank, E. V. and Lentz, H., Ber. Bunsenges. Phys. Chem., 79 (1975), 897

178. Srinivasan, K. R. and Kay, R. L., J. Soln. Chem., 6 (1977), 357

179. Schroeder, J., Schiemann, V. H., Sharko, P. T. and Jonas, J., J. Chem. Phys., 66 (1977), 3215

180. Landau, R. and Wurflinger, A., Rev. Sci. Instrum., 51 (1980), 533

181. Easteal, A. J. and Woolf, L. A., J. Chem. Thermodyn., 14 (1982), 755

182. Easteal, A. J. and Woolf, L. A., Int. J. Thermophys., 6 (1985), 331

183. Hayward, A. T., Br. J. Appl. Phys., 18 (1967), 965

184. Bridgman, P. W., Proc. Am. Acad. Arts. Sci., 61 (1926), 57

185. Ageav, N. A. and Golubev, Dokl. Akad. Nauk., SSSR 151 (1963), 597

186. Brazier, D. W. and Freeman, G. R., Can. J. Chem., 47 (1969), 893

187. Isdale, J. D., Dymond, J. H. and Brawn, T. A., High Temp. High Press. 11 (1979), 571

188. Krall, A. H., Nieuwoudt, J. C. and Sengers, J. V., Fluid Phase Equilib., 36 (1987), 207

189. Malhotra, R., Personal Communication.

190. Dymond, J. H., Young, K. J. and Isdale, J. D., J. Chem. Thermodyn., 11 (1979), 887

191. Dymond, J. H., Glen, N. F., Robertson, J. and Isdale, J. D., J. Chem. Thermodyn., 14 (1982), 1149

192. Grigg, R. B., Goates, J. R., Ott, J. B. and Thomas, D. L., J. Chem. Thermodyn., 14 (1982), 27

193. Letcher, T. M. and Scoones, B. W. H., J. Chem. Thermodyn., 14 (1982), 185

194. Grolier, J.-P., Inglese, E. and Wilhelm, E., J. Chem. Thermodyn., 14 (1982), 523

195. Weissberger, A., "Physical Methods of Organic Chemistry", Part 1 (Interscience, New York), 1959, Ch. 4

196. Rowlinson, J. S. and Swinton, F. L.," Liquids and Liquid Mixtures", (Butterworths, London, 3rd. Ed.), 1981

197. Grolier, J.-P., Int. Data Series, Selected Data on Mixtures, Ser. A (1980), p. 141

198. Dymond, J. H. and Malhotra, R., Int. J. Thermophys., 9 (1988), 941

199. Cutler, W. G., McMikle, R. H., Webb, W. and Schiessler, R. W., J. Chem. Phys., 29 (1958), 727

200. Thomson, G. H., Grobst, K. R. and Hankinson, R. W., AIChE J., 28 (1982), 671

201. Kumagi, A. and Iwasaki, H., J. Chem. Eng. Data, 24 (1979), 261

202. Gibson, R. E. and Loeffler, O. H., J. Am. Chem. Soc., 63 (1941), 898

203. Gibson, R. E. and Kincaid, J. F., J. Am. Chem. Soc., 60 (1938), 511

204. Irving, J. B., N. E. L. Report No. 631, National Engineering Laboratory, East Kilbride, Glasgow, 1977

205. Hurle, R. L. and Woolf, L. A., J. Chem. Soc. Faraday Trans.1, 78 (1982), 2921

206 Chan, T. C., J. Chem. Phys., 79 (1983), 3591

207 Wakeham, W. A., Personal Communication.

208 Retsina, T., Richardson, S. M. and Wakeham, W. A., Appl. Sci. Res., 43 (1987), 325

APPENDIX 1

BLOCK DIAGRAM OF DIFFUSION APPARATUS

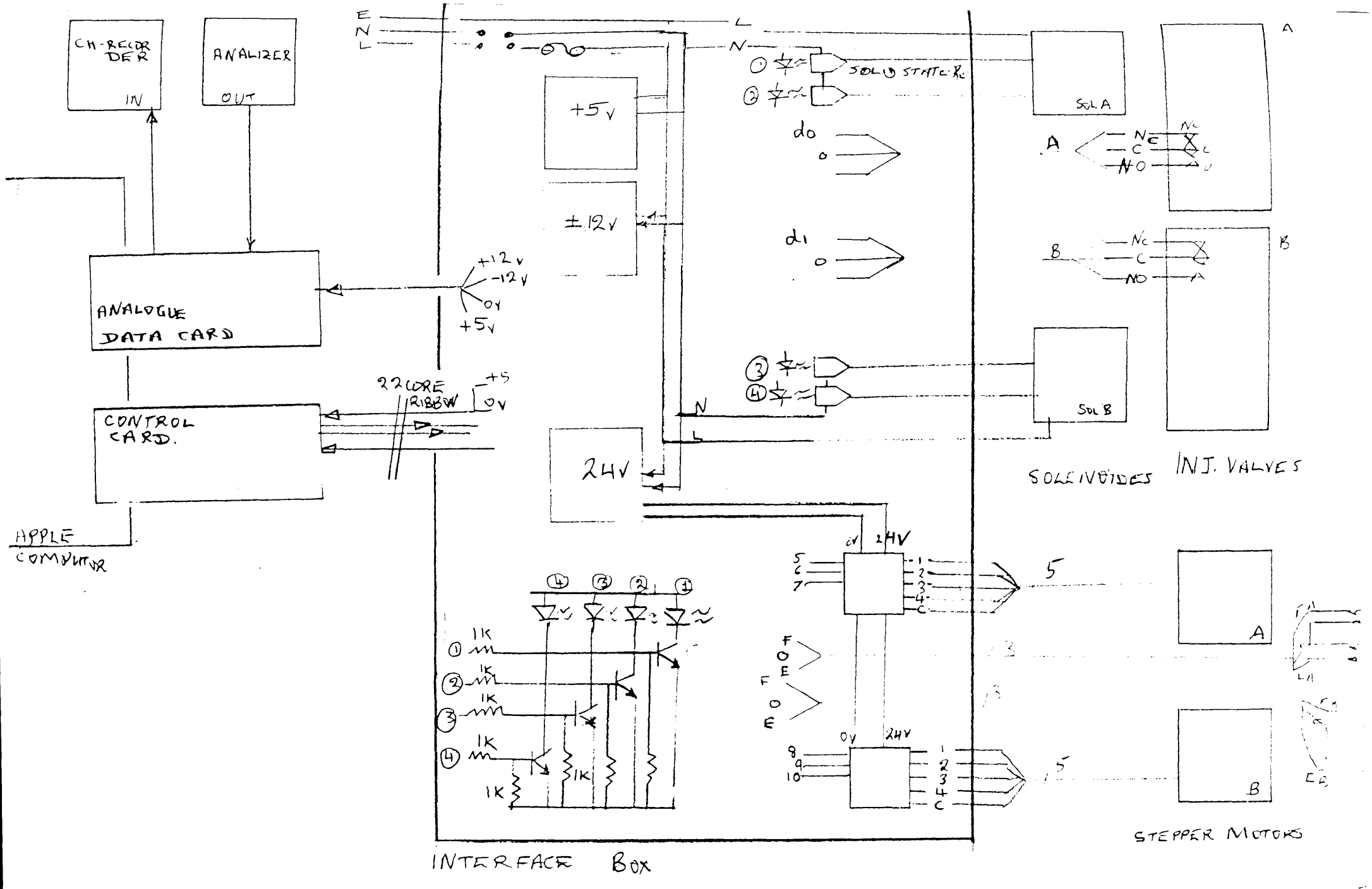
CH-RECORDER IN
ANALIZER OUT
ANALOGUE DATA CARD
CONTROL CARD.
APPLE COMPUTER
22 CORE RIBBON
+5
0V
+12V
-12V
0V
+5V
E
N
L
+5V
±12V
24V
SOLID STATE RL
SOL A
SOL B
SOLENOIDES
INJ. VALVES
NC
C
NO
A
B
1K
INTERFACE BOX
STEPPER MOTORS

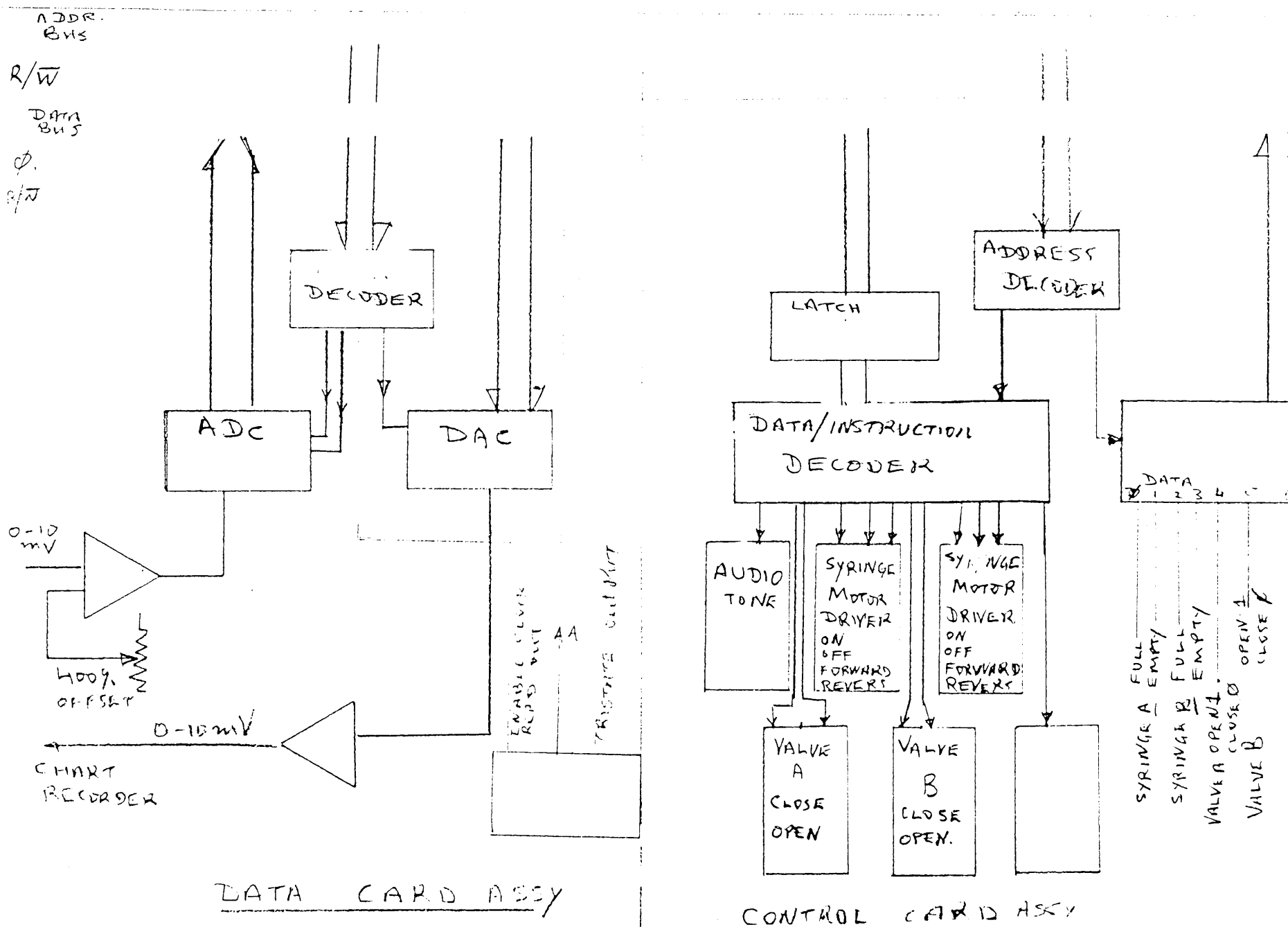

DATA CARD ASSY

CONTROL CARD ASSY

J.S.B. Mar...

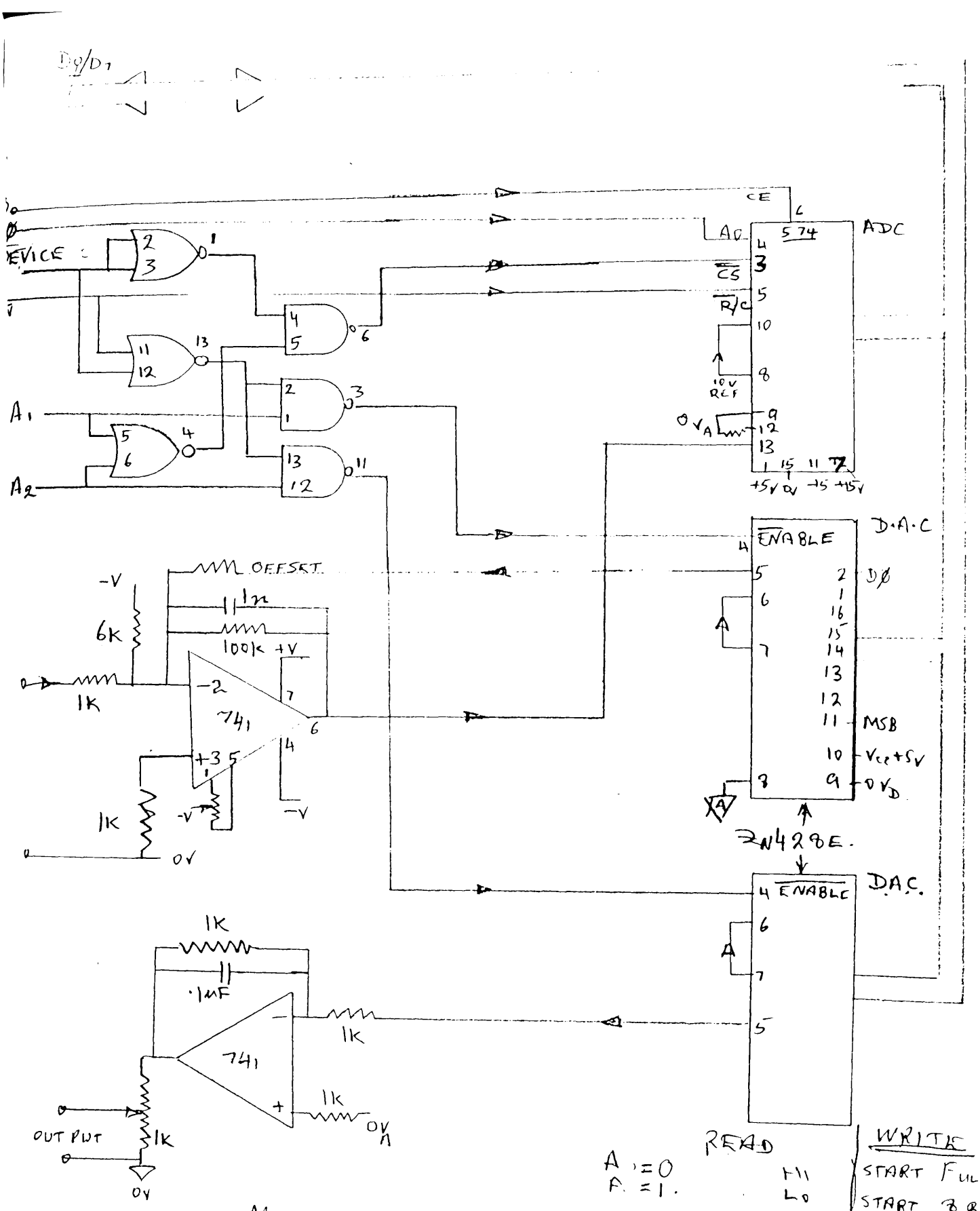

NOTES : Source impedance A1=2 : A1=HIGH NO READ
≃ 160Ω A=4 : A2=H1 NO READ
: Source Voltage 10mV, 1mV
OR Source Current 100μA. 1mA.

1. LS00
1. LS02
1. 32
1. 574 : RS 303-725 @
2. 2N428E RS: 303-523@
2. 741.

ANALOGUE INPUT OUT PUT CIRCUIT
APPLE IIE

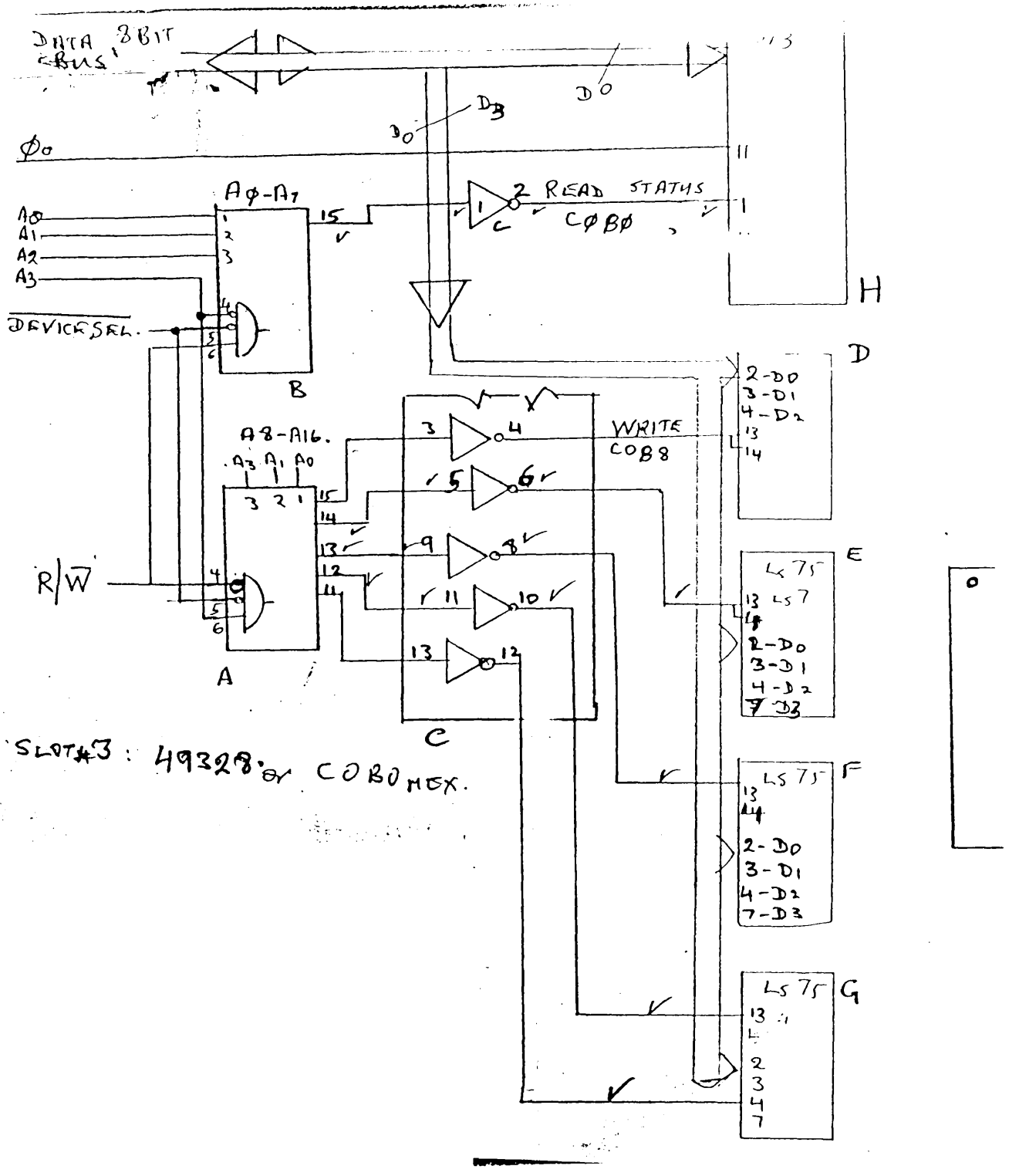
DATA 8 BIT BUS
D0
D3
Ø0
A0
A1
A2
A3
A0-A7
B
DEVICESEL.
2 READ STATUS
C0B0
H
D
2-D0
3-D1
4-D2
WRITE C0B8
A8-A16.
A3 A1 A0
R/W
A
C
E
LS75
2-D0
3-D1
4-D2
F
LS75
2-D0
3-D1
4-D2
7-D3
G
LS75
2
3
4
7
SLOT#3 : 49328. or C0B0MEX.